

**Exploring Theoretical Origins of the Toxicity of Organic
Quaternary Ammonium Salts towards *Escherichia coli* Using
Machine Learning Approaches**

A thesis submitted to the University of Manchester for the degree of
Doctor of Philosophy

2014

Alexandria Olessia Naden

School of Chemistry

List of Contents

List of Figures	7
List of Tables	11
List of Abbreviations	16
Abstract	17
Declaration	18
Copyright statement	19
Dedication	20
Acknowledgements	21
1. Introduction	22
1.1 Quaternary ammonium salts and their bio-activity.	22
1.2 Quantitative structure-activity relationships.	25
1.2.1 Theoretical descriptors of lipophilicity and electronic properties of imidazolium carboxylates.	26
1.2.1.1 Theoretical descriptors of lipophilicity.	28
1.2.1.2 Theoretical descriptors of Hammett sigma constants.	32
1.2.1.2.1 The theory of Atoms in Molecules.	34
1.2.1.2.2 Quantum molecular topological similarity descriptors.	35

1.3 Toxicological data for imidazolium carboxylates.	37
1.3.1 Agar diffusion test - an evaluation of a research hypothesis.	39
1.3.1.1 A research hypothesis.	39
1.3.1.2 Agar diffusion test.	40
1.4 The nature of C – H – – O electrostatic interactions in 1-ethyl-3-methylimidazolium acetate.	41
1.4.1 The nature of a hydrogen bond.	42
1.5 A summary of research objectives.	46
2 Materials and Methods	47
2.1 Minimum inhibitory concentrations of 1-ethyl-, 1-butyl-3-methylimidazolium carboxylates towards <i>Escherichia coli</i> in a liquid medium.	47
2.1.1 Propagation of <i>Escherichia coli</i> .	47
2.1.2 Preparation of a range of concentrations of 1-ethyl-, 1-butyl-3-methylimidazolium carboxylates.	49
2.1.3 The workflow of toxicological screening.	51
2.2 Agar diffusion test.	54
2.2.1 Agar well test.	56
2.3 Computational modelling of imidazolium carboxylates.	59

2.3.1 Chemical structures of imidazolium cations and carboxylate anions.	59
2.3.2 Optimization of imidazolium cations and carboxylate anions to their equilibrium geometries.	61
2.3.3 Optimization of imidazolium carboxylates to their equilibrium geometries.	65
2.3.4 Generation of wavefunction files of imidazolium carboxylates.	66
2.3.5 Computation of quantum topological molecular similarity descriptors of imidazolium carboxylates.	68
2.3.6 Computation of distribution coefficients of imidazolium carboxylates.	71
2.4 Statistical correlation of experimental and computational data for imidazolium carboxylates.	73
2.4.1 The mathematical format of experimental and computational data.	77
2.4.2 Multivariate linear regression algorithms in the MATLAB 7.10 program.	79
3. Results and discussions	80
3.1 Minimum inhibitory concentrations of 1-ethyl-, 1-butyl-3-methylimidazolium carboxylates	80

towards *Escherichia coli*.

3.2 Agar diffusion test.	82
3.2.1 A theoretical evaluation of the agar diffusion test for toxicological screening of ionic liquids.	82
3.2.2 An experimental evaluation of the agar diffusion test for toxicological screening of ionic liquids.	86
3.3 Distribution coefficients and QTMS descriptors of imidazolium carboxylates.	89
3.4 The nature of C – H – O electrostatic interactions in 1-ethyl-3-methylimidazolium acetate.	92
3.4.1 A topological assessment of C – H – O interactions.	92
3.4.1.1 Terminology of the theory of Atoms in Molecules.	97
3.4.1.2 Assessment criteria, results and discussions.	98
3.5 Quantitative structure activity relationships.	121
3.5.1 Linear regression of Log(1/MIC) values of imidazolium carboxylates on their topological connectivity indices.	122
3.5.2 Linear regression of LogD values of imidazolium carboxylates on their QTMS descriptors.	124
3.5.3 Linear regression of Log(1/MIC) values of	126

imidazolium carboxylates on their LogD and	
QTMS descriptors.	
3.6 Topological analysis of the long side chains on	137
imidazolium cations.	
4. Conclusions	141
5. Future work	143
6. References	145
Appendix 1: Reprint licences.	159
Appendix 2: QTMS descriptors of imidazolium carboxylates.	165
Appendix 3: The data processing script written in Matlab 7.10.	209

Total word count: 54133

List of Figures

Figure 1. The mechanism of a bio-action of a quaternary ammonium cation on a bacterial cell wall on an example of benzalkonium chloride.	23
Figure 2. A graphical representation of an imidazolium carboxylate monomer.	24
Figure 3. A graphical representation of an inter-atomic surface, an atomic interaction line and a bond critical point as defined in the theory of Atoms in Molecules.	35
Figure 4. The workflow of a regression analysis based on QTMS descriptors.	36
Figure 5. Chemical structures of 1-alkyl, 1-alkoxymethylimidazolium lactates from the dataset of Pernak and colleagues (Pernak et al., 2004).	37
Figure 6. The observation of an adaptation of a microorganism towards an antibiotic in the Agar Diffusion Test.	41
Figure 7. The concentrations of imidazolium carboxylates which were used for toxicological screening of <i>Escherichia coli</i> .	50
Figure 8. Stages of a bacterial growth which can be quantitatively observed in a liquid medium.	52
Figure 9. Four stages of the transfer of a filter paper disk	55

from a vial on an agar surface.

Figure 10. A pocket well in the Agar Well Test.	57
Figure 11. The sealed end of a glass Pasteur pipette.	57
Figure 12. The chemical structures of imidazolium cations.	59
Figure 13. The chemical structures of carboxylate anions.	60
Figure 14. A geometrical configuration of a combined imidazolium carboxylate structure.	65
Figure 15. A sample of the content of a wavefunction file.	67
Figure 16. An atomic numbering scheme in 1-ethyl-3-methylimidazolium acetate.	95
Figure 17. Schematics of the topological portrait of electronic charge distribution in the region between two interacting atoms.	97
Figure 18. The atomic labelling scheme of the inter-ionic region of 1-ethyl-3-methylimidazolium acetate.	98
Figure 19. Bond critical points and atomic interaction lines observed in H—O interactions of 1-ethyl-3-methylimidazolium acetate in HF electronic charge density.	101
Figure 20. Bond critical points and atomic interaction lines observed in H—O interactions of 1-ethyl-3-methylimidazolium acetate in electronic charge density.	102

Figure 21. Topological portraits of formaldehyde - chloroform and acetone - chloroform van der Waals complexes.	110
Figure 22. A sample plot of predicted versus experimental $\text{Log}(1/\text{MIC})$ values of imidazolium carboxylates by a QSAR based on the topological connectivity indices and the partial least squares regression.	124
Figure 23. An illustrative plot of predicted versus Computed LogD values of imidazolium carboxylates based on the partial least squares regression.	125
Figure 24. Histograms of QSARs based on the LogD and the QTMS descriptors generated using partial least squares (PLS) regression.	128
Figure 25. Histograms of QSARs based on the QTMS descriptors of the imidazoiium cations and the LogD descriptors of the salts generated using partial least squares (PLS) regression.	131
Figure 26. Histograms of QSARs based on the QTMS descriptors of the imidazoiium cations and the LogD descriptors of the salts generated using partial least squares (PLS) regression with principal component analysis data pre-processing.	132

Figure 27. Histograms of QSARs based on the QTMS descriptors of the long side chains on imidazolioium cations and the LogD descriptors of the salts generated using partial least squares (PLS) regression.	135
Figure 28. Histograms of QSARs based on the QTMS descriptors of the long side chains on imidazolioium cations and the LogD descriptors of the salts generated using partial least squares (PLS) regression with principal component analysis data pre-processing.	136
Figure 29. Intra-ionic C–H– \cdots H–C interactions in 1-alkylimidazolium cations.	139
Figure 30. Intra-ionic C–H– \cdots H–C interactions in 1-alkoxymethylimidazolium cations.	139

List of Tables

Table 1. Minimum inhibitory concentrations of 1-alkyl-, 1-alkoxymethylimidazolium lactates towards <i>Escherichia coli</i> .	38
Table 2. Minimal inhibitory concentrations of 1-ethyl, 1-butyl-imidazolium carboxylates towards <i>Escherichia coli</i> .	80
Table 3. The maximum specific growth rates of <i>Escherichia coli</i> with a range of concentrations of 1-ethyl-, 1-butyl-3-methylimidazolium carboxylates reported as growth rate percent of the control.	81
Table 4. Qualitative toxicological profiling of 1-ethyl-, 1-butyl-3-methylimidazolium carboxylates with <i>Escherichia coli</i> in the agar diffusion test and the agar well test.	87
Table 5. The comparison of the initial in-well concentrations of 1-ethyl-, 1-butyl-3-methylimidazolium carboxylates in the agar well test with their MICs in a liquid medium.	88
Table 6. Theoretical distribution coefficients of 1-ethyl, 1-butyl-3-methylimidazolium carboxylates and 1-alkyl, 1-alkoxymethylimidazolium L-lactates at pH 5, 7, 9.	91
Table 7. Distances between the atoms of 1-ethyl-3-methylimidazolium cation and the acetate anion facing the inter-ionic region.	95

Table 8. Inter-atomic distances in H – – O	99
interactions, and the distances between the atoms	
and a bond critical point.	
Table 9. The values of HF and MP2 electronic charge	103
density of H – – O bond critical points of	
1-ethyl-3-methylimidazolium acetate.	
Table 10. The Laplacian of the HF electronic charge	105
density at the H – – O bond critical points of	
1-ethyl-3-methylimidazolium acetate.	
Table 11. The Laplacian of the MP2 electronic charge	106
density at H – – O bond critical points of	
1-ethyl-3-methylimidazolium acetate.	
Table 12. The radii of atoms in H – – O inter-ionic	108
interactions and their free atomic radii computed at the HF and	
the MP2 geometries of 1-ethyl-3-methylimidazolium acetate.	
Table 13. Changes in atomic radii of hydrogen atoms	109
and oxygen atoms in H – – O inter-ionic interactions compared	
to their free radii computed for the HF and the MP2 geometry of	
1-ethyl-3-methylimidazolium acetate.	
Table 14. Changes in electronic charge on hydrogen	111

atoms upon formation of H – – O inter-ionic interactions
 compared to their free radii computed in the HF geometry of
 1-ethyl-3-methylimidazolium acetate.

Table 15. Changes in electronic charge on hydrogen 111

atoms upon formation of H – – O inter-ionic interactions
 compared to their free radii computed in the MP2 geometry of
 1-ethyl-3-methylimidazolium acetate.

Table 16. Total atomic energies of free hydrogen atoms 113

and their energy in H – – O inter-ionic interactions in the HF
 geometry of 1-ethyl-3-methylimidazolium acetate.

Table 17. Total atomic energies of free hydrogen atoms 113

and their energy in H – – O inter-ionic interactions in the HF
 geometry of 1-ethyl-3-methylimidazolium acetate.

Table 18. Dipolar polarization of free hydrogen atoms and 115

their dipolar polarization in H – – O inter-ionic interactions in the
 HF geometry of 1-ethyl-3-methylimidazolium acetate.

Table 19. Dipolar polarization of free hydrogen atoms and 115

their dipolar polarization in H – – O inter-ionic interactions in the
 MP2 geometry of 1-ethyl-3-methylimidazolium acetate.

Table 20. Point dipole moments at bond critical points of 118

H – – O interactions computed in the HF and MP2 geometry of 1-ethyl-3-methylimidazolium acetate.

Table 21. Topological volumes of free hydrogen atoms 119

and their topological volumes in H – – O inter-ionic interactions in the HF and the MP2 geometry of 1-ethyl-3-methylimidazolium acetate.

Table 22. Statistical parameters quantifying the predictivity 123

of a linear regression model based on the topological connectivity indices of imidazolium carboxylates as an average of 1000 random models.

Table 23. Statistical parameters of a linear regression 124

model correlating the QTMS descriptors of imidazolium carboxylates with their LogD values as an average of 1000 random models.

Table 24. Statistical parameters quantifying the predictivity 126

of a linear regression model based on the QTMS and the LogD descriptors of imidazolium carboxylates as an average of 1000 random models.

Table 25. Statistical parameters quantifying the predictivity 129

of a linear regression model based on the QTMS and QTMS with

LogD descriptors of the imidazolium cations as an average of 1000 random models.

Table 26. Statistical parameters quantifying the predictivity of a linear regression model based on the QTMS descriptors of structural fragments of imidazolium cations as an average of 1000 random models. 133

Table 27. Topological parameters at bond critical points of H – – H interactions in the alkyl side chains of 1-alkyl, 1-alkoxymethylimidazolium cations. 140

Abbreviations

MIC - minimum inhibitory concentrations

ADT- agar diffusion test

AWT- agar well test

QTMS- quantum topological molecular similarity

MLR- multiple linear regression

PCA- principal component analysis

PCA₁ - first principal component of the principal component analysis

PLS- partial least squares

PLS₆ - partial least squares regression with six latent variables

Abstract

The University of Manchester

Alexandria Olessia Naden

Doctor of Philosophy

Exploring Theoretical Origins of the Toxicity of Organic Quaternary
Ammonium Salts towards *Escherichia coli* Using Machine Learning
Approaches

08.03.2014

Quaternary ammonium salts are surface active bactericides. A mechanism of their biological activity has been well studied experimentally, and it encompasses two stages. The first stage involves electrostatic interactions of polar functional groups of the salts with oppositely charged functional groups on a bacterial cell surface, and the second stage includes incorporation of their lipophilic groups into a bacterial cell membrane. However, despite numerous experimental studies, computational modelling of this mechanism with the aim to support experimental observations with theoretical conclusions, to the author's knowledge, has not yet been reported.

In the current study, linear regression models correlating theoretical descriptors of lipophilicity and electronic properties of mono- and di-substituted imidazolium carboxylates with their biological activity towards *Escherichia coli* have been developed. These models established that biological activity of these salts is governed by the chemical structures of imidazolium cations, and that the centre of this biological activity is located in the long alkyl side chains of the cations. It was also found that these side chains have an intrinsic electronic potential to form internal C–H–...H–C electrostatic interactions when their lengths reach seven carbon atoms. Additionally, the nature of the C–H–...O–C inter-ionic electrostatic interactions in imidazolium carboxylates has been explored via a topological analysis of these interactions in 1-ethyl-3-methylimidazolium acetate. Thus, it was established that these electrostatic interactions are hydrogen bonds.

Declaration

I declare that no portion of the work referred to in the thesis has been submitted in support of an application for another degree or qualification of this or any other university or other institute of learning.

Copyright Statement

- i. The author of this thesis (including any appendices and/or schedules to this thesis) owns certain copyright or related rights in it (the “Copyright”) and s/he has given The University of Manchester certain rights to use such Copyright, including for administrative purposes.
- ii. Copies of this thesis, either in full or in extracts and whether in hard or electronic copy, may be made **only** in accordance with the Copyright, Designs and Patents Act 1988 (as amended) and regulations issued under it or, whether appropriate, in accordance with licensing agreements which the University has from time to time. This page must form part of any such copies made.
- iii. The ownership of certain Copyright, patents, designs, trade marks and other intellectual property (the “Intellectual Property”) and any reproductions of copyright works in the thesis, for example graphs and tables (“Reproductions”), which may be described in this thesis, may not be owned by the author and may be owned by third parties. Such Intellectual Property and Reproductions cannot and must not be made available for use without the prior written permission of the owner(s) of the relevant Intellectual Property and/or Reproductions.
- iv. Further information on the conditions under which disclosure, publication and commercialisation of this thesis, the Copyright and Intellectual Property and/or Reproductions described in it may take place is available in the University IP Policy (see <http://documents.manchester.ac.uk/DocuInfo.aspx?DocID=487>), in any relevant Thesis restriction declarations deposited in the University Library, The University Library’s regulations (see <http://www.manchester.ac.uk/library/aboutus/regulations>) and in The University’s policy on Presentation of Theses.

Dedication

To my daughter

Acknowledgements

I would like to thank Dr. Mike Croucher and Mr. Ian Cottam for their help with computational software used in the current project (both) and MATLAB programming (Mike). I would also like to thank Prof. Gill Stephens for several discussions on experimental work conducted in the current study and Prof. Paul Popelier for a copy of the MORPHY98 program. Many thanks to Prof. Roy Goodacre for his advice on microbiological and statistical aspects of the current work, and for not restraining research directions of the current project to the area of his own research. I would also like to acknowledge all members of the research group for an opportunity to discuss machine learning methods relevant for the current study.

In addition, I thank my family simply for being here.

1. Introduction

1.1 Quaternary ammonium salts and their bio-activity.

Quaternary ammonium salts are formed by quaternary ammonium cations with alkyl or aryl side chains and inorganic or organic anions. These salts have been synthesized since 1851 (Hofmann, 1851), and initially assessed for their bio-activity in 1916 by Jacobs who concluded that it was of a non-specific origin (Jacobs, 1916a; Jacobs et al., 1916). The first systematic study of a correlation between a biological activity of quaternary ammonium salts and their chemical structures was conducted by Domagk who reported on the dependence of a biological activity of these salts on alkyl side chain lengths on their cations (Domagk, 1935; Rahn and Van Eseltine, 1947). Consequently, quaternary ammonium salts were classed as surface active cationic bactericides (Resuggan, 1952). Surface active bactericides act on a bacterial cell by incorporating into a cell membrane and disrupting its integrity (Figure 1). The mechanism of a biological activity of surface active bactericides is based on two stages (Hotchkiss, 1946):

- An interaction of surface active ions with oppositely charged ions on a bacterial cell surface (a reversible process).
- An incorporation of hydrophobic groups of surface active ions into a bacterial cell membrane leading to the disruption of its integrity and the cell death (an irreversible process).

This mechanism was supported by numerous experimental studies (Lawrence, 1950; Salt and Wiseman, 1968; Gilbert and Moore, 2005; Buffet-Bataillon et al., 2012; Wessels and Ingmer, 2013a).

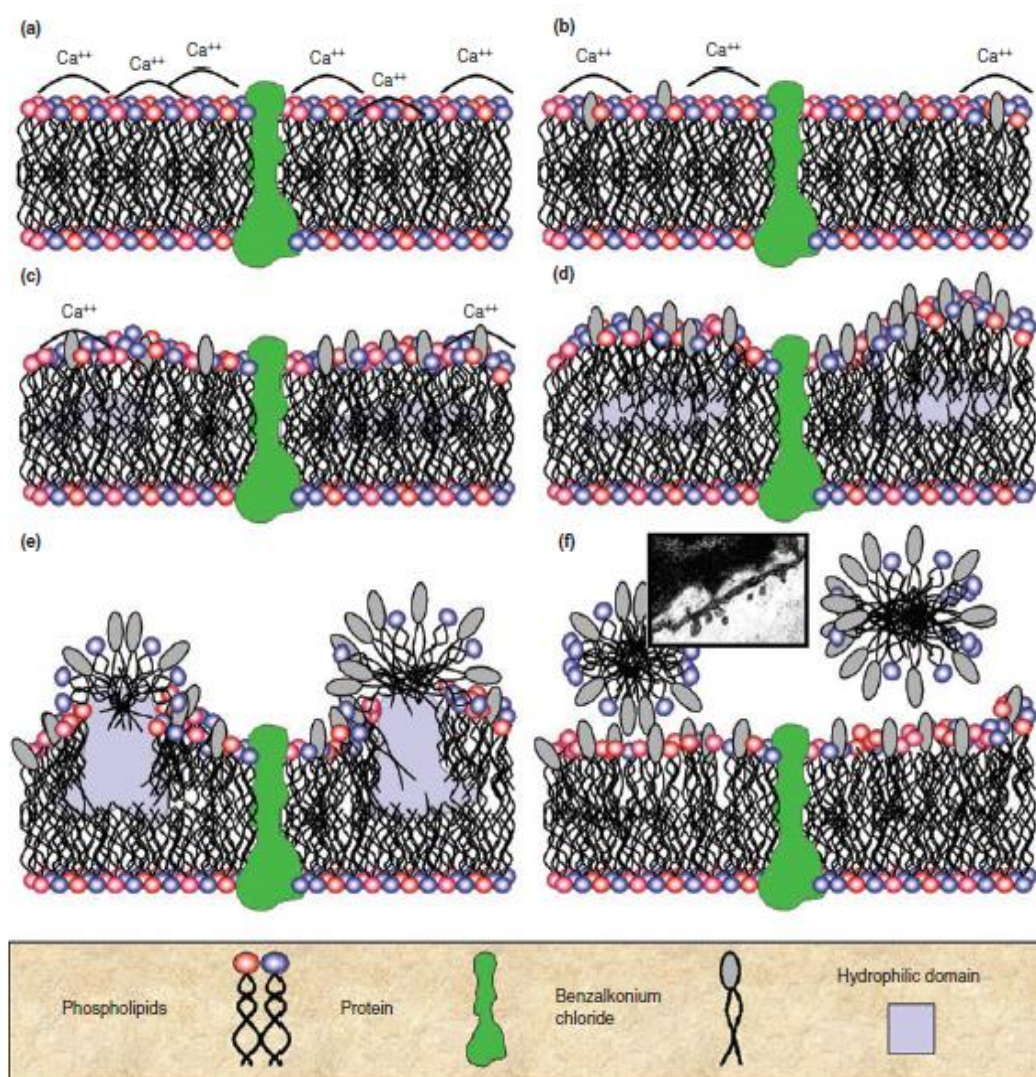


Figure 1. The mechanism of a biological action of a quaternary ammonium cation on a bacterial cell wall on an example of benzalkonium chloride: (a.) the surface of a bacterial cell; (b.) interaction of the positively charged nitrogen with phospholipids; (c.) integration of the alkyl side chain into the cell membrane; (d.- f.) the bio-action on the cell membrane leading to its loss of integrity. Reprinted with the permission from the publisher from (Gilbert and Moore, 2005). Copyright (2014) John Wiley and Sons, Inc. The Licence for this reprint is included in Appendix 1.

In the current study, theoretical origins of this two-stage mechanism of a biological activity of surface active bactericides will be explored by developing computational models relating intrinsic properties of organic quaternary ammonium salts with their biological activity.

Computational modelling of this mechanism will be performed by developing quantitative structure-activity relationships (QSARs). QSARs are computational regression models that are developed to predict a biological activity of novel chemicals based on the knowledge of the biological activity of existing chemicals modelled by their mathematical descriptors (Kubinyi, 2002). A success of a QSAR strongly depends on a descriptor's ability to preserve enough structural information about a set of chemicals so a pattern of a structure-activity correlation can be established by a regression algorithm.

Herein, quantitative structure-activity relationships will be developed with the theoretical descriptors of the intrinsic potential of mono- and di-substituted imidazolium carboxylates (Figure 2) to electrostatically interact with a bacterial cell membrane, and to partition into it from an aqueous phase will be correlated with their minimum inhibitory concentrations towards a bacterium *Escherichia coli*.

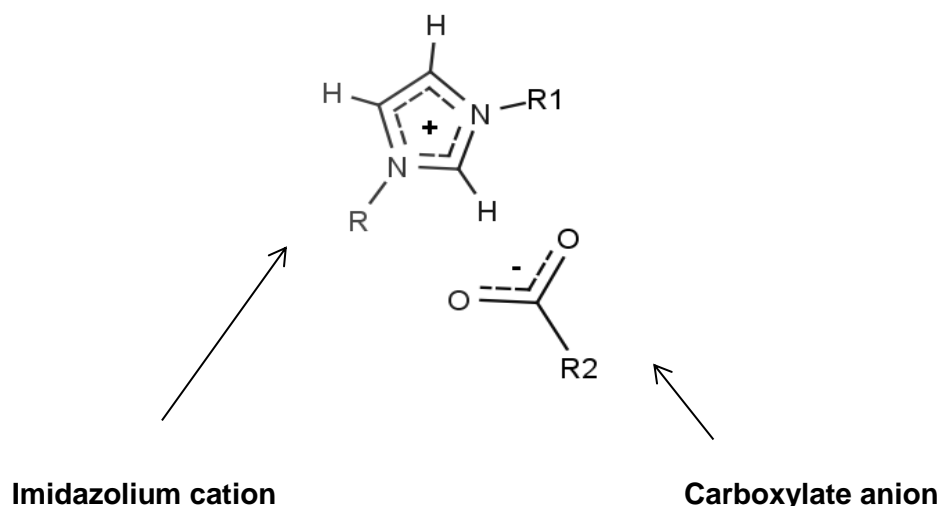


Figure 2. A graphical representation of an imidazolium carboxylate monomer (R, R1, R2 indicate the regions of structural variation of imidazolium carboxylates). The positive charge is concentrated on the central carbon atom in N – C – N bond.

1.2 Quantitative structure-activity relationships.

Quantitative structure-activity relationships (QSARs) are statistical models which correlate the structural features of chemicals with their biological activities (Kubinyi, 2002; Nikolova and Jaworska, 2004). In these relationships, chemical structures can be encoded as indices, which represent the whole chemical structure by a scalar, or as an array of scalars in which each number represents a single feature of a chemical structure. Index descriptors of chemical structures were developed prior to array descriptors due to limitations in computational power, so that QSARs could be developed with simple linear regression algorithms. With the advances in computational power, improvement in regression algorithms (Pollock, 2013), and the introduction of multivariate methods (Wold et al., 1986; Mellinger, 1987; Rajalahti and Kvalheim, 2011), chemical structures started to be encoded as arrays of scalars which allowed a more explicit representation of their structural features, and enhanced the potential of QSARs to localize the centre of a biological action within them.

Currently, both index and array type descriptors are used in QSARs alongside each other. The choice of the type of a descriptor is governed by a personal preference of the researcher, an ability of a descriptor algorithm to differentiate and encode relevant features of chemical structures and the type of a data analysis method used. All developed structure-activity relationships must be validated by an independent set of chemicals within their applicability domain. This is performed to ensure that the developed QSARs are of a sufficient quality, free of bias and lead to reliable conclusions (Golbraikh and Tropsha, 2002; Scior et al., 2009; Tropsha, 2010; Gramatica, 2013).

1.2.1 Theoretical descriptors of lipophilicity and electronic properties of imidazolium carboxylates.

The most challenging stage in the development of a QSAR model is finding an appropriate theoretical descriptor of chemical structures which can most explicitly mimic the mechanism of their biological action. In the current study, theoretical descriptors of imidazolium carboxylates must be able to mimic both stages of the two-stage mechanism of a biological activity of surface active agents reported earlier (p. 22). The first stage of the above mechanism involves electrostatic interactions of surface active functional groups of ions with oppositely charged groups on a bacterial cell surface. Hence, this stage requires theoretical descriptors of electronic properties of imidazolium carboxylates. The second stage of the mechanism is based on the ability of lipophilic functional groups of surface active ions to partition into a cell membrane. Therefore, this stage requires theoretical descriptors of lipophilicity of these salts.

The choice of descriptors of lipophilicity of imidazolium carboxylates is a straightforward process because all of these descriptors are based on the same principle, i.e. they compute the preference of a chemical structure for an aqueous or an organic phase. Hence, these descriptors differ only in their algorithms. In contrary, the choice of descriptors of electronic properties of imidazolium carboxylates is a complex process because there are numerous theoretical ways to compute these properties. Thus, they can be computed as atomic charges, orbital and total energies, electronic charge densities, polarizabilities, polarity etc. (Karelson et al., 1996). The main criteria which will govern the choice of a theoretical descriptor of electronic properties of

imidazolium carboxylates in the current study will be its ability to mimic Hammett sigma constants.

Hammett sigma constants are coefficients in the Hammett equation which relates changes in rates and outcomes of organic reactions of aromatic chemical structures with the structures and positions of substituents on their aromatic rings (Eq. 1).

$$\log K = \log K^0 + \sigma\rho \quad (\text{Eq. 1})$$

where:

K is a rate or an equilibrium constant of a substituted reactant.

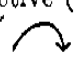
K^0 is a rate or an equilibrium constant of a parent molecule.

σ is a substituent coefficient which depends on a structure and a position of a substituent.

ρ is a reaction coefficient which depends on the type of a reaction, temperature and a dielectric constant of a reaction medium.

Hammett supported the validity of the above equation by the Electronic Theory of Organic Reactions which was an umbrella term introduced by Ingold (Ingold, 1934). This term encompassed fundamental theories of that time relating changes in a reactivity of organic chemicals to re-distribution of electronic charge within them (Lewis, 1913; Lowry, 1923; Ingold and Ingold, 1926; (Pauling and Sherman, 1933) which Ingold summarized as follows:

“The relationship between the four polar effects, their electrical classification, and their electronic mechanism, may be represented as in the following scheme: ”

ELECTRONIC MECHANISM	ELECTRICAL CLASSIFICATION	
	Polarization	Polarizability
General inductive (\rightarrow) (<i>I</i>)	Inductive	Inductomeric
Tautomeric () (<i>T</i>)	Mesomeric (<i>M</i>)	Electromeric (<i>E</i>)

(Ingold, 1934)*

*The image of the scheme is reprinted with the permission from the publisher from (Ingold, 1934). Copyright (2014) American Chemical Society. The Licence for this reprint is included in Appendix 1.

A detailed explanation of the terminology used by Ingold can be found in the original publication (Ingold, 1934).

1.2.1.1 Theoretical descriptors of lipophilicity.

A theory on the partitioning of a chemical between two immiscible solvents was developed as early as 1872 (Leo et al., 1971), and a number of computational schemes for the calculation of partition coefficients (LogP values) of chemicals between octanol and water have since been reported (Reis et al., 2013). All of these schemes are based on the computation of a ratio between the concentration of a neutral chemical structure in an organic phase and its concentration in an aqueous phase of a bi-phasic reaction system.

The first published algorithm for computation of LogP values was based on a fragment substitution approach (Fujita et al., 1964). In this approach partition coefficients of substituted aromatic chemical structures were estimated by adding various structural fragments to an unsubstituted aromatic ring for which the LogP value was experimentally determined. A number of later

algorithms are based on this approach. These algorithms are described as constructionistic computational methods (Mannhold et al., 2009), and are represented by such algorithms as CLOGP (Leo et al., 1971; Chou and Jurs, 1979) and ACD/LogP (Petrauskas and Kolovanov, 2000) which are implemented in the software of BioByte, Inc and Advanced Chemistry Development, Inc (ACD/Labs) respectively.

An alternative approach to the estimation of LogP values of chemicals is provided by reductionistic computational methods (Mannhold et al., 2009). These methods linearly regress experimental LogP values of chemicals on their chemical structures, and use the derived regression coefficients to estimate LogP values of structurally similar compounds for which experimental data are unavailable. They are represented by algorithms of Computer Automated Structure Evaluation (CASE) program (Klopman et al., 1994) and the KOWWINTM program (Meylan and Howard, 1995) which is a part of the Estimation Program Interface (EPI) Suite (US EPA, 2012).

In a contrast to the fragment based approach, several algorithms compute LogP values based on individual atoms of a chemical structure; these are implemented in programs ALOGP (Ghose and Crippen, 1986; Viswanadhan et al., 1989), Dragon (Talete srl.), XLOGP (Wang et al., 1997), SmilogP (Convard et al., 1994). Some software, such as MarvinSketch (ChemAxon) and PrologP (CompuDrug International Inc.), includes both fragment and atom based algorithms to compute LogP values.

Computation of LogP values is based on a neutral form of chemical structure because the bi-phasic partitioning potential of a chemical is assumed to be pH independent. Thus, it is believed that a neutral form of a chemical

structure partitions between aqueous and organic phases exclusively due to the influence of lipophilic or hydrophilic fragments within it. The pH independent view on the bi-phasic partitioning of chemicals significantly constrains a reaction system because it ignores any solute-solvent and solute-solute interactions which will inevitably occur. Consequently, LogP values are only estimates of a true state of a bi-phasic partitioning of a neutral chemical specie.

Imidazolium carboxylates are formed by positively charged cations and negatively charged anions. Hence, their bi-phasic partitioning behaviour will be significantly affected by solute-solvent and solute-solute interactions. Hence, modified LogP algorithms which account for the ionized forms of chemical structures and compute their pH dependent bi-phasic partitioning potential (LogD values) which will give a more realistic view on the behaviour of an ionized chemical specie in a bi-phasic system are required (Eq. 2).

$$\text{LogD} = \text{Log} \left(\frac{C_{ioct} \times C_{oct}}{C_{iw} \times C_w} \right) \quad (\text{Eq. 2})$$

where:

C_{ioct} is the concentration of an ionized form of a chemical structure in octanol at a defined pH.

C_{oct} is the concentration of a neutral form of a chemical structure in octanol at a defined pH.

C_{iw} is the concentration of an ionized form of a chemical structure in water at a defined pH.

C_w is the concentration of a neutral form of a chemical structure in water at a defined pH.

These coefficients can be computed by such computational methods as an algorithm of the ACD/LogD module of ACD/Percepta Platform (Advanced Chemistry Development, Inc.) and an algorithm of Csizmadia and colleagues (Csizmadia et al., 1997) which is implemented in the program PrologD (CompuDrug International Inc.) and in the Calculator Plugins module of a MarvinSketch program (ChemAxon).

Experimental determination of LogD values for ionisable compounds is challenging because the structural identity of these species between the two phases is rarely preserved due to various degrees of solvent-solute and solute-solute interactions in water and octanol. Thus, to the author's knowledge, LogD values for the imidazolium carboxylates utilized in the current study, have not yet been reported. Hence, these values will be estimated using the algorithm implemented in the ChemAxon software. The algorithm of Csizmadia and colleagues (Csizmadia et al., 1997) estimates LogD values by computation of microspecies of a chemical present in octanol and water phases at a defined pH, where the term *microspecies* refers to all possible ionized forms of a chemical structure.

1.2.1.2 Theoretical descriptors of Hammett sigma constants.

Hammett sigma constants are experimentally derived values. This fact limits their availability to a finite set of aromatic chemical structures for which these constants exist. Numerous computational efforts have been made to overcome this limitation by correlating Hammett sigma constants with quantifiable electronic parameters of chemical structures in an attempt to find their electrostatic analogue. Reported linear correlations between the electronic analogues and Hammett sigma constants were based on semi-empirical (Gilliom et al., 1985; Ertl, 1997; Monaco and Gardiner, 1995) and ab initio atomic charges (Kochetova and Klyuev, 2008), the strength of an aromatic π -conjugation (Fernandez and Frenking, 2006), ab initio electronic charge density (Jaffé, 1952); (O'Brien and Popelier, 2001) and molecular orbital energies combined with topological indices (Sullivan et al., 2000) or partial atomic charges (Genix et al., 1996).

The first attempt to correlate sigma Hammett constants with ab initio electronic charge densities of aromatic chemical structures was made by Jaffé who tested the hypothesis that:

“... the change of the electron densities in the *meta* and *para* position of benzene upon monosubstitution should be related to Hammett's σ -values through a single proportionality factor.”

(Jaffé, 1952)

Thus, the electronic charge densities of a benzene ring in meta- or para-substituted benzene derivatives were calculated using the Linear Combination of Atomic Orbitals Molecular Orbital method, and correlated with Hammett sigma constants of meta- and para- substituents on a benzene ring using a simple linear regression. Based on the calculations, Jaffé concluded

that Hammett sigma constants are monotonically dependent on the ab initio electronic charge density of a benzene ring in mono-substituted benzene derivatives. However, he stressed that at that time:

“An absolute calculation of σ -values is impossible, since the electron densities are very sensitive to the choice of the parameters (α and γ) required for numerical calculations by the MO method, and no good method for the determination of these parameters exists.”

(Jaffé, 1952)*

*The parameters α and γ in the above quotation refer to Coulomb and resonance integrals respectively. The Licence for both excerpts is provided in Appendix 1.

More than five decades later another study reported a successful correlation of Hammett sigma constants of mono- and di-substituted phenols, toluenes and bromophenethylamines with the functions of their ab initio electronic charge densities (Smith and Popelier, 2005). This approach was based on the theory of Atoms in Molecules (Bader, 1990; Popelier, 2000; Matta and Boyd, 2007) which introduced the topological analysis of scalar fields used in Linear Algebra into the research of electronic properties of chemical structures.

1.2.1.2.1 The theory of Atoms in Molecules.

The theory of Atoms in Molecules is an interpretative theory that analyses electronic charge density of a chemical structure, and partitions it into a continuous set of topological atoms (Bader et al., 1971). These atoms are finite topological volumes of the electronic charge around each nucleus (Bader et al., 1987). The boundaries of each topological atom are determined by the size and the distribution of its electronic charge cloud in that direction. A shared boundary between two interacting topological atoms is called an inter-atomic surface (Bader and Essen, 1984). Each inter-atomic surface has an equilibrium point at which its electronic charge density is at its maximum compared to the other points. The mathematical term for this point is a saddle critical point (SCP), where the word *saddle* underlines the topological instability of this point due to the directional dependency of the values of its electronic charge density. However, Bader referred to this point as a bond critical point (BCP) (Bader, 2010), where the word *bond* stresses that this point is found between two interacting topological atoms (Figure 3). The BCP is a starting point for a topological trajectory which runs in the direction perpendicular to the inter-atomic surface, and connects the nuclei of two interacting topological atoms. This trajectory is called an atomic interaction line (AIL) (Bader, 2009), and the electronic charge density at the BCP in the direction of the AIL is at its minimum compared to the other points.

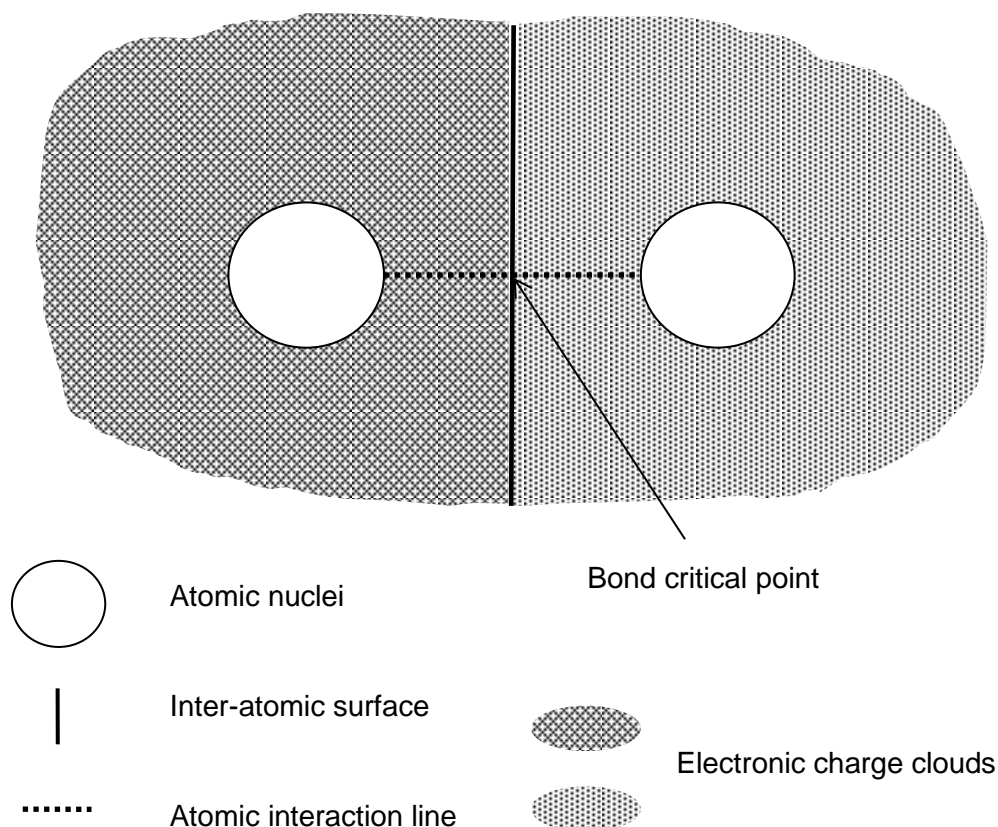


Figure 3. A graphical representation of an inter-atomic surface, an atomic interaction line and a bond critical point as defined in the theory of Atoms in Molecules.

1.2.1.2.2 Quantum topological molecular similarity descriptors

Smith and Popelier computed three functions of the electronic charge density at bond critical points of mono- and di-substituted phenols, toluenes and bromophenethylamines whose geometry was optimized at HF level of the electronic structure theory (Smith and Popelier, 2005). These functions were the Laplacian of the electronic charge density (Bader et al., 1984), its ellipticity (Bader et al., 1983) and kinetic energy density (Bader and Preston, 1969). A detailed discussion on each of these functions will be presented in the Results and Discussions section of the current thesis.

The values of the above functions of electronic charge density together with the values of electronic charge density themselves, were collectively named as quantum topological molecular similarity descriptors (QTMS) (O'Brien and Popelier, 2001). These descriptors were successfully regressed on the Hammett sigma constants using partial least squares (PLS) regression, PLS combined with a principal component analysis (PCA/PLS) or a genetic algorithm feature selection methods. The workflow reported by O'Brien and Popelier for regression models based on QTMS descriptors is summarized in the Figure 4.

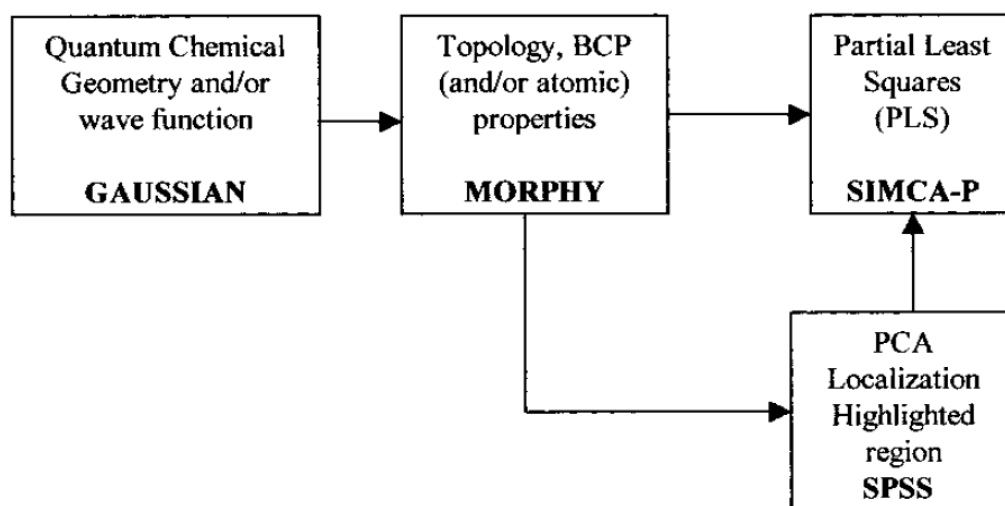


Figure 4. The workflow of a regression analysis based on QTMS descriptors. The bold text represents software used by the authors. Reprinted with permission from the publisher from (O'Brien and Popelier, 2001). Copyright 2014 American Chemical Society. The Licence for this reprint is included in Appendix 1.

The above workflow will be used in the current study for generation of QSARs for imidazolium carboxylates based on the QTMS descriptors. In addition, a multiple linear regression will be performed on the data after the principal component analysis (PCA/MLR).

1.3 Toxicological data for imidazolium carboxylates.

Quantitative structure-activity relationships require the presence of both theoretical descriptors of chemical structures and their toxicological data. Hence, the choice of quaternary ammonium salts for which QSARs can be developed depends on the availability of their experimental toxicological data. In the current study, a set of organic quaternary ammonium salts, i.e. 1-alkyl-, 1-alkoxymethylimidazolium L-lactates, will be used as a basis for regression models (Figure 5, Table 1) (Pernak et al., 2004). However, due to the small size of this dataset, toxicological data for a set of 1-ethyl-, 1-butyl-3-methylimidazolium carboxylates will be experimentally generated in the current study and included in QSARs.

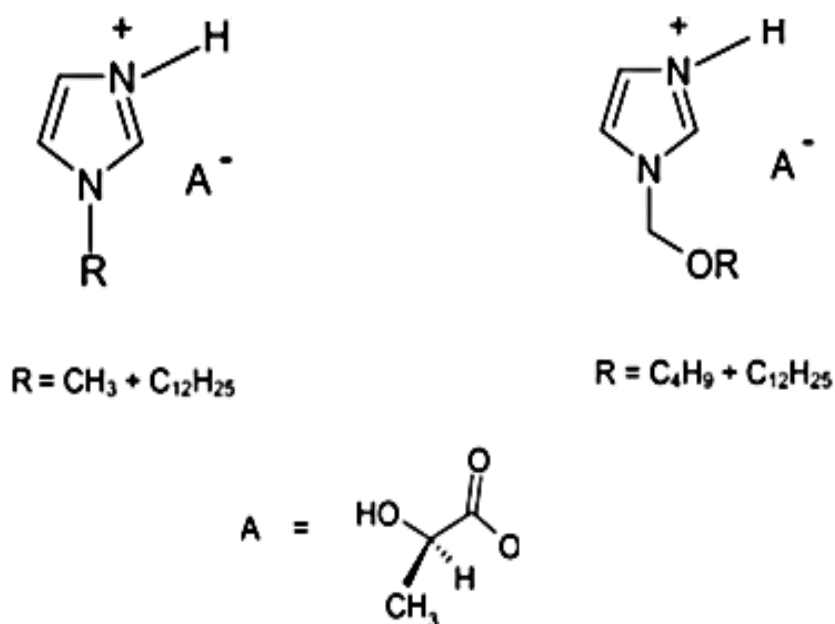


Figure 5. Chemical structures of 1-alkyl, 1-alkoxymethylimidazolium lactates from the dataset of Pernak and colleagues (Pernak et al., 2004). Reproduced in part from Pernak et al., 2004 with the permission of the Royal Society of Chemistry (RSC). The Licence for this reprint is included in Appendix 1.

Table 1. Minimum inhibitory concentrations of 1-alkyl-,
1-alkoxymethylimidazolium lactates towards *Escherichia coli*. Reproduced in part
from Pernak et al., 2004 with the permission of The Royal Society of Chemistry
(RSC). The Licence for this reprint is included in Appendix 1.

Quaternary ammonium salt	[]*	Minimum inhibitory concentration (μ M)
1-[]-imidazolium L-lactates		
3a	CH ₃	>5814
3b	C ₂ H ₅	>5814
3c	C ₃ H ₇	>5814
3d	C ₄ H ₉	>5814
3e	C ₅ H ₁₁	>5814
3f	C ₆ H ₁₃	2066
3g	C ₇ H ₁₅	977
3h	C ₈ H ₁₇	463
3i	C ₉ H ₁₉	220
3j	C ₁₀ H ₂₁	105
3k	C ₁₁ H ₂₃	50
3l	C ₁₂ H ₂₅	48
1-[]-methylimidazolium L-lactates		
4a	OC ₄ H ₉	4098
4b	OC ₅ H ₁₁	1938
4c	OC ₆ H ₁₃	919
4d	OC ₇ H ₁₅	437
4e	OC ₈ H ₁₇	208
4f	OC ₉ H ₁₉	199
4g	OC ₁₀ H ₂₁	95
4h	OC ₁₁ H ₂₃	183
4i	OC ₁₂ H ₂₅	88

* The symbol [] refers to a side chain on the imidazolium ring.

1.3.1 Agar diffusion test - the evaluation of a research hypothesis.

1.3.1.1 A research hypothesis

In 2009, a research hypothesis stating that the agar diffusion test (ADT) could be used for the toxicological classification of ionic liquids (Seddon, 1997) was published (Rebros et al., 2009). The authors supported the proposed novel application of ADT by a partial correlation between qualitative toxicological classification of quaternary ammonium ionic liquids in the ADT with their half maximal effective concentrations (EC_{50}) towards *Clostridium Butyricum* in a liquid medium. Thus, it was reported that:

“... the absence of an inhibition zone in the Agar Diffusion test provides a reliable indication that the ionic liquids are sufficiently biocompatible to merit further investigation for use as green solvents. Conversely, the ionic liquids which do produce an inhibition zone are toxic enough to be rejected from further study.”

(Rebros et al., 2009)*

*The licence for the above excerpt is provided in the Appendix 1.

Three years later, another study reported on a partial correlation between qualitative classification of the toxicity of quaternary ammonium ionic liquids towards *Escherichia coli* in ADT with their toxicological data from a liquid medium (Wood et al., 2011). However, in a contrast to the earlier reported publication (Rebros et al., 2009), toxicological data for the ionic liquids from a liquid medium test was reported as the growth rate present of a control sample of *Escherichia coli* and not as EC_{50} values. The toxicological screening was conducted in an automated incubator-plate reader Bioscreen C (Thermo Fisher Scientific Corporation, Basingstoke, UK).

In the current study, the toxicological screening of 1-ethyl-, 1-butyl-3-methylimidazolium carboxylates, all of which are ionic liquids, will also be conducted in a Bioscreen C plate reader (Thermo Fisher Scientific Corporation, Basingstoke, UK) with the same strain of *Escherichia coli* (K-12 MG1655) as utilized in the study of Wood and colleagues (Wood et al., 2011). Therefore, experimental work conducted herein will be marginally extended to encompass the toxicological classification of 1-ethyl-, 1-butyl-3-methylimidazolium carboxylates using the agar diffusion test, so that the validity of the proposed by Rebros and colleagues research hypothesis (Rebros et al., 2009) for the above ionic liquids could be assessed.

1.3.1.2 Agar diffusion test.

The agar diffusion test (ADT) is a toxicological screening method which was designed to evaluate a progressive adaptation of a micro-organism to a defined concentration of an antibiotic (Bauer et al., 1966). It is performed on an agar based bacterial growth medium which is a solid at temperatures below 85 °C. In its originally published form, the ADT is performed by streaking a bacterial culture in its steady-state onto the surface of an agar with a cotton swab, and pressing down filter paper discs saturated with an antibiotic on the top of the bacterial culture prior to its incubation. The adaptation of a microorganism towards an antibiotic is assessed by comparing the density of its growth around the filter paper disks with that of a control micro-organism (Figure 6).

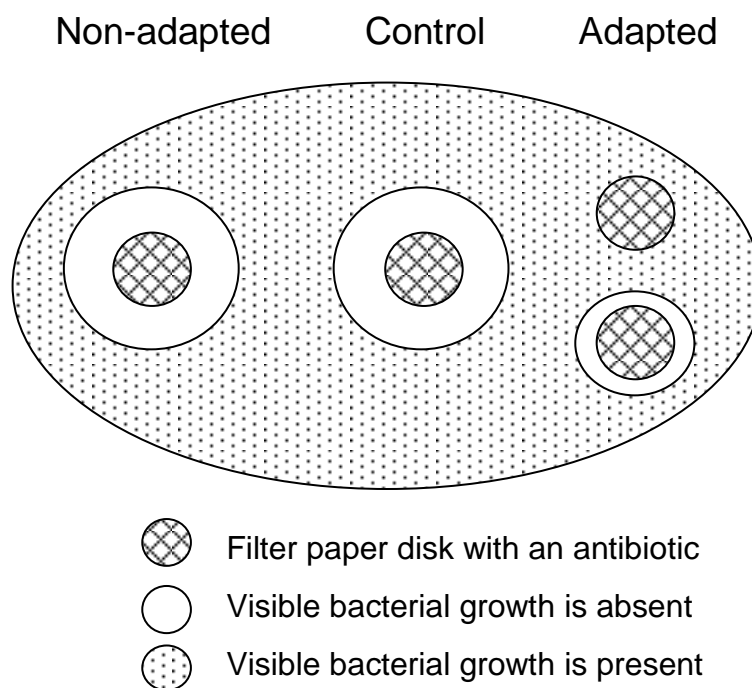


Figure 6. The observation of an adaptation of a micro-organism towards an antibiotic in the agar diffusion test.

1.4 The nature of C–H···O electrostatic interactions in

1-ethyl-3-methylimidazolium acetate.

All of the imidazolium carboxylates utilized in the current study are ionic liquids formed by mono- or di-substituted imidazolium cations and carboxylate anions that are held together by electrostatic C–H···O interactions. The exact nature of these interactions in imidazolium based ionic liquids is still an open area of research (Kempter and Kirchner, 2010). It was reported earlier (p. 22) that the first stage of the two-stage mechanism of a biological activity of surface active bactericides is based on electrostatic interactions between their charged functional groups with the oppositely charged functional groups on a bacterial cell surface. Hence, imidazolium cations can potentially interact with carboxylate groups present on a bacterial cell surface (Metzler, 1977).

It was reported earlier (p. 36) that the electronic properties of imidazolium carboxylates for the development of QSARs in the current study will be computed by the QTMS descriptors which are based on principles of the theory of Atoms in Molecules. In 1995, a set of criteria which described C – H – – O hydrogen bonds in the context of this theory was published (Koch and Popelier, 1995). Therefore, the computational work of the current study will be extended to theoretically evaluate the nature of C – H – – O interactions in imidazolium carboxylates. The evaluation will be conducted on the structure of 1-ethyl-3-methylimidazolium acetate because the morphology of inter-ionic interactions in this ionic liquid, and their effect on its physical properties have been extensively studied (Kiefer et al., 2008; Dhumal et al., 2009; Bowron et al., 2010; Almeida et al., 2012; Brehm et al., 2012; Shi et al., 2012; Clough et al., 2013; Chen et al., 2014).

1.4.1 The nature of a hydrogen bond.

There are many various definitions of an interaction which should be defined as a hydrogen bond (Pauling, 1938; Koch and Popelier, 1995; Henschman and Irudayam, 2010; Desiraju, 2011), and the unification of this definition has been a subject of debate for many years. In 2011, the International Union of Pure and Applied Chemistry (IUPAC) accepted the following unified definition of a hydrogen bond:

“The hydrogen bond is an attractive interaction between a hydrogen atom from a molecule or a molecular fragment X–H in which X is more electronegative than H, and an atom or a group of atoms in the same or a different molecule, in which there is evidence of bond

formation...The evidence for hydrogen bond formation may be experimental or theoretical, or ideally, a combination of both.”

(Arunan et al., 2011a; Arunan et al., 2011b)

The above definition is quite broad and allows to investigate the presence of a hydrogen bond using a number of experimental and theoretical approaches. For example, the presence of a hydrogen bond can be assessed by IR, Raman (Badger and Bayer, 1937; Murthy and Rao, 1968; Grabowski, 2006) which look for the changes in the vibrational, rotational and stretching frequencies of the chemical bonds, NMR spectroscopy and conductivity measurements (Avent et al., 1994) which look for the proton chemical shifts and the presence of a cooperativity of a chemical network respectively, crystallography (Jeffrey and Lewis, 1978; Steiner, 2003; Jeffrey, 2003) which evaluates the changes in the electronic charge density distribution, pKa measurements (Gill et al., 2009) which can be used to estimate the strength of a hydrogen bond, and theoretical methods which computationally assess the presence of hydrogen bonds via the analysis of the electronic charge density (Koch and Popelier, 1995) or a potential energy surface of a chemical network of atoms (Henchman and Irudayam, 2010). The IUPAC definition of a hydrogen bond does not restrict it to a particular set of geometrical and energy cut-off parameters which are at present required for differentiation between bonded and non-bonded states of a chemical network of atoms. However, attempts to overcome this limitation have been made (Henchman and Irudayam, 2010).

Inter-ionic C – H – –O electrostatic interactions in 1-ethyl-3-methylimidazolium acetate have been previously investigated by Dhumal and colleagues using a combination of density functional theory, IR and Raman spectroscopy and

natural bond orbital and partial topological analysis (Dhumal et al., 2009) and by Bowron and colleagues using a combination of molecular dynamics and neutron diffraction (Bowron et al, 2010). Both studies established the presence of identifiable C–H–O inter-ionic interactions, and agreed that the most energetically stable inter-ionic interaction is formed when the acetate anion approaches the imidazolium ring from its N–C–N side.

In the current study, the nature of C–H–O electrostatic interactions on the N–C–N side of the imidazolium cation in 1-ethyl-3-methylimidazolium acetate will be explored via the topological assessment of its inter-ionic region using the theory of Atoms in Molecules and a set of criteria for the C–H–O hydrogen bonds (Koch and Popelier, 1995). This approach was chosen for the current study because the theory of Atoms in Molecules was utilized to generate the QTMS descriptors of imidazolium carboxylates in the current study. Therefore, the topological investigation of the C–H–O interactions in 1-ethyl-3-methylimidazolium acetate will provide an additional insight on the topology of the electronic charge density in the inter-ionic region of these salts.

These topological criteria are:

1. The presence of a bond critical point and an atomic interaction line between the hydrogen and oxygen atoms.
2. The electronic charge density at the bond critical point must be within the range of 0.002 – 0.034 au.
3. The Laplacian of the electronic charge density at the bond critical point must be within the range of 0.024 - 0.139 au.

4. The radii of the hydrogen atom and the oxygen atom involved in $C-H \cdots O$ interaction must be shorter than their radii in the absence of this interaction.
5. The electronic charge on the hydrogen atom involved in $C-H \cdots O$ interaction must be less than its electronic charge in the absence of the oxygen atom.
6. The total atomic energy of the hydrogen atom involved in $C-H \cdots O$ interaction must be smaller than its total atomic energy in the absence of the oxygen atom.
7. The dipolar polarization of the hydrogen atom involved in $C-H \cdots O$ interaction must decrease compared to its dipolar polarization in the absence of the oxygen atom.
8. The topological volume of the hydrogen atom involved in $C-H \cdots O$ interaction must be smaller than its topological volume in the absence of the oxygen atom.

1.5 A summary of the research objectives.

The work which will be conducted in the current study is integrated but it can be summarized in three parts according to the type of work which will be undertaken. These parts and their research objectives are detailed below:

Experimental part:

1. To determine minimum inhibitory concentrations of 1-ethyl, 1-butyl-3-methylimidazolium carboxylates towards *Escherichia coli* in a liquid medium.
2. To evaluate the validity of the research hypothesis on the applicability of agar diffusion test for toxicological classification of ionic liquids.

Computational and theoretical part:

1. To generate two and three dimensional structures of 1-alkyl-, 1-alkoxymethylimidazolium L-lactates and 1-ethyl-, 1-butyl-3-methylimidazolium carboxylates.
2. To compute distribution coefficients (LogD values) and descriptors of electronic properties (QTMS descriptors) of the imidazolium carboxylates.
3. To establish the nature of C – H – – O electrostatic interactions in 1-ethyl-3-methylimidazolium acetate.

Statistical part:

1. To develop quantitative structure-activity relationships for imidazolium carboxylates.

2. Materials and methods

2.1 Minimum inhibitory concentrations of 1-ethyl-, 1-butyl-3-methylimidazolium carboxylates towards *Escherichia coli* in a liquid medium.

Aseptic conditions were maintained during all microbiological work described in the current chapter. Equipment and materials were either purchased already sterile or steam sterilized locally at a temperature of 121 °C for min. The analytical balance was calibrated to the accuracy of four decimal places before each experiment with a 50.0000 g control weight. The toxicity of 1-ethyl-, 1-butyl-3-methylimidazolium carboxylates was evaluated in a liquid medium in an automated incubator-plate reader Bioscreen C (Thermo Fisher Scientific Corporation, Basingstoke, UK). The instrument can control the incubation temperature, the frequency of the plates shaking during incubation phase and the wavelength during the measurements of turbidity of samples. It also equipped with software which automatically generates bacterial growth curves based on the turbidity data.

2.1.1 Propagation of *Escherichia coli*.

Luria Broth with Miller modification (LB-Mm) was prepared as follows:

Tryptone (Formedium, Batch 07/MFM/498)	10 g
Yeast extract powder (Formedium, Batch 07/MFM/428)	5 g
NaCl (Sigma-Aldrich, Batch 0751508)	10 g
Deionized water	up to 1 L

A magnetic stirrer was used to mix the components. The broth pH was adjusted to 7 at $19 \pm 2^\circ\text{C}$ with 1 M NaOH before autoclaving. The pH of the sterilized broth was re-measured at 37°C (pH test strips; Sigma-Aldrich, pH range 1-14) to confirm that the initial pH did not change at the experimental temperature. This measurement at 37°C pH was within the pH 7 test strip indicator range for all experiments. The sterilized broth (50 mL) was transferred in glass Erlenmeyer flasks (cotton wool plug), and used for bacterial incubation within 2 h from the preparation.

LB-Mm agar was prepared as described above with an addition of 15 g of agar (Sigma-Aldrich, Batch 18211) to the initial broth recipe before the sterilization. Warm LB-Mm agar (20 mL) was poured into Petri dishes and left to cool. The prepared dishes were sealed with PARAFILM® M and stored at -4°C in an inverted position for up to 10 d.

The dormant culture of *Escherichia coli* K-12, MG1655 was obtained from Prof. Gill Stephens (The University of Nottingham, UK) in a cryogenic vial (-80°C , LB-Mm with 15% v/v of glycerol). The micro-organism was re-activated by incubating on LB-Mm agar (20 mL, inverted Petri dish; 24 h., 37°C). Once active, an individually growing colony was transferred in a glass Erlenmeyer flask (cotton wool plug, 80% free head space) with freshly prepared LB-Mm (50 mL, 37°C , pH 7.0), and cultivated for 24 h at 37°C in a Ceromat BS-1 incubator with shaking at 200 rpm. Then, the culture was streaked on LB-Mm agar and incubated further (20 mL, inverted Petri dish; 24 h, 37°C).

Five single colonies were transferred from the LB-Mm agar into cryogenic vials (LB-Mm with 15% v/v of glycerol) to be kept at -80°C as a parent culture

stock. At the same time, the sixth colony was cultivated further in LB-Mm and then into LB-Mm agar as described above to obtain a working stock culture for on-going experiments. The working stock culture on LB-Mm agar was sealed with PARAFILM® M and stored at -4 °C in an inverted position for up to 4 w. Then, it was replaced by the re-activation of a parent stock culture as described above.

2.1.2 Preparation of a range of concentrations of 1-ethyl-, 1-butyl-3-methylimidazolium carboxylates.

Several drops of each imidazolium carboxylate obtained from Prof. Gill Stephens (The University of Nottingham, UK) were dispensed into pre-weighed 2 mL Eppendorf® Safe-Lock microcentrifuge tubes (Sigma-Aldrich). These tubes were weighed again, and the mass of the ionic liquids was calculated (Eq. 3).

$$M_{IL} = M_2 - M_1 \quad (\text{Eq. 3})$$

where:

M_{IL} is the mass of an ionic liquid in a tube (g)

M_1 is the mass of an empty labelled tube (g)

M_2 is the mass of the tube with an ionic liquid (g)

The volume of deionized water (pH 7) required for a dilution of the stock ionic liquids to a 1 M concentration was calculated (Eq. 4), and added into the vials.

$$V_{IL} = \frac{C \times W}{M} \quad (\text{Eq. 4})$$

where:

V_{IL} is a volume of deionized water (L)

C is a required concentration of an ionic liquid (mol/L)

W is the molecular weight of an ionic liquid (g/mol)

M is the mass of an ionic liquid in a vial (g)

The obtained 1 M liquids were diluted further to give a range of aqueous concentrations of ionic liquids (Figure 7, Eq. 5).

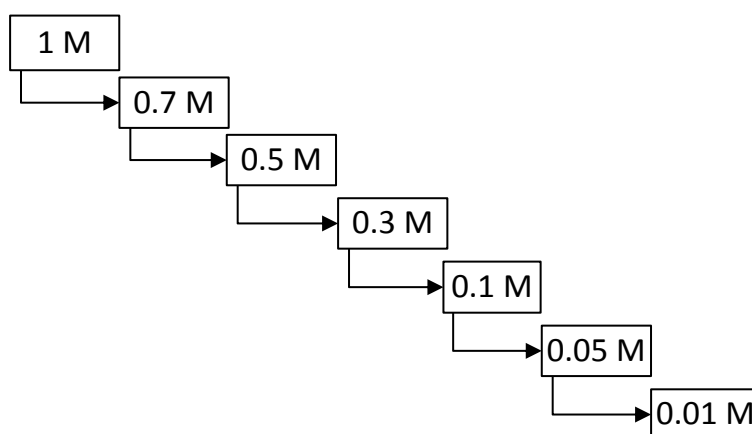


Figure 7. The concentrations of imidazolium carboxylates which were used for toxicological screening of *Escherichia coli*.

$$V_{water} = \frac{C_d \times V_d}{C_s} \quad (\text{Eq. 5})$$

where:

V_{water} is a volume of deionized water required for a serial dilution (L)

C_d is a required lower concentration of an ionic liquid (M)

V_d is a required volume of an ionic liquid of the lower concentration (L)

C_s is a concentration of the stock solution (M)

Stock imidazolium carboxylates were used without prior sterilization as they had been reported to be self-sterile (Rebros et al., 2009). They were stored at a room temperature of $19 \pm 2^\circ\text{C}$ between the experiments. All of the diluted imidazolium carboxylates were stored at -4°C , and vortexed for 1 min before use to eliminate any phase separation between water and ionic liquids.

2.1.3 The workflow of toxicological screening in a liquid medium.

A single colony of *Escherichia coli* was transferred from the LB-Mm agar stock Petri dish into LB-Mm and incubated as described earlier (p. 48). Then, 1 mL of the incubated culture was dispensed into a glass Erlenmeyer flask with 100 mL of fresh LB-Mm and mixed for 1 min. Afterwards, 180 μL of the bacterial broth were pipetted into each of 100 wells of a Bioscreen C honeycomb plate, and followed by the addition of 20 μL of imidazolium carboxylates of various concentrations. Every concentration of an IL was tested in a triplicate, and triplicate control wells containing the *Escherichia*

coli broth with added 20 μL of sterile distilled water were included on each plate.

Minimal inhibitory concentrations (MICs) of imidazolium carboxylates towards *Escherichia coli* were determined from the 16 h bacterial growth curves at 37 °C temperature in an automated incubator-plate reader Bioscreen C (Labsystems, Basingstoke, UK). Optical density measurements at 600 nm (OD_{600}) were automatically taken every 5 min, and the shaking of the plates was performed for 1 min before and after each measurement. On-line data collection and processing was performed by Research Express software (Transgalactic Ltd., Finland, version 1.05). The maximum specific growth rates (MSGRs) were calculated from the exponential part of a growth curve (Figure 8, Eq. 6).

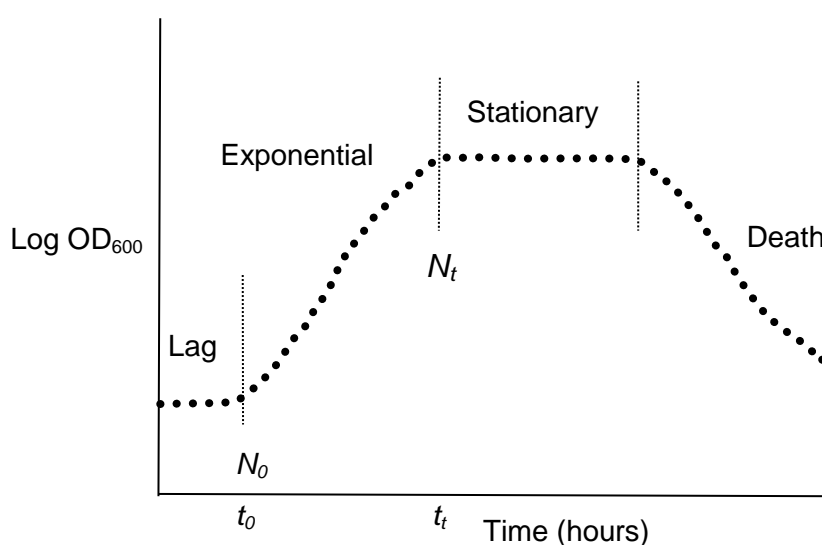


Figure 8. Stages of a bacterial growth which can be quantitatively observed in a liquid medium.

$$\mu = \frac{\ln(N_t) - \ln(N_0)}{t_t - t_0} \quad (\text{Eq. 6})$$

where:

μ is a maximum specific growth rate.

N_0 is OD₆₀₀ at time t_0 hours, where t_0 is time at the start of the exponential part of a bacterial growth curve.

N_t is OD₆₀₀ at time t_t hours, where t_t is time at the end of the exponential part of a bacterial growth curve.

MICs of imidazolium carboxylates towards *Escherichia coli* were found by comparing the MSGRs of the microorganism in the presence of the ionic liquids with the growth rates of the *Escherichia coli* control on the same honeycomb plate (Eq. 7).

$$G_{rpct} = \frac{G_s}{G_c} \times 100\% \quad (\text{Eq. 7})$$

where:

G_{rpct} is the maximum specific growth rate of *Escherichia coli* in the presence of an ionic liquid as a percentage of the MSGR of the control microorganism.

G_s is the average of three MSGRs of *Escherichia coli* in the presence of an ionic liquid (h^{-1}).

G_c is the average of three MSGRs of the *Escherichia coli* controls (h^{-1}).

2.2 Agar Diffusion Test.

A single colony of *Escherichia coli* from a working-stock Petri dish was incubated in LB-Mm as described earlier (p. 48). Once cultivated, 100 μ L of the bacterial broth were dispensed onto LB-Mm agar using an automatic single channel pipette, and evenly spread on the agar surface. Customized filter paper disks (Whatman 3mm thickness, 7mm diameter) were transferred into Eppendorf vials with undiluted ionic liquids (15 μ L). Three disks were placed in the same vial. The vials were closed and left to stand for 30 min at 19 \pm 2 $^{\circ}$ C temperature. Then, the filter paper disks were placed directly onto the pre-prepared bacterial LB-Mm agar using a novel two-needle transfer approach (Figure 9). Once disks were in place, the Petri dishes were closed, inverted and placed in an incubator set at 37 $^{\circ}$ C temperature for 12 h. Each ionic liquid was tested in a triplicate in the presence of a control disk containing distilled water.

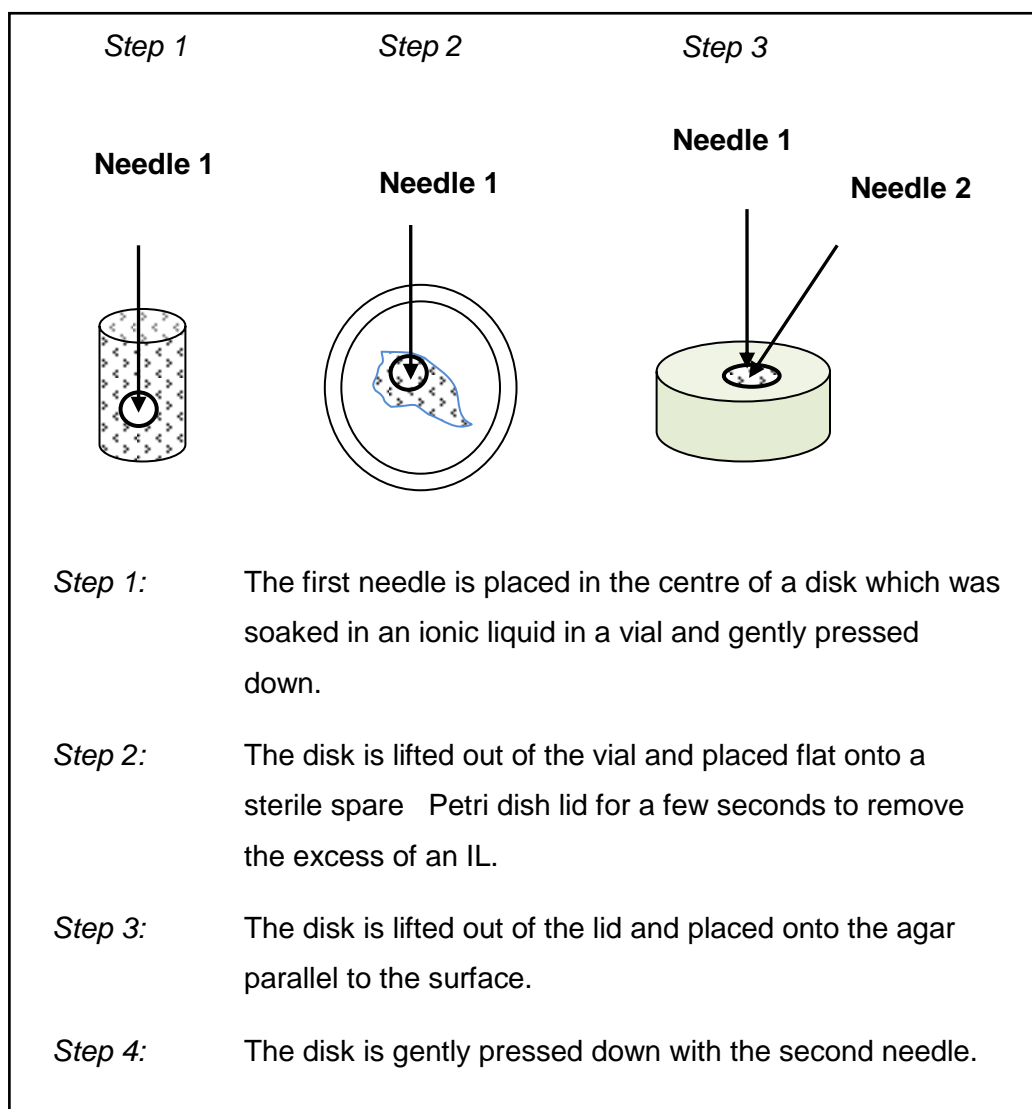


Figure 9. Four stages of the transfer of a filter paper disk from a vial on an agar surface.

The biocompatibility of 1-ethyl, 1-butyl-3-methylimidazolium carboxylates towards *E. coli* was assessed qualitatively. Thus, Petri dishes with the incubated bacteria were placed on a light box, and assessed for the absence of a visible bacterial population around the disks. If such zones were observed the ionic liquids were classed as growth inhibiting, otherwise they were classed as biocompatible.

The mass of an IL on each disk was estimated as follows (Eq. 8):

$$M_{id} = \frac{(M_3 - M_4) - (M_2 - M_1)}{3} \quad (\text{Eq. 8})$$

where:

M_{id} is the mass of an ionic liquid on a filter paper disk

M_1 is the mass of an empty labelled vial

M_2 is the mass of the vial with three filter paper disks

M_3 is the mass of the vial with three disks and 15 μL of an ionic liquid

M_4 is the mass of the vial after three disks soaked with an ionic liquid

were removed

2.2.1 Agar well test.

The agar well test is a modified version of the agar diffusion test in which the cellulose filter paper disks are replaced with the indentations on the agar surface. The version described herein was developed in the current study.

This modification of the agar diffusion test was made, so that the initial concentrations of ionic liquids in a contact with *Escherichia coli* on the agar based medium could be estimated, and compared with their minimum inhibitory concentrations in a liquid medium. Thus, pocket shape indentations were melted on LB-Mm agar surface with a metal rod which was dipped in 70% ethanol and flamed for 30 s. Once heated, the rod was gently pressed

down into the agar with a circular motion until a pocket shape indentation as melted (Figure 10).

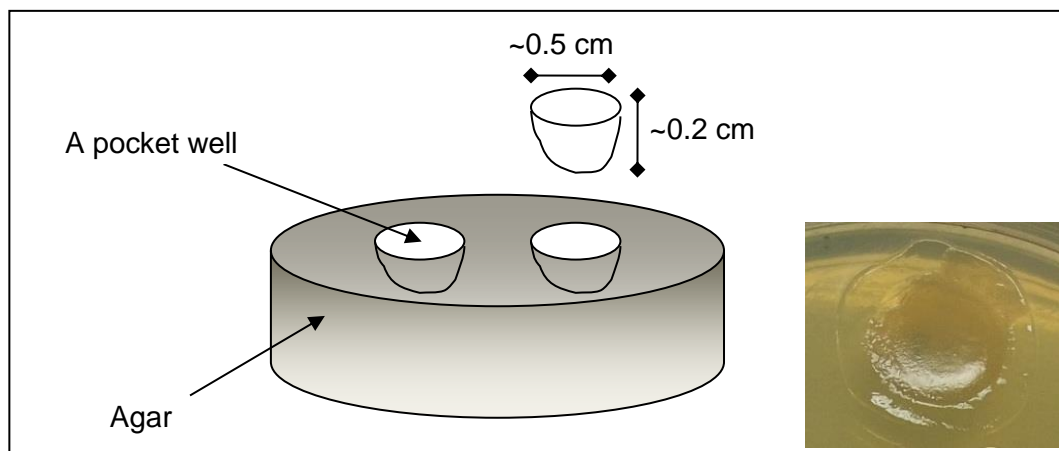


Figure 10. A pocket well in the Agar Well Test. Dimensions are approximate. Inset: The photograph of a typical well made using this approach.

A single drop of an imidazolium carboxylate was obtained by touching the surface of the stock ionic liquid with a warm, sealed narrow end of a glass Pasteur pipette (Figure 11). A single pipette was used for the transfer of three drops of the same IL and then discarded.

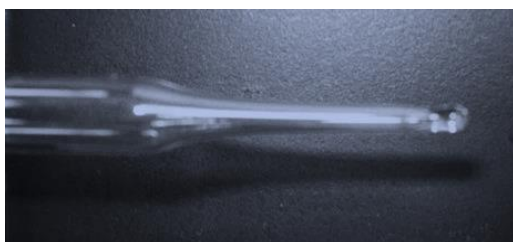


Figure 11. A sealed end of a glass Pasteur pipette.

The drop was added into the wells and followed by 5 μL of the bacterial broth which was prepared as described earlier (p. 47). The Petri dishes were closed and placed in an incubator set at 37 $^{\circ}\text{C}$ in an upright position for 1 h and in inverted position for further 11 h. The biocompatibility of 1-ethyl, 1-

butyl-3-methylimidazolium carboxylates towards *Escherichia coli* was assessed qualitatively. In order to achieve this, Petri dishes with the incubated bacteria were placed on a light box, and assessed for the absence of the visible bacterial population inside the wells. If the wells without the visible layer of *Escherichia coli* were observed the ionic liquids were classed as growth inhibiting, otherwise they were classed as biocompatible.

The mass of an ionic liquid in a well was estimated as follows (Eq. 9):

$$\frac{M_w = (M_{vs} - M_{ve}) - (M_{pe} - M_{ps})}{3} \quad (\text{Eq. 9})$$

where:

M_w is the mass of an ionic liquid in an agar well.

M_{vs} is the starting mass of a labelled vial with an ionic liquid.

M_{ve} is the mass of the vial after three touch drops of an ionic liquid were removed.

M_{ps} is the starting mass of a pipette.

M_{pe} is the mass of the pipette after three drops of an ionic liquid were taken.

2.3 Computational modelling of imidazolium carboxylates.

2.3.1 Chemical structures of imidazolium cations and carboxylate anions.

The following chemical structures of imidazolium cations and carboxylate anions were modelled computationally (Figure 12, Figure 13). All of the carboxylate anions were combined with 1-ethyl-3-methylimidazolium cation to form 1-ethyl-3-methylimidazolium carboxylates; formate, furoate and i-butanoate anions were combined with 1-butyl-3-methylimidazolium cation to form 1-butyl-3-methylimidazolium carboxylates and the L-lactate anion was combined with 1-alkyl-, 1-alkoxymethylimidazolium cations to form 1-alkyl-, 1-alkoxymethyl L-lactates.

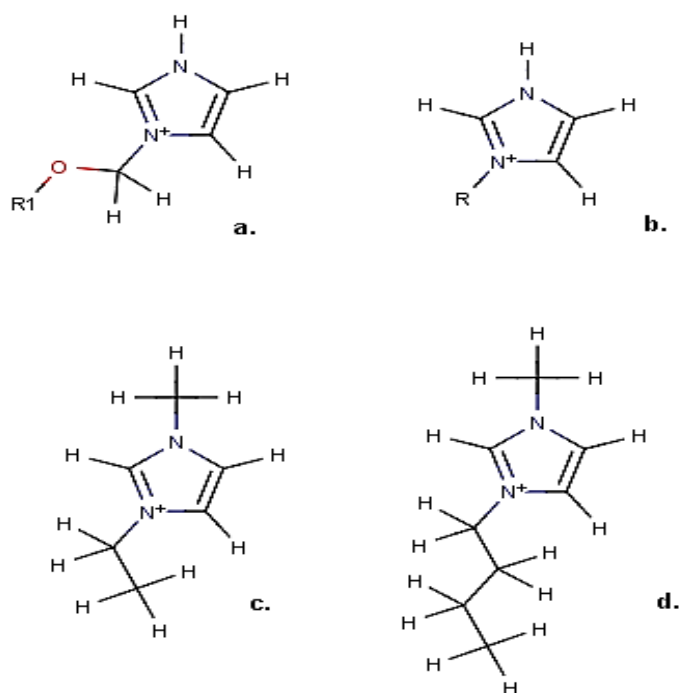


Figure 12. The chemical structures of imidazolium cations: (a.) 1-alkoxymethylimidazolium, (b.) 1-alkylimidazolium, (c.) 1-ethyl-3-methylimidazolium, (d.) 1-butyl-3-methylimidazolium. R, R₁ refer to the alkyl chains the length of which was reported in the Figure 5 (p. 37).

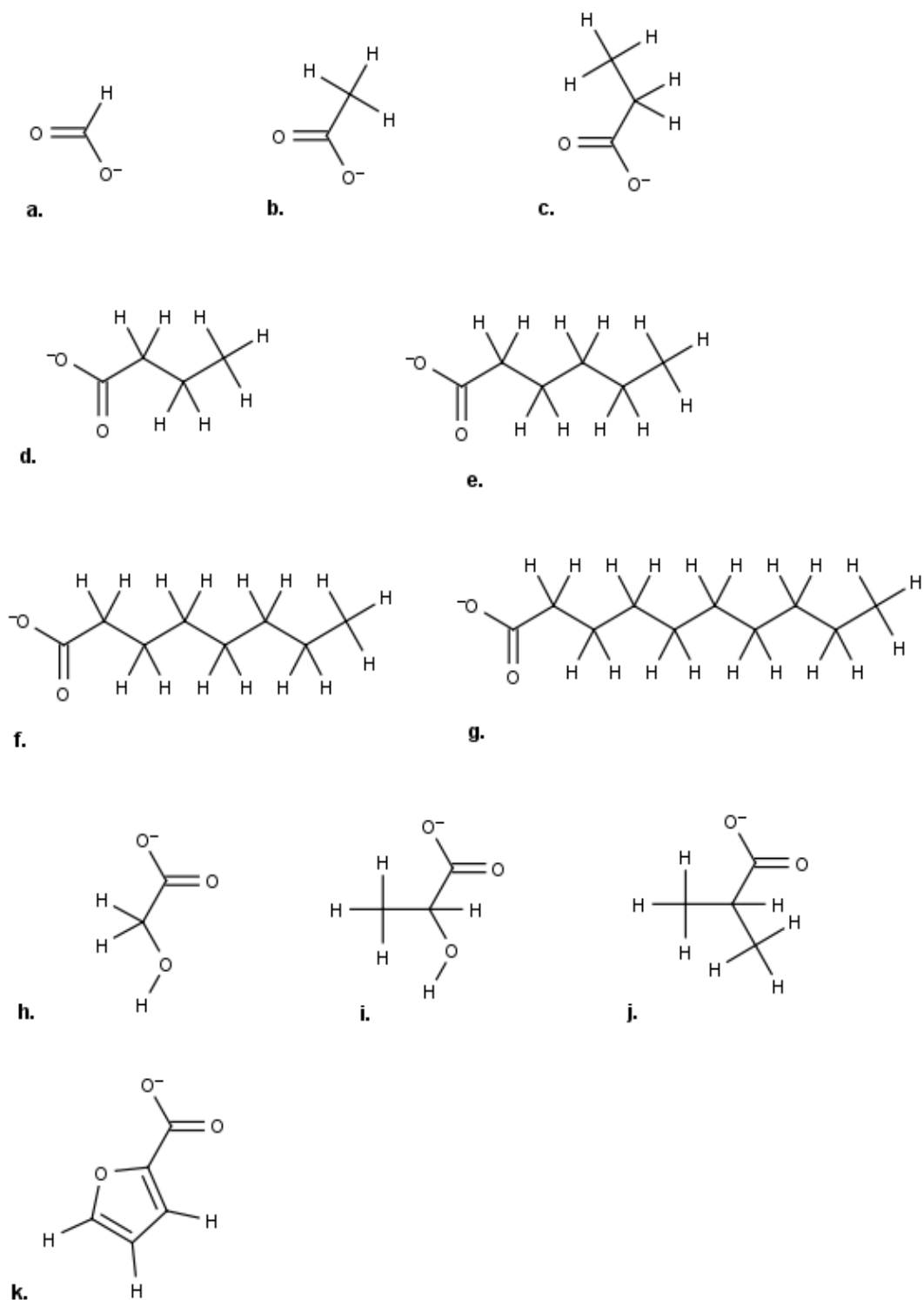


Figure 13. The chemical structures of carboxylate anions: (a.) formate, (b.) acetate, (c.) propanoate, (d.) butanoate, (e.) hexanoate, (f.) octanoate, (g.) decanoate, (h.) glycolate, (i.) L-lactate, (j.) i-butanoate, (k.) furoate.

2.3.2 Optimization of imidazolium cations and carboxylate anions to their equilibrium geometries.

The workflow of computational modelling of the chemical structures of imidazolium cations and carboxylate anions can be described in two stages. The first stage involved an initial encoding of the chemical structures in a form accessible by the Gaussian 03 program (Frisch et al., 2003), and the second stage produced the matrices of their nuclear Cartesian coordinates at the equilibrium geometry. Initially, isolated structures of imidazolium cations and carboxylate anions were generated in the program Avogadro 0.9.7 (Hanwell et al., 2012). These structures were optimized to their equilibrium geometry at a molecular mechanics level using the Merck (Halgren, 1996), and then transferred into the program Gaussian 03 (Frisch et al., 2003) for ab initio optimization at Hartree-Fock (Hartree, 1928; Lowdin, 1955) level of the electronic structure theory using 6-31++G* basis set (Hehre et al., 1969).

A force field optimization of the geometry of the chemical structures was aimed at finding their most energetically stable state at a molecular mechanics level, so that their initial Hessian during ab initio geometry optimizations was as close to their most energetically stable state as possible. The Hessian of a chemical structure is a matrix of force constants describing the second derivatives of the potential energy surface of a chemical system with respect to their Cartesian coordinates.

A test for the absence of computed negative vibrational frequencies, which are the second derivatives of energy, was performed for all chemical structures once a stationary point on their potential energy surface has been found. The absence of the negative frequencies at a stationary point ensures

that the found geometry of a chemical structure describes its potential energy minimum and not in a transitional state.

A summary of the algorithms and the parameters utilized during each stage of the computational modelling are presented below:

Stage 1

- Computational software: Avogadro 0.9.7 (Hanwell et al., 2012).
- Coordinate system: Cartesian.
- Level of electronic structure theory: Molecular mechanics.
- Molecular forcefield: Merck Molecular Force Field (Halgren, 1996).
- Forcefield algorithm: Open Babel MMFF94 (O'Boyle et al., 2011).
- Developer's forcefield validation method: MMFF94 validation suite (Merck and Co., Inc.).
- Energy minimization method: Steepest Descent (Booth, 1949; Steinmetz, 1966).
- Energy minimization algorithm: Open Babel steepest descent.
 - Maximum number of steps: 500.
 - Function minimization method: Analytical gradients.
 - Energy convergence threshold: 10^{-6} kcal mol⁻¹.

Stage 2:

- Computational software: Gaussian 03 (Frisch et al., 2003).

- Electronic structure method: Hartree-Fock (HF)(Hartree, 1928; Lowdin, 1955).
- Basis set: 6-31++G* (Hehre et al., 1969).
- Energy minimization method: Self consistent field method of molecular orbital approximation via linear combination of atomic orbitals (LCAO-MO-SCF).
- The SCF convergence acceleration algorithm:
 - Early stages of optimization: A modification of Direct inversion of the iterative subspace (DIIS) (Pulay, 1980) algorithm (EDIIS) (Kudin et al., 2002).
 - Later stages of optimization: CDIIS (Frisch et al., 2003).
- SCF energy convergence threshold: 1.6×10^{-4} Hartrees ($0.1 \text{ kcal mol}^{-1}$).
- Search for the energy minima:
 - Initial: Linear.
 - Close to convergence:
 - Newton-Raphson (reviewed in (Ypma, 1995)).
 - Rational function approximation (Simons et al., 1983).
- Number of optimization steps: twenty plus the number of redundant internal coordinates.
- Maximum step size (initial trust radius): $N = 30$
 - Distance: $0.01 N$ Bohrs.
 - Angle: $0.01 N$ radians.

- Trust radius update: Update for energy minima using Fletcher method (Fletcher, 1970).
- Requested energy convergence cut-off: 1×10^{-7} Hartree (6×10^{-5} kcal mol⁻¹).
- Orbital symmetry constraints used: No.
- Initial HF wavefunction guess: Diagonalized Harris functional (Harris, 1985).
- Calculation of one electron integrals: Prism algorithm (Gill, 1994).
- Initial estimation of a Hessian matrix: Berny optimization algorithm (Schlegel, 1982).
 - Atom connectivity is based on: Atomic radii and force constants (Schlegel, 1984).
- The Hessian update method: Analytical first derivatives.
- The Hessian update algorithm: Broyden-Fletcher-Goldfarb-Shanno (BFGS) (Head and Zerner, 1985).

2.3.3 Optimization of imidazolium carboxylates to their equilibrium geometries.

The chemical structures of 1-ethyl-, 1-butyl-3-methylimidazolium carboxylates and 1-alkyl-, 1-alkoxymethylimidazolium L-lactates described earlier were generated in the program Avogadro (Hanwell et al., 2012). The salts were modeled by combining the optimized structures of the imidazolium cation and the carboxylate anion. The generated matrices were transferred into the program Gaussian 03 (Frisch et al., 2003) without any force-field energy minimization.

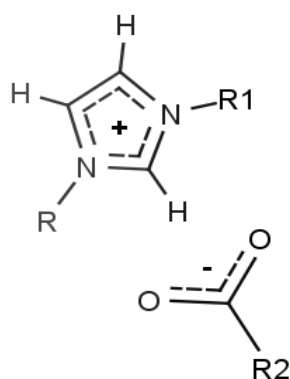


Figure 14. A geometrical configuration of a combined imidazolium carboxylate structure.

The structural integrity of each imidazolium carboxylate in a combined matrix was checked after its transfer into the Gaussian 03 program to ensure that each cation-anion combination was seen by the program as single entity and not as a pair of separate ions. Thus, the integrity of an imidazolium carboxylate was confirmed if the number of degrees of freedom for a combined cation-anion structure was less than the sum of a number of degrees of freedom of its separate ions. Once the structural integrity of an imidazolium carboxylate was confirmed it was optimized in the Gaussian 03

program as described earlier (p. 61), and the matrix of its nuclear Cartesian coordinates at the equilibrium geometry was computed.

An additional ab initio optimization of the chemical structure of 1-ethyl-3-methylimidazolium acetate was conducted using second order Moller-Plesset (MP2) level of the EST under the settings reported earlier (p. 61). The MP2 method adds corrections to the correlation energy computed by the HF method, and it was evoked for the computational evaluation of the topology of the C-H--O inter-ionic interactions in 1-ethyl-3-methylimidazolium acetate. The frozen core option of Gaussian 03, was used to compute the correlation energy of the chemical structure. Hence, the inner-shells of the atoms were excluded from the calculations.

2.3.4 Generation of wavefunction files of imidazolium carboxylates.

It was reported earlier (p. 35) that the QTMS descriptors of chemical structures are based on the principles of the theory of the Atoms in Molecules. This theory is an interpretative theory which computes and analyses the wavefunctions and the electronic charge density of chemical structures but does not generate the electronic parameters which are used for the computation of these wavefunctions. Hence, the wavefunction files of 1-ethyl-, 1-butyl-3-methylimidazolium carboxylates and 1-alkyl-, 1-alkoxymethylimidazolium L-lactates which contained the data on their electronic structures at their equilibrium geometries were generated by the Gaussian 03 program. An example of a wavefunction file format which was used for the generation of the QTMS descriptors in the current study is illustrated in the Figure 15.

```

Block 0 { A title
          GAUSSIAN 16 MOL ORBITALS 119 PRIMITIVES 7 NUCLEI
Block 1 { C 1 (CENTRE 1) -0.00272697 -0.01547303 -0.00731799 CHARGE = 6.0
          O 2 (CENTRE 2) 0.03859847 0.01261931 2.38239638 CHARGE = 8.0
Block 2 { CENTRE ASSIGNMENTS 1 1 1 1 1 1 1 1 1 1 1 1 1 1 1
          CENTRE ASSIGNMENTS 1 1 1 1 1 1 2 2 2 2 2 2 2 2 2
Block 3 { TYPE ASSIGNMENTS 1 1 1 1 1 1 1 1 1 2 2 2 3 3 3 4
          TYPE ASSIGNMENTS 3 4 1 2 3 4 1 1 1 1 1 1 1 1 1 2
Block 4 { EXPONENTS 0.3047525D+04 0.4573695D+03 0.1039487D+03 0.2921016D+02
          EXPONENTS 0.3163927D+01 0.7868272D+01 0.1881289D+01 0.5442493D+00
Block 5 { MO 1 MO 0.0 OCC NO = 2.0000000 ORB. ENERGY = -20.305798
          0.72774366D-04 0.13425450D-03 0.21672838D-03 0.28211596D-03
          MO 2 MO 0.0 OCC NO = 2.0000000 ORB. ENERGY = -20.304163
          0.77453537D-04 0.14288665D-03 0.23066336D-03 0.30025516D-03
Block 6 { END DATA
          THE HF ENERGY = -227.145709239089 THE VIRIAL(-V/T)= 2.00011908

```

where:

- Block 0:** Title, Gaussian type AOs, number of MOs, number of primitive Gaussian functions, total number of nuclei
- Block 1:** Atomic label, nuclear centre number, nuclear Cartesian coordinates (x,y,z), nuclear charge
- Block 2:** Replicates of the nuclear centre numbers whose quantity corresponds to the number of primitive Gaussian functions to represent MOs of a centre
- Block 3:** Types of primitive Gaussian functions assigned to each centre number
- Block 4:** Exponents of primitive Gaussian functions
- Block 5:** Molecular orbital number, the number of electrons, orbital energy, MO coefficients
- Block 6:** Total energy of a chemical structure, the ratio of kinetic to potential energy

Figure 15. A sample of the content of a wavefunction file. The illustrated format of the file is generated by the Gaussian 03 program.

2.3.5 Computation of the quantum topological molecular similarity descriptors of imidazolium carboxylates.

A wavefunction file of each imidazolium carboxylate was analyzed by the MORPHY98 program (Popelier, 1998), and the following parameters were computed:

- The electronic charge density (Eq. 10).

$$\rho_n = N_i \times \psi_{ni}^2 \quad (\text{Eq. 10})$$

where:

ρ_n is the electronic charge density scalar field based on n scalars.

N_i is the occupational number of an i^{th} molecular orbital.

ψ_{ni}^2 is the square of a wavefunction of an i^{th} molecular orbital, where ψ is defined according to the type of a molecular orbital:

$$\psi_s = \exp[-\alpha \times rd^2] \times c$$

$$\psi_p = \exp[-\alpha \times rd^2] \times rd \times c$$

$$\psi_d = \exp[-\alpha \times rd^2] \times rd^2 \times c$$

where:

α is an exponent of a primitive Gaussian function.

rd^2 is a squared distance between the nucleus and an MO.

rd is a distance between the nucleus and an MO.

c is a primitive Gaussian function.

- The Laplacian of electronic charge density (Eq. 11).

$$\nabla^2 \rho_n = H_{xx}(\rho_n) + H_{yy}(\rho_n) + H_{zz}(\rho_n) \quad (\text{Eq. 11})$$

where:

ρ_n is the electronic charge density scalar field based on n scalars.

$\nabla^2 \rho_n$ is the Laplacian of electronic charge density.

$H_{xx}(\rho_n), H_{yy}(\rho_n), H_{zz}(\rho_n)$ are the variables along the main diagonal of the Hessian of ρ_n at its n^{th} scalar point.

- Kinetic energy density (Eq. 12).

$$G_n = \frac{N_i \times (\nabla \psi_{ni})^2}{2} \quad (\text{Eq. 12})$$

where:

G_n is a kinetic energy density.

N_i is the occupational number of an i^{th} molecular orbital.

$\nabla \psi_{ni}$ is $\left(\nabla \psi_{ni} = \frac{\partial \psi}{\partial x} l + \frac{\partial \psi}{\partial y} j + \frac{\partial \psi}{\partial z} k \right)$ where l, j, k are unit vectors,

where ψ_{ni} is a wavefunction of an i^{th} MO at its n^{th} primitive Gaussian function.

- Kinetic energy density (Eq. 13).

$$K = \frac{N_i \times \psi_{ni} \times \nabla^2 \psi_{ni}}{2} \quad (\text{Eq. 13})$$

where:

N_i is the occupation number of an i^{th} molecular orbital.

ψ_{ni} is a wavefunction of an i^{th} MO at its n^{th} primitive Gaussian function.

$\nabla^2 \psi_{ni}$ is the Laplacian of the wavefunction of an i^{th} MO at its n^{th} primitive Gaussian function.

- The ellipticity of the electronic charge density (Eq. 14).

$$\varepsilon = \frac{\lambda_1}{\lambda_2} - I \equiv \frac{\lambda_1 - \lambda_2}{\lambda_2} \quad (\text{Eq. 14})$$

where:

ε is the ellipticity of the electronic charge density around a saddle critical point.

λ_1 and λ_2 are the negative eigenvalues of the Hessian of the electronic charge density.

Further information on the algorithms of the MORPHY98 program and the default threshold values can be found in the original publications (Popelier, 1996a; 1996b; 1994; 1998) and in the pseudocode of the MORPHY1.0 program (Popelier, 1996c) which is deposited at the Computer Physics Communications Program Library (The Queen's University of Belfast).

2.3.6 Computation of the distribution coefficients of imidazolium carboxylates.

It was reported earlier (p. 31) that the experimental LogD values for imidazolium carboxylates utilized in the current study, to the author's knowledge, has not yet been reported. Therefore, distribution coefficients of 1-ethyl-, 1-butyl-3-methylimidazolium carboxylates and 1-alkyl-, 1-alkoxymethylimidazolium L-lactates were calculated in the program MarvinSketch (ChemAxon) which utilizes the algorithm of Csizmadia and colleagues (Csizmadia et al., 1997). The overall computational approach to the estimation of LogD values is outlined below.

Initially, pre-processing algorithm determined all of the possible ionization sites of a chemical structure. Then, a partition coefficient of a neutral form of a chemical was calculated as a sum of LogP values of atomic fragments of a structure at a pH 7.4. The atomic fragments were generated according to the atom types proposed by Viswanadhan and colleagues (Viswanadhan et al., 1989). Individual LogP values for each fragment were taken from three available fragment pools: VG (Viswanadhan et al., 1989), KLOP (Klopman et al., 1994) and PHYSPROP (PhysProp[®] database, SRC Inc.).

Afterwards, an ionization constant for every microspecie ($pK_{a_{micro}}$) was evaluated as a function of the atomic partial charge distribution and polarizabilities, and the LogD value of a chemical structure was calculated using Eq. 15.

$$\text{LogD} = \text{Log} \left(\frac{\sum_i P_i \times m_{water_i}}{\sum_i m_{water_i}} \right) \equiv \text{Log} \left(\frac{\sum_i m_{oct_i}}{\sum_i m_{water_i}} \right) \quad (\text{Eq. 15})$$

where:

m_{solvent} are the concentrations of all possible ionized forms plus the major unionized form of a chemical in octanol or water at a defined pH, where the extent of the ionization at that pH was determined from the $\text{pK}_{\text{a}_{\text{micro}}}$ values.

P is a partition coefficient of a chemical between octanol and water.

In the current study, the LogD values were computed at acidic (pH 5), neutral (pH 7) and basic pH (pH 9). This range of pH values was chosen to encompass all possible shifts from a neutral pH during experimental determination of the MICs of imidazolium carboxylates which could be caused by the excretion of metabolic products a microorganism leading to the changes in a chemical composition of a bacterial medium. The support electrolyte concentration, which is the concentration of available pairing ions Cl^- , Na^+ , K^+ for the ionic microspecies was set to 0.1 M; only the major tautomeric form was considered.

In addition to the LogD values, the MarvinSketch (ChemAxon) was also used to compute the Platt (Platt, 1952) and Randic (Randic, 1975) topological indices of the imidazolium carboxylates. These indices encoded the chemical structures as scalars based on the topological connectivity of their atoms, excluding the connectivity of hydrogen atoms. Both, the Platt and the Randic indices were based on the number of bonds in a chemical structure but only the Randic index considered its branching.

2.4 Statistical correlation of experimental and computational data for imidazolium carboxylates.

Multivariate linear regression equations correlating minimal inhibitory concentrations of 1-ethyl-, 1-butyl-3-methylimidazolium carboxylates and 1-alkyl-, 1-alkoxymethylimidazolium L-lactates were generated in MATLAB using the algorithms of Statistics toolbox (MATLAB and Statistics Toolbox Release 2010a, 2010). The script integrating the relevant MATLAB functions was written by the author. The pseudo-code of this script is outlined below. The MATLAB functions which were included in the script and the file format of the input data files are reported in brackets.

Module 1: Data pre-processing:

This part of the script prepared the input data for the linear regression analysis.

- Data files (.csv) with theoretical descriptors of imidazolium carboxylates were read into two dimensional (2D) arrays and randomly divided into a training and a test set of equal lengths (f: cvpartition). Each training and test set contained 17 chemical structures in all QSARs. The term *theoretical descriptors* refers to the following data in a data file:

Topological connectivity indices, i.e. a combination of the Platt and the Randic indices, which were in a form of a row vector.

LogD values which were in a form of a matrix, the rows of which represented a cation and an anion and the columns of which were their LogD values at pH 5, 7 and 9.

QTMS descriptors which were in a form of a matrix, the rows of which represented electronic charge density, its Laplacian, ellipticity and two terms of kinetic energy terms, and the columns of which were the

values of these descriptors at bond critical points of a chemical structure.

A combination of the QTMS descriptors and the LogD values of a chemical structure, which was represented by a matrix, the rows of which included the descriptors and the columns included their values.

- The arrays in both sets were indexed and linked to the Log(1/MICs) of corresponding imidazolium carboxylates. This generated a constant link between the descriptors of a chemical structure and its toxicity.
- The 2D training and test set arrays were concatenated into three dimensional (3D) training and test set arrays (f: cat). These arrays were generated in a *closed book shape* where each page represented a 2D descriptor array of a structure. This was performed to enhance the ease of the data retrieval by the MATLAB program, and the speed of the regression analysis. Bond critical points of the identical bonds within the chemical structures were fully aligned. The absence of a particular bond critical point within a chemical structure was encoded by a null value.
- The data within each set were normalized (f: zscore) and mean-centered (f: detrend).

Module 2: The generation of regression equations (training set):

This part of the script performed the regression analysis of the data.

- The 3D training set array was transformed into a 2D array, in which each row represented a structure and columns represented the descriptors of that structure. This was performed, so that a regression algorithm could simultaneously analyze a matrix of the descriptors of a of all 17 chemical structures.
- The descriptors of imidazolium carboxylates were correlated with their Log(1/MICs) using partial least squares regression (PLS) (f: plsregress),

and PLS and multiple linear regression (MLR) of the first principal components (PC_1) of the descriptors computed via the principal component analysis (PCA). The latter type of the regression was conducted as follows:

- The 3D training set array was analyzed (f: princomp).
- PCA scores PC_1 for all training set arrays were grouped in a 2D array.
- A regression analysis was performed using partial least squares regression (f: plsregress) and multiple linear regression (f: regress).

Principal component analysis is a statistical approach used to reduce the dimensionality of data by maximizing its variance via the elimination of linear dependencies of its variables. The PCA algorithm analyzes the variables and project them into a space of principal components, in which the scores of the first principal component represent the maximum computed variance of the initial data. Partial least squares regression is statistical approach which is similar in its goal to the principal component analysis but approaches is from a different angle. Thus, PLS algorithms project the initial linearly dependent variables into a space of latent variables which are linearly independent projections of the initial variables maximizing their variance in a correlation with a response variable. The optimal number of the latent variables for generation of regression equations is determined experimentally. Thus, in the current study, the number of significant PLS latent variables was determined by plotting the contribution of each variable to the total explained variance until no further change was observed.

Module 3: The validation of the regression equations (test set):

This part of the script tested the statistical reliability of the developed by the Module 2 regression models.

- The 3D test array was transformed into a 2D array, in which each row represented a structure and columns represented the descriptors for that structure.

PLS:

- The descriptors were mean-centered with the mean of the training set from the Module 2 (f: bsxfun).
- The Log(1/MICs) values for the test set of imidazolium carboxylates were predicted using the PLS regression equation generated in the Module 2.

PCA/MLR and PCA/PLS:

- The descriptors were mean-centered with the mean of the training set from the Module 2.
- PCA scores PC₁ were computed for each imidazolium carboxylate (f: princomp) and combined in a 2D array.
- PC₁ scores were mean-centered with the mean of the PC1 training set scores from the Module 2 (f: bsxfun).
- The Log(1/MICs) values for the test set of imidazolium carboxylates were predicted using the partial least squares regression equation and the multiple least squares regression equation from the Module 2.

The statistical performance of the generated regression models was assessed as follows:

The values of R^2 predicted (Eq. 16), R^2 (data from f: *regstat*) and root mean

squared error of prediction (RMSE) (squared root of the data from f:regstat) were computed for all generated regression equations. The values reported in the Results and Discussion chapter for each statistical parameter are the averages of the values computed for 1000 randomly generated combinations of a training and a test set of chemical structures each containing 17 imidazolium carboxylates.

$$R^2_{predicted} = \frac{\sum (y_{test} - x_{test})^2}{\sum (x_{test} - \bar{x}_{train})^2} \quad (\text{Eq. 16})$$

where:

y_{test} are predicted Log(1/MICs) of a test set.

x_{test} are experimental Log(1/MICs) of a test set.

\bar{x} is the average of experimental Log(1/MICs) values of a training set.

Y-permutation tests, in which wrong Log(1/MICs) were assigned to the chemical structures of a training set and a test set were performed using a random permutation function of the MATLAB program (f: randsample).

2.4.1 The mathematical format of experimental and computational data.

Experimental data:

Y is a row matrix of $\left[\log \frac{1}{\text{MIC}_1}, \log \frac{1}{\text{MIC}_2}, \dots, \log \frac{1}{\text{MIC}_m} \right]$ values of MICs of imidazolium carboxylates towards *Escherichia coli*.

- Matrix dimensions: $[a \times m]$, where $a = 1$ and each column m is a unique imidazolium carboxylate.

- Matrix type: Dense.
- Correlated variables:
 - Row variables: No.
 - Column variables: No.
- Matrix rank:
 - Row rank: Full and equal to a , where $a = 1$.
 - Column rank: Full and equal to m , where $m = 17$.
 - Total rank: Deficient, i.e. $m \neq a$.

Computational data:

X is a rectangular matrix of the QTMS descriptors for every structure.

- Matrix dimensions: $[m \times n]$, where each row m is a unique imidazolium carboxylate and the columns within that row are its QTMS descriptors.
- Matrix type: Dense.
- Correlated variables:
 - Row variables: No.
 - Column variables: Yes.
- Matrix rank:
 - Row rank: Full and equal to m , where $m = 17$.
 - Column rank: Deficient and equal to n .
 - Total rank: Deficient, i.e. $m < n$.

2.4.2 Multivariate linear regression algorithms in the MATLAB 7.10 program.

Partial least squares regression:

- SIMPLS (De Jong, 1993).
 - Matrix decomposition subroutine: Singular value decomposition (SVD) algorithm (INTEL® MKL LAPACK).
 - Matrix orthogonalization algorithm: Modified Gram-Schmidt (INTEL® MKL LAPACK).
 - Type of linear regression: Least squares fit.

Multiple linear regression:

- Data pre-processing: Orthogonal triangular decomposition algorithm.
- MATLAB internal regression algorithm.
- Type of linear regression: Least squares fit.

Principal component analysis algorithm:

Matrix decomposition subroutine: Singular value decomposition (SVD) algorithm (INTEL® MKL LAPACK).

3. Results and Discussions

3.1 Minimum inhibitory concentrations of 1-ethyl-, 1-butyl-3-methylimidazolium carboxylates towards *Escherichia coli*.

The minimum inhibitory concentrations (MICs) of 1-ethyl-, 1-butyl-3-methylimidazolium carboxylates towards *Escherichia coli* K-12 MG1655 are summarized below (Table 2). A concentration of an ionic liquid was classed as a minimum inhibitory concentration if the maximum specific growth rate (MSGR) of *Escherichia coli* in the presence of an ionic liquid was less than 20 percent of that of the control. The MSGRs of *Escherichia coli* are reported in the Table 3.

Table 2. Minimal inhibitory concentrations of 1-ethyl, 1-butyl-imidazolium carboxylates towards *Escherichia coli*.

1-R- 3-methylimidazolium	Anion	Relative molecular mass (g/mol)	Carbon content (%)	Minimum inhibitory concentration (M)
R= ethyl	formate	158	52	0.07
	acetate	172	54	0.07
	propanoate	186	57	0.07
	butanoate	200	59	0.07
	hexanoate	228	62	0.05
	octanoate	256	65	0.07
	decanoate	284	67	0.01
	furoate	224	57	0.07
	L-lactate	202	52	0.10
	glycolate	188	50	0.10
	i-butanoate	200	59	0.10
R=butyl	formate	186	57	0.07
	i-butanoate	228	62	0.07
	furoate	252	60	0.10

Table 3. The maximum specific growth rates of *Escherichia coli* with a range of concentrations of 1-ethyl-, 1-butyl-3-methylimidazolium carboxylates reported as growth rate percent of the control.

1-R- 3-methylimidazolium	Anion	In-well concentrations of ionic liquids (M)						
		0.100	0.070	0.050	0.030	0.010	0.005	0.001
R= ethyl	formate	0	0	97±4	93±4	94±4	96±6	109±5
	acetate	0	0	53±2	60±3	112±5	107±7	100±5
	propanoate	0	0	69±3	94±4	100±5	97±6	113±5
	butanoate	0	0	83±4	85±4	88±4	105±7	101±5
	hexanoate	0	0	18±1	19±1	42±2	86±6	93±6
	octanoate	0	19±1	24±1	50±2	54±3	89±6	103±5
	decanoate	0	0	0	0	29±1	91±6	97±4
	furoate	0	14±1	70±3	89±4	80±4	104±7	99±5
	L-lactate	0	44±2	100±5	87±4	100±5	101±7	100±5
	glycolate	0	46±2	94±4	99±5	92±4	103±7	103±5
	i-butanoate	0	63±3	77±4	95±4	88±4	103±7	105±5
R=butyl	formate	0	0	69±3	95±4	94±4	102±7	93±4
	i-butanoate	0	0	76±3	95±4	84±4	99±7	107±5
	furoate	0	82±4	79±4	99±4	74±3	97±7	99±5

All of 1-ethyl-, 1-butyl-3-methylimidazolium carboxylate were biocompatible with *Escherichia coli* at their in-well concentrations of up to 0.01 M, and all of them were toxic at their 0.1 M concentration under the reported test conditions. The observed MICs of these ionic liquids were in the agreement with the MICs of 1-alkyl, 1-alkoxymethylimidazolium L-lactates towards *Escherichia coli* with alkyl side chains of up to five carbon atoms which were reported of being higher than 0.005 M and 0.004 M respectively (Pernak et al., 2004). Thus, all of 1-ethyl-, 1-butyl-3-methylimidazolium carboxylates were biocompatible with *Escherichia coli* at the concentrations of up to 0.01 M, which are by an order of a magnitude higher than the biocompatible concentrations of 1-alkyl-, 1-alkoxymethylimidazolium L-lactates. This

observation indicated that the chemical structures of the anions did not have a significant effect on the toxicity of these ionic liquids. In addition, a visual inspection of the pattern of MICs of 1-ethyl-, 1-butyl-3-methylimidazolium carboxylates reported earlier (Table 2, p. 80) suggested that their biological activity is not linearly correlated with the number of carbon atoms in their chemical structures or with their relative molecular mass. The determined MICs of the ionic liquids were electronically recorded in comma-separated values files (.csv) and used in a development of QSARs.

3.2 Agar diffusion test.

It was reported earlier (p. 39) that the agar diffusion test was proposed to be used as a reliable toxicological screen for ionic liquids (Rebros et al., 2009; Wood et al., 2011). Herein, the validity of this research hypothesis for 1-ethyl-, 1-butyl-3-methylimidazolium carboxylates is assessed theoretically and experimentally.

3.2.1 A theoretical evaluation of the agar diffusion test for toxicological screening of ionic liquids.

The theoretical assessment of the reliability of the agar diffusion test is performed by critically evaluating the approaches which were used to validate the ADT for its toxicological screening of ionic liquids.

Thus, in both earlier reported studies (Rebros et al., 2009; Wood et al., 2011) the validation of the ADT was based on the correspondence of the toxicological data between the ADT and liquid medium tests which were performed in automated incubator-plate readers. However, a reaction system based on an agar medium is significantly different from a reaction system

based on a liquid medium. Hence, it is questionable that a proper validation of the ADT could be conducted via its comparison with a liquid medium test. Thus, the agar diffusion test is an open reaction system and a liquid medium test is a closed reaction system. The nature of each of the reaction system can be described as follows:

- Closed reaction system (liquid medium):
 - Nothing leaves. The initial concentration of a chemical changes only due to its reaction within the system. The waste products of a microorganism cannot leave the system.
 - Nothing enters. No supply of fresh nutrients from outside are available for a microorganism.
- Open reaction system (agar medium):
 - Something leaves. A concentration gradient of a chemical forms as some of the chemical leaves the initial area by diffusion. Hence, the initial concentration of the chemical changes not only due to its reaction within the system but also due to its physical movement away from a microorganism. The waste products of a microorganism can leave the system.
 - Something enters. Continuous supply of fresh nutrients for a microorganism which can diffuse from areas of higher concentration to areas of lower concentration (Piddock, 1990).

Further differences between the agar diffusion test and a liquid medium test conducted in automated incubator-plate readers are summarized below:

The first difference between the agar diffusion test and the liquid medium test is in the presence of additional chemical structures in the agar based medium:

- Agar is a complex natural material originated from seaweed. A highly purified agar consists of a mixture of polysaccharides: a linear neutral polymer agarose and a heterogeneous mixture of smaller agaropeptin molecules which are negatively charged due to the presence of sulphate and carboxyl groups. These anionic groups can interact with the positively charged ions during toxicological screening, hence, affecting the outcome of the tests (Piddock, 1990).

The second difference between the tests is the density of an initial bacterial inoculum, which can be explicitly defined in a liquid medium test but is unknown in the agar diffusion test:

- The quantitative value of the bacterial density is measured as the initial turbidity of a bacterial broth at the start of the toxicological screening in a liquid medium.
- The uniformity of the bacterial biofilm on an agar surface cannot be quantified.

The third difference between the agar diffusion test and a liquid medium test is in the growth stage of a bacterial culture:

- A bacterial culture in its exponential growth phase is used in a liquid medium test. Thus, the micro-organism develops competitively and adaptively in the presence of a chemical.

- A bacterial culture is at its steady state growth stage in the agar diffusion test. Thus, fully developed bacterial cells survive and multiply in the presence of a chemical.

The forth difference between the agar diffusion test and a liquid medium screening is the availability of the oxygen to the bacteria.

- The oxygen is uniformly available for all of the cells in a liquid medium test due to repeated automatic shaking of a reaction vessel.
- The oxygen accessibility varies between the bacterial cells in the agar diffusion test depending on the density of a biofilm and their position within it.

The fifth difference between the ADT and a liquid medium test is the extent of a physical contact between a chemical and a microorganism:

- In a liquid medium this contact is continuous due to the shaking of the reaction vessels.
- In the agar diffusion test this contact is limited contact and is initiated by the mobility of a microorganism and the initial bacterial population density.

The listed differences between the agar diffusion test and a liquid medium test performed in automated incubator-plate reader systems explain theoretical reasons for the incomparability of the results of these tests.

3.2.2 An experimental evaluation of the agar diffusion test for the toxicological screening of ionic liquids.

It was reported previously (p. 39) that in the agar diffusion test was validated for the toxicological screening of ionic liquids by a liquid medium test conducted in an automated incubator-plate reader (Rebros et al., 2009).

This validation was based on the comparison of the qualitative data from the ADT for a set of quaternary ammonium ionic liquids with their half maximal effective concentrations in a liquid medium (Rebros et al., 2009), and with their growth rates percent data (Wood et al., 2011). Hence, in both studies, the reported correlations between the outcomes of the ADT and the liquid medium tests were based on the comparison of a different format of the experimental data. In the current study, this inconsistency in the experimental data format was addressed by introducing an agar well test (AWT). In this test a bacterial culture and ionic liquids are dispensed directly into the wells on an agar surface. Hence, the initial concentrations of ionic liquids in a direct contact with a micro-organism can be estimated, and compared with the minimum inhibitory concentrations of these ionic liquids in a liquid medium.

A development of the agar well test underwent several stages and its final version was reported in the Materials and Methods chapter (p. 56). Once the agar well test was developed it was validated by the agar diffusion test performed under the same conditions (Table 4).

Table 4. Qualitative toxicological profiling of 1-ethyl-, 1-butyl-3-methylimidazolium carboxylates with *Escherichia coli* in the agar diffusion test and the agar well test.

1-R-3-methyl imidazolium	Anion	ADT		AWT	
		Mass of an ionic liquid on the disk (mg)	Bacterial growth inhibition (Yes / No)	Mass of the ionic liquid in an agar well (mg)	Bacterial growth inhibition (Yes / No)
R= ethyl	formate	20	No	3	No
	acetate	30	Yes	3	Yes
	propanoate	10	No	4	No
	butanoate	10	Yes	3	Yes
	hexanoate	10	Yes	4	Yes
	octanoate	10	Yes	3	Yes
	decanoate	20	Yes	4	Yes
	furoate	10	No	3	No
	L-lactate	10	Yes	3	No
	glycolate	10	No	4	No
	i-butanoate	10	No	4	No
R=butyl	formate	20	No	3	No
	i-butanoate	30	Yes	3	Yes
	furoate	10	No	3	No

* Bold font represents toxic ionic liquids.

In the ADT, the ionic liquids were classed as toxic if zones without visible bacterial growth were observed around the filter paper disks, irrespective of their diameter. In the AWT, the toxic ionic liquids were determined by the absence of a visual bacterial growth inside agar wells. The assessment established that the toxicological classification of 1-ethyl, 1-butyl-3-methylimidazolium carboxylates into toxic and biocompatible groups in the ADT and the AWT was in a ninety three percent agreement, indicating that agar well diffusion test could be used as a representative of the agar diffusion

test in the current study. Thus, only the classification of 1-ethyl-3-methylimidazolium L-lactate was in a disagreement between the tests. It is hypothesized that 1-ethyl-3-methylimidazolium L-lactate was classed as a biocompatible ionic liquid in the ADT due to a very small zone of a bacterial growth inhibition around the filter paper disk which could not be identified upon a visual examination. Once the AWT was validated, the initial in-well concentrations of the ionic liquids in agar wells were estimated and compared with the MICs in a liquid medium test (Table 5).

Table 5. The comparison of the initial in-well concentrations of 1-ethyl-, 1-butyl-3-methylimidazolium carboxylates in the agar well test with their MICs in a liquid medium.

1-R-3-methylimidazolium	Anion	In well concentration of an ionic liquid	
		Agar well test (M)	Liquid medium test (M)
R= ethyl	formate	3.8	0.07
	acetate	3.4	0.07
	propanoate	4.2	0.07
	butanoate	3.0	0.07
	hexanoate	3.4	0.05
	octanoate	2.4	0.07
	decanoate	2.8	0.01
	furoate	2.6	0.07
	L-lactate	3.0	0.10
	glycolate	4.2	0.10
	i-butanoate	4.0	0.10
R=butyl	formate	3.2	0.07
	i-butanoate	2.6	0.07
	furoate	2.4	0.10

* Bold font represents toxic ionic liquids

The data in Table 5 show that the in-well concentrations of the biocompatible according to the AWT (and the ADT) ionic liquids were higher than their minimum inhibitory concentrations in a liquid medium. For example, the initial in-well concentration of 1-ethyl-3-methylimidazolium formate was 3.8 M in the AWT, but its minimum inhibitory concentration in a liquid medium was 0.07 M. Thus, if the differences between the agar based and a liquid medium based reaction systems were negligible, then the 3.8 M concentration of 1-ethyl-3-methylimidazolium formate would have resulted in the absence of a bacterial growth, and the ionic liquid would have been classed as toxic. However, the biocompatible response of *Escherichia coli* was observed in the AWT (and the ADT). This indicates that the open nature of the agar based reaction system had a significant influence on the results of the toxicological classification of this ionic liquid, and correspondently, of other biocompatible ionic liquids reported in the Table 5 (p. 88). Consequently, establishing that the research hypothesis of Rebros and colleagues (Rebros et al., 2009), stating that the agar diffusion test (ADT) could be reliably used for the toxicological classification of ionic liquids, was invalid for 1-ethyl-, 1-butyl-3-methylimidazolium carboxylates.

3.3 Distribution coefficients and QTMS descriptors of imidazolium carboxylates.

The distribution coefficients (LogD values) and the QTMS descriptors of 1-ethyl, 1-butyl-3-methylimidazolium carboxylates and 1-alkyl, 1-alkoxymethylimidazolium carboxylates were computed as described earlier (p. 68) and prepared for a development of QSARs. The theoretical LogD values of imidazolium carboxylates are summarized in Table 6. The QTMS

descriptors of each imidazolium carboxylate are provided in Appendix 2 due to the long length of the data arrays. The numbers in brackets identify the structures in the Table 1 (p. 38). The structure 3k in the Table 1 was randomly chosen to be omitted from the statistical modelling so that a dataset with an even number of ionic liquids could be generated. The generated descriptors of for all imidazolium carboxylates were transferred into comma-separated values files (.csv) for the development of QSARs.

Table 6. Theoretical distribution coefficients of 1-ethyl, 1-butyl-3-methylimidazolium carboxylates and 1-alkyl, 1-alkoxymethylimidazolium L-lactates at pH 5, 7, 9.

Identification of an ionic liquid	Distribution coefficient		
	pH 5	pH 7	pH 9
1-ethyl-3-methylimidazolium	-3.11	-3.11	-3.11
acetate	-0.81	-2.65	-3.70
butanoate	0.57	-1.16	-2.50
decanoate	3.26	1.55	0.17
formate	-1.08	-2.94	-3.78
furoate	-1.18	-2.68	-2.84
glycolate	-2.52	-4.24	-4.57
hexanoate	1.55	-0.09	-1.57
i-butanoate	0.65	-1.10	-2.41
L-lactate	-1.71	-3.52	-3.99
octanoate	2.48	0.89	-0.65
propanoate	0.04	-1.75	-2.98
1-butyl-3-methylimidazolium	-2.15	-2.15	-2.15
formate	-1.08	-2.94	-3.78
furoate	-1.18	-2.68	-2.84
i-butanoate	0.65	-1.10	-2.41
L-lactate*	-1.71	-3.52	-3.99
Im_CH ₃	-0.49	-0.07	0.08
Im_C ₂ H ₅	-0.49	-0.07	-0.08
Im_C ₃ H ₇	0.39	0.81	0.96
Im_C ₄ H ₉	0.83	1.26	1.40
Im_C ₅ H ₁₁	1.84	1.85	1.85
Im_C ₆ H ₁₃	1.72	2.15	2.29
Im_C ₇ H ₁₅	2.15	2.59	2.73
Im_C ₈ H ₁₇	2.61	3.04	3.18
Im_C ₉ H ₁₉	3.05	3.48	3.62
Im_C ₁₀ H ₂₁	3.05	3.48	3.62
Im_C ₁₂ H ₂₅	4.39	4.81	4.96
Im_CH ₂ OC ₄ H ₉	0.91	1.37	1.46
Im_CH ₂ OC ₅ H ₁₁	1.35	1.81	1.91
Im_CH ₂ OC ₆ H ₁₃	1.80	2.26	2.35
Im_CH ₂ OC ₇ H ₁₅	2.24	2.70	2.80
Im_CH ₂ OC ₈ H ₁₇	2.69	3.15	3.24
Im_CH ₂ OC ₉ H ₁₉	3.13	3.59	3.69
Im_CH ₂ OC ₁₀ H ₂₁	3.57	4.04	4.13
Im_CH ₂ OC ₁₁ H ₂₃	4.02	4.48	4.58
Im_CH ₂ OC ₁₂ H ₂₅	4.39	4.81	4.96

* Im represents imidazolium ring and the part after the underline represents 1-alkyl-, 1-alkoxymethyl side chains.

3.4 The nature of electrostatic interactions in 1-ethyl-3-methylimidazolium acetate.

3.4.1 A topological assessment of C – H – – O electrostatic interactions.

A topological analysis of the electronic charge density of in the inter-ionic region of 1-ethyl-3-methylimidazolium acetate was performed using the principles of the theory of Atoms in Molecules and a set of criteria reported earlier (p. 44). The assessment was performed by the MORPHY98 program using the Gaussian 03 wavefunction files describing the equilibrium geometry of 1-ethyl-3-methylimidazolium acetate generated at the HF and MP2 levels of the electronic structure theory (EST). The MP2 level of the EST was evoked for the topological analysis of the C – H – – O interactions because it is more accurate in the estimation of the electron correlation energy than the HF method. The correlation energy is especially important for weak inter-atomic interactions such as hydrogen bonds which are formed by the outer regions of the electronic charge clouds of the atoms which are easily distorted. Hence, the results of the topological analysis of the MP2 electronic charge density should be regarded as the primary results, and the results from the topological analysis of the HF electronic charge density should be regarded as complimentary.

Both, HF and MP2 geometry optimizations of 1-ethyl-methylimidazolium acetate were started from the same force field geometry of the chemical structure. Initially, identical convergence criteria were used for both methods.

These criteria were as follows:

Maximum force	0.000015 Hartree
RMS force	0.000010 Hartree
Maximum displacement	0.000060 Bohr
RMS displacement	0.000040 Bohr

A stationary point was found in both optimizations. However, the analysis of the vibrational frequencies established that the MP2 optimized geometry of 1-ethyl-3-methylimidazolium acetate was at a transitional state because several imaginary frequencies were computed. Hence, the optimization of the structure was repeated from the force field geometry with tighter convergence criteria, which were as follows:

Maximum force	0.000450 Hartree
Root mean squared force	0.000300 Hartree
Maximum displacement	0.001800 Bohr
RMS displacement	0.001200 Bohr

The frequency analysis of the geometry of 1-ethyl-3-methylimidazolium acetate optimized with tighter convergence criteria established that the chemical structure was at its potential energy minimum.

Geometrical parameters of the inter-ionic region of 1-ethyl-3-methylimidazolium acetate at the equilibrium geometry established at the HF and the MP2 levels of the EST are reported in the Table 7 (Figure 16). Only the geometry of 1-ethyl-3-methylimidazolium acetate illustrated in the Figure 16 was considered in the current study. The choice of this geometry was

influenced by the publications of Dhumal and colleagues (Dhumal et al., 2009) and Bowron and colleagues (Bowron et al., 2010) which were based on a combined experimental and theoretical data and concluded that the $N_1 - C_5 - N_4$ side of the imidazolium ring (Figure 16) was the most likely side of the anion approach. The approach of an anion from the $N_1 - C_5 - N_4$ side of the imidazolium ring also agrees with the reactivity scale of Allerhand and colleagues (Allerhand et al., 1963) which groups the C – H group to act as a proton donor for a hydrogen bond formation decreases with the increase of the orbital hybridization of the carbon atom, and increases with the number of electron withdrawing groups attached to it. All of the carbon atoms in the imidazolium ring are sp^2 hybridized. However, the C_5 carbon atom (Figure 16) has two nitrogen atoms attached to it, hence, it has stronger proton donating ability than the C_2 and C_3 carbon atoms of the imidazolium ring.

However, the above in -plane approach is only one of several possible approaches of the acetate anion towards the imidazolium ring. Thus, an out-of-plane approach of anions towards the imidazolium ring have been reported (Matthews et al., 2014). In addition, alternative conformations of the alkyl side chains are possible on the approach of an anion towards mono- or di-substituted imidazolium cation. These are due to internal rotations of the side chains. However, these side chain rotations do not directly affect the acidity of the acidic hydrogen atom (Niedermeyer et al., 2013), i.e. the hydrogen atom in $C_5 - H_9$ bond.

Table 7. Distances between the atoms of 1-ethyl-3-methylimidazolium cation and the acetate anion facing the inter-ionic region.

Interacting atoms	Distance			
	HF		MP2	
	au	Å	au	Å
$C_6 - H_{17}$	2.04	1.08	2.07	1.09
$C_5 - H_9$	2.03	1.07	2.08	1.10
$C_{10} - H_{15}$	2.04	1.08	2.08	1.10
$C_6 - N_1$	2.78	1.47	2.81	1.49
$N_1 - C_5$	2.50	1.32	2.57	1.36
$C_5 - N_4$	2.51	1.33	2.57	1.36
$N_4 - C_{10}$	2.79	1.48	2.83	1.50
$C_{20} - O_{21}$	2.40	1.27	2.49	1.32
$C_{20} - O_{22}$	2.40	1.27	2.48	1.31

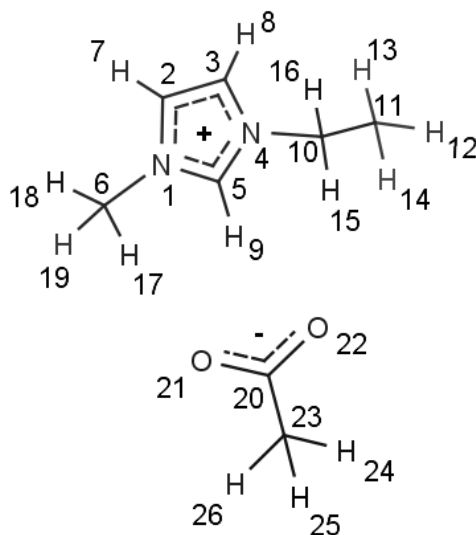


Figure 16. An atomic numbering scheme in 1-ethyl-3-methylimidazolium acetate.

The analysis of the computed bond lengths in the structure of 1-ethyl-3-methylimidazolium acetate established that the positive charge was concentrated on the C₅ carbon atom rather than on either of the nitrogen atoms because the C₅ – N₁ and C₅ – N₄ bond lengths were the same at the MP2 level of the EST. This is supported by the idea of the Ingold's mesomeric effect (Ingold, 1934), which is also known as a resonance, which Ingold defined as a permanent state of a polarizability within a chemical structure in which the system is permanently in-between non-polar and dipolar forms. Thus in a 1-ethyl-3-methylimidazolium cation the electronic charge is in a permanent dynamic state of delocalization around the imidazolium ring which provides additional stability of a chemical structure, and potentially leads to the formation of a stable carbene. Carbene is a chemical species with a divalent carbon atom. Imidazolium carbenes are formed when the carbon atom in N – C – N bond of the imidazolium ring, i.e. C₅ in the Figure 16 (p. 95), loses its hydrogen atom. Imidazolium carbenes are stable due to the resonance but still active. These chemical species are active nucleophiles and will react with metals and p-block elements (Hopkinson et al., 2014). The above could potentially affect their ability to reach a bacterial cell surface to form an initial electrostatic contact with the functional groups on it. For example, theoretical investigation of formation of 1-ethyl-3-methyl imidazolium carbene in the presence of acetate anion, and its reactivity towards glucose has been published (Du et al., 2011).

3.4.1.1 Terminology of the theory of Atoms in Molecules.

Terminology which is used in the context of the theory of Atoms in Molecules was introduced by Bader during its development (Bader, 1990). The terminology is rooted in the terminology of Linear Algebra. The correlation between the terms used in the Atoms in Molecules theory and in Linear Algebra is illustrated in the Figure 17.

Bader's terminology	Linear Algebra terminology
Bond critical point (BCP)	Saddle critical point (SCP)
Atomic interaction line (AIL)	Diverging trajectory
Nuclear critical point (NCP)	Node critical point (NCP)
Interatomic surface (IAS)	Two converging trajectories

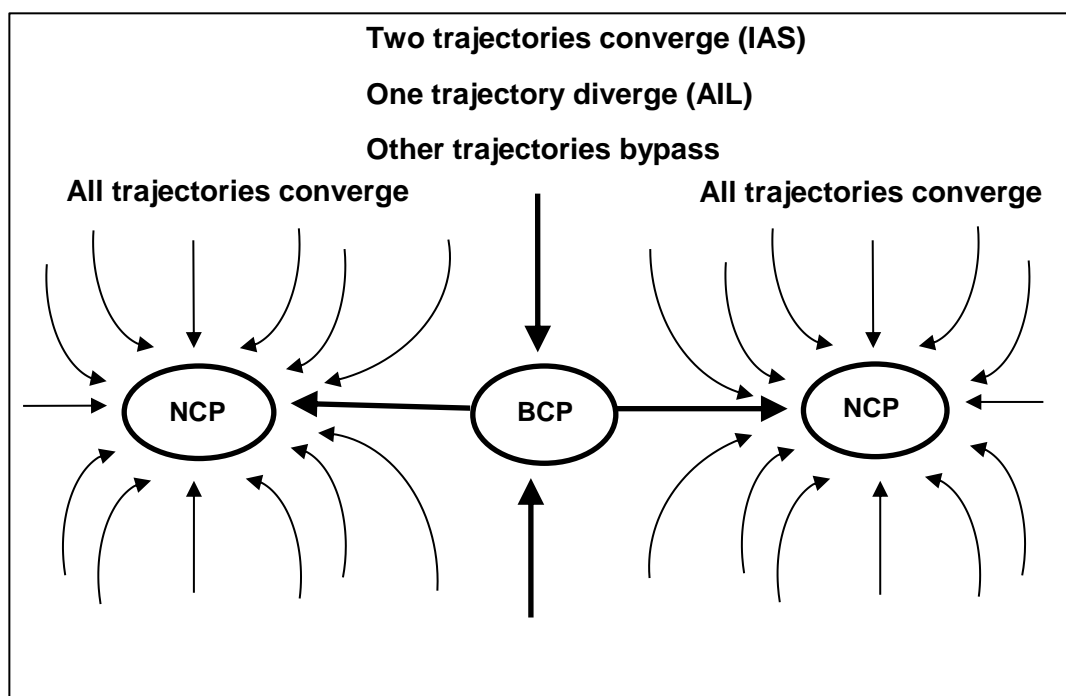


Figure 17. Schematics of the topological portrait of electronic charge distribution in the region between two interacting atoms.

3.4.1.2 Assessment criteria, results and discussions.

The assessment of the nature of C–H–O electrostatic interactions in the equilibrium geometry of 1-ethyl-3-methylimidazolium acetate was conducted using the set of topological criteria listed earlier (p. 44). The atomic numbering scheme for the inter-ionic region of 1-ethyl-3-methylimidazolium acetate is illustrated in Figure 18. Four ring critical points, which are critical points in the electronic charge density formed by a ring of bond critical points were found within each structure. The presence of ring critical points in the geometry of 1-ethyl-3-methylimidazolium acetate at the HF and the MP2 level of the EST indicated that the geometry was topologically stable.

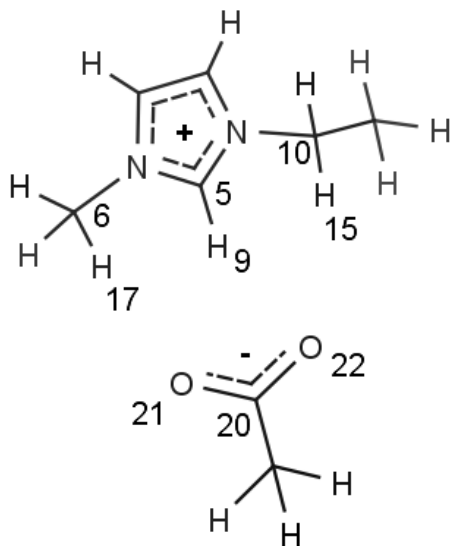


Figure 18. The atomic labelling scheme of the inter-ionic region of 1-ethyl-3-methylimidazolium acetate.

Criterion 1: The presence of a bond critical point and an atomic interaction line between the hydrogen and oxygen atoms.

Results:

Bond critical points and corresponding atomic interaction lines were found in four H – O inter-ionic regions of electronic charge density of 1-ethyl-3-methylimidazolium acetate (Figure 19, p. 101; Figure 20, p. 102). These points were shifted from the midpoint of the computed H – O distances towards the hydrogen atoms in all of the interactions (Table 8). The distances were computed in the MATLAB 7.10 program and in the MORPHY98 program.

Table 8. Inter-atomic distances in H – O interactions, and the distances between the atoms and a bond critical point. The conversion of atomic units into SI unit in the current table and all of the tables in the current chapter is performed using conversion factors from Koch and Popelier, 1995. These factors were as follows:

distance (5.29×10^{-11} m), electronic charge density (1.08×10^{12} C m⁻³), the Laplacian of charge density (3.86×10^{32} C m⁻⁵), dipole moment (8.48×10^{-30} C m).

Level of the EST	Atoms	Distance (MATLAB)				Distance (MORPHY98)					
		Total		Midpoint		Total		H - BCP		O - BCP	
		au	Å	au	Å	au	Å	au	Å	au	Å
HF	H ₉ ⁻ -O ₂₁	3.96	2.10	1.98	1.05	3.97	2.09	1.47	0.78	2.50	1.32
	H ₉ ⁻ -O ₂₂	3.69	1.95	1.84	0.97	3.70	1.96	1.33	0.70	2.37	1.25
	H ₁₇ ⁻ -O ₂₁	4.21	2.23	2.10	1.11	4.22	2.23	1.65	0.87	2.57	1.36
	H ₁₅ ⁻ -O ₂₂	4.63	2.45	2.31	1.22	4.65	2.46	1.87	0.99	2.78	1.47
MP2	H ₉ ⁻ -O ₂₁	3.53	1.87	1.76	0.93	3.53	1.87	1.24	0.66	2.29	1.21
	H ₉ ⁻ -O ₂₂	4.18	2.21	2.09	1.11	4.18	2.21	1.57	0.83	2.61	1.38
	H ₁₇ ⁻ -O ₂₁	4.78	2.53	2.39	1.26	4.80	2.54	1.93	1.02	2.87	1.52
	H ₁₅ ⁻ -O ₂₂	4.04	2.14	2.02	1.07	4.06	2.15	1.58	0.83	2.48	1.31

NB. 1 atomic unit of length is equal to 5.29×10^{-11} m.

Discussion:

The electronic charge density of an atom is a continuous differentiable function of a distance from its nucleus. In a chemical structure, this continuity of electronic charge density will continue if distances between neighbouring atoms are shorter than their free radii because at these distances the electronic charge clouds of neighbouring atoms form shared inter-atomic boundaries. These inter-atomic boundaries unify the electronic charge of the whole chemical structure, and its electronic charge density becomes a continuous differentiable function of the atomic coordinates. In the context of the Atoms in Molecules theory, a chemical structure is a continuous network of topological atoms which are finite non-overlapping volumes of a topological space. Each topological atom is centered around a nuclear critical point and its boundaries are determined by positions of inter-atomic surfaces on all of its interacting sides. A non-interacting side of a topological atom is defined by a cut-off point which is set to 0.001 au for atoms in a gas phase.

In Linear Algebra, the continuity of a differentiable function in a region defined by two critical points is confirmed by the presence of another critical point between them. This confirmation is based on Rolle's theorem developed as early as 1690 (Thomas and Finney, 1996). Topologically, atomic nuclei are critical points. The distance between the neighbouring atoms is an interval in which another critical point will be found if the electronic charge distribution between them is continuous. The data in the Table 8 (p. 99) show that the critical points were computed within all reported H – – O distances. This establishes that the electronic charge distribution between all

pairs of the hydrogen atom and the oxygen atom in the inter-ionic region of 1-ethyl-3-methylimidazolium acetate is continuous. Consequently, the atoms are interacting with each other. Reported in Table 8 (p. 99) are shifts of bond critical points from mid-points of the inter-atomic distances, which were observed in all H – – O bond critical points are related to unequal contributions of the electronic charges of the interacting atoms towards the inter-atomic boundary.

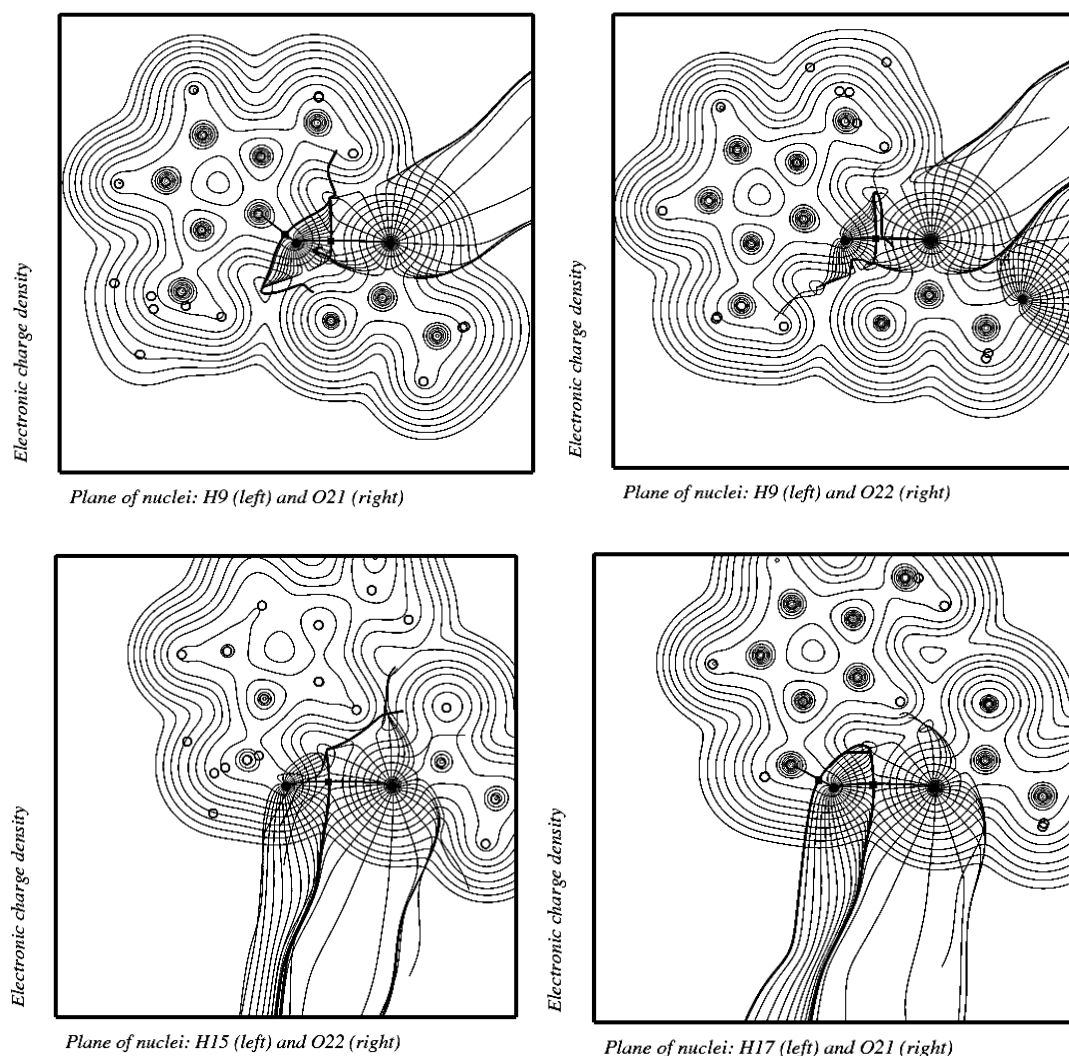


Figure 19. Bond critical points and atomic interaction lines observed in H – – O interactions of 1-ethyl-3-methylimidazolium acetate in HF electronic charge

density. The dark coloured circles represent nuclei lying within the plane. The hydrogen atoms are positioned on the left side of a bond critical point and the oxygen atoms are on the right side. The straggling lines are the gradient paths lying outside of the plane.

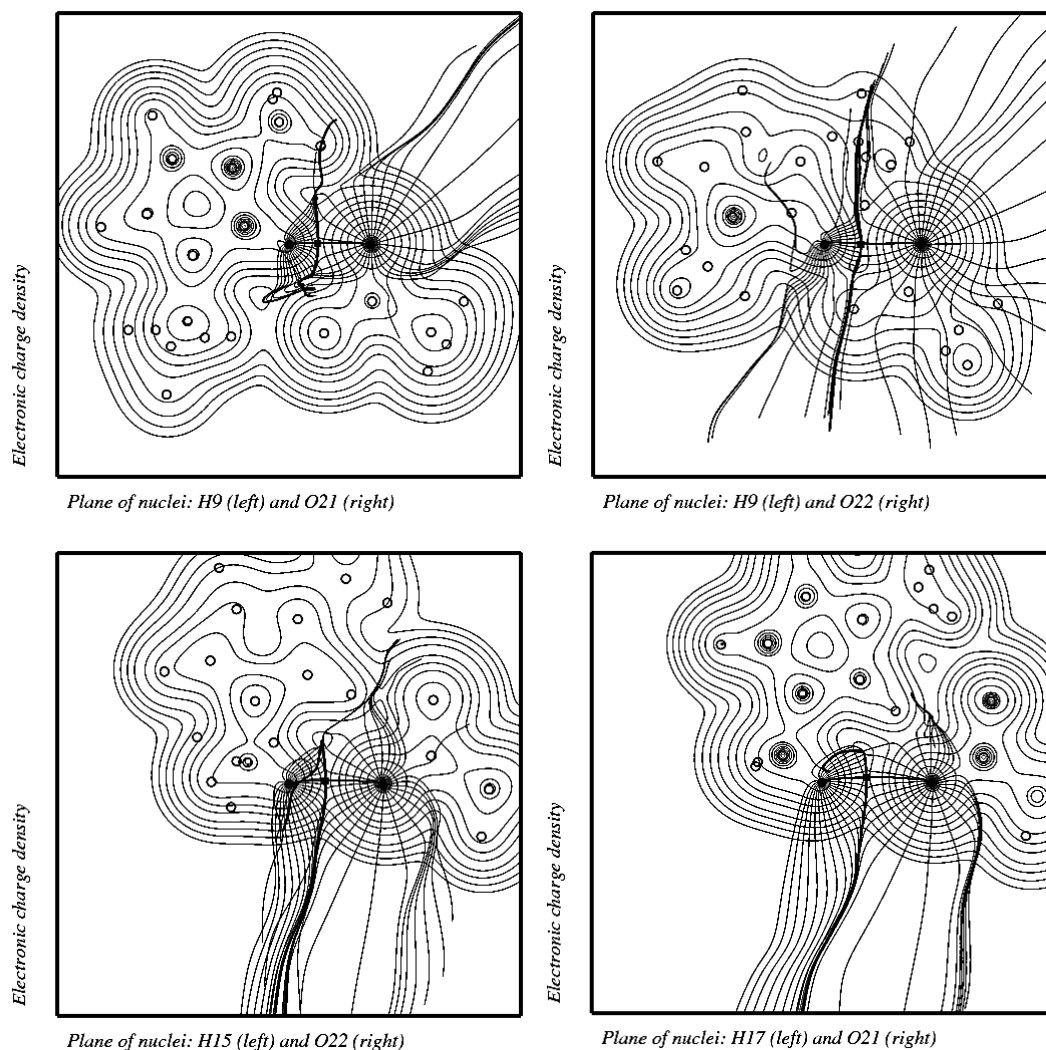


Figure 20. Bond critical points and atomic interaction lines observed in H—O interactions of 1-ethyl-3-methylimidazolium acetate in MP2 electronic charge density. The dark coloured circles represent nuclei lying within the plane. The hydrogen atoms are positioned on the left side of a bond critical point and the oxygen atoms are on the right side. The straggling lines are the gradient paths lying outside of the plane.

Criterion 2: The electronic charge density at a H – – O bond critical point must be within the range of 0.002 – 0.034 au.

Results:

Electronic charge density of all reported H – – O bond critical points was within the required range (Table 9).

Table 9. The values of HF and MP2 electronic charge density of H – – O bond critical points of 1-ethyl-3-methylimidazolium acetate.

Interacting atoms	Electronic charge density			
	HF		MP2	
	au	$\times 10^{10} \text{ Cm}^{-3}$	au	$\times 10^{10} \text{ Cm}^{-3}$
H ₉ - -O ₂₁	0.021	2.258	0.033	3.611
H ₉ - -O ₂₂	0.028	3.001	0.017	1.805
H ₁₇ - -O ₂₁	0.014	1.554	0.007	0.813
H ₁₅ - -O ₂₂	0.009	0.984	0.018	1.910

Discussion:

Electronic charge density of a chemical structure is a function of its atomic coordinates. It has the highest values at the positions of nuclei and the lowest values at the outer boundaries of electronic charge clouds of atoms. A bond critical point is located on an inter-atomic boundary where the electronic charge clouds of two atoms interact. The position of this boundary depends on the strength of an inter-atomic interaction which is topologically defined by

their distance from each other. For every inter-atomic interaction there is the shortest and the longest inter-atomic distances at which topologically detectable inter-atomic interactions are possible. Topologically, the strength of an inter-atomic interaction is evaluated by the electronic charge density of an electronic charge cloud of an atom involved in the inter-atomic interaction. The electronic charge density of an atom is a function of a distance from its nucleus. Hence, the strength of inter-atomic interactions increases with the decrease of the distance between the atoms because deeper regions of their electronic charge clouds (with higher electronic charge density) contribute to the shared inter-atomic boundary.

The shortest feasible inter-atomic distance will be largely governed by nuclear-nuclear repulsions, and the longest feasible inter-atomic distance will depend on the initial size of electronic charge clouds of atoms. Thus, the longest feasible inter-atomic distance depends on an ability of atoms to approach each other close enough for their electronic charge clouds to form an inter-atomic boundary, because only then will the continuity of the electronic charge density be preserved. Therefore, the longest feasible inter-atomic distance for two interacting atoms must be equal to or less than the sum of their free radii.

In the context of the Atoms in Molecules theory, free radii of atoms are defined by distances from a nuclear critical point to a threshold value of electronic charge density which, in the current study, was set to 0.001 au. The imposed constraint on the outer contour of an electronic charge density of an atom means that its value at a bond critical point cannot be less than 0.002 au because of the mutual contribution of to the inter-atomic boundary. Consequently, this value will characterise weak inter-atomic interactions

formed at the longest feasible inter-atomic distances. Hence, the presence of a bond critical point at the values of electronic charge density higher than 0.002 au will indicate stronger inter-atomic interactions due to shorter inter-atomic distances. The above correlation is observed for the data reported in the Table 9 (p. 103) for H – – O inter-ionic interactions in the HF and the MP2 electronic charge density of 1-ethyl-3-methylimidazolium acetate.

Criterion 3: The Laplacian of the electronic charge density at a bond critical point must be within the range of 0.024 - 0.139 au.

Results:

Values of the Laplacian of the HF and MP2 electronic charge density at bond critical points of 1-ethyl-3-methylimidazolium acetate and the corresponding eigenvalues are summarized in Tables 10 and 11 respectively.

Table 10. The Laplacian of the HF electronic charge density at the H – – O bond critical points of 1-ethyl-3-methylimidazolium acetate.

Interacting atoms	The Laplacian of the electronic charge density		Eigenvalues of the Laplacian		
	au	$\times 10^{31} \text{ Cm}^{-5}$	au		
H ₉ - -O ₂₁	0.075	2.909	-0.0246	-0.0195	0.1195
H ₉ - -O ₂₂	0.095	3.677	-0.0363	-0.0354	0.1669
H ₁₇ - -O ₂₁	0.057	2.210	-0.0156	-0.0154	0.0883
H ₁₅ - -O ₂₂	0.038	1.479	-0.0090	-0.0083	0.0556

Table 11. The Laplacian of the MP2 electronic charge density at the H–O bond critical points of 1-ethyl-3-methylimidazolium acetate.

Interacting atoms	The Laplacian of the electronic charge density		Eigenvalues of the Laplacian		
	au	$\times 10^{31} \text{ Cm}^{-5}$	au		
H ₉ -O ₂₁	0.111	4.278	-0.0473	-0.0462	0.2043
H ₉ -O ₂₂	0.065	2.493	-0.0181	-0.0076	0.0903
H ₁₇ -O ₂₁	0.032	1.250	-0.0073	-0.0063	0.0460
H ₁₅ -O ₂₂	0.069	2.648	-0.0205	-0.0194	0.1085

Discussion:

The Laplacian of electronic charge density is the sum of eigenvalues along the main diagonal of the Hessian of electronic charge density which is computed as:

$$\text{The Hessian}(\rho) = \begin{bmatrix} \frac{\partial^2 \rho}{\partial x^2} & \frac{\partial^2 \rho}{\partial x \partial y} & \frac{\partial^2 \rho}{\partial x \partial z} \\ \frac{\partial^2 \rho}{\partial y \partial x} & \frac{\partial^2 \rho}{\partial y^2} & \frac{\partial^2 \rho}{\partial y \partial z} \\ \frac{\partial^2 \rho}{\partial z \partial x} & \frac{\partial^2 \rho}{\partial z \partial y} & \frac{\partial^2 \rho}{\partial z^2} \end{bmatrix}$$

The signs and the magnitudes of these eigenvalues specify the vertical direction and the rate of change of electronic charge density from a bond critical point in the direction of nuclear critical points. Thus, the negative eigenvalues show that electronic charge density is at its maximum at a bond critical point, and a positive eigenvalue shows the opposite. Therefore, at a

bond critical point, negative eigenvalues are computed along trajectories on an inter-atomic surface, and a positive eigenvalue is computed along a trajectory in the directions of atomic nuclei (Figure 17, p. 97). Consequently, the sign of the Laplacian of electronic charge density at a bond critical point shows the preference of electronic charge to accumulate at an inter-atomic surface or to disperse from it. The accumulation of the electronic charge in an inter-atomic region is observed in covalent bonds and its dispersion from an inter-atomic surface towards individual atoms is noted in electrostatic interactions. The data in the Table 10 (p. 105) and the Table 11 (p. 106) characterise the H – – O inter-ionic interactions in 1-ethyl-3-methylimidazolium acetate as electrostatic interactions because the Laplacian of the electronic charge density at all of the BCPs is positive, thus, indicating that the dispersion of electronic charge from an inter-atomic surface towards the individual atoms dominates its accumulation on it.

Criterion 4: The radii of atoms in H – – O interaction must be smaller than their free radii.

Results:

In the context of the Atoms in Molecules theory, atomic radii are computed as follows:

- The radius of an atom in an inter-atomic interaction is computed as the distance between its nuclear critical point and a bond critical point.
- A free atomic radius is computed a distance between its nuclear critical point and a defined threshold of electronic charge density, which in the current study was set to 0.001 au.

The atomic radii of the hydrogen atoms and the oxygen atoms in H – – O interactions and their free radii are reported in Table 12, and the changes in the atomic radii upon formation of H – – O interaction are summarized in Table 13 below.

Table 12. The radii of atoms in H – – O inter-ionic interactions and their free atomic radii computed at the HF and the MP2 geometries of 1-ethyl-3-methylimidazolium acetate.

Level of the EST	Interacting atoms	Atomic radius in H – – O interaction (Atom - BCP)				Free atomic radius (Atom - threshold of 0.001 au)			
		H		O		H		O	
		au	Å	au	Å	au	Å	au	Å
HF	H ₉ ⁻ -O ₂₁	1.47	0.77	2.50	1.32	2.29	1.16	4.33	2.29
	H ₉ ⁻ -O ₂₂	1.33	0.71	2.37	1.25	2.29	1.16	3.57	1.89
	H ₁₇ ⁻ -O ₂₁	1.65	0.87	2.57	1.36	2.52	1.33	4.33	2.29
	H ₁₅ ⁻ -O ₂₂	1.87	0.99	2.78	1.47	2.51	1.33	3.57	1.89
MP2	H ₉ ⁻ -O ₂₁	1.24	0.66	2.29	1.21	2.92	1.54	4.04	2.14
	H ₉ ⁻ -O ₂₂	1.57	0.83	2.61	1.38	2.92	1.54	3.55	1.88
	H ₁₇ ⁻ -O ₂₁	1.93	1.02	2.87	1.52	2.51	1.33	4.04	2.14
	H ₁₅ ⁻ -O ₂₂	1.58	0.84	2.48	1.31	2.54	1.34	3.55	1.88

Table 13. Changes in atomic radii of hydrogen atoms and oxygen atoms in H – – O inter-ionic interactions compared to their free radii computed for the HF and the MP2 geometry of 1-ethyl-3-methylimidazolium acetate.

Level of the EST	Interacting atoms	Decrease in atomic radii (Free radius - radius in H – – O interaction)			
		H		O	
		au	Å	au	Å
HF	H ₉ - -O ₂₁	0.82	0.43	1.83	0.97
	H ₉ - -O ₂₂	0.96	0.51	1.20	0.63
	H ₁₇ - -O ₂₁	0.87	0.46	1.76	0.93
	H ₁₅ - -O ₂₂	0.64	0.34	0.79	0.42
MP2	H ₉ - O ₂₁	1.68	0.89	1.75	0.93
	H ₉ - O ₂₂	1.35	0.71	0.94	0.50
	H ₁₇ - O ₂₁	0.58	0.31	1.17	0.62
	H ₁₅ - O ₂₂	0.96	0.51	1.07	0.57

Discussion:

A bond critical point is computed between the two atoms when the electronic charge density in their inter-atomic region is continuous (and differentiable). It was reported earlier (p. 100) that the continuity of the electronic charge distribution is achieved when the inter-atomic distance between the two atoms is equal to or less than the sum of their free atomic radii. Hence, the computed decrease in atomic radii will be observed in most instances when a bond critical point is found. However, there are some exceptions. Thus, Koch and Popelier reported two instances when the radius of a hydrogen atom in C–H––Cl interaction increased compared to its free radii (Figure 21) (Koch and Popelier, 1995). A decrease in the atomic radii was computed in all

H – – O inter-ionic interactions of 1-ethyl-3-methylimidazolium acetate reported in the Table 13 (p. 109).

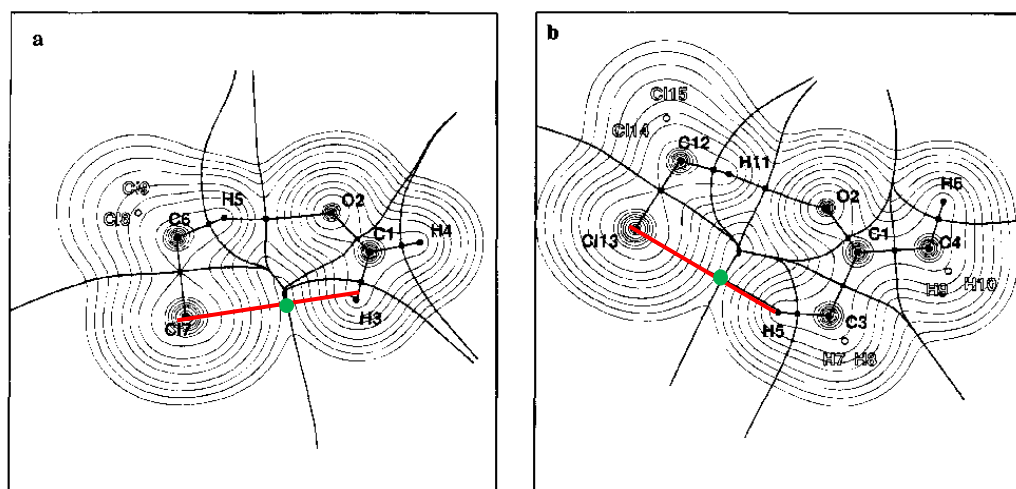


Figure 21. Topological portraits of (a) formaldehyde - chloroform and (b) acetone - chloroform van der Waals complexes. Red lines highlight H – – Cl atomic interaction lines. Green circles represent bond critical points. Adapted with permission from the publisher from Koch and Popelier, 1995. Copyright 2013 American Chemical Society. The licence for this reprint is included in Appendix 1.

Criterion 5: The electronic charge on a hydrogen atom in H – – O interaction must decrease compared to its free electronic charge.

Results:

The differences between electronic charges on hydrogen atoms in their free states and in H – – O inter-ionic interactions in HF and MP2 geometry are summarized in Table 14 and 15 respectively.

Table 14. Changes in electronic charge on hydrogen atoms upon formation of H – – O inter-ionic interactions compared to their free radii computed in the HF geometry of 1-ethyl-3-methylimidazolium acetate.

Interacting atoms	Electronic charge on a hydrogen atom					
	Free state		H – – O interaction		Difference	
	au	$\times 10^{-19}$ C	au	$\times 10^{-19}$ C	au	$\times 10^{-19}$ C
H ₉ ⁻ -O ₂₁	0.8484	1.3593	0.6582	1.0546	-0.1902	-0.3047
H ₉ ⁻ -O ₂₂	0.8484	1.3593	0.6582	1.0546	-0.1902	-0.3047
H ₁₇ ⁻ -O ₂₁	0.8698	1.3936	0.8452	1.3542	-0.0246	-0.0394
H ₁₅ ⁻ -O ₂₂	0.9772	1.5657	0.8935	1.4315	-0.0837	-0.1342

Table 15. Changes in electronic charge on hydrogen atoms upon formation of H – – O inter-ionic interactions compared to their free radii computed in the MP2 geometry of 1-ethyl-3-methylimidazolium acetate.

Interacting atoms	Electronic charge on a hydrogen atom					
	Free state		H – – O interaction		Difference	
	au	$\times 10^{-19}$ C	au	$\times 10^{-19}$ C	au	$\times 10^{-19}$ C
H ₉ ⁻ -O ₂₁	0.8304	1.3305	0.6348	1.0171	-0.1956	-0.3134
H ₉ ⁻ -O ₂₂	0.8304	1.3305	0.6348	1.0171	-0.1956	-0.3134
H ₁₇ ⁻ -O ₂₁	0.8559	1.3713	0.8744	1.4009	0.0185	0.0296
H ₁₅ ⁻ -O ₂₂	0.9663	1.5482	0.8447	1.3534	-0.1218	-0.1216

Discussion:

Bader's atomic charges are calculated by integrating electronic charge density over a topological volume of an atom. The topological volume of an atom is a closed region of space around a nuclear critical point defined by its distances with bond critical points and a threshold value of the electronic charge density on its non-interacting side, which in the current study was set

to 0.001 au. Hence, a decrease in the electronic charge of a hydrogen atom in H – – O interaction compared to its electronic charge in a free state indicates that some of it was permanently donated towards an inter-atomic boundary. The data in the Table 14 (p. 111) show that this decrease in the electronic charge of a hydrogen atom was computed in all H – – O inter-ionic interactions in the HF geometry of 1-ethyl-3-methylimidazolium acetate. However, the data in Table 15 (p. 111) for the MP2 geometry of the salt show that the decrease in the electronic charge was computed in three out of four H – – O inter-ionic interactions. Thus, an increase in the electronic charge on the hydrogen atom was computed in the $H_{17} - - O_{21}$ interaction which involves the hydrogen atom of the methyl group on an imidazolium ring (Figure 16, p. 95), hence, indicating that a permanent transfer of electronic charge from the hydrogen atom towards the inter-atomic boundary in $H_{17} - - O_{21}$ did not occur.

Criterion 6: The total atomic energy of the hydrogen atom in H – – O interaction must decrease compared to the total atomic energy of its free state.

Results:

The differences between the total atomic energies of hydrogen atoms in their free states and in H – – O inter-ionic interactions in HF and MP2 geometry are summarized in Tables 16 and 17 respectively.

Table 16. Total atomic energies of free hydrogen atoms and their energy in H – – O inter-ionic interactions in the HF geometry of 1-ethyl-3-methylimidazolium acetate.

Interacting atoms	Atomic energy of the hydrogen atom					
	Free state		H – – O interaction		Difference	
	au	$\times 10^3$ kJ/mol	au	$\times 10^3$ kJ/mol	au	$\times 10^3$ kJ/mol
H ₉ - -O ₂₁	-0.5598	-1.4698	-0.4780	-1.2550	-0.0818	-0.215
H ₉ - -O ₂₂	-0.5598	-1.4698	-0.4780	-1.2550	-0.0818	-0.215
H ₁₇ - -O ₂₁	-0.5661	-1.4863	-0.5628	-1.4776	-0.0033	-0.009
H ₁₅ - -O ₂₂	-0.6254	-1.6420	-0.5907	-1.5509	-0.0347	-0.091

Table 17. Total atomic energies of free hydrogen atoms and their energy in H – – O inter-ionic interactions in the HF geometry of 1-ethyl-3-methylimidazolium acetate.

Interacting atoms	Atomic energy of the hydrogen atom					
	Free state		H – – O interaction		Difference	
	au	$\times 10^3$ kJ/mol	au	$\times 10^3$ kJ/mol	au	$\times 10^3$ kJ/mol
H ₉ - -O ₂₁	-0.5428	-1.4251	-0.4550	-1.1946	-0.0878	-0.230
H ₉ - -O ₂₂	-0.5428	-1.4251	-0.4550	-1.1946	-0.0878	-0.230
H ₁₇ - -O ₂₁	-0.5514	-1.4477	-0.5670	-1.4887	0.0156	0.041
H ₁₅ - -O ₂₂	-0.6121	-1.6071	-0.5618	-1.4750	-0.0503	-0.132

Discussion:

Bader's total atomic energy is computed by integrating the total atomic energy density of an atom over its topological volume, which was defined earlier (p. 111). A decrease in the total atomic energy of a hydrogen atom in an H – – O interaction compared to its free state indicates an energetic

destabilization of an atom compared to its free state, which is caused by the transfer of electronic charge from the hydrogen atom towards the inter-atomic boundary. Therefore, the energetic destabilization of a hydrogen atom in H – – O interaction is observed alongside the decrease of its electronic charge. The data reported in Table 16 (p. 113) show that that decrease was computed in all H – – O inter-ionic interactions in the HF geometry of 1-ethyl-3-methylimidazolium acetate. The decrease in the total atomic energy was also observed in all of the H – – O inter-ionic interactions in the MP2 geometry of 1-ethyl-3-methylimidazolium acetate for which a decrease in the electronic charge of a hydrogen atom was reported (Table 17, p. 113). Consequently, the only H – – O inter-ionic interaction of the salt for which a decrease in the total atomic energy of a hydrogen atom was not computed was the H₁₇ – – O₂₁ interaction.

Criterion 7: Dipolar polarization of a hydrogen atom in H – – O interaction must decrease compared to its dipolar polarization in a free state.

Results:

The differences between dipolar polarization of hydrogen atoms in their free states and in H – – O inter-ionic interactions in HF and MP2 geometry are summarized in Tables 18 and 19 respectively.

Table 18. Dipolar polarization of free hydrogen atoms and their dipolar polarization in H – – O inter-ionic interactions in the HF geometry of 1-ethyl-3-methylimidazolium acetate.

Interacting atoms	Dipolar polarization of a hydrogen atom					
	Free state		H – – O interaction		Difference	
	au	$\times 10^{-30}$ Cm	au	$\times 10^{-30}$ Cm	au	$\times 10^{-30}$ Cm
H ₉ ⁻ -O ₂₁	0.1153	0.9776	0.0869	0.7368	0.0284	0.2408
H ₉ ⁻ -O ₂₂	0.1153	0.9776	0.0869	0.7368	0.0284	0.2408
H ₁₇ ⁻ -O ₂₁	0.1183	1.0030	0.1009	0.8555	0.0174	0.1475
H ₁₅ ⁻ -O ₂₂	0.1307	1.1081	0.1076	0.9123	0.0231	0.1958

Table 19. Dipolar polarization of free hydrogen atoms and their dipolar polarization in H – – O inter-ionic interactions in the MP2 geometry of 1-ethyl-3-methylimidazolium acetate.

Interacting atoms	Dipolar polarization of a hydrogen atom					
	Free state		H – – O interaction		Difference	
	au	$\times 10^{-30}$ Cm	au	$\times 10^{-30}$ Cm	au	$\times 10^{-30}$ Cm
H ₉ ⁻ -O ₂₁	0.1126	0.9547	0.0814	0.6901	0.0312	0.2645
H ₉ ⁻ -O ₂₂	0.1126	0.9547	0.0814	0.6901	0.0312	0.2645
H ₁₇ ⁻ -O ₂₁	0.1160	0.9835	0.1067	0.9046	0.0093	0.0788
H ₁₅ ⁻ -O ₂₂	0.1288	1.0920	0.0988	0.8377	0.0300	0.2543

Discussion:

A dipolar polarization of an atom quantifies the degree of asymmetry of its electronic charge cloud around the nucleus caused by the presence of an interacting atom with it. It counter-balances the transfer of an electronic charge from an atom towards an inter-atomic boundary, and it accompanies the decrease in the electronic charge of a hydrogen atom in H – – O

interaction. The decrease in dipolar polarization of hydrogen atoms in its $H \cdots O$ inter-ionic interactions of 1-ethyl-3-methylimidazolium acetate was computed for all of the interactions in its HF geometry, and for all interactions in MP2 geometry. A small decrease in dipolar polarization of the hydrogen atom in $H_{17} \cdots O_{21}$ interaction was computed despite the absence of the decrease in the electronic charge of this atom. The electronic charge of a hydrogen atom and its dipolar polarization are computed within a defined topological volume of an atom. Herein, an attempt to develop an equation which could be used to calculate a point dipole moment directly at a bond critical point between two atoms was made (Eq. 17).

$$\mu_{\text{bcp}} = \frac{\rho^3}{(\nabla^2 \rho)^2} \quad (\text{Eq. 17})$$

where:

μ_{bcp} is a dipole moment of the electronic charge density at a bond critical point.

ρ is the electronic charge density at a bond critical point (C m^{-3}).

$\nabla^2 \rho$ is the Laplacian of the electronic charge density at a bond critical point (C m^{-5}).

The development of the above equation was motivated by the fact that any chemical structure is a dynamic system in which electronic charge is in a constant movement. A bond critical point is a stationary point in the electronic charge density of a chemical structure, and any property evaluated at that point has a constant value. Currently, the topological dipole moment is a

property which depends on the accuracy of the computed topological volume of an atom. A developed equation eliminates this dependency because it estimates the dipole moment at a stationary point at an inter-atomic boundary. The equation was derived by correlating the electronic charge density at a bond critical point with the rate of its change from the bcp as described by its Laplacian. This was performed by equalizing the SI units of the electronic charge density and its Laplacian so that a vector of an electronic charge distribution could be obtained:

$$\mu_{\text{bcp}} = \frac{\left(\frac{\text{C}}{\text{m}^3}\right)^3}{\left(\frac{\text{C}}{\text{m}^5}\right)^2} = \frac{\frac{\text{C}^3}{\text{m}^9}}{\frac{\text{C}^2}{\text{m}^{10}}} = \frac{\text{C}^3}{\text{m}^9} \times \frac{\text{m}^{10}}{\text{C}^2} = \text{C m}$$

where:

C m is the SI unit of a dipole moment

$\frac{\text{C}}{\text{m}^3} = \text{C m}^{-3}$ is the SI unit of electronic charge density

$\frac{\text{C}}{\text{m}^5} = \text{C m}^{-5}$ is the SI unit of the Laplacian of electronic charge density

The point dipole moments at BCPs of H – O interactions in 1-ethyl-3-methylimidazolium acetate are reported in Table 20.

Table 20. Point dipole moments at bond critical points of H – – O interactions computed in the HF and MP2 geometry of 1-ethyl-3-methylimidazolium acetate.

Interacting atoms	Dipole moment at a BCP	
	HF geometry	MP2 geometry
	$\times 10^{-30}$ C m	
H ₉ - -O ₂₁	0.0136	0.0257
H ₉ - -O ₂₂	0.0201	0.0094
H ₁₇ - -O ₂₁	0.0768	0.0034
H ₁₅ - -O ₂₂	0.0043	0.0099

The data show that the developed equation (Eq. 17, p. 116) was capable of computing the point dipole moments at bond critical points of H – – O inter-ionic interactions of 1-ethyl-3-methylimidazolium acetate at its HF and MP2 geometries, qualitatively corresponding with the earlier reported data (p. 99) on the presence of an assymetry of electronic charge clouds of the hydrogen atom and the oxygen atom in H – – O inter-ionic interactions of the salt.

However, at present, the quantitative treatment of the data should not be performed as further research on the meaning of these point dipole moments is necessary. This is largely due to the fact that the Laplacian of the electronic charge density is a summative descriptor of the rates and the directions of change of electronic charge from a bond critical point. Hence, further analysis of the effect of this summative nature of the Laplacian of the electronic charge density on the reliability of the computed point dipole moments is required. The possible research directions of the above are discussed in the Conclusions and Future Work chapter of the current thesis.

Criterion 8: The topological volume of a hydrogen atom in the H – – O interaction must decrease compared to its topological volume in a free state.

Results:

The differences between topological volume of hydrogen atoms in their free states and in H – – O inter-ionic interactions are summarized in Table 21 below.

Table 21. Topological volumes of free hydrogen atoms and their topological volumes in H – – O inter-ionic interactions in the HF and the MP2 geometry of 1-ethyl-3-methylimidazolium acetate.

Interacting atoms	The topological volume of the hydrogen atom (au)					
	Free state		H – – O interaction		Difference	
Level of the EST	HF	MP2	HF	MP2	HF	MP2
H ₉ ⁻ -O ₂₁	39.03	39.14	19.68	19.73	-19.35	-19.41
H ₉ ⁻ -O ₂₂	39.03	39.03	19.68	19.73	-19.35	-19.41
H ₁₇ ⁻ -O ₂₁	40.02	40.28	34.04	38.52	-5.98	-1.76
H ₁₅ ⁻ -O ₂₂	44.31	44.87	37.36	33.29	-6.74	-11.58

Discussion:

The topological volume of an atom is a closed region of space around a nuclear critical point defined by its distances from bond critical points and a threshold value of electronic charge density on its non-interacting side. It was discussed earlier (p. 100) that topological continuity of electronic charge distribution between two atoms is possible when their separation distance is equal to or less than the sum of their free atomic radii. However, a decrease in a topological volume of an atom in an inter-atomic interaction compared to its free state is observed only at the latter inter-atomic distances. Thus, in the

reported data (Table 21, p. 119) a decrease the topological volume of a hydrogen atom was observed in all H – – O inter-ionic interactions of 1-ethyl-3-methylimidazolium acetate salt in its HF and MP2 geometries. However, a computed decrease in the topological volume of the hydrogen atom in the $H_{17} - O_{21}$ interaction of the MP2 geometry of 1-ethyl-3-methylimidazolium acetate was marginal compared to the data for other H – – O inter-ionic interactions of the salt at the MP2 geometry. The decrease in the topological volume of the hydrogen atom in the $H_{15} - O_{22}$ interaction was smaller than for both H – – O interactions involving the H_9 atom. However, it is by an order of magnitude larger than that of the $H_{17} - O_{21}$ interaction, so it cannot be dismissed. It was reported earlier that the MP2 level of the EST is more explicit in its computation of the electron correlation energy than the HF method. Hence, a disagreement between the pattern of the changes in the topological volume of the hydrogen atoms is attributed to the difference in the electronic charge density distribution between the HF and the MP2 methods.

3.5 Quantitative structure-activity relationships.

Herein, the results of a multivariate linear regression of Log(1/MIC) values of imidazolium carboxylates on LogD and QTMS descriptors are reported. The reported statistical parameters for each QSAR are the averages of the 1000 randomizations of a training and a test set of imidazolium carboxylates. Thus, a set of 34 chemical structures was randomly divided into a training and a test sets each containing 17 non-repeating imidazolium carboxylates. This random generation of a training and a test set was repeated 1000 times, and a regression analysis was performed on every computer generated combination.

In the current study a QSAR was considered as statistically significant if the following thresholds were reached:

$$R^2_{\text{predicted}} > 0.80$$

$$R^2 > 0.90$$

The comparison of the predictive ability between the models was conducted by comparing root mean squared error (RMSE) of prediction, which was smaller for models with higher predictivity.

Two additional linear regression relationships were developed prior to generation of QSARs based on the LogD and the QTMS descriptors and Log(1/MIC) values of imidazolium carboxylates. The first linear regression correlated connectivity indices of imidazolium carboxylates with their Log(1/MIC) values to establish if the biological activity of these salt could be described merely by the connectivity of atoms in their chemical structures. The second linear regression correlated LogD and QTMS descriptors to

ensure that they are truly independent in their representation of imidazolium carboxylates.

3.5.1 Linear regression of Log(1/MIC) values of imidazolium carboxylates on their topological connectivity indices.

It was discussed earlier (p. 25) that chemical structures can be encoded as indices, i.e. scalars, rather than as an array descriptors. Herein, four topological indices were assessed for their suitability to encode the chemical structures of imidazolium carboxylates. All of the chosen topological connectivity indices encode a chemical structure based on the patterns of the connectivity of atoms within it. Thus, these descriptors are based purely on the consideration of the neighbouring elements within a chemical structure, and hence, they are very fast to compute. Consequently, these indices were utilized to ensure that the involvement of more computationally demanding QTMS descriptors to encode the chemical structures of imidazolium carboxylates was justified.

Four types of connectivity indices were attempted to be computed in the program Marvin (ChemAxon):

- Balaban index (Balaban, 1982)
- Wiener index (Wiener, 1947)
- Randic index (Randic, 1975)
- Platt index (Platt, 1952)

The distance based algorithms which compute the Balaban index and the Wiener index failed to generate these indices for the imidazolium carboxylates. However, the path based algorithms which compute the Randic

index and the Platt index were successful in their encoding of the salts. Hence, they were correlated with the Log(1/MIC) values of imidazolium carboxylates (Table 22).

Table 22. Statistical parameters quantifying the predictivity of a linear regression model based on the topological connectivity indices of imidazolium carboxylates as an average of 1000 random models.

Statistical parameters	PCA / MLR	PCA / PLS	PLS
R ² predicted	0.16 ±0.32	<0	0.39 ±0.33
R ²	0.38 ±0.20	0.05 ±0.05	0.58 ±0.17
RMSE	2.09 ±0.39	2.63 ±0.21	1.70 ±0.34

The data reported in Table 22 show that a linear correlation between the biological activity of imidazolium carboxylates and their connectivity indices does not exist because both statistical parameters (R² predicted and R²) were below the defined thresholds. An illustrative example of the predictivity this model is reported in Figure 22.

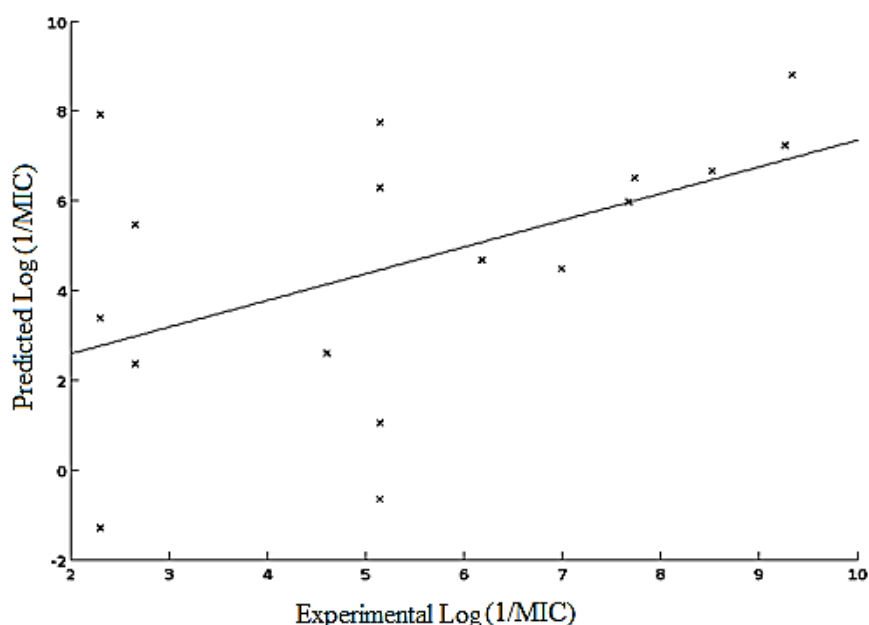


Figure 22. A sample plot of predicted versus experimental Log(1/MIC) values of imidazolium carboxylates by a QSAR based on the topological connectivity indices and the partial least squares regression.

3.5.2 Linear regression of LogD values of imidazolium carboxylates on their QTMS descriptors.

The QTMS descriptors of imidazolium carboxylates were required to predict the LogD values of these salts at pH 7 (Table 23). The LogD values for each structure were encoded as a sum of the LogD value of a cation and the LogD value of an anion at pH 7 (Table 6, p. 91).

Table 23. Statistical parameters of a linear regression model correlating the QTMS descriptors of imidazolium carboxylates with their LogD values as an average of 1000 random models.

Statistical parameters	PCA / MLR	PCA ₁ / PLS ₆	PLS ₆
R ² predicted	<0	0.18 ±0.34	0.25 ±0.29
R ²	0.15 ±0.14	0.33 ±0.18	0.36 ±0.17
RMSE	2.52 ±0.30	2.23 ±0.34	2.18 ±0.34

The data in the Table 23 show that the QTMS descriptors of imidazolium carboxylates could not predict the values of requested LogD descriptors of the salts. An illustrative example of the predictivity of this model is reported in Figure 23. The plot shows that the QTMS descriptors could successfully model the LogD values of some imidazolium carboxylates but failed with the others. It was reported earlier that the LogD values of imidazolium carboxylates for the current regression model were computed as a sum of the LogD values of a cation and an anion at pH 7. Hence, the inability of the QTMS descriptors to successfully compute the LogD values of imidazolium carboxylates refers only to the absence of their correlation with the combined LogD values of the cations and the anions.

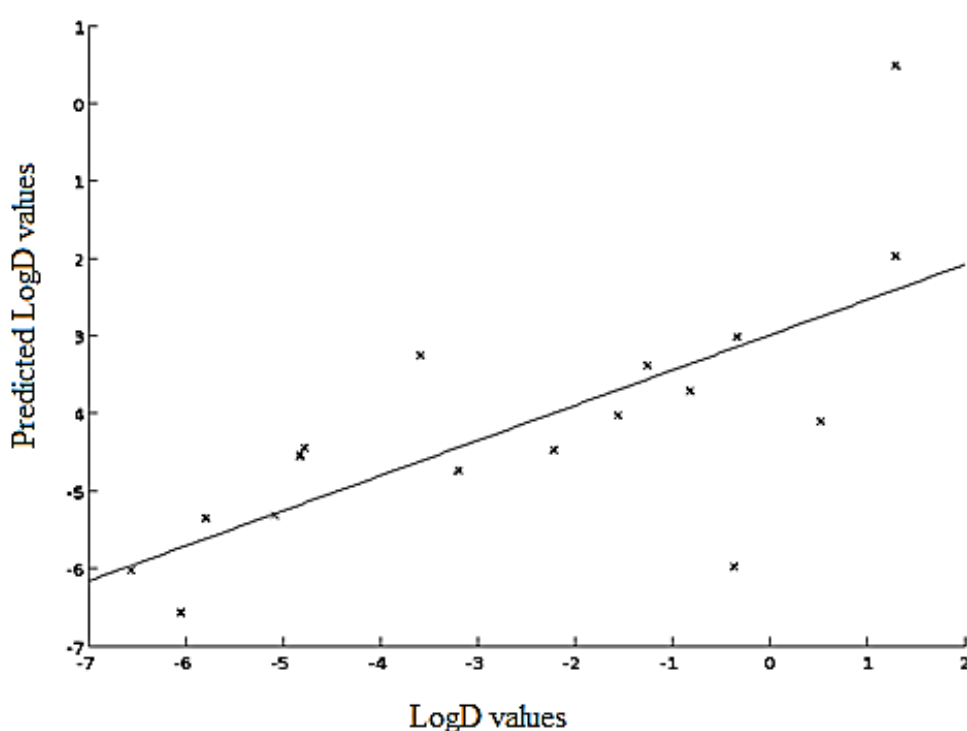


Figure 23. An illustrative plot of predicted versus computed LogD values of imidazolium carboxylates based on the partial least squares regression.

3.5.3 Linear regression of Log(1/MIC) values of imidazolium carboxylates on their LogD and QTMS descriptors.

Statistical parameters evaluating the ability of the QTMS and the LogD descriptors of imidazolium carboxylates to model the Log(1/MIC) values of the salts are reported in Table 24.

Table 24. Statistical parameters quantifying the predictivity of a linear regression model based on the QTMS and the LogD descriptors of imidazolium carboxylates as an average of 1000 random combinations of a training and a test set.

Statistical parameters	PCA ₁ / MLR	PCA ₁ / PLS ₆	PLS ₆
<i>LogD and QTMS full</i>			
R ² predicted	0.75 ±0.21	0.96 ±0.02	0.96 ±0.02
R ²	0.80 ±0.14	0.97 ±0.02	0.97 ±0.02
RMSE	1.13 ±0.37	0.46 ±0.11	0.48 ±0.10
<i>LogD</i>			
R ² predicted	<0	<0	0.83 ±0.10
R ²	0.08 ±0.11	0.06 ±0.08	0.84 ±0.07
RMSE	2.57 ±0.26	2.62 ±0.23	1.04 ±0.21
<i>QTMS full</i>			
R ² predicted	0.64 ±0.32	0.95 ±0.02	0.95 ±0.02
R ²	0.75 ±0.16	0.96 ±0.02	0.95 ±0.02
RMSE	1.30 ±0.39	0.52 ±0.12	0.57 ±0.11

Linear regression of Log(1/MIC) values of imidazolium carboxylates on their QTMS and LogD descriptors established that the two stage mechanism of a biological activity of surface active bactericides (p. 22) can be computationally modelled for these quaternary ammonium salts. Thus, the data in the Table 24 show that either of the theoretical descriptors of imidazolium carboxylates was capable of explaining the biological activity of

these salts towards *Escherichia coli* using partial least squares regression. However, the QSARs based on the QTMS descriptors were more accurate in their prediction of Log(1/MIC) values than the regression models based on the LogD values.

Regression models with a simultaneous inclusion of the QTMS and the LogD descriptors were, overall, more accurate in their prediction of the Log(1/MIC) values of imidazolium carboxylates. Thus, indicating that the LogD values complemented the QTMS descriptors in their description of the whole structures of imidazolium carboxylates in QSARs derived using partial least squares regression. The histograms of the statistical parameters for the statistically significant QSARs (PLS regression) are reported in Figure 24. The histograms below and in the later parts of the thesis illustrate the distribution of the statistical values across 1000 randomly chosen combinations of a test and a training set of imidazolium carboxylates. Thus, the area of each bar in a histogram represents a number of QSARs which had a particular value of a statistical parameter.

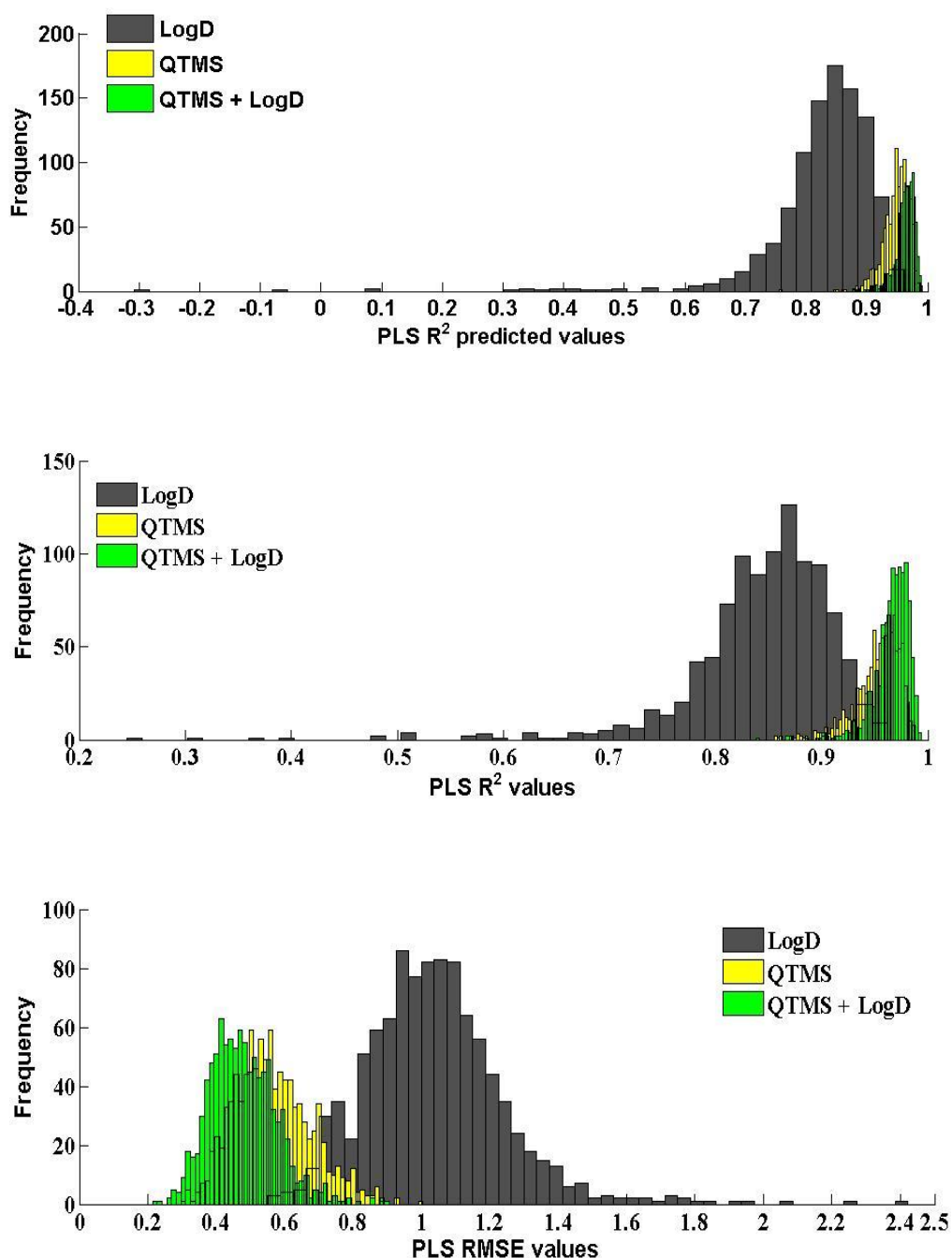


Figure 24. Histograms of QSARs based on the LogD and the QTMS descriptors generated using partial least squares (PLS) regression.

Further theoretical exploration of the two stage mechanism of biological activity of imidazolium carboxylates was conducted by developing QSARs based on the QTMS descriptors of the imidazolium cations only (Table 25). Thus, descriptors of the salts representing the cations only were isolated

from the overall set of descriptors of each imidazolium carboxylate and correlated with Log(1/MIC) values of the salts. An effect of addition of the LogD values of the cations at pH 5, 7 and 9 to the QTMS descriptors of the cations was also evaluated.

Table 25. Statistical parameters quantifying the predictivity of a linear regression model based on the QTMS and QTMS with LogD descriptors of the imidazolium cations as an average of 1000 random combinations of a training and a test set.

Statistical parameters	PCA ₁ / MLR	PCA ₁ / PLS ₆	PLS ₆
<i>QTMS cation</i>			
R ² predicted	<0	0.96 ±0.02	0.96 ±0.02
R ²	0.56 ±0.22	0.96 ±0.02	0.96 ±0.03
RMSE	1.72 ±0.42	0.50 ±0.10	0.49 ±0.12
<i>QTMS cation with LogD</i>			
R ² predicted	<0	0.96±0.02	0.94±0.03
R ²	0.67±0.22	0.96±0.02	0.94±0.03
RMSE	1.47±0.47	0.50±0.11	0.59±0.17

Linear regression analysis of Log(1/MIC) of imidazolium carboxylates on the QTMS descriptors of their imidazolium cations established that the biological activity of these quaternary ammonium salts can be computationally modelled by the isolated electronic properties of the cations. This theoretical conclusion is supported by the experimental observations that the biological activity of quaternary ammonium salts is governed by the chemical structures of their cations (Domagk, 1935). The data in the Table 25 show that the addition of the LogD values of the cations does not affect the predictive ability of QSARs derived using PCA₁/PLS regression. However, it decreases the predictive ability of the QSARs developed using PLS regression. This can be attributed by the differences in the data pre-processing algorithms (p. 75)

The comparison of the QSARs based on the PLS regression reported on Table 24 (p. 126) and Table 25 (p. 129) shows that the predictivity of QSARs based on the QTMS descriptors for imidazolium cations is better than that of the QSARs based on the QTMS descriptors of the whole chemical structures of the salts. However, in a contrast to the latter models, an addition of the LogD values to the QSARs based on the QTMS descriptors of the imidazolium cations decreased their predictivity. This could be explained by referring to the two stage mechanism of the biological activity of quaternary ammonium salts described earlier (p. 22) in which an electrostatic interaction of a cation with a bacterial cell wall is a precursor for its lipophilic incorporation into it. The histograms of the statistical parameters for the statistically significant QSARs (PCA/PLS regression and PLS regression) are reported in Figures 25 and 26 respectively.

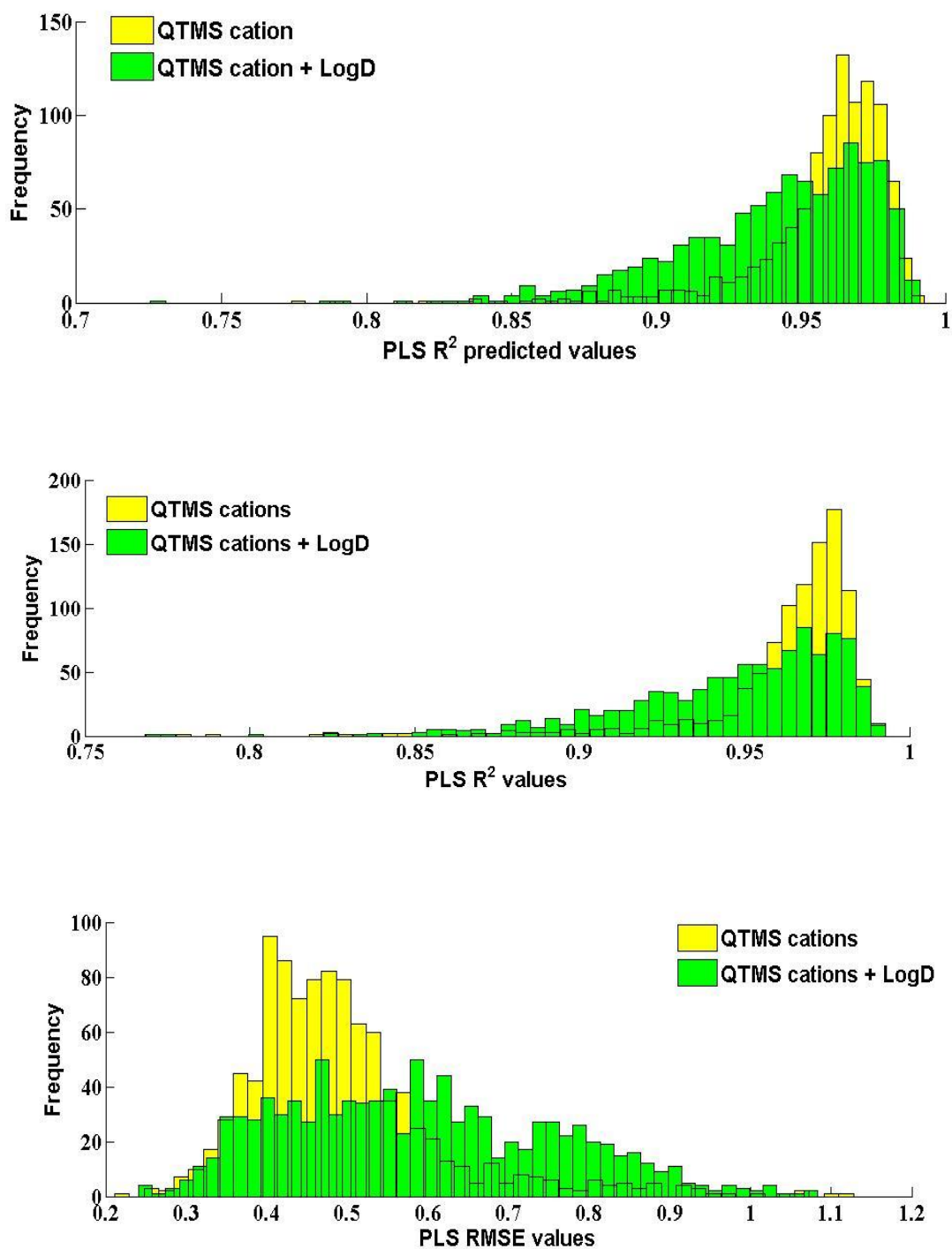


Figure 25. Histograms of QSARs based on the QTMS descriptors of the imidazoiium cations and the LogD descriptors of the salts generated using partial least squares (PLS) regression.

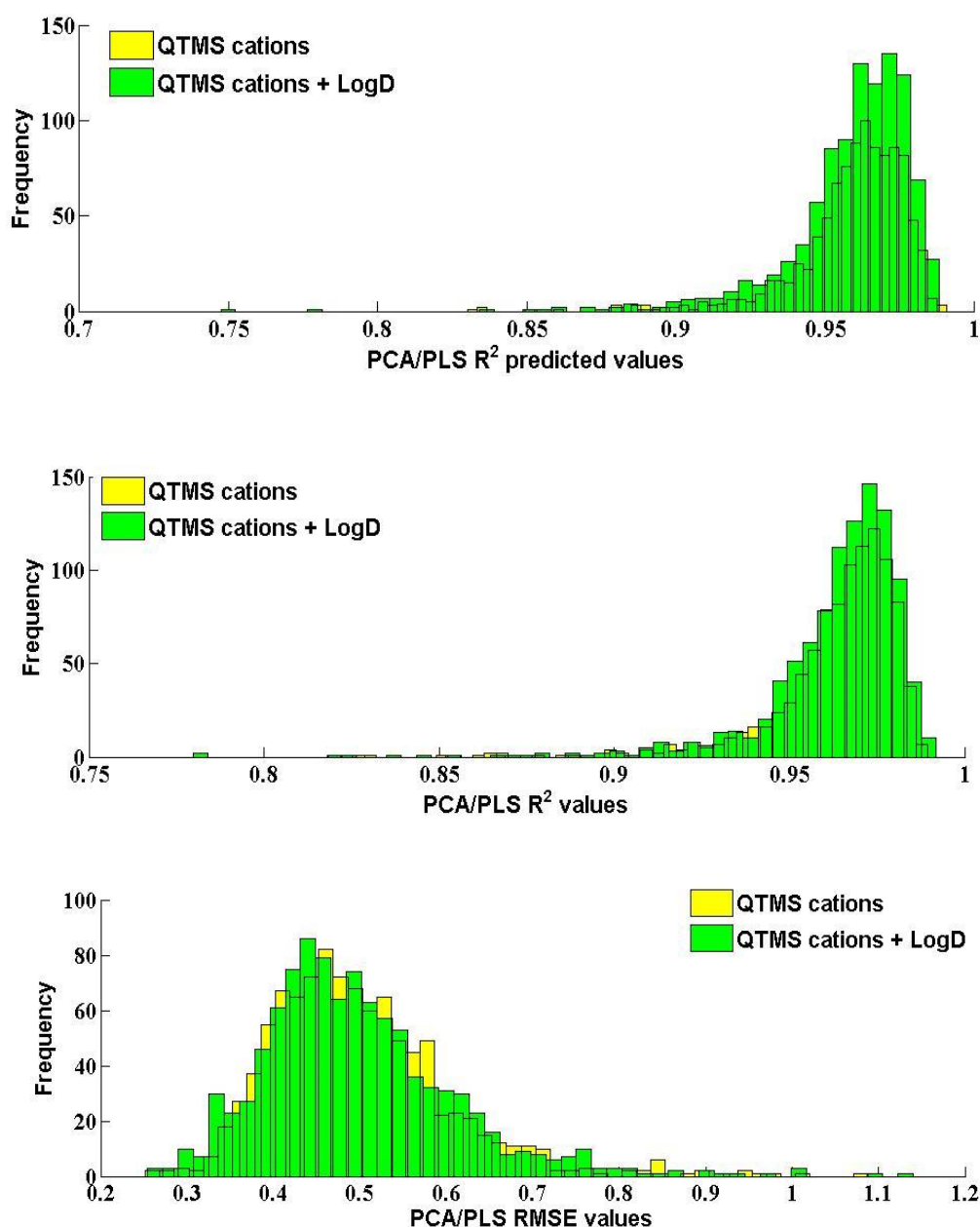


Figure 26. Histograms of QSARs based on the QTMS descriptors of the imidazolum cations and their LogD values at pH 5, 7, 9 generated using partial least squares (PLS) regression with principal component analysis data pre-processing (p. 75).

It was established by the earlier reported QSARs (p. 129) that the biological activity of imidazolium carboxylates towards *Escherichia coli* could be explained by the theoretical descriptors of the electronic properties of their cations. Hence, QSAR based on the QTMS descriptors of isolated structural

features the cations were developed (Table 26). Their aim was to localize the centre of a biological action within the imidazolium cations.

Table 26. Statistical parameters quantifying the predictivity of a linear regression model based on the QTMS descriptors of structural fragments of imidazolium cations as an average of 1000 random combinations of a training and a test set.

Statistical parameters	PCA ₁ / MLR	PCA ₁ / PLS ₆	PLS ₆
<i>QTMS long chain of imidazolium ring</i>			
R ² predicted	0.67 ±0.31	0.96 ±0.02	0.95 ±0.02
R ²	0.75 ±0.17	0.97 ±0.02	0.96 ±0.02
RMSE	1.29 ±0.39	0.48 ±0.11	0.50 ±0.10
<i>QTMS long chain with LogD</i>			
R ² predicted	<0	0.34±0.55	0.88±0.04
R ²	0.09±0.12	0.59±0.22	0.89±0.04
RMSE	2.56±0.24	1.67±0.48	0.86±0.13
<i>QTMS imidazolium ring with short chain</i>			
R ² predicted	<0	<0	<0
R ²	0.08±0.09	0.13±0.10	0.34
RMSE	2.59±0.24	2.51±0.24	2.14

Linear regression of the QTMS descriptors of the isolated structural fragments of imidazolium cations established that the centre of the biological action of imidazolium cations is located in their long side chains. Thus, both PCA/PLS and PLS regression approaches generated statistically predictive regression models. The theoretical observation that the biological activity of imidazolium cations is correlated with the electronic properties of their long side chains, to the author's knowledge, has not yet being reported.

The predictive failure of the QSARs based on the descriptors of the imidazolium ring and a short side chain only shows that the ring itself does not significantly influence the toxicity of the cations. This can be supported by the experimentally observed two-stage mechanism of the biological activity of quaternary ammonium cations (Hotchkiss, 1946). Thus, it is hypothesized, that developed QSARs show that an imidazolium ring facilitates an initial electrostatic contact with functional groups on a bacterial cell surface, either via hydrogen bonding or pi interactions. This electrostatic contact does not toxicologically affect the cell but it leads to a subsequent incorporation of alkyl side chains into a bacterial cell membrane which disruption of the integrity of a bacterial cell membrane (Gilbert and Moore, 2005; Wessels and Ingmer, 2013b) leading to a bacterial cell death.

The preference of alkyl side chains for a lipophilic phase will increase with the number of carbon atoms within them this could potentially explain the obtained correlation of the alkyl side chains with the toxicity data. However, it was reported earlier (p. 123) that the topological indices which describe the changes in the number of carbon atoms in a chemical structure did not successfully correlate with the toxicity data. Therefore, it is proposed that a toxicity of the alkyl side chains is not a function of the number of carbon atoms within them. Consequently, it is hypothesized that the toxicity of alkyl side chains is a function of the strength, i.e. number, of their dispersion interactions within a bacterial cell membrane which will increase with the increase in the length of their carbon chains. The results of the preliminary evaluation of this hypothesis are reported further in the current thesis.

The histograms of the statistical parameters for the statistically significant QSARs (PCA/PLS regression and PLS regression) are reported in Figures 27 and 28.

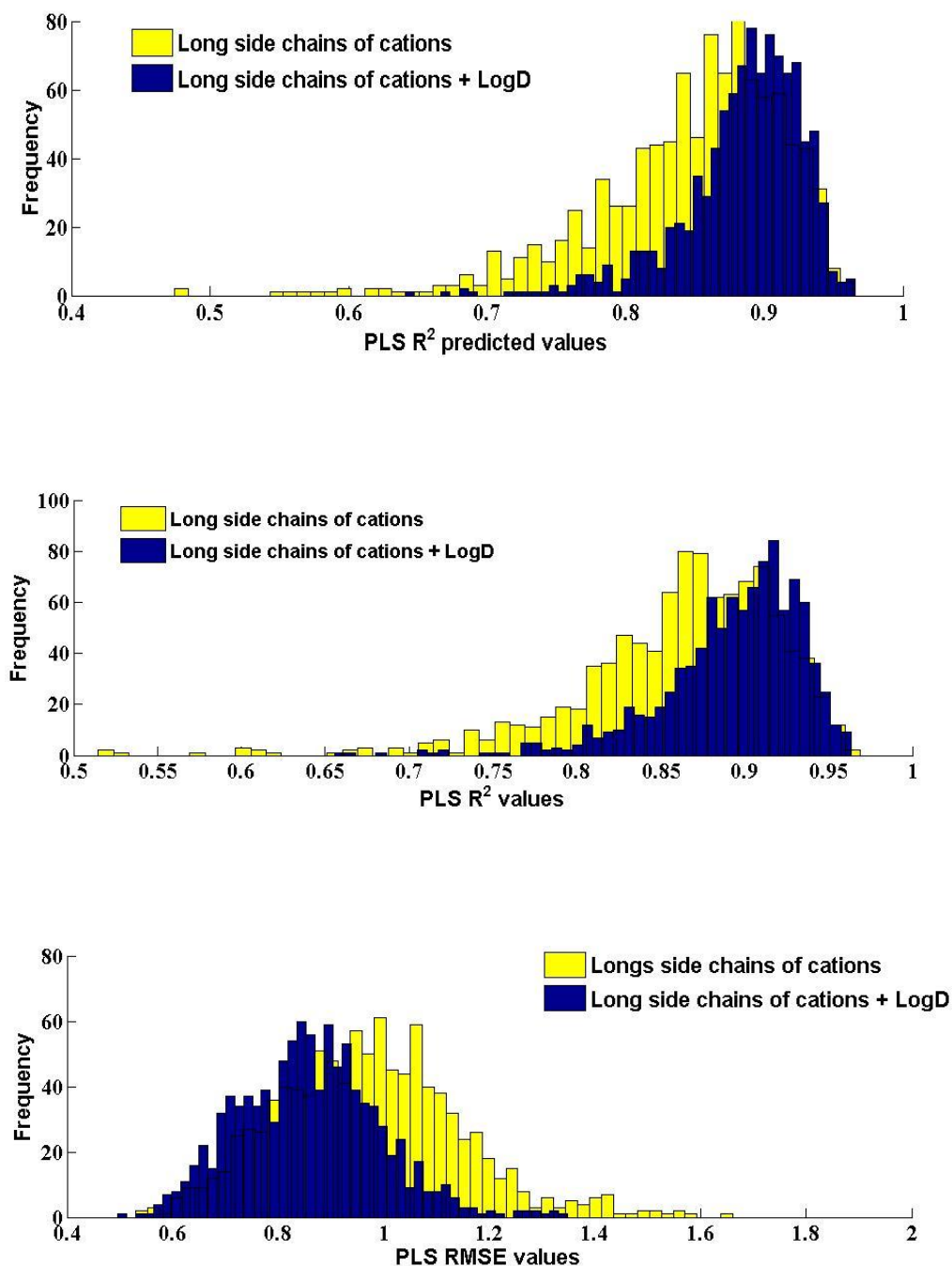


Figure 27. Histograms of QSARs based on the QTMS descriptors of the long side chains on imidazoiium cations and the LogD descriptors of the salts generated using partial least squares (PLS) regression.

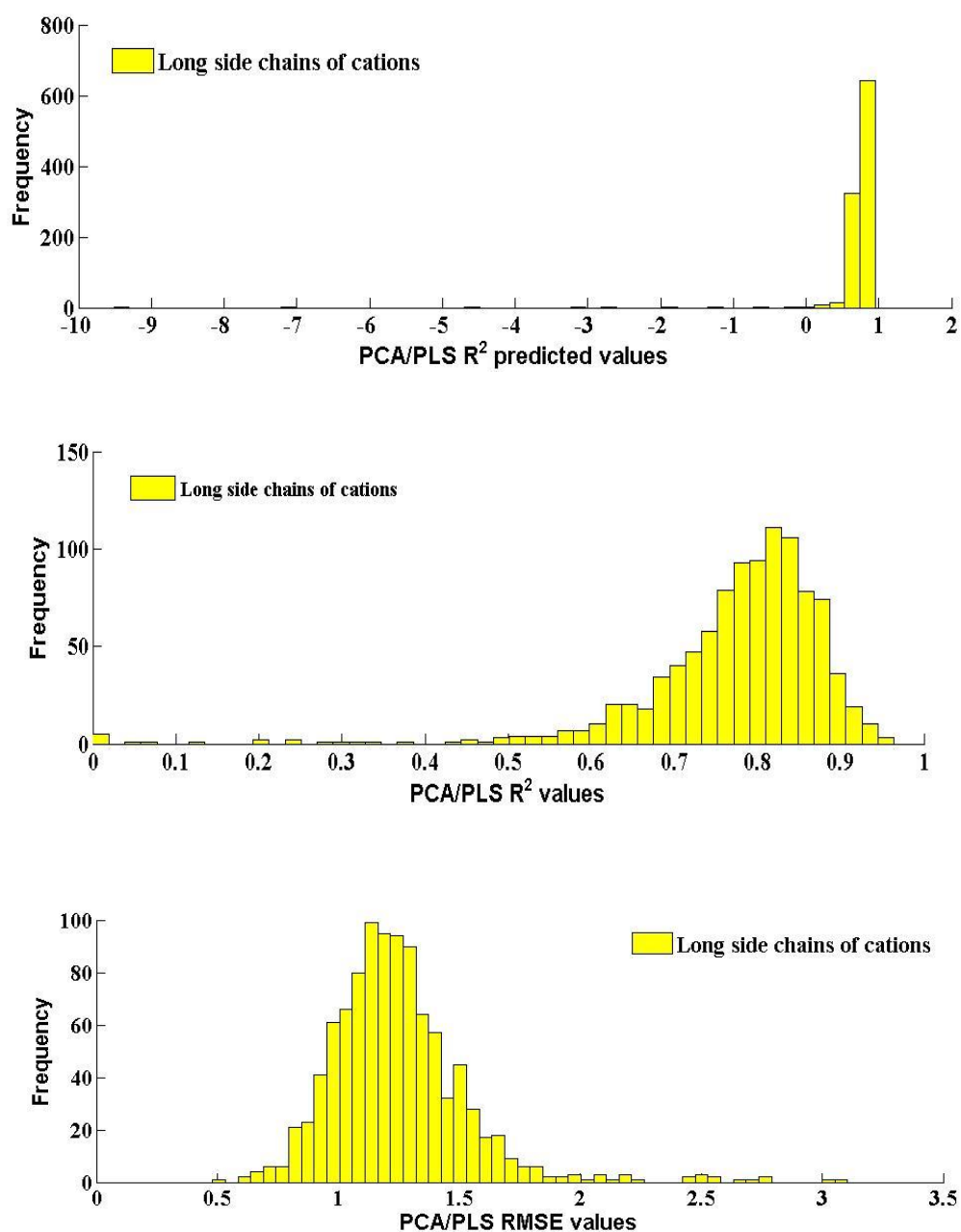


Figure 28. Histograms of QSARs based on the QTMS descriptors of the long side chains on imidazoiium cations and the LogD descriptors of the salts generated using partial least squares (PLS) regression with principal component analysis data pre-processing (p. 75).

3.6 Topological analysis of the long side chains on imidazolium cations.

Chemical structures of imidazolium cations were optimized to their HF equilibrium geometries as described earlier (p. 61). The analysis of the electronic charge density of alkyl- and the alkyl part of alkoxymethylimidazolium cations established topologically detectable C–H–H–C dispersion interactions which in the side chains with seven to eleven carbon atoms. These interactions were observed between the hydrogen atoms of the third and the seventh carbon atoms in the 1-alkylimidazolium cations (Figure 29), and between the hydrogen atoms of the third and the seventh carbon atoms of the alkyl part of 1-alkoxymethylimidazolium cations (Figure 30). Bifurcated H–H interactions were observed in the alkyl- and the alkyl part of the alkoxymethyl side chains with eleven carbon atoms.

Dispersion interactions are formed due to the created induced dipoles which are temporarily delocalizations of electronic charge within atoms caused by their close proximity to each other. It has been experimentally observed that the magnitude of dispersion interactions in unbranched alkanes is related to the number of carbon atoms in their side chains (Loudon, 2002). For example, it has been reported that the boiling points of unbranched alkanes increase by 20-30 °C per carbon atom. In the context of a QSAR, the changes in a magnitude, i.e. strength, of these interactions could potentially be used to explain an increase in a biological toxicity of imidazolium cations with an increase in their alkyl side chain lengths. It has been reported earlier (p. 22) that the toxicological mechanism of quaternary ammonium cations undergoes two stages, i.e. an initial electrostatic interaction of the cations with oppositely charged groups on a bacterial cell surface and the

incorporation of their hydrophobic groups into a cell membrane leading to its disruption. The second stage is irreversible. Thus, it was hypothesised (p.139) that the strength of $C-H\cdots H-C$ dispersion interactions between the alkyl side chains of imidazolium cations and lipophilic groups of a bacterial membrane governs the second, irreversible, stage of the toxicological mechanism of imidazolium cations. It has been reported by Pernak and colleagues (Pernak et al., 2004) that an experimentally observed toxicity of 1-alkyl and 1-alkoxymethylimidazolium L-Lactates increases considerably when the length of alkyl side chains on the cations exceeds six carbon atoms. The topological analysis of the side chains of these cations conducted in the current study established the presence of internal $C-H\cdots H-C$ dispersion interactions in the alkyl chains with seven or more carbon atoms. Thus, agreeing with the experimental data.

The topological parameters computed at bond critical points of all established $C-H\cdots H-C$ interactions are reported in the Table 27. These interactions were not topologically observed in the structures of the cations which were optimized in the presence of the L-Lactate anion under the same computational settings. This corresponds to the experimental findings of Pernak and colleagues (Pernak et al., 2004) who reported on the absence of a linear decrease in the boiling points of 1-alkyl and 1-alkoxymethylimidazolium L-lactates which were measured in the presence of the L-lactate anion. The above fact indicates that the side chains of the imidazolium cations did not form significant $C-H\cdots H-C$ interactions in the presence of the L-lactate anion. However, based on the earlier reported dependency of the boiling points of pure alkanes on the number of their carbon atoms, it is hypothesized that the theoretically established

C–H–H–C intra-ionic dispersion interactions in 1-alkyl-, 1-alkoxymethylimidazolium cations with long side chains which were optimized in the absence of the L-lactate anion, potentially uncover the reason for an increase in their biological toxicity. However, further investigation of this hypothesis is necessary prior to making any definitive conclusion.

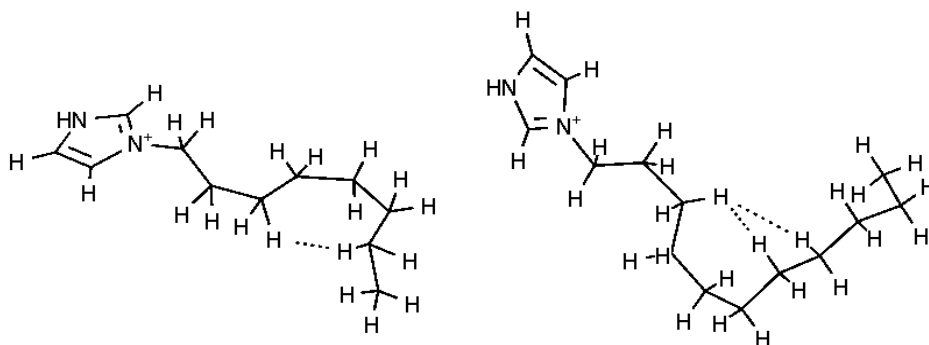


Figure 29. Intra-ionic C–H–H–C interactions in 1-alkylimidazolium cations. A bifurcated H–H interaction was observed in the alkyl chain with eleven carbon atoms. Dashed lines connect the interacting hydrogen atoms.

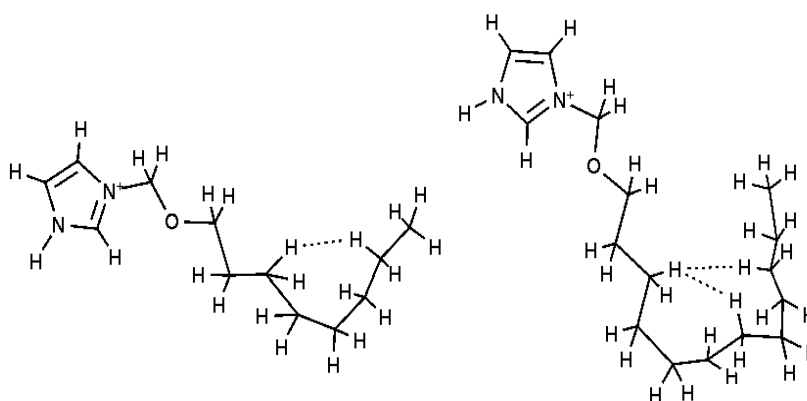


Figure 30. Intra-ionic C–H–H–C interactions in 1-alkoxymethylimidazolium cations. A bifurcated interaction was observed in the alkyl part of alkoxyethyl chain with eleven carbon atoms.

Table 27. Topological parameters at bond critical points of H – – H interactions in the alkyl side chains of 1-alkyl, 1-alkoxymethylimidazolium cations.

Number of carbons	Electronic charge density	The Laplacian of density	Eigenvalues of the Laplacian			Inter-atomic distance	
	au	au	au			au	$\times 10^{-10}$ Å
Alkyl chain:							
7	0.006	0.026	-0.004	-0.004	0.034	4.47	2.36
8	0.006	0.026	-0.004	-0.004	0.035	4.45	2.35
9	0.006	0.026	-0.005	-0.004	0.035	4.44	2.35
10	0.006	0.026	-0.005	-0.004	0.036	4.43	2.34
11	0.006	0.026	-0.005	-0.004	0.036	4.43	2.34
11	0.004	0.017	-0.003	-0.001	0.020	4.85	2.57
12	0.007	0.027	-0.005	-0.004	0.036	4.43	2.34
Alkyl part of alkoxyethyl chain:							
7	0.006	0.026	-0.004	-0.004	0.035	4.46	2.36
8	0.006	0.025	-0.004	-0.004	0.032	4.53	2.40
9	0.006	0.024	-0.004	-0.004	0.032	4.54	2.40
10	0.006	0.026	-0.004	-0.004	0.034	4.47	2.36
11	0.006	0.025	-0.004	-0.004	0.034	4.48	2.37
12	0.006	0.025	-0.004	-0.004	0.034	4.49	2.38
12	0.003	0.010	-0.002	-0.001	0.012	5.05	2.67

4. Conclusions

In the course of the current study it was established that the two-stage mechanism of biological activity of surface active bactericides can be computationally modelled to describe the toxicity of imidazolium carboxylates towards *Escherichia coli*. Thus, it was demonstrated that statistically significant QSARs can be developed by regressing the Log(1/MIC) values of imidazolium carboxylates towards *Escherichia coli* on the theoretical descriptors of their lipophilicity (LogD descriptors) and the descriptors of their electronic properties (QTMS descriptors). However, a linear correlation of the QTMS descriptors of these quaternary ammonium salts results in QSARs with higher accuracy.

It was established that the partial least squares (PLS) regression and the PLS regression after the principal component data pre-processing (PCA/PLS) were suitable multivariate linear regression approaches for modelling the biological activity of imidazolium carboxylates towards *Escherichia coli* under the reported experimental and computational parameters, and that the multiple linear regression after the principal component data analysis was unsuitable for this purpose because this algorithm failed to generate statistically significant QSARs in instances when the PLS and PCA/PLS algorithms were successful.

It was found that the electronic properties of the imidazolium cations play a major role in the biological activity of 1-ethyl-, 1-butylimidazolium carboxylates and 1-alkyl-, 1-alkoxymethylimidazolium L-lactates, and that the centre of the biological activity is located within their long side chains. A topological investigation of the electronic charge distribution of the long side chains of the cations was conducted, and it was established that the

imidazolium cations whose alkyl side chains and the alkyl part of alkoxymethyl side chains contain seven to twelve carbon atoms formed intra-ionic C–H–H–C dispersion interactions. Hence, a hypothesis explaining an increase in a biological activity of imidazolium carboxylates by an increase in their intrinsic electronic potential to engage in C–H–H–C dispersion interactions with lipophilic functional groups of a bacterial cell membrane was proposed and preliminary tested.

The nature of C–H–O–C inter ionic electrostatic interactions in 1-ethyl-3-methylimidazolium acetate was topologically evaluated and it was determined that these interactions can be described as hydrogen bonds. In the process of the topological analysis an equation which can be used to compute a limiting dipole moment of a bond was developed and these values for the C–H–O hydrogen bonds in 1-ethyl-3-methylimidazolium acetate were computed.

The validity of a research hypothesis (Rebros et al., 2009) proposing the use of the agar diffusion test was evaluated for the toxicological classification of ionic liquids. The invalidity of this hypothesis was demonstrated via a combination of theoretical reasoning and experimental work. In the process of the topological analysis an agar well test, which allows to estimate initial in-well concentrations of ionic liquids was developed, and its suitability for the toxicological screening of 1-ethyl-, 1-butyl-3-methylimidazolium carboxylates was validated by the agar diffusion test performed under identical experimental conditions.

5. Future work

The following research directions can be explored as a continuation of the current project:

QSARs

- A wider range of multivariate linear regression approaches can be implemented to generate the regression equations relating the biological activity of the imidazolium carboxylates with the descriptors of their lipophilicity and their electronic properties.
- Non-linear regression approaches can be utilized to correlate the biological activity of imidazolium carboxylates with their lipophilicity.
- Alternative theoretical descriptors of the electronic properties of imidazolium carboxylates and the algorithms for the estimation of their lipophilicity can be utilized.
- Experimental distribution coefficients (when available) can be utilized in regression models.

$C-H \cdots H-C$ electrostatic interactions

- The nature of these electrostatic interactions can be explored via their topological analysis.
- A molecular dynamic simulation of the interaction between 1-alkyl-, 1-alkoxymethylimidazolium cations and a lipophilic chemical structure of a biological cell membrane can be attempted.
- An investigation of the topological parameters for these interactions in other chemical structures can be performed.

C–H–O hydrogen bonds

- The geometry of 1-ethyl-3-methylimidazolium acetate can be optimized in the presence of a solvent, such as water, and the effect of inclusion of a solvent during the geometry optimization on the topological properties of the electronic charge density in inter-ionic region can be investigated.
- The nature of C–H–O interactions in other imidazolium carboxylates, such as 1-alkyl-, 1-alkoxymethylimidazolium carboxylates can be topologically evaluated.
- The applicability, usefulness and reliability of the developed equation for the calculation of a point dipole moment in a bond critical point can be assessed by the computation of the point dipole moments for other imidazolium carboxylates and other chemical structures.

6. References

- Allerhand, A., Schleyer, P. V., 1963. A survey of C-H groups as proton donors in hydrogen bonding. *J. Am. Chem. Soc.* 85, 1715-1723.
- Almeida, H.F.D., Passos, H., Lopes-da-Silva, J.A., Fernandes, A.M., Freire, M.G., Coutinho, J.A.P., 2012. Thermophysical Properties of Five Acetate-Based Ionic Liquids. *J. Chem. Eng. Data* 57, 3005–3013.
- Arunan, E., Desiraju, G.R., Klein, R.A., Sadlej, J., Scheiner, S., Alkorta, I., Clary, D.C., Crabtree, R.H., Dannenberg, J.J., Hobza, P., Kjaergaard, H.G., Legon, A.C., Mennucci, B., Nesbitt, D.J., 2011a. Definition of the hydrogen bond (IUPAC Recommendations 2011). *Pure Appl. Chem.* 83, 1637–1641.
- Arunan, E., Desiraju, G.R., Klein, R.A., Sadlej, J., Scheiner, S., Alkorta, I., Clary, D.C., Crabtree, R.H., Dannenberg, J.J., Hobza, P., Kjaergaard, H.G., Legon, A.C., Mennucci, B., Nesbitt, D.J., 2011b. Defining the hydrogen bond: An account (IUPAC Technical Report). *Pure Appl. Chem.* 83, 1619–1636.
- Avent, A.G., Chaloner, P.A., Day, M.P., Seddon, R., Welton, T., 1994, Evidence for Hydrogen Bonding in Solutions of 1-Ethyl-3-methylimidazolium Halides, and its Implications for Room-temperature Halogenoaluminate(III) Ionic Liquids. *J. Chem. Soc. Dalton Trans.* 3405–3413.
- Bader, R., 1990. *Atoms in Molecules. A Quantum Theory.* Oxford University Press, New York.
- Bader, R., Carrol, M., Cheeseman, J., Chang, C., 1987. Properties of Atoms in Molecules - Atomic Volumes. *J. Amer. Chem. Soc.* 109, 7968–7979.

- Bader, R., Essen, H., 1984. The Characterization of Atomic Interactions. J. Chem. Phys. 80, 1943–1960.
- Bader, R., MacDougall, P., Lau, C., 1984. Bonded and nonbonded charge concentrations and their relation to molecular geometry and reactivity. J. Amer. Chem. Soc. 106, 1594–1605.
- Bader, R.F.W., 2009. Bond Paths Are Not Chemical Bonds. J. Phys. Chem. A 113, 10391–10396.
- Bader, R.F.W., 2010. Definition of Molecular Structure: By Choice or by Appeal to Observation? J. Phys. Chem. A 114, 7431–7444.
- Bader, R.F.W., Beddall, P.M., Cade, P.E., 1971. Partitioning and characterization of molecular charge distributions. J. Amer. Chem. Soc. 93, 3095–3107.
- Bader, R.F.W., Preston, H.J.T., 1969. The kinetic energy of molecular charge distributions and molecular stability. Int. J. Quantum Chem. 3, 327–347.
- Bader, R.F.W., Slee, T.S., Cremer, D., Kraka, E., 1983. Description of conjugation and hyperconjugation in terms of electron distributions. J. Amer. Chem. Soc. 105, 5061–5068.
- Badger, R.M, Bauer, S.H., 1937. Spectroscopic Studies of the Hydrogen Bond. II. The Shift of the O-H Vibrational Frequency in the Formation of the Hydrogen Bond. J. Chem. Phys. 5, 839-851.
- Balaban, A., 1982. Highly Discriminating Distance-based Topological Index. Chem. Phys. Lett. 89, 399–404.
- Bauer, A., Kirby, W., Sherris, J., Turck, M., 1966. Antibiotic Suseptibility Testing by a Standardized Single Disk Method. Am. J. Clin. Path. 45, 493–496.

- Booth, A.D., 1949. An Application of the Method of the Steepest Descents to the solution of Systems of Non-linear Simultaneous Equations. *Q. J. Mech. Appl. Math.* 2, 460–468.
- Bowron, D.T., D'Agostino, C., Gladden, L.F., Hardacre, C., Holbrey, J.D., Lagunas, M.C., McGregor, J., Mantle, M.D., Mullan, C.L., Youngs, T.G.A., 2010. Structure and Dynamics of 1-Ethyl-3-methylimidazolium Acetate via Molecular Dynamics and Neutron Diffraction. *J. Phys. Chem. B* 114, 7760–7768.
- Brehm, M., Weber, H., Pensado, A.S., Stark, A., Kirchner, B., 2012. Proton transfer and polarity changes in ionic liquid-water mixtures: a perspective on hydrogen bonds from ab initio molecular dynamics at the example of 1-ethyl-3-methylimidazolium acetate-water mixtures- Part 1. *Phys. Chem. Chem. Phys.* 14, 5030–5044.
- Buffet-Bataillon, S., Tattevin, P., Bonnaure-Mallet, M., Jolivet-Gougeon, A., 2012. Emergence of resistance to antibacterial agents: the role of quaternary ammonium compounds—a critical review. *Int. J. Antimicrob. Ag.* 39, 381 – 389.
- Chen, Y., Cao, Y., Mu, T., 2014. A New Application of Acetate-Based Ionic Liquids: Potential Usage as Drying Materials. *Chem. Eng. Technol.* 37, 527–534.
- Chou, J., Jurs, P., 1979. Computer-assisted Computation of Partition Coefficients from Molecular Structures Using Fragment Constants. *J. Chem. Inf. Comput. Sci.* 19, 172–178.
- Clough, M.T., Geyer, K., Hunt, P.A., Mertes, J., Welton, T., 2013. Thermal decomposition of carboxylate ionic liquids: trends and mechanisms. *Phys. Chem. Chem. Phys.* 15, 20480–20495.

- Convard, T., Dubost, J., Lesolleu, H., Kummer, E., 1994. SMILOGP - A Program for a Fast Evaluation of Theoretical LogP from the SMILES Code of a Molecule. *Quant. Struct.-Act. Relat.* 13, 34–37.
- Csizmadia, F., Tsantili-Kakoulidou, A., Panderi, I., Darvas, F., 1997. Prediction of distribution coefficient from structure. 1. Estimation method. *J. Pharm. Sci.* 86, 865–871.
- De Jong, S., 1993. SIMPLS: An Alternative Approach to Partial Least Squares Regression. *Chemom. Intell. Lab. Syst.* 18, 251–263.
- Desiraju, G.R., Steiner, T., 1999, *The Weak Hydrogen Bond*, Oxford University Press, Oxford.
- Dhumal, N.R., Kim, H.J., Kiefer, J., 2009. Molecular Interactions in 1-Ethyl-3-methylimidazolium Acetate Ion Pair: A Density Functional Study. *J. Phys. Chem. A* 113, 10397–10404.
- Domagk, G., 1935. A new class of disinfectant. *Deut. Med. Wochenschr.* 61, 829–832.
- Du, H., Qian, X., 2011. The effects of Acetate Anion on Cellulose dissolution and Reaction in Imidazolium Ionic Liquids. *Carb. Res.* 346, 1985-1900.
- Ertl, P., 1997. Simple Quantum Chemical Parameters as an Alternative to the Hammett Sigma Constants in QSAR Studies. *Quant. Struct.-Act. Relat.* 16, 377-382
- Henchman, R.H., Irudayam, S. J., 2010. Topological Hydrogen-Bond Definition to Characterize the Structure and Dynamics of Liquid Water. *J. Phys. Chem. B* 114, 16792-16810.

- Fernandez, I., Frenking, G., 2006. Correlation between Hammett substituent constants and directly calculated pi-conjugation strength. *J. Org. Chem.* 71, 2251–2256.
- Fletcher, R., 1970. A new approach to variable metric algorithms. *Comput. J.* 13, 317–322.
- Frisch, M., Trucks, G., Schlegel, H., Scuseria, G., Robb, M., et al., 2003. Gaussian 03, Revision D.01.
- Fujita, T., Iwasa, J., Hansch, C., 1964. A New Substituent Constant, π , Derived from Partition Coefficients. *J. Am. Chem. Soc.* 86, 5175–5180.
- Genix, P., Jullien, H., Le Goas, R., 1996. Estimation of Hammett sigma constants from calculated atomic charges using partial least squares regression. *J. Chemom.* 10, 631–636.
- Ghose, A.K., Crippen, G.M., 1986. Atomic Physicochemical Parameters for Three-Dimensional Structure-Directed Quantitative Structure-Activity Relationships I. Partition Coefficients as a Measure of Hydrophobicity. *J. Comput. Chem.* 7, 565–577.
- Gilbert, P., Moore, L.E., 2005. Cationic antiseptics: diversity of action under a common epithet. *J. Appl. Microbiol.* 99, 703–715.
- Gill, P.M.W., 1994. Molecular Integrals over Gaussian Basis Functions, in: John R. Sabin and Michael C. Zerner (Ed.), *Advances in Quantum Chemistry*. Academic Press, pp. 141–205.
- Gilli, P., Pretto, L., Bertolasi, V., Gili, G., 2009. Predicting Hydrogen-Bond Strengths from Acid-Base Molecular Properties. The pKa Slide Rule: Toward the Solution of a Long-Lasting Problem. *Acc. Chem. Res.* 42, 33–44.

- Gilliom, R., Beck, J., Purcell, W., 1985. An MNDO Treatment of Sigma Values. *J. Comput. Chem.* 6, 437–440.
- Golbraikh, A., Tropsha, A., 2002. Beware of q^2 ! *J. Mol. Graphics Modell.* 20, 269 – 276.
- Grabowski, S., 2006. *Hydrogen Bonding—New Insights*, Springer.
- Gramatica, P., 2013. On the Development and Validation of QSAR Models, in: Reisfeld, B., Mayeno, A.N. (Eds.), *Computational Toxicology, Methods in Molecular Biology*. Humana Press, pp. 499–526.
- Hamett, L. P., 1937. The Effect of Structure upon the Reactions of Organic Compounds. Benzene Derivatives. *J. Am. Chem. Soc.* 59 (1), 96-103.
- Halgren, T.A., 1996. Merck molecular force field .1. Basis, form, scope, parameterization and performance of MMFF94. *J. Comput. Chem.* 17, 490–519.
- Hanwell, M.D., Curtis, D.E., Lonie, D.C., Vandermeersch, T., Zurek, E., Hutchison, G.R., 2012. Avogadro: an advanced semantic chemical editor, visualization, and analysis platform. *J. Cheminform.* 4.
- Harris, J., 1985. Simplified method for calculating the energy of weakly interacting fragments. *Phys. Rev. B* 31, 1770–1779.
- Hartree, D.R., 1928. The Wave Mechanics of an Atom with a Non-Coulomb Central Field. Part I. Theory and Methods. *Math. Proc. Cambridge* 24, 89–110.
- Head, J.D., Zerner, M.C., 1985. A Broyden—Fletcher—Goldfarb—Shanno optimization procedure for molecular geometries. *Chem. Phys. Lett.* 122, 264–270.

- Hehre, W.J., Stewart, R.F., Pople, J.A., 1969. Self-Consistent Molecular-Orbital Methods. I. Use of Gaussian Expansions of Slater-Type Atomic Orbitals. *J. Chem. Phys.* 51, 2657–2664.
- Hofmann, A.W., 1851. XXV.-Researches on the volatile organic bases. *Q. J. Chem. Soc.* 3, 231–240.
- Hopkinson, M.N., Richter, C., Schedler, M., Glorious, F., An Overview of N-heterocyclic Carbenes. *Nature*, 510, 485-496.
- Hotchkiss, R., 1946. The Nature of the Bactericidal Action of Surface Active Agents. *Ann. N. Y. Acad. Sci.* 46, 479–493.
- Ingold, C.K., 1934. Principles of an Electronic Theory of Organic Reactions. *Chem. Rev.* 15, 225–274.
- Ingold, C.K., Ingold, E.H., 1926. CLXIX.-The nature of the alternating effect in carbon chains. Part V. A discussion of aromatic substitution with special reference to the respective roles of polar and non-polar dissociation; and a further study of the relative directive efficiencies of oxygen and nitrogen. *J. Chem. Soc.* 129, 1310–1328.
- Jacobs, W., 1916a. The bactericidal properties of the quaternary salts of hexamethylenetetramine. I. The problem of the chemotherapy of experimental bacterial infections. *Journal of Experimental Medicine* 23, 563–568.
- Jacobs, W., Heidelberger, M., Bull, C., 1916. The relation between constitution and bactericidal action in the quaternary salts obtained from halogenacetyl compounds. *J. Exp. Med.* 23, 577–599.
- Jaffé, H.H., 1952. Correlation of Hammett's Values with Electron Densities Calculated by Molecular Orbital Theory. *J. Chem. Phys.* 20, 279–284.
- Jeffrey, G.A., 2003. Hydrogen-Bonding: An update. *Crystallogr. Rev.*, 9, 135–176.

- Karelson, M., Lobanov, V.S., Katritzky, A.R., 1996. Quantum-chemical descriptors in QSAR/QSPR studies. *Chem. Rev.* 96, 1027–1043.
- Kempton, V., Kirchner, B., 2010. The role of hydrogen atoms in interactions involving imidazolium-based ionic liquids. *J. Mol. Struct.* 972, 22 – 34.
- Kiefer, J., Obert, K., Himmler, S., Schulz, P.S., Wasserscheid, P., Leipertz, A., 2008. Infrared Spectroscopy of a Wilkinson Catalyst in a Room-Temperature Ionic Liquid. *ChemPhysChem* 9, 2207–2213.
- Klopman, G., Li, J.-Y., Wang, S., Dimayuga, M., 1994. Computer Automated log P Calculations Based on an Extended Group Contribution Approach. *J. Chem. Inf. Comput. Sci.* 34, 752–781.
- Koch, U., Popelier, P., 1995. Characterization of C-H - -O Hydrogen Bonds on the Basis of the Charge Density. *J. Phys. Chem.* 99, 9747–9754.
- Kochetova, L.B., Klyuev, M.V., 2008. Quantum-chemical interpretation of the effect of substitution in the benzene ring on the reactivity of monosubstituted benzenes. *Russ. J. Gen. Chem.* 78, 1389–1392.
- Kubinyi, H., 2002. From narcosis to hyperspace: The history of QSAR. *Quant. Struct.-Act. Relat.* 21, 348–356.
- Kudin, K.N., Scuseria, G.E., Cancès, E., 2002. A black-box self-consistent field convergence algorithm: One step closer. *J. Chem. Phys.* 116, 8255–8261.
- Lawrence, C., 1950. Mechanism of Action and Neutralizing Agents for Surface - Active Materials upon Microorganisms. *Ann. N.Y. Acad. Sci.* 53, 66–75.
- Loe, A., Hansch, C., Elkins, D., 1971. Partition coefficients and their User. *Chem. Rev.* 71, 525-616.

- Loudon, G.M., 2002. Organic Chemistry, Oxford University Press, Inc., New York.
- Lewis, G., 1913. The free energy of chemical substances. Introduction. J. Am. Chem. Soc. 35, 1–30.
- Lowdin, P., 1955. Quantum Theory of Many-particle Systems. II. Study of the Ordinary Hartree-Fock Approximation. Phys. Rev. 97, 1490–1508.
- Lowry, T.M., 1923. The electronic theory of valency. Part I. Intramolecular ionisation. Trans. Faraday Soc. 18, 285–295.
- Mannhold, R., Poda, G.I., Ostermann, C., Tetko, I.V., 2009. Calculation of Molecular Lipophilicity: State-of-the-Art and Comparison of Log P Methods on More Than 96,000 Compounds. J. Pharm. Sci. 98, 861–893.
- MATLAB and Statistics Toolbox Release 2010a, 2010. The MathWorks, Inc., Natick, Massachusetts, United States.
- Matta, C.F., Boyd, R.J., 2007. The Quantum Theory of Atoms in Molecules: From Solid State to DNA and Drug Design. Wiley-VCH, Weinheim.
- Matthews, R.P., Welton, T., Hunt, P.A., 2014. Competitive pi interactions and hydrogen bonding within imidazolium ionic liquids. Phys. Chem. Chem. Phys. 16, 3238–3253.
- Mellinger, M., 1987. Multivariate data analysis: Its methods. Chemometr. Intell. Lab. 2, 29 – 36.
- Meylan, W., Howard, P., 1995. Atom Fragment Contribution Method for Estimating Octanol - Water Partition Coefficients. J. Pharm. Sci. 84, 83–92.
- Metzler, D. E., 1997, Biochemistry: The Chemical Reactions of Living Cells, Academic Press, Inc., New York.

- Monaco, R., Gardiner, W., 1995. Substituent Effects in Monosubstituted Bensenes - Semiempirical SCF Studies of the Hammett Constants. J. Phys. Org. Chem. 8, 629–636.
- Murthy, A.S.N., Rao, C.N.R., 1968. Spectroscopic Studies of the Hydrogen Bond. Appl. Spectrosc. Rev. 2, 69–91.
- Niedermeyer, H., Ashworth, C., Brandt, A., Welton, T., Hunt, P. A., 2013. A step towards the *a priori* design of ionic liquids. Phys. Chem. Chem. Phys. 15, 11566-11578.
- Nikolova, N., Jaworska, J., 2004. Approaches to measure chemical similarity - A review. QSAR Comb. Sci. 22, 1006–1026.
- O'Boyle, N., Banck, M., James, C., Morley, C., Vandermeersch, T., Hutchison, G., 2011. Open Babel: An open chemical toolbox. J. of Cheminform. 3, 33.
- O'Brien, S.E., Popelier, P.L.A., 2001. Quantum Molecular Similarity. 3. QTMS Descriptors. J. Chem. Inf. Comput. Sci. 41, 764–775.
- Pauling, L., Sherman, J., 1933. The nature of the chemical bond. VII. The calculation of resonance energy in conjugated systems. J. Chem. Phys. 1, 679–686.
- Pauling, L., 1938. The Nature of a Chemical Bond, 1960, Cornell University Press, Ithaca, NY.
- Pernak, J., Goc, I., Mirska, I., 2004. Anti-microbial activities of protic ionic liquids with lactate anion. Green Chem. 6, 323–329.
- Petrauskas, A., Kolovanov, E., 2000. ACD/Log P method description. Perspect. Drug Discovery Des. 19, 99–116.

- Piddock, L., 1990. Techniques used for the Determination of Antimicrobial Resistance and Sensitivity in Bacteria. *J. Appl. Bacteriol.* 68, 307–318.
- Platt, J., 1952. Prediction of Isomeric Differences in Paraffin Properties. *J. Phys. Chem.* 56, 328–336.
- Pollock, S., 2013. Econometrics: an historical guide for the uninitiated. *Interdiscipl. Sci, Rev.* 38, 169–186.
- Popelier, P., 1996a. On the differential geometry of interatomic surfaces. *Can. J. Chem.* 74, 829–838.
- Popelier, P., 1996b. Integration of atoms in molecules: A critical examination. *Mol. Phys.* 87, 1169–1187.
- Popelier, P., 1996c. MORPHY, a program for an automated “atoms in molecules” analysis. *Comput. Phys. Commun.* 93, 212–240.
- Popelier, P., 1998. A method to integrate an atom in a molecule without explicit representation of the interatomic surface. *Comput. Phys. Commun.* 108, 180–190.
- Popelier, P.L.A., 1994. A robust algorithm to locate automatically all types of critical points in the charge density and its Laplacian. *Chem. Phys. Lett.* 228, 160–164.
- Popelier, P.L.A., 2000. *Atoms in Molecules: An Introduction*. Prentice Hall, London.
- Pulay, P., 1980. Convergence Acceleration of Iterative Sequences - the Case of SCF Iteration. *Chem. Phys. Lett.* 73, 393–398.
- Rahn, O., Van Eseltine, W.P., 1947. Quaternary Ammonium Compounds. *Annu. Rev. Microbiol.* 1, 173–192.
- Rajalahti, T., Kvalheim, O.M., 2011. Multivariate data analysis in pharmaceuticals: A tutorial review. *Int. J. Pharm.* 417, 280 – 290.

- Randic, M., 1975. Characterization of molecular branching. *J. Am. Chem. Soc.* 97, 6609–6615.
- Rebros, M., Gunaratne, H.Q.N., Ferguson, J., Seddon, K.R., Stephens, G., 2009. A high throughput screen to test the biocompatibility of water-miscible ionic liquids. *Green Chem.* 11, 402–408.
- Reis, R.R. dos, Sampaio, S.C., Melo, E.B. de, 2013. The effect of different log P algorithms on the modeling of the soil sorption coefficient of nonionic pesticides. *Water Res.* 47, 5751 – 5759.
- Regussan, J., 1952. The Anti-bacterial Action of Quaternary Ammonium Compounds. *Chem. Ind.* 267–268.
- Salt, W.G., Wiseman, D., 1968. The uptake of cetyltrimethylammonium bromide by *Escherichia coli*. *J. Pharm. Pharmacol.* 20, 14S–17S.
- Schlegel, H.B., 1982. Optimization of equilibrium geometries and transition structures. *J. Comput. Chem.* 3, 214–218.
- Scior, T., Medina-Franco, J.L., Do, Q.-T., Martinez-Mayorga, K., Yunes Rojas, J.A., Bernard, P., 2009. How to Recognize and Workaround Pitfalls in QSAR Studies: A Critical Review. *Curr. Med. Chem.* 16, 4297–4313.
- Seddon, K.R., 1997. Ionic liquids for clean technology. *J. Chem. Technol. Biotechnol.* 68, 351–356.
- Shi, W., Damodaran, K., Nulwala, H.B., Luebke, D.R., 2012. Theoretical and experimental studies of water interaction in acetate based ionic liquids. *Phys. Chem. Chem. Phys.* 14, 15897–15908.
- Schlegel, H., 1984. Estimating the hessian for gradient-type geometry optimizations. *Theoret. Chim. Acta* 66, 333–340.

- Simons, J., Jorgensen, P., Taylor, H., Ozment, J., 1983. Walking on Potential Energy Surfaces. *J. Phys. Chem.* 87, 2745–2753.
- Smith, P.J., Popelier, P.L.A., 2005. Quantum chemical topology (QCT) descriptors as substitutes for appropriate Hammett constants. *Org. Biomol. Chem.* 3, 3399–3407.
- Steinmetz, H.L., 1966. Using the Method of Steepest Descent. *Ind. Eng. Chem.* 58, 33–39.
- Steiner, T., 2003. C-H \cdots O hydrogen bonding in crystals. *Crystallogr. Rev.* 9, 177–228.
- Sullivan, J., Jones, A., Tanji, K., 2000. QSAR treatment of electronic substituent effects using frontier orbital theory and topological parameters. *J. Chem. Inf. Comput. Sci.* 40, 1113–1127.
- Szegezdi, J., Csizmadia, F., 2004. Prediction of distribution coefficient using microconstants. *Abst. Pap. Am. Chem. S.* 227, 1, U1019
- Thomas, G.B., Finney, R.L., 1996. *Calculus and Analytic Geometry*, 9th ed. Addison-Wesley Publishing Company, Inc.
- Tropsha, A., 2010. Best Practices for QSAR Model Development, Validation, and Exploitation. *Mol. Inf.* 29, 476–488.
- Viswanadhan, V.N., Ghose, A.K., Revankar, G.R., Robins, R.K., 1989. Atomic physicochemical parameters for three dimensional structure directed quantitative structure-activity relationships. 4. Additional parameters for hydrophobic and dispersive interactions and their application for an automated superposition of certain naturally occurring nucleoside antibiotics. *J. Chem. Inf. Comput. Sci.* 29, 163–172.

- Wang, R., Fu, Y., Lai, L., 1997. A New Atom-Additive Method for Calculating Partition Coefficients. *J. Chem. Inf. Comput. Sci.* 37, 615–621.
- Wessels, S., Ingmer, H., 2013a. Modes of action of three disinfectant active substances: A review. *Regul. Toxicol. Pharm.* 67, 456–467.
- Wessels, S., Ingmer, H., 2013b. Modes of action of three disinfectant active substances: A review. *Regul. Toxicol. Pharm.* 67, 456 – 467.
- Wiener, H., 1947. Structural Determination of Parafin Boiling Points. *J. Am. Chem. Soc.* 69, 17–20.
- Wold, S., Sjöström, M., Carlson, R., Lundstedt, T., Hellberg, S., Skagerberg, B., Wikström, C., Öhman, J., 1986. Multivariate design. *Anal. Chim. Acta* 191, 17 – 32.
- Wood, N., Ferguson, J.L., Gunaratne, H.Q.N., Seddon, K.R., Goodacre, R., Stephens, G.M., 2011. Screening ionic liquids for use in biotransformations with whole microbial cells. *Green Chem.* 13, 1843–1851.
- Ypma, T.J., 1995. Historical Development of the Newton-Raphson Method. *SIAM Rev.* 37, 531–551.

Appendix 1: Reprint licences

This is a License Agreement between Alexandria Naden ("You") and John Wiley and Sons ("John Wiley and Sons") provided by Copyright Clearance Center ("CCC"). The license consists of your order details, the terms and conditions provided by John Wiley and Sons, and the payment terms and conditions.

All payments must be made in full to CCC. For payment instructions, please see information listed at the bottom of this form.

License Number	3332431181407
License date	Feb 19, 2014
Licensed content publisher	John Wiley and Sons
Licensed content publication	Journal of Applied Microbiology
Licensed content title	Cationic antiseptics: diversity of action under a common epithet
Licensed copyright line	Copyright © 2005, John Wiley and Sons
Licensed content author	P. Gilbert, L.E. Moore
Licensed content date	Jul 1, 2005
Start page	703
End page	715
Type of use	Dissertation/Thesis
Requestor type	University/Academic
Format	Print and electronic
Portion	Figure/table
Number of figures/tables	1
Original Wiley figure/table number(s)	Figure 2
Will you be translating?	No
Title of your thesis / dissertation	Exploring theoretical origins of the toxicity of organic quaternary ammonium salts towards Escherichia coli using machine learning approaches
Expected completion date	Mar 2014
Expected size (number of pages)	160
Total	0.00 USD

ROYAL SOCIETY OF CHEMISTRY LICENSE
TERMS AND CONDITIONS

Jan 24, 2014

This is a License Agreement between Alexandria Naden ("You") and Royal Society of Chemistry ("Royal Society of Chemistry") provided by Copyright Clearance Center ("CCC"). The license consists of your order details, the terms and conditions provided by Royal Society of Chemistry, and the payment terms and conditions.

All payments must be made in full to CCC. For payment instructions, please see information listed at the bottom of this form.

License Number	3315361098487
License date	Jan 24, 2014
Licensed content publisher	Royal Society of Chemistry
Licensed content publication	Green Chemistry
Licensed content title	Anti-microbial activities of protic ionic liquids with lactate anion
Licensed content author	Juliusz Pernak, Izabela Goc, Ilona Mirska
Licensed content date	Jun 22, 2004
Volume number	6
Issue number	7
Type of Use	Thesis/Dissertation
Requestor type	academic/educational
Portion	figures/tables/images
Number of figures/tables /images	3
Format	print and electronic
Distribution quantity	3
Will you be translating?	no
Order reference number	
Title of the thesis/dissertation	Exploring theoretical origins of the toxicity of organic quaternary ammonium salts towards Escherichia coli using machine learning approaches
Expected completion date	Mar 2014
Estimated size	120
Total	0.00 GBP

This is a License Agreement between Alexandria Naden ("You") and Royal Society of Chemistry ("Royal Society of Chemistry") provided by Copyright Clearance Center ("CCC"). The license consists of your order details, the terms and conditions provided by Royal Society of Chemistry, and the payment terms and conditions.

All payments must be made in full to CCC. For payment instructions, please see information listed at the bottom of this form.

License Number	3337040134087
License date	Feb 27, 2014
Licensed content publisher	Royal Society of Chemistry
Licensed content publication	Green Chemistry
Licensed content title	A high throughput screen to test the biocompatibility of water-miscible ionic liquids
Licensed content author	Martin Rebros,H.Q. Nimal Gunaratne,Jamie Ferguson,Kenneth R. Seddon,Gillian Stephens
Licensed content date	Jan 23, 2009
Volume number	11
Issue number	3
Type of Use	Thesis/Dissertation
Requestor type	non-commercial (non-profit)
Portion	excerpt (<= 400 words)
Format	print and electronic
Distribution quantity	3
Will you be translating?	no



Title: Characterization of C-H-O
Hydrogen Bonds on the Basis of
the Charge Density
Author: U. Koch and P. L. A. Popelier
Publication: The Journal of Physical
Chemistry B
Publisher: American Chemical Society
Date: Jun 1, 1995
Copyright © 1995, American Chemical Society

Logged in as:

Alexandria Naden

Account #:
3000742786[LOGOUT](#)**PERMISSION/LICENSE IS GRANTED FOR YOUR ORDER AT NO CHARGE**

This type of permission/license, instead of the standard Terms & Conditions, is sent to you because no fee is being charged for your order. Please note the following:

- Permission is granted for your request in both print and electronic formats, and translations.
- If figures and/or tables were requested, they may be adapted or used in part.
- Please print this page for your records and send a copy of it to your publisher/graduate school.
- Appropriate credit for the requested material should be given as follows: "Reprinted (adapted) with permission from (COMPLETE REFERENCE CITATION). Copyright (YEAR) American Chemical Society." Insert appropriate information in place of the capitalized words.
- One-time permission is granted only for the use specified in your request. No additional uses are granted (such as derivative works or other editions). For any other uses, please submit a new request.



Title: Principles of an Electronic
Theory of Organic Reactions.
Author: Christopher K. Ingold
Publication: Chemical Reviews
Publisher: American Chemical Society
Date: Oct 1, 1934

Copyright © 1934, American Chemical Society

Logged in as:
Alexandria Naden
Account #:
3000742786

LOGOUT

PERMISSION/LICENSE IS GRANTED FOR YOUR ORDER AT NO CHARGE

This type of permission/license, instead of the standard Terms & Conditions, is sent to you because no fee is being charged for your order. Please note the following:

- Permission is granted for your request in both print and electronic formats, and translations.
- If figures and/or tables were requested, they may be adapted or used in part.
- Please print this page for your records and send a copy of it to your publisher/graduate school.
- Appropriate credit for the requested material should be given as follows: "Reprinted (adapted) with permission from (COMPLETE REFERENCE CITATION). Copyright (YEAR) American Chemical Society." Insert appropriate information in place of the capitalized words.
- One-time permission is granted only for the use specified in your request. No additional uses are granted (such as derivative works or other editions). For any other uses, please submit a new request.

All payments must be made in full to CCC. For payment instructions, please see information listed at the bottom of this form.

License Number	3337031021096
Order Date	Feb 27, 2014
Publisher	AIP Publishing LLC
Publication	Journal of Chemical Physics
Article Title	Correlation of Hammett's σ -Values with Electron Densities Calculated by Molecular Orbital Theory
Author	H. H. Jaffé
Online Publication Date	Dec 23, 2004
Volume number	20
Issue number	2
Type of Use	Thesis/Dissertation
Requestor type	Student
Format	Print and electronic
Portion	Excerpt (< 800 words)
Will you be translating?	No
Title of your thesis / dissertation	Exploring theoretical origins of the toxicity of organic quaternary ammonium salts towards Escherichia coli using machine learning approaches
Expected completion date	Mar 2014
Estimated size (number of pages)	160
Total	0.00 GBP

Appendix 2: QTMS descriptors of imidazolium carboxylates.

Structure 1: 1-ethyl-3-methylimidazolium acetate

Bond critical points							
BCP #	=	1	2	3	4	5	6
n1-n2	=	2- 1	5- 4	5- 1	6- 1	2- 3	9-21
A - B	=	C - N	C - N	C - N	C - N	C - C	H - O
x	=	0.02069	2.94778	1.61251	-1.38333	1.20707	2.51619
y	=	0.03027	-0.00331	0.00997	0.03773	0.01967	-0.03640
z	=	1.64448	-0.07365	-0.51166	-1.17788	2.98814	-4.06532
RHO	=	0.27776	0.32346	0.32404	0.21838	0.32393	0.02088
LAP	=	-0.60092	-0.76471	-0.76913	-0.21113	-0.84717	0.07534
ellip	=	0.03614	0.00982	0.00604	0.07798	0.27069	0.26162
K(r)	=	0.38473	0.49982	0.50107	0.27176	0.32729	0.00030
G(r)	=	0.23450	0.30864	0.30878	0.21898	0.11550	0.01914
BCP #	=	7	8	9	10	11	12
n1-n2	=	9- 5	3- 4	7- 2	8- 3	10- 4	11-10
A - B	=	H - C	C - N	H - C	H - C	C - N	C - C
x	=	2.90740	2.95964	-1.10366	2.92098	5.76112	7.27945
y	=	-0.01271	0.00098	0.03984	0.00052	-0.02550	1.26122
z	=	-2.15081	2.60637	3.23514	4.55656	1.14393	1.53770
RHO	=	0.28196	0.27753	0.27840	0.27846	0.21642	0.23175
LAP	=	-1.17214	-0.60308	-0.93049	-0.93049	-0.23421	-0.43935
ellip	=	0.01236	0.03483	0.03177	0.03152	0.08260	0.04967
K(r)	=	0.31604	0.38374	0.27271	0.27279	0.26527	0.16785
G(r)	=	0.02301	0.23297	0.04009	0.04017	0.20671	0.05801
BCP #	=	13	14	15	16	17	18
n1-n2	=	9-22	17- 6	18- 6	19- 6	17-21	20-21
A - B	=	H - O	H - C	H - C	H - C	H - O	C - O
x	=	4.12554	-1.65488	-2.80615	-2.83358	-0.07013	3.28032
y	=	-0.06188	0.02596	1.09729	-0.98963	-0.01701	-0.10825
z	=	-3.56586	-3.00947	-1.55344	-1.53619	-4.63839	-6.76460
RHO	=	0.02782	0.27435	0.26825	0.26826	0.01437	0.34866
LAP	=	0.09524	-0.91595	-0.80799	-0.80814	0.05723	-0.70706
ellip	=	0.02491	0.04446	0.07109	0.07103	0.01919	0.12214
K(r)	=	0.00101	0.26507	0.24869	0.24871	-0.00102	0.55699
G(r)	=	0.02482	0.03608	0.04669	0.04668	0.01328	0.38023
BCP #	=	19	20	21	22	23	24
n1-n2	=	20-22	15-10	16-10	15-22	12-11	13-11
A - B	=	C - O	H - C	H - C	H - O	H - C	H - C
x	=	4.69950	7.01959	7.11306	6.44950	9.10694	7.53831
y	=	-0.13180	-0.29551	-0.98916	-0.28049	2.41198	2.75962
z	=	-6.34282	-0.14767	1.84611	-2.54135	1.85465	3.11597
RHO	=	0.34818	0.27596	0.26938	0.00910	0.26137	0.25989
LAP	=	-0.69241	-0.89715	-0.80916	0.03830	-0.75274	-0.73353
ellip	=	0.12237	0.04440	0.06619	0.09037	0.01856	0.02023
K(r)	=	0.55596	0.26287	0.24890	-0.00126	0.23864	0.23621
G(r)	=	0.38286	0.03858	0.04661	0.00831	0.05045	0.05283
BCP #	=	25	26	27	28	29	
n1-n2	=	14-11	23-20	24-23	25-23	26-23	
A - B	=	H - C	C - C	H - C	H - C	H - C	
x	=	7.44895	4.51771	6.15530	4.39777	4.44078	
y	=	3.41269	-0.17491	-0.19867	0.76723	-1.26884	
z	=	1.16974	-8.35130	-9.77686	-10.29159	-10.21044	
RHO	=	0.26319	0.24281	0.26456	0.25950	0.25882	
LAP	=	-0.76596	-0.47868	-0.77321	-0.73957	-0.73494	
ellip	=	0.01692	0.01864	0.01376	0.01409	0.01394	
K(r)	=	0.24138	0.18098	0.24441	0.23651	0.23543	
G(r)	=	0.04989	0.06131	0.05111	0.05162	0.05169	

Structure 2: 1-ethyl-3-methylimidazolium butanoate

----- Bond critical points -----							
BCP #	=	1	2	3	4	5	6
n1-n2	=	2- 1	5- 1	6- 1	3- 2	5- 4	9- 5
A - B	=	C - N	C - N	C - N	C - C	C - N	H - C
x	=	0.04175	1.65060	-1.33203	1.22117	2.98253	2.91989
y	=	0.03045	-0.02709	0.01935	0.02775	-0.04483	-0.06560
z	=	1.60384	-0.54446	-1.23401	2.95164	-0.09769	-2.18713
RHO	=	0.27742	0.32329	0.22011	0.32391	0.32431	0.28209
LAP	=	-0.59301	-0.75446	-0.23354	-0.84702	-0.77794	-1.17411
ellip	=	0.03533	0.01206	0.05933	0.27079	0.00471	0.01232
K(r)	=	0.38487	0.49995	0.27421	0.32724	0.50127	0.31650
G(r)	=	0.23662	0.31134	0.21582	0.11549	0.30678	0.02298
BCP #	=	7	8	9	10	11	12
n1-n2	=	9-22	3- 4	7- 2	8- 3	11- 4	10-11
A - B	=	H - O	C - N	H - C	H - C	C - N	C - C
x	=	2.71715	2.97666	-1.09140	2.92593	5.79227	7.26470
y	=	-0.06805	-0.00902	0.07671	0.02206	-0.08245	-1.40127
z	=	-4.04191	2.57773	3.18621	4.52877	1.14263	1.57855
RHO	=	0.02742	0.27775	0.27831	0.27853	0.21487	0.23175
LAP	=	0.09432	-0.60984	-0.92971	-0.93127	-0.21485	-0.43924
ellip	=	0.03795	0.03546	0.03207	0.03122	0.10067	0.05098
K(r)	=	0.00096	0.38336	0.27256	0.27292	0.26317	0.16778
G(r)	=	0.02454	0.23090	0.04014	0.04010	0.20946	0.05797
BCP #	=	13	14	15	16	17	18
n1-n2	=	9-20	12- 6	13- 6	14- 6	13-22	19-20
A - B	=	H - O	H - C	H - C	H - C	H - O	C - O
x	=	4.31849	-2.78510	-1.58644	-2.75070	0.20321	5.20577
y	=	-0.06913	-1.00479	0.00786	1.08368	-0.02461	-0.06222
z	=	-3.54230	-1.61446	-3.06109	-1.63261	-4.63570	-6.20158
RHO	=	0.02158	0.26854	0.27386	0.26854	0.01070	0.34980
LAP	=	0.07751	-0.81083	-0.90102	-0.81095	0.04439	-0.66756
ellip	=	0.23365	0.06866	0.04576	0.06861	0.05596	0.12882
K(r)	=	0.00042	0.24916	0.26253	0.24917	-0.00122	0.56004
G(r)	=	0.01980	0.04645	0.03727	0.04643	0.00987	0.39315
BCP #	=	19	20	21	22	23	24
n1-n2	=	19-22	17-10	18-10	15-20	32-10	15-11
A - B	=	C - O	H - C	H - C	H - O	H - C	H - C
x	=	3.79930	7.46324	7.37921	6.70807	9.05546	7.07012
y	=	-0.06112	-2.87861	-3.56431	0.09809	-2.59741	0.12645
z	=	-6.65764	3.18774	1.25317	-2.46948	1.94037	-0.14848
RHO	=	0.34649	0.25966	0.26312	0.01232	0.26138	0.27673
LAP	=	-0.71401	-0.73141	-0.76535	0.04976	-0.75293	-0.91184
ellip	=	0.12873	0.01999	0.01669	0.04743	0.01813	0.04319
K(r)	=	0.55162	0.23584	0.24128	-0.00115	0.23867	0.26545
G(r)	=	0.37312	0.05299	0.04994	0.01130	0.05044	0.03749
BCP #	=	25	26	27	28	29	30
n1-n2	=	16-11	21-19	23-21	23-24	30-21	31-21
A - B	=	H - C	C - C	C - C	C - C	H - C	H - C
x	=	7.15801	5.07433	6.89987	8.63718	4.92345	4.93773
y	=	0.85615	-0.05261	-0.03590	-0.01924	0.96262	-1.05970
z	=	1.84173	-8.22790	-9.77164	-11.37570	-10.09729	-10.10269
RHO	=	0.26911	0.24115	0.23044	0.22604	0.25941	0.25931
LAP	=	-0.80654	-0.46949	-0.42876	-0.41374	-0.72979	-0.72906
ellip	=	0.06848	0.03362	0.02460	0.01359	0.01494	0.01487
K(r)	=	0.24846	0.17846	0.16531	0.16039	0.23454	0.23437
G(r)	=	0.04682	0.06109	0.05812	0.05696	0.05209	0.05210
BCP #	=	31	32	33	34	35	
n1-n2	=	28-23	29-23	25-24	26-24	27-24	
A - B	=	H - C	H - C	H - C	H - C	H - C	
x	=	8.80896	8.82263	8.53095	10.23215	8.51742	
y	=	0.98519	-1.03316	-1.02820	-0.00374	1.00048	
z	=	-9.42669	-9.43265	-13.37982	-12.96382	-13.37363	

RHO	=	0.26299	0.26304	0.25805	0.25859	0.25805
LAP	=	-0.75302	-0.75342	-0.72016	-0.72513	-0.72021
ellip	=	0.01573	0.01570	0.00827	0.00890	0.00827
K(r)	=	0.23990	0.23998	0.23327	0.23438	0.23328
G(r)	=	0.05164	0.05162	0.05323	0.05310	0.05323

Structure 3 : 1-ethyl-3-methylimidazolium decanoate

----- Bond critical points -----

BCP #	=	1	2	3	4	5	6
n1-n2	=	2- 1	5- 4	5- 1	6- 1	23- 5	23-13
A - B	=	C - N	C - N	C - N	C - N	H - C	H - O
x	=	0.07330	2.93929	1.59082	-1.43290	2.85647	2.44647
y	=	-0.16277	-0.10958	-0.09554	-0.07614	-0.05047	-0.01073
z	=	1.68600	-0.12904	-0.52136	-1.07747	-2.20666	-4.22068
RHO	=	0.27791	0.32249	0.32374	0.21800	0.27878	0.01697
LAP	=	-0.60486	-0.75533	-0.77325	-0.20497	-1.15582	0.06711
ellip	=	0.03639	0.01484	0.00539	0.08408	0.01233	3.97022
K(r)	=	0.38462	0.49788	0.50011	0.27128	0.31192	-0.00012
G(r)	=	0.23341	0.30904	0.30680	0.22003	0.02297	0.01666
BCP #	=	7	8	9	10	11	12
n1-n2	=	2- 3	3- 4	21- 2	7- 4	22- 3	8- 7
A - B	=	C - C	C - N	H - C	C - N	H - C	C - C
x	=	1.30323	3.04161	-0.99756	5.78912	3.06837	7.31021
y	=	-0.20562	-0.19375	-0.21729	-0.14222	-0.25891	1.14795
z	=	2.99015	2.55126	3.31289	0.99625	4.50003	1.37966
RHO	=	0.32412	0.27755	0.27839	0.21741	0.27839	0.23174
LAP	=	-0.84837	-0.60115	-0.93044	-0.24558	-0.92976	-0.43931
ellip	=	0.27064	0.03421	0.03163	0.07352	0.03155	0.04901
K(r)	=	0.32771	0.38407	0.27269	0.26666	0.27265	0.16785
G(r)	=	0.11561	0.23378	0.04008	0.20526	0.04021	0.05802
BCP #	=	13	14	15	16	17	18
n1-n2	=	23- 9	24-13	24- 6	25- 6	26- 6	27- 9
A - B	=	H - O	H - O	H - C	H - C	H - C	H - O
x	=	3.90163	-0.35048	-1.77623	-2.87742	-2.88525	6.23288
y	=	-0.03114	0.00240	-0.02922	0.98019	-1.10562	-0.25945
z	=	-3.67538	-4.62756	-2.89957	-1.35926	-1.41164	-2.73658
RHO	=	0.03341	0.01586	0.27460	0.26811	0.26811	0.00765
LAP	=	0.11343	0.06197	-0.92169	-0.80670	-0.80679	0.03331
ellip	=	0.02319	0.00643	0.04403	0.07190	0.07185	0.15360
K(r)	=	0.00137	-0.00090	0.26617	0.24846	0.24847	-0.00129
G(r)	=	0.02972	0.01459	0.03575	0.04678	0.04677	0.00703
BCP #	=	19	20	21	22	23	24
n1-n2	=	27- 7	28- 7	29- 8	30- 8	31- 8	11-12
A - B	=	H - C	H - C	H - C	H - C	H - C	C - C
x	=	7.00719	7.17580	7.44612	9.13660	7.60897	4.02822
y	=	-0.35808	-1.11362	3.31141	2.30672	2.59652	0.02897
z	=	-0.34020	1.62105	1.07624	1.67102	2.99596	-8.53410
RHO	=	0.27558	0.26947	0.26320	0.26135	0.26000	0.24077
LAP	=	-0.89007	-0.81004	-0.76605	-0.75256	-0.73456	-0.46749
ellip	=	0.04498	0.06493	0.01700	0.01874	0.02028	0.03397
K(r)	=	0.26170	0.24903	0.24139	0.23860	0.23638	0.17802
G(r)	=	0.03918	0.04652	0.04988	0.05046	0.05274	0.06115
BCP #	=	25	26	27	28	29	30
n1-n2	=	12- 9	10-11	10-14	14-15	32-10	33-10
A - B	=	C - O	C - C	C - C	C - C	H - C	H - C
x	=	4.23061	3.35110	2.73932	3.93372	1.50174	1.61938
y	=	0.00646	0.06259	-0.01249	1.00049	-0.86880	1.14205
z	=	-6.52166	-10.82579	-13.13467	-15.00806	-11.52366	-11.63042
RHO	=	0.34505	0.22976	0.22621	0.22680	0.26351	0.26143
LAP	=	-0.71455	-0.42579	-0.41270	-0.41339	-0.75661	-0.74035
ellip	=	0.13057	0.02207	0.01022	0.01697	0.01528	0.01560
K(r)	=	0.54804	0.16451	0.15989	0.16066	0.24060	0.23727
G(r)	=	0.36941	0.05806	0.05671	0.05731	0.05145	0.05218

BCP #	=	31	32	33	34	35	36
n1-n2	=	34-11	35-11	12-13	15-16	36-14	37-14
A - B	=	H - C	H - C	C - O	C - C	H - C	H - C
x	=	5.20162	5.15916	2.80555	5.02818	3.85889	2.16277
y	=	1.03382	-0.98687	0.02516	2.03898	-1.17053	-0.26279
z	=	-9.99414	-10.02729	-6.91208	-16.89548	-14.66672	-15.26191
RHO	=	0.26089	0.25893	0.35146	0.22692	0.25808	0.25890
LAP	=	-0.73910	-0.72586	-0.65632	-0.41384	-0.71317	-0.71919
ellip	=	0.01439	0.01570	0.12737	0.01786	0.00962	0.00980
K(r)	=	0.23720	0.23376	0.56410	0.16077	0.23179	0.23318
G(r)	=	0.05243	0.05230	0.40002	0.05731	0.05350	0.05339
BCP #	=	37	38	39	40	41	42
n1-n2	=	16-17	17-18	38-15	39-15	40-16	41-16
A - B	=	C - C	C - C	H - C	H - C	H - C	H - C
x	=	6.20236	6.44037	4.03766	5.76527	5.93607	4.29674
y	=	2.99399	5.35130	3.18540	2.24607	0.82960	1.89849
z	=	-18.80667	-19.35859	-15.28657	-14.83932	-18.49824	-18.98043
RHO	=	0.22575	0.22679	0.26010	0.26006	0.25951	0.25854
LAP	=	-0.41061	-0.41321	-0.72684	-0.72671	-0.72410	-0.71720
ellip	=	0.00826	0.01845	0.00901	0.00845	0.01043	0.00981
K(r)	=	0.15927	0.16058	0.23541	0.23526	0.23407	0.23249
G(r)	=	0.05661	0.05728	0.05370	0.05358	0.05304	0.05319
BCP #	=	43	44	45	46	47	48
n1-n2	=	18-19	42-17	43-17	19-20	44-18	45-18
A - B	=	C - C	H - C	H - C	C - C	H - C	H - C
x	=	6.66718	8.10547	7.42621	7.81818	4.76798	5.46120
y	=	7.70337	4.10720	3.73405	8.64287	6.59785	6.97853
z	=	-19.91950	-18.62437	-20.48454	-21.83077	-20.08416	-18.22900
RHO	=	0.22591	0.25843	0.26082	0.22573	0.25825	0.26161
LAP	=	-0.41107	-0.71639	-0.73178	-0.41186	-0.71492	-0.73848
ellip	=	0.00895	0.00982	0.00959	0.00958	0.01111	0.00950
K(r)	=	0.15943	0.23232	0.23656	0.15980	0.23206	0.23776
G(r)	=	0.05666	0.05323	0.05361	0.05683	0.05333	0.05314
BCP #	=	49	50	51	52	53	
n1-n2	=	46-19	47-19	48-20	49-20	50-20	
A - B	=	H - C	H - C	H - C	H - C	H - C	
x	=	8.58161	6.93958	8.80894	8.79725	7.08062	
y	=	8.80311	9.87259	7.49834	9.51959	8.47194	
z	=	-19.77058	-20.24238	-23.48857	-23.64339	-23.93170	
RHO	=	0.25954	0.26038	0.26035	0.25904	0.25844	
LAP	=	-0.72574	-0.73101	-0.73664	-0.72857	-0.72372	
ellip	=	0.01186	0.01272	0.01073	0.01130	0.01077	
K(r)	=	0.23414	0.23558	0.23721	0.23501	0.23387	
G(r)	=	0.05271	0.05282	0.05305	0.05287	0.05294	

Structure 4: 1-ethyl-3-methylimidazolium formate

----- Bond critical points -----							
BCP #	=	1	2	3	4	5	6
n1-n2	=	2- 1	5- 1	6- 1	3- 2	5- 4	9-21
A - B	=	C - N	C - N	C - N	C - C	C - N	H - O
x	=	0.11034	1.71311	-1.27204	1.29139	3.04744	2.71955
y	=	-0.02587	0.15837	0.12688	-0.08435	0.16396	0.41852
z	=	1.40439	-0.73878	-1.42726	2.74931	-0.29255	-4.27383
RHO	=	0.27738	0.32390	0.21926	0.32384	0.32470	0.02327
LAP	=	-0.59168	-0.76246	-0.22472	-0.84670	-0.77706	0.08045
ellip	=	0.03499	0.00601	0.06275	0.27052	0.00223	0.09821
K(r)	=	0.38495	0.50100	0.27289	0.32708	0.50224	0.00065
G(r)	=	0.23703	0.31039	0.21671	0.11540	0.30797	0.02076
BCP #	=	7	8	9	10	11	12
n1-n2	=	9- 5	3- 4	7- 2	8- 3	10- 4	11-10
A - B	=	H - C	C - N	H - C	H - C	C - N	C - C
x	=	2.99237	3.04500	-1.02081	2.99795	5.85804	7.32222

y	=	0.29307	-0.01302	-0.16483	-0.14717	0.16245	1.46207
z	=	-2.36312	2.37788	2.98281	4.32425	0.93928	1.46077
RHO	=	0.28372	0.27758	0.27845	0.27864	0.21483	0.23176
LAP	=	-1.17335	-0.60495	-0.93131	-0.93264	-0.21578	-0.43940
ellip	=	0.01251	0.03476	0.03199	0.03129	0.09546	0.05034
K(r)	=	0.31676	0.38363	0.27286	0.27319	0.26300	0.16787
G(r)	=	0.02342	0.23239	0.04003	0.04003	0.20906	0.05802
BCP #	=	13	14	15	16	17	18
n1-n2	=	9-22	17- 6	18- 6	19- 6	17-21	20-22
A - B	=	H - O	H - C	H - C	H - C	H - O	C - O
x	=	4.35005	-1.53186	-2.73045	-2.68550	0.19520	5.11567
y	=	0.41139	0.23322	1.16223	-0.92293	0.38962	0.61331
z	=	-3.73815	-3.25217	-1.74842	-1.87507	-4.86088	-6.43904
RHO	=	0.02319	0.27394	0.26861	0.26860	0.01139	0.35109
LAP	=	0.08019	-0.90362	-0.81159	-0.81151	0.04631	-0.63421
ellip	=	0.10020	0.04582	0.06923	0.06923	0.03857	0.12580
K(r)	=	0.00065	0.26294	0.24929	0.24928	-0.00115	0.56324
G(r)	=	0.02070	0.03704	0.04639	0.04640	0.01043	0.40468
BCP #	=	19	20	21	22	23	24
n1-n2	=	20-21	15-10	16-10	15-22	12-11	13-11
A - B	=	C - O	H - C	H - C	H - O	H - C	H - C
x	=	3.71234	7.13038	7.23700	6.70097	9.10423	7.51923
y	=	0.61959	0.05605	-0.81135	0.23297	2.64559	2.82163
z	=	-6.90057	-0.36600	1.56476	-2.70646	1.89337	3.16935
RHO	=	0.35072	0.27646	0.26933	0.01120	0.26147	0.25978
LAP	=	-0.63437	-0.90682	-0.80871	0.04558	-0.75382	-0.73242
ellip	=	0.12624	0.04385	0.06793	0.05296	0.01840	0.02037
K(r)	=	0.56234	0.26453	0.24884	-0.00116	0.23881	0.23605
G(r)	=	0.40375	0.03783	0.04666	0.01023	0.05036	0.05294
BCP #	=	25	26				
n1-n2	=	14-11	23-20				
A - B	=	H - C	H - C				
x	=	7.41335	4.94001				
y	=	3.64278	0.73848				
z	=	1.28900	-8.26603				
RHO	=	0.26318	0.27133				
LAP	=	-0.76584	-0.83756				
ellip	=	0.01700	0.01065				
K(r)	=	0.24138	0.24974				
G(r)	=	0.04992	0.04035				

Structure 5: 1-ethyl-3-methylimidazolium furoate

----- Bond critical points -----

BCP #	=	1	2	3	4	5	6
n1-n2	=	2- 1	5- 1	6- 1	2- 3	5- 4	9-26
A - B	=	C - N	C - N	C - N	C - C	C - N	H - O
x	=	0.07617	2.14068	-0.52360	0.85672	3.29470	4.00007
y	=	-0.53957	0.11318	-0.17124	-0.64343	0.21087	0.92678
z	=	1.23144	-0.35161	-1.84263	2.83980	0.44680	-3.40299
RHO	=	0.27754	0.32393	0.21900	0.32391	0.32429	0.02449
LAP	=	-0.59351	-0.76410	-0.22023	-0.84713	-0.77455	0.08634
ellip	=	0.03493	0.00541	0.06397	0.27063	0.00321	0.10461
K(r)	=	0.38518	0.50100	0.27258	0.32723	0.50138	0.00063
G(r)	=	0.23680	0.30997	0.21753	0.11544	0.30774	0.02222

BCP #	=	7	8	9	10	11	12
n1-n2	=	9- 5	3- 4	7- 2	8- 3	10- 4	11-10
A - B	=	H - C	C - N	H - C	H - C	C - N	C - C
x	=	3.76972	2.61579	-1.39744	2.07939	5.64953	6.72418
y	=	0.61055	-0.32341	-1.01829	-0.72272	0.36170	1.75043
z	=	-1.53513	2.98120	2.41058	4.81381	2.40846	3.42099
RHO	=	0.28353	0.27758	0.27844	0.27855	0.21544	0.23174
LAP	=	-1.17441	-0.60295	-0.93129	-0.93178	-0.22207	-0.43933
ellip	=	0.01248	0.03456	0.03189	0.03139	0.09006	0.05019
K(r)	=	0.31692	0.38392	0.27283	0.27300	0.26396	0.16785
G(r)	=	0.02332	0.23319	0.04000	0.04005	0.20845	0.05801
BCP #	=	13	14	15	16	17	18
n1-n2	=	9-27	17- 6	18- 6	19- 6	17-26	20-27
A - B	=	H - O	H - C	H - C	H - C	H - O	C - O
x	=	5.39783	-0.31087	-1.98384	-1.59814	1.72638	6.81335
y	=	1.03178	0.14494	0.72015	-1.31016	0.68064	1.61167
z	=	-2.49807	-3.64954	-2.45220	-2.76219	-4.69047	-4.84366
RHO	=	0.02303	0.27423	0.26861	0.26862	0.01174	0.35146
LAP	=	0.08168	-0.90655	-0.81164	-0.81185	0.04874	-0.77825
ellip	=	0.14630	0.04589	0.06951	0.06944	0.04177	0.08575
K(r)	=	0.00055	0.26361	0.24930	0.24933	-0.00126	0.56290
G(r)	=	0.02097	0.03697	0.04639	0.04637	0.01092	0.36833
BCP #	=	19	20	21	22	23	24
n1-n2	=	15-10	16-10	15-27	12-11	13-11	14-11
A - B	=	H - C	H - C	H - O	H - C	H - C	H - C
x	=	7.22649	6.93472	7.41443	8.14009	6.26161	6.55176
y	=	0.55094	-0.51499	0.96086	3.06911	2.91680	3.93279
z	=	1.50975	3.31494	-0.85827	4.43084	5.21833	3.45599
RHO	=	0.27635	0.26935	0.01056	0.26139	0.25985	0.26317
LAP	=	-0.90355	-0.80894	0.04365	-0.75302	-0.73316	-0.76587
ellip	=	0.04413	0.06719	0.05413	0.01850	0.02025	0.01696
K(r)	=	0.26402	0.24886	-0.00123	0.23868	0.23615	0.24136
G(r)	=	0.03813	0.04662	0.00968	0.05042	0.05285	0.04989
BCP #	=	25	26	27	28	29	30
n1-n2	=	20-21	22-21	21-25	20-26	22-23	24-25
A - B	=	C - C	C - C	C - O	C - O	C - C	C - O
x	=	7.11288	9.21002	7.54801	5.56534	10.64949	7.98181
y	=	1.93411	2.47903	2.29522	1.51933	2.93701	2.76193
z	=	-6.69073	-7.98042	-8.63858	-5.66045	-9.43749	-11.30806
RHO	=	0.25914	0.32317	0.25045	0.35812	0.26801	0.25847
LAP	=	-0.56265	-0.84808	-0.02328	-0.72509	-0.57269	-0.06395
ellip	=	0.06581	0.23488	0.05328	0.08433	0.09545	0.08941
K(r)	=	0.20365	0.32947	0.33528	0.58050	0.22310	0.35129
G(r)	=	0.06299	0.11745	0.32946	0.39923	0.07993	0.33530
BCP #	=	31	32	33	34		
n1-n2	=	28-22	23-24	29-23	30-24		
A - B	=	H - C	C - C	H - C	H - C		
x	=	11.26615	9.77076	11.94217	8.17293		
y	=	2.70881	3.06689	3.43318	3.06235		
z	=	-7.18427	-11.32604	-11.32255	-13.12690		
RHO	=	0.27566	0.32183	0.27230	0.28061		
LAP	=	-0.90018	-0.84750	-0.86215	-0.94351		
ellip	=	0.00386	0.23428	0.01109	0.03755		
K(r)	=	0.26742	0.33067	0.26123	0.27543		
G(r)	=	0.04238	0.11880	0.04570	0.03955		

Structure 6: 1-ethyl-3-methylimidazolium glucolate

----- Bond critical points -----

BCP #	=	1	2	3	4	5	6
n1-n2	=	2- 1	5- 4	5- 1	6- 1	2- 3	9- 5
A - B	=	C - N	C - N	C - N	C - N	C - C	H - C
x	=	0.10763	3.02339	1.68873	-1.30185	1.29172	2.97326
y	=	-0.17275	0.20950	0.13806	-0.05086	-0.19020	0.37427
z	=	1.83527	0.13742	-0.30719	-0.98213	3.17775	-1.92177

RHO	=	0.27763	0.32378	0.32436	0.21806	0.32408	0.28348
LAP	=	-0.59318	-0.76962	-0.77394	-0.20757	-0.84822	-1.16534
ellip	=	0.03409	0.00203	0.00163	0.07197	0.27030	0.01272
K(r)	=	0.38549	0.50023	0.50148	0.27128	0.32753	0.31489
G(r)	=	0.23719	0.30783	0.30800	0.21939	0.11548	0.02356
BCP #	=	7	8	9	10	11	12
n1-n2	=	3- 4	7- 2	8- 3	10- 4	11-10	9-22
A - B	=	C - N	H - C	H - C	C - N	C - C	H - O
x	=	3.03595	-1.01195	3.00339	5.82815	7.22178	4.19879
y	=	-0.01599	-0.40286	-0.18746	0.34069	1.72687	0.56921
z	=	2.80871	3.41195	4.75073	1.37137	1.88591	-3.37302
RHO	=	0.27737	0.27857	0.27862	0.21629	0.23171	0.02579
LAP	=	-0.59474	-0.93320	-0.93314	-0.23317	-0.43936	0.08984
ellip	=	0.03283	0.03167	0.03148	0.07448	0.04881	0.03157
K(r)	=	0.38449	0.27313	0.27321	0.26507	0.16795	0.00078
G(r)	=	0.23580	0.03983	0.03992	0.20678	0.05811	0.02324
BCP #	=	13	14	15	16	17	18
n1-n2	=	9-23	17- 6	18- 6	19- 6	17-23	20-22
A - B	=	H - O	H - C	H - C	H - C	H - O	C - O
x	=	2.57829	-1.58524	-2.81941	-2.65199	-0.00442	4.74640
y	=	0.49287	0.07400	0.90135	-1.17463	0.32827	0.81164
z	=	-3.86678	-2.80531	-1.26482	-1.43318	-4.44817	-6.15472
RHO	=	0.01965	0.27455	0.26857	0.26857	0.01378	0.34720
LAP	=	0.07192	-0.91336	-0.81127	-0.81139	0.05530	-0.66893
ellip	=	0.26153	0.04551	0.07056	0.07051	0.01790	0.14033
K(r)	=	0.00011	0.26488	0.24924	0.24925	-0.00108	0.55365
G(r)	=	0.01809	0.03654	0.04642	0.04641	0.01275	0.38642
BCP #	=	19	20	21	22	23	24
n1-n2	=	15-10	16-10	15-22	12-11	13-11	14-11
A - B	=	H - C	H - C	H - O	H - C	H - C	H - C
x	=	7.10825	7.26198	6.53532	8.93512	7.33826	7.19231
y	=	0.29526	-0.55140	0.47531	3.00658	3.10172	3.90607
z	=	0.07910	2.00452	-2.35074	2.31369	3.58570	1.69982
RHO	=	0.27583	0.26973	0.00829	0.26153	0.26017	0.26320
LAP	=	-0.89165	-0.81262	0.03532	-0.75439	-0.73603	-0.76606
ellip	=	0.04570	0.06528	0.09278	0.01907	0.02076	0.01760
K(r)	=	0.26217	0.24948	-0.00127	0.23888	0.23663	0.24139
G(r)	=	0.03926	0.04632	0.00756	0.05029	0.05263	0.04987
BCP #	=	25	26	27	28	29	30
n1-n2	=	21-20	20-23	21-24	26-21	27-21	25-22
A - B	=	C - C	C - O	C - O	H - C	H - C	H - O
x	=	4.56268	3.32352	5.90291	4.39301	4.54045	7.23792
y	=	0.94735	0.74364	1.14739	2.11743	0.04861	1.05465
z	=	-8.13313	-6.56970	-9.53398	-9.96938	-10.12334	-7.05725
RHO	=	0.24569	0.35554	0.23103	0.27043	0.27040	0.02350
LAP	=	-0.48684	-0.68919	-0.32511	-0.82329	-0.82302	0.09185
ellip	=	0.06693	0.12066	0.05850	0.05163	0.05164	0.48143
K(r)	=	0.18217	0.57412	0.27501	0.25128	0.25121	0.00031
G(r)	=	0.06046	0.40182	0.19373	0.04546	0.04546	0.02327
BCP #	=	31					
n1-n2	=	25-24					
A - B	=	H - O					
x	=	8.22327					
y	=	1.22723					
z	=	-8.43349					
RHO	=	0.34607					
LAP	=	-1.72340					
ellip	=	0.02394					
K(r)	=	0.49773					
G(r)	=	0.06688					

Structure 7: 1-ethyl-3-methylimidazolium hexanoate

----- Bond critical points -----						
BCP #	=	1	2	3	4	5
n1-n2	=	2- 1	5- 4	5- 1	6- 1	2- 3
A - B	=	C - N	C - N	C - N	C - N	C - C
x	=	0.00024	2.88787	1.54473	-1.47236	1.21424
y	=	0.00008	-0.00210	-0.00154	-0.00291	-0.00011
						-0.00901

z	=	1.68893	-0.09217	-0.50094	-1.09419	3.00856	-2.17123
RHO	=	0.27790	0.32243	0.32368	0.21797	0.32412	0.27878
LAP	=	-0.60450	-0.75333	-0.77119	-0.20424	-0.84844	-1.15571
ellip	=	0.03661	0.01438	0.00497	0.08436	0.27057	0.01242
K(r)	=	0.38463	0.49781	0.50005	0.27126	0.32771	0.31190
G(r)	=	0.23350	0.30947	0.30725	0.22020	0.11560	0.02298
BCP #	=	7	8	9	10	11	12
n1-n2	=	9-26	3- 4	7- 2	8- 3	10- 4	11-10
A - B	=	H - O	C - N	H - C	H - C	C - N	C - C
x	=	2.44212	2.95781	-1.09031	2.96093	5.72416	7.23979
y	=	-0.03478	-0.00094	-0.00354	-0.00376	0.00272	1.30601
z	=	-4.18921	2.59067	3.30358	4.54070	1.06824	1.42809
RHO	=	0.01697	0.27754	0.27840	0.27839	0.21738	0.23174
LAP	=	0.06707	-0.60091	-0.93047	-0.92981	-0.24498	-0.43934
ellip	=	3.77098	0.03442	0.03166	0.03157	0.07363	0.04902
K(r)	=	-0.00012	0.38406	0.27270	0.27266	0.26665	0.16786
G(r)	=	0.01665	0.23384	0.04008	0.04021	0.20540	0.05803
BCP #	=	13	14	15	16	17	18
n1-n2	=	9-22	17- 6	18- 6	19- 6	17-26	25-22
A - B	=	H - O	H - C	H - C	H - C	H - O	C - O
x	=	3.89365	-1.79326	-2.91369	-2.91997	-0.34667	4.25707
y	=	-0.03523	-0.01473	1.04267	-1.04378	-0.03757	-0.08757
z	=	-3.62715	-2.92090	-1.42721	-1.41276	-4.63131	-6.46900
RHO	=	0.03339	0.27461	0.26811	0.26812	0.01586	0.34504
LAP	=	0.11341	-0.92185	-0.80672	-0.80685	0.06199	-0.71431
ellip	=	0.02319	0.04404	0.07194	0.07189	0.00633	0.13057
K(r)	=	0.00136	0.26620	0.24846	0.24848	-0.00090	0.54803
G(r)	=	0.02971	0.03573	0.04678	0.04677	0.01460	0.36945
BCP #	=	19	20	21	22	23	24
n1-n2	=	25-26	15-10	16-10	15-22	12-11	13-11
A - B	=	C - O	H - C	H - C	H - O	H - C	H - C
x	=	2.83674	6.95837	7.10341	6.21299	9.06193	7.51811
y	=	-0.08388	-0.25532	-0.94674	-0.23249	2.47505	2.80641
z	=	-6.87697	-0.24565	1.74101	-2.65307	1.70390	3.00002
RHO	=	0.35149	0.27559	0.26947	0.00765	0.26135	0.26000
LAP	=	-0.65726	-0.89016	-0.81004	0.03329	-0.75256	-0.73457
ellip	=	0.12726	0.04500	0.06497	0.15338	0.01876	0.02029
K(r)	=	0.56418	0.26172	0.24903	-0.00129	0.23861	0.23638
G(r)	=	0.39987	0.03918	0.04652	0.00703	0.05046	0.05274
BCP #	=	25	26	27	28	29	30
n1-n2	=	14-11	23-24	24-25	20-23	23-29	29-30
A - B	=	H - C	C - C	C - C	H - C	C - C	C - C
x	=	7.37840	3.42971	4.07899	1.71571	2.84471	4.06312
y	=	3.45853	-0.15611	-0.12820	0.91172	-0.29340	0.65904
z	=	1.05625	-10.78333	-8.48344	-11.63997	-13.09642	-14.98581
RHO	=	0.26320	0.22971	0.24075	0.26137	0.22625	0.22722
LAP	=	-0.76610	-0.42556	-0.46739	-0.73989	-0.41288	-0.41505
ellip	=	0.01701	0.02208	0.03391	0.01572	0.01032	0.01921
K(r)	=	0.24139	0.16444	0.17798	0.23718	0.15994	0.16111
G(r)	=	0.04987	0.05804	0.06114	0.05220	0.05672	0.05734
BCP #	=	31	32	33	34	35	36
n1-n2	=	21-24	28-24	27-23	30-31	32-29	33-29
A - B	=	H - C	H - C	H - C	C - C	H - C	H - C
x	=	5.27764	5.21994	1.58180	5.18703	2.29267	3.97868
y	=	0.82560	-1.19488	-1.09435	1.62519	-0.60472	-1.49936
z	=	-9.95731	-9.93279	-11.47648	-16.87844	-15.22283	-14.58108
RHO	=	0.26097	0.25887	0.26358	0.22613	0.25888	0.25793
LAP	=	-0.73967	-0.72555	-0.75724	-0.41365	-0.71887	-0.71233
ellip	=	0.01441	0.01562	0.01529	0.00978	0.00963	0.00925
K(r)	=	0.23733	0.23368	0.24073	0.16041	0.23316	0.23157
G(r)	=	0.05241	0.05229	0.05143	0.05699	0.05345	0.05349
BCP #	=	37	38	39	40	41	
n1-n2	=	34-30	35-30	36-31	37-31	38-31	
A - B	=	H - C	H - C	H - C	H - C	H - C	
x	=	5.88793	4.17357	4.51946	6.23530	6.21684	
y	=	1.91570	2.83702	1.38272	0.43839	2.45617	
z	=	-14.82214	-15.35137	-19.00057	-18.45991	-18.69375	

RHO	=	0.26127	0.25939	0.25863	0.25859	0.25892
LAP	=	-0.73672	-0.72394	-0.72488	-0.72499	-0.72793
ellip	=	0.00998	0.01186	0.00990	0.00992	0.01062
K(r)	=	0.23727	0.23399	0.23417	0.23410	0.23484
G(r)	=	0.05309	0.05301	0.05295	0.05286	0.05285

Structure 8: 1-ethyl-3-methylimidazolium i-butanoate

Bond critical points							
BCP #	=	1	2	3	4	5	6
n1-n2	=	2- 1	5- 4	5- 1	6- 1	2- 3	9- 5
A - B	=	C - N	C - N	C - N	C - N	C - C	H - C
x	=	0.02997	2.95893	1.62431	-1.37321	1.21421	2.92923
y	=	0.00172	0.00641	0.00824	0.00869	-0.00341	0.00674
z	=	1.64993	-0.06454	-0.50421	-1.17170	2.99561	-2.14209
RHO	=	0.27783	0.32313	0.32398	0.21822	0.32400	0.28115
LAP	=	-0.60199	-0.76167	-0.77080	-0.20836	-0.84763	-1.16770
ellip	=	0.03606	0.01112	0.00539	0.08055	0.27066	0.01237
K(r)	=	0.38479	0.49914	0.50084	0.27158	0.32745	0.31491
G(r)	=	0.23429	0.30873	0.30814	0.21949	0.11554	0.02298
BCP #	=	7	8	9	10	11	12
n1-n2	=	9-22	3- 4	7- 2	8- 3	10- 4	11-10
A - B	=	H - O	C - N	H - C	H - C	C - N	C - C
x	=	2.52001	2.96709	-1.09681	2.92597	5.76963	7.27528
y	=	-0.01254	-0.00239	-0.00797	-0.01279	0.00696	1.30731
z	=	-4.07565	2.61677	3.23903	4.56660	1.15866	1.56118
RHO	=	0.01961	0.27752	0.27840	0.27844	0.21678	0.23174
LAP	=	0.07219	-0.60181	-0.93056	-0.93031	-0.23827	-0.43934
ellip	=	0.40137	0.03450	0.03170	0.03154	0.07879	0.04936
K(r)	=	0.00015	0.38388	0.27271	0.27275	0.26578	0.16785
G(r)	=	0.01820	0.23343	0.04007	0.04017	0.20621	0.05802
BCP #	=	13	14	15	16	17	18
n1-n2	=	9-23	17- 6	18- 6	19- 6	17-22	32-23
A - B	=	H - O	H - C	H - C	H - C	H - O	C - O
x	=	4.11011	-1.64503	-2.80624	-2.81258	-0.09424	4.63469
y	=	-0.01995	0.00284	1.05552	-1.03145	-0.01643	-0.06847
z	=	-3.56450	-3.00423	-1.54073	-1.53338	-4.64447	-6.36149
RHO	=	0.02939	0.27444	0.26819	0.26820	0.01503	0.34658
LAP	=	0.10028	-0.91821	-0.80748	-0.80765	0.05930	-0.67256
ellip	=	0.00794	0.04427	0.07139	0.07132	0.01588	0.13136
K(r)	=	0.00112	0.26550	0.24859	0.24862	-0.00096	0.55226
G(r)	=	0.02619	0.03594	0.04672	0.04671	0.01387	0.38412
BCP #	=	19	20	21	22	23	24
n1-n2	=	15-10	16-10	15-23	12-11	13-11	14-11
A - B	=	H - C	H - C	H - O	H - C	H - C	H - C
x	=	7.03342	7.13101	6.42565	9.09073	7.51695	7.42346
y	=	-0.24419	-0.94661	-0.22033	2.47437	2.79962	3.46205
z	=	-0.13017	1.85829	-2.53811	1.88636	3.14744	1.20454
RHO	=	0.27583	0.26942	0.00853	0.26137	0.25994	0.26319
LAP	=	-0.89442	-0.80960	0.03630	-0.75279	-0.73399	-0.76593
ellip	=	0.04467	0.06564	0.11202	0.01863	0.02028	0.01698
K(r)	=	0.26243	0.24896	-0.00128	0.23864	0.23629	0.24137
G(r)	=	0.03883	0.04656	0.00780	0.05044	0.05279	0.04989
BCP #	=	25	26	27	28	29	30
n1-n2	=	31-21	31-20	31-32	24-20	25-20	26-20
A - B	=	C - C	C - C	C - C	H - C	H - C	H - C
x	=	4.39144	4.36519	4.46601	4.27058	2.61698	4.30377
y	=	1.06227	-1.32365	-0.09979	-2.56252	-2.54670	-3.55648
z	=	-10.39962	-10.36153	-8.39238	-12.20135	-10.99289	-10.42910
RHO	=	0.22502	0.22503	0.24151	0.25803	0.26238	0.25920
LAP	=	-0.40760	-0.40763	-0.47148	-0.71985	-0.75685	-0.72993
ellip	=	0.01140	0.01139	0.00775	0.01465	0.01039	0.01411
K(r)	=	0.15906	0.15907	0.17861	0.23346	0.24003	0.23511
G(r)	=	0.05716	0.05716	0.06074	0.05350	0.05082	0.05262
BCP #	=	31	32	33	34	35	
n1-n2	=	27-21	28-21	29-21	32-22	30-31	
A - B	=	H - C	H - C	H - C	C - O	H - C	

x	=	4.32299	4.37933	2.67024	3.22109	6.12649
y	=	2.24338	3.29260	2.30287	-0.06070	-0.13920
z	=	-12.27827	-10.53881	-11.06996	-6.78454	-9.71228
RHO	=	0.25803	0.25918	0.26238	0.34814	0.26693
LAP	=	-0.71986	-0.72980	-0.75686	-0.67016	-0.77568
ellip	=	0.01464	0.01412	0.01038	0.13344	0.00291
K(r)	=	0.23347	0.23508	0.24003	0.55599	0.24509
G(r)	=	0.05350	0.05263	0.05082	0.38845	0.05117

Structure 9: 1-ethyl-3-methylimidazolium L-lactate

----- Bond critical points -----						
BCP #	=	1	2	3	4	5
n1-n2	=	2- 1	5- 4	5- 1	6- 1	2- 3
A - B	=	C - N	C - N	C - N	C - N	C - C
x	=	-0.01314	3.14696	1.90772	-0.92576	0.92542
y	=	0.18939	0.13521	0.39051	0.90166	-0.21657
z	=	1.86400	0.62333	0.00502	-1.06757	3.33357
RHO	=	0.27768	0.32357	0.32429	0.21801	0.32411
LAP	=	-0.59433	-0.76764	-0.77446	-0.20650	-0.84845
ellip	=	0.03418	0.00324	0.00142	0.07366	0.27033
K(r)	=	0.38548	0.49981	0.50131	0.27124	0.32762
G(r)	=	0.23689	0.30789	0.30769	0.21962	0.11551
BCP #	=	7	8	9	10	11
n1-n2	=	3- 4	7- 2	8- 3	10- 4	11-10
A - B	=	C - N	H - C	H - C	C - N	C - C
x	=	2.70641	-1.38446	2.34415	5.70157	7.23750
y	=	-0.37066	0.03098	-0.73681	-0.45037	0.55341
z	=	3.21956	3.23770	5.10004	2.21604	3.08976
RHO	=	0.27737	0.27856	0.27860	0.21651	0.23170
LAP	=	-0.59463	-0.93305	-0.93287	-0.23563	-0.43932
ellip	=	0.03277	0.03164	0.03149	0.07272	0.04868
K(r)	=	0.38452	0.27310	0.27316	0.26538	0.16794
G(r)	=	0.23586	0.03984	0.03994	0.20647	0.05811
BCP #	=	13	14	15	16	17
n1-n2	=	9-25	17- 6	18- 6	19- 6	17-25
A - B	=	H - O	H - C	H - C	H - C	H - O
x	=	3.37851	-0.89729	-2.17744	-2.37591	0.91823
y	=	0.95202	1.28575	2.16905	0.13525	1.39971
z	=	-3.33412	-2.87700	-1.40592	-1.84081	-4.25757
RHO	=	0.01905	0.27461	0.26851	0.26852	0.01418
LAP	=	0.07051	-0.91484	-0.81079	-0.81088	0.05661
ellip	=	0.33260	0.04534	0.07074	0.07072	0.01725
K(r)	=	0.00004	0.26516	0.24915	0.24916	-0.00105
G(r)	=	0.01766	0.03645	0.04646	0.04644	0.01310
BCP #	=	19	20	21	22	23
n1-n2	=	15-10	16-10	15-24	12-11	13-11
A - B	=	H - C	H - C	H - O	H - C	H - C
x	=	7.13306	6.82597	6.96202	9.07608	7.34998
y	=	-0.62128	-1.68309	-0.05063	1.39642	1.68385
z	=	1.10666	2.90178	-1.33502	3.90526	4.96115
RHO	=	0.27577	0.26974	0.00803	0.26152	0.26018
LAP	=	-0.89039	-0.81267	0.03441	-0.75431	-0.73613
ellip	=	0.04579	0.06504	0.10522	0.01911	0.02078
K(r)	=	0.26197	0.24948	-0.00128	0.23887	0.23665
G(r)	=	0.03938	0.04631	0.00732	0.05029	0.05262
BCP #	=	25	26	27	28	29
n1-n2	=	21-20	22-21	21-23	20-25	26-21
A - B	=	C - C	C - C	C - O	C - O	H - C
x	=	6.02061	6.12567	7.58926	4.53198	6.38777
y	=	1.52021	0.83377	1.64632	1.37201	2.96407
z	=	-7.21653	-9.49648	-8.34908	-5.86401	-8.79060
RHO	=	0.24399	0.23389	0.22878	0.35525	0.27105
LAP	=	-0.47929	-0.44700	-0.32372	-0.67374	-0.81974
ellip	=	0.06362	0.04116	0.04974	0.12369	0.04697
K(r)	=	0.17946	0.17026	0.26869	0.57345	0.25059
G(r)	=					
BCP #	=	30				
n1-n2	=	27-22				
A - B	=	H - C				
x	=	4.40294				
y	=	0.13653				
z	=	-10.65584				
RHO	=	0.26265				
LAP	=	-0.76000				
ellip	=	0.01508				
K(r)	=	0.24079				
G(r)	=					

G(r)	=	0.05964	0.05851	0.18776	0.40501	0.04566	0.05079
BCP #	=	31	32	33	34		
n1-n2	=	28-22	29-22	30-24	30-23		
A - B	=	H - C	H - C	H - O	H - O		
x	=	5.86685	6.24692	8.46845	9.65364		
y	=	-1.22111	0.21208	0.98314	1.16336		
z	=	-10.16511	-11.57308	-5.72340	-6.88545		
RHO	=	0.26049	0.26175	0.02512	0.34584		
LAP	=	-0.74099	-0.75161	0.09760	-1.72461		
ellip	=	0.01501	0.01497	0.37700	0.02324		
K(r)	=	0.23725	0.23945	0.00049	0.49811		
G(r)	=	0.05200	0.05155	0.02489	0.06696		

Structure 10: 1-ethyl-3-methylimidazolium propanoate

----- Bond critical points -----							
BCP #	=	1	2	3	4	5	6
n1-n2	=	2- 1	5- 1	6- 1	2- 3	5- 4	9- 5
A - B	=	C - N	C - N	C - N	C - C	C - N	H - C
x	=	0.09499	1.77591	-1.17028	1.21597	3.08448	3.12256
y	=	-0.28962	0.22447	0.08961	-0.42756	0.25887	0.61521
z	=	1.55127	-0.47392	-1.31197	2.94246	0.03703	-2.01344
RHO	=	0.27763	0.32385	0.21898	0.32390	0.32385	0.28248
LAP	=	-0.59798	-0.76379	-0.21881	-0.84695	-0.76995	-1.17584
ellip	=	0.03580	0.00813	0.07111	0.27076	0.00767	0.01233
K(r)	=	0.38480	0.50090	0.27264	0.32722	0.50054	0.31693
G(r)	=	0.23531	0.30996	0.21793	0.11548	0.30805	0.02297
BCP #	=	7	8	9	10	11	12
n1-n2	=	9-22	3- 4	7- 2	8- 3	10- 4	11-10
A - B	=	H - O	C - N	H - C	H - C	C - N	C - C
x	=	2.88374	2.97662	-1.09345	2.85167	5.82992	7.18606
y	=	0.89813	-0.21289	-0.66918	-0.56444	0.28402	1.61433
z	=	-3.89051	2.67121	3.04679	4.58628	1.40487	2.11221
RHO	=	0.02357	0.27758	0.27837	0.27848	0.21586	0.23176
LAP	=	0.08284	-0.60527	-0.93020	-0.93077	-0.22721	-0.43934
ellip	=	0.13090	0.03509	0.03187	0.03143	0.08895	0.05014
K(r)	=	0.00061	0.38355	0.27265	0.27284	0.26453	0.16783
G(r)	=	0.02132	0.23223	0.04010	0.04014	0.20773	0.05800
BCP #	=	13	14	15	16	17	18
n1-n2	=	9-21	17- 6	18- 6	19- 6	17-22	20-22
A - B	=	H - O	H - C	H - C	H - C	H - O	C - O
x	=	4.46911	-1.35406	-2.67739	-2.48887	0.37002	3.89023
y	=	0.93289	0.37946	1.06151	-0.98867	0.77960	1.38353
z	=	-3.31390	-3.12870	-1.59144	-1.93783	-4.61525	-6.47524
RHO	=	0.02517	0.27417	0.26836	0.26836	0.01297	0.34726
LAP	=	0.08759	-0.91046	-0.80905	-0.80920	0.05241	-0.71147
ellip	=	0.08143	0.04493	0.07021	0.07015	0.03099	0.12843
K(r)	=	0.00079	0.26411	0.24886	0.24888	-0.00111	0.55350
G(r)	=	0.02269	0.03650	0.04660	0.04658	0.01199	0.37564
BCP #	=	19	20	21	22	23	24
n1-n2	=	15-10	16-10	15-21	12-11	13-11	14-11
A - B	=	H - C	H - C	H - O	H - C	H - C	H - C
x	=	7.16628	7.23901	6.78298	8.86852	7.21634	7.14952
y	=	0.37050	-0.65950	0.75521	2.85543	2.82291	3.80355
z	=	0.16486	2.01200	-2.19093	2.74070	3.94104	2.13682
RHO	=	0.27625	0.26928	0.01026	0.26137	0.25981	0.26316
LAP	=	-0.90249	-0.80821	0.04250	-0.75278	-0.73279	-0.76566
ellip	=	0.04396	0.06700	0.06763	0.01839	0.02012	0.01683
K(r)	=	0.26380	0.24873	-0.00123	0.23864	0.23608	0.24133
G(r)	=	0.03818	0.04668	0.00939	0.05044	0.05288	0.04991
BCP #	=	25	26	27	28	29	30
n1-n2	=	20-21	23-20	24-23	28-23	29-23	25-24
A - B	=	C - O	C - C	C - C	H - C	H - C	H - C
x	=	5.28043	5.20169	7.05578	5.02538	5.18599	8.90530
y	=	1.41420	1.72030	2.09243	2.99514	1.00342	3.19089
z	=	-5.97275	-7.97858	-9.41806	-9.67755	-9.98560	-8.88720

RHO	=	0.34896	0.24107	0.22909	0.26023	0.26019	0.26166
LAP	=	-0.66713	-0.46855	-0.42571	-0.73674	-0.73649	-0.75014
ellip	=	0.13119	0.03493	0.01304	0.01704	0.01701	0.01173
K(r)	=	0.55800	0.17831	0.16408	0.23596	0.23590	0.23927
G(r)	=	0.39122	0.06117	0.05765	0.05178	0.05178	0.05173
BCP #	=	31	32				
n1-n2	=	26-24	27-24				
A - B	=	H - C	H - C				
x	=	8.76116	9.06665				
y	=	2.43933	1.18882				
z	=	-10.77533	-9.19603				
RHO	=	0.25757	0.26170				
LAP	=	-0.71563	-0.75048				
ellip	=	0.01482	0.01169				
K(r)	=	0.23284	0.23933				
G(r)	=	0.05394	0.05171				

Structure 11: 1-butyl-3-methylimidazolium formate

Bond critical points							
BCP #	=	1	2	3	4	5	6
n1-n2	=	2- 1	5- 1	6- 1	3- 2	5- 4	9-27
A - B	=	C - N	C - N	C - N	C - C	C - N	H - O
x	=	-0.02929	1.49330	-1.51230	1.20494	2.84408	2.56489
y	=	0.01724	-0.01072	-0.01917	0.03535	-0.00448	-0.06003
z	=	1.72693	-0.48950	-1.05258	3.02147	-0.09590	-4.02901
RHO	=	0.27698	0.32239	0.22166	0.32397	0.32515	0.03067
LAP	=	-0.58092	-0.74387	-0.25433	-0.84760	-0.79235	0.10276
ellip	=	0.03508	0.01293	0.04188	0.27033	0.00357	0.01796
K(r)	=	0.38516	0.49810	0.27631	0.32735	0.50248	0.00129
G(r)	=	0.23994	0.31213	0.21273	0.11545	0.30439	0.02698
BCP #	=	7	8	9	10	11	12
n1-n2	=	3- 4	7- 2	8- 3	13- 4	12-13	9-28
A - B	=	C - N	H - C	H - C	C - N	C - C	H - O
x	=	2.94333	-1.09764	2.97420	5.70599	7.21199	4.15823
y	=	0.03011	0.04271	0.05857	-0.00078	-1.33983	-0.04836
z	=	2.57474	3.35175	4.52597	1.03732	1.33876	-3.61753
RHO	=	0.27826	0.27831	0.27869	0.21345	0.23178	0.01649
LAP	=	-0.61309	-0.92964	-0.93351	-0.19048	-0.43806	0.06323
ellip	=	0.03392	0.03257	0.03078	0.10599	0.05956	1.16951
K(r)	=	0.38452	0.27259	0.27326	0.26184	0.16793	-0.00021
G(r)	=	0.23125	0.04018	0.03988	0.21422	0.05842	0.01560
BCP #	=	13	14	15	16	17	18
n1-n2	=	9- 5	14- 6	15- 6	16- 6	15-27	26-27
A - B	=	H - C	H - C	H - C	H - C	H - O	C - O
x	=	2.67658	-2.96741	-1.84842	-2.96661	0.07691	3.80906
y	=	-0.03122	-1.06836	-0.04269	1.02249	-0.06729	-0.09527
z	=	-2.18484	-1.37356	-2.86084	-1.40084	-4.48675	-6.60601
RHO	=	0.28108	0.26888	0.27334	0.26887	0.00745	0.34898
LAP	=	-1.15780	-0.81427	-0.88664	-0.81421	0.03233	-0.63779
ellip	=	0.01264	0.06636	0.04730	0.06637	0.13831	0.12851
K(r)	=	0.31287	0.24973	0.26025	0.24972	-0.00127	0.55814
G(r)	=	0.02342	0.04617	0.03859	0.04616	0.00681	0.39870
BCP #	=	19	20	21	22	23	24
n1-n2	=	10-11	11-12	19-10	20-10	21-10	22-11
A - B	=	C - C	C - C	H - C	H - C	H - C	H - C
x	=	11.21984	9.22770	13.05923	11.36346	11.54256	10.95056
y	=	-3.87375	-2.58097	-5.12060	-6.05001	-5.48104	-2.27212
z	=	1.73208	1.53292	1.92927	1.28833	3.23636	0.21429
RHO	=	0.22655	0.22716	0.26038	0.25999	0.25867	0.26344
LAP	=	-0.41563	-0.41606	-0.74056	-0.73666	-0.72497	-0.75898
ellip	=	0.01399	0.02486	0.01355	0.01315	0.01410	0.01102
K(r)	=	0.16087	0.16161	0.23708	0.23618	0.23421	0.23990
G(r)	=	0.05696	0.05759	0.05194	0.05202	0.05296	0.05016

BCP #	=	25	26	27	28	29	30
n1-n2	=	23-11	24-12	25-12	17-28	17-13	18-13
A - B	=	H - C	H - C	H - C	H - O	H - C	H - C
x	=	11.13276	7.44267	7.26650	6.64693	6.93746	7.08054
y	=	-1.70768	-2.88867	-3.45050	0.21501	0.29703	0.90277
z	=	2.15755	2.83488	0.88483	-2.53862	-0.28419	1.75057
RHO	=	0.25944	0.25910	0.26326	0.01484	0.27686	0.26811
LAP	=	-0.72382	-0.71958	-0.75724	0.05803	-0.91572	-0.79797
ellip	=	0.01646	0.01595	0.01066	0.05205	0.04354	0.07103
K(r)	=	0.23398	0.23348	0.23984	-0.00095	0.26622	0.24677
G(r)	=	0.05302	0.05358	0.05053	0.01355	0.03729	0.04727
BCP #	=	31	32				
n1-n2	=	26-28	29-26				
A - B	=	C - O	H - C				
x	=	5.21900	5.01709				
y	=	-0.08344	-0.10947				
z	=	-6.16495	-7.99296				
RHO	=	0.35311	0.27122				
LAP	=	-0.62778	-0.83661				
ellip	=	0.12334	0.01068				
K(r)	=	0.56809	0.24952				
G(r)	=	0.41115	0.04036				

Structure 12: 1-butyl-3-methylimidazolium furoate

----- Bond critical points -----							
BCP #	=	1	2	3	4	5	6
n1-n2	=	2- 1	5- 1	6- 1	2- 3	5- 4	9- 5
A - B	=	C - N	C - N	C - N	C - C	C - N	H - C
x	=	-0.00138	1.54360	-1.46172	1.21569	2.88961	2.77564
y	=	-0.00028	0.00162	0.00293	-0.00127	0.00101	0.00511
z	=	1.69246	-0.50134	-1.10295	3.00551	-0.09219	-2.16698
RHO	=	0.27740	0.32381	0.21938	0.32386	0.32459	0.28349
LAP	=	-0.59051	-0.76091	-0.22495	-0.84687	-0.77781	-1.17301
ellip	=	0.03554	0.00597	0.06095	0.27059	0.00163	0.01260
K(r)	=	0.38514	0.50088	0.27314	0.32710	0.50195	0.31661
G(r)	=	0.23751	0.31065	0.21690	0.11538	0.30750	0.02336
BCP #	=	7	8	9	10	11	12
n1-n2	=	9-33	3- 4	7- 2	8- 3	13- 4	12-13
A - B	=	H - O	C - N	H - C	H - C	C - N	C - C
x	=	2.48704	2.95875	-1.08993	2.96577	5.73221	7.24376
y	=	-0.00431	-0.00177	0.00338	-0.00072	-0.01371	-1.35329
z	=	-4.04332	2.58402	3.30603	4.53417	1.06286	1.36652
RHO	=	0.02535	0.27774	0.27839	0.27856	0.21567	0.23173
LAP	=	0.08894	-0.60284	-0.93062	-0.93218	-0.21646	-0.43798
ellip	=	0.07905	0.03348	0.03210	0.03129	0.08142	0.05841
K(r)	=	0.00070	0.38448	0.27273	0.27302	0.26511	0.16792
G(r)	=	0.02294	0.23376	0.04007	0.03998	0.21100	0.05843
BCP #	=	13	14	15	16	17	18
n1-n2	=	9-31	14- 6	15- 6	16- 6	15-33	29-33
A - B	=	H - O	H - C	H - C	H - C	H - O	C - O
x	=	4.09528	-2.90881	-1.77464	-2.90727	-0.07424	3.39046
y	=	0.01468	-1.04053	0.00478	1.04927	-0.00363	-0.00512
z	=	-3.60928	-1.44645	-2.92185	-1.44425	-4.57055	-6.71124
RHO	=	0.02199	0.26864	0.27411	0.26863	0.01118	0.35790
LAP	=	0.07865	-0.81200	-0.90382	-0.81190	0.04670	-0.72635
ellip	=	0.19142	0.06903	0.04604	0.06905	0.04815	0.08438
K(r)	=	0.00045	0.24935	0.26312	0.24933	-0.00128	0.57994
G(r)	=	0.02012	0.04635	0.03717	0.04636	0.01039	0.39835
BCP #	=	19	20	21	22	23	24
n1-n2	=	29-31	10-11	11-12	19-10	20-10	21-10
A - B	=	C - O	C - C	C - C	H - C	H - C	H - C
x	=	4.82956	11.25331	9.25999	13.09170	11.40257	11.56294
y	=	0.01215	-3.88386	-2.59069	-5.12750	-6.05715	-5.49381
z	=	-6.30810	1.78627	1.57285	1.99599	1.33631	3.28816

RHO	=	0.35188	0.22654	0.22719	0.26046	0.26007	0.25886
LAP	=	-0.77768	-0.41562	-0.41606	-0.74126	-0.73731	-0.72655
ellip	=	0.08527	0.01365	0.02470	0.01396	0.01356	0.01445
K(r)	=	0.56394	0.16086	0.16160	0.23720	0.23629	0.23448
G(r)	=	0.36952	0.05696	0.05759	0.05189	0.05196	0.05285
BCP #	=	25	26	27	28	29	30
n1-n2	=	22-11	23-11	24-12	25-12	17-31	17-13
A - B	=	H - C	H - C	H - C	H - C	H - O	H - C
x	=	10.99658	11.15916	7.46565	7.30497	6.49738	6.96736
y	=	-2.27629	-1.71696	-2.90381	-3.46238	0.24801	0.28983
z	=	0.27391	2.21825	2.85967	0.90722	-2.60067	-0.24259
RHO	=	0.26286	0.25963	0.25945	0.26327	0.01066	0.27586
LAP	=	-0.75359	-0.72537	-0.72252	-0.75732	0.04394	-0.89687
ellip	=	0.01123	0.01558	0.01606	0.01110	0.06057	0.04497
K(r)	=	0.23903	0.23424	0.23401	0.23983	-0.00124	0.26280
G(r)	=	0.05063	0.05290	0.05338	0.05050	0.00974	0.03859
BCP #	=	31	32	33	34	35	36
n1-n2	=	18-13	27-30	28-32	30-26	26-32	34-26
A - B	=	H - C	C - C	C - O	C - C	C - O	H - C
x	=	7.11085	7.21388	4.45031	5.82362	4.10254	3.76482
y	=	0.89063	0.02119	-0.01034	-0.00525	-0.02687	-0.03961
z	=	1.78182	-11.95622	-10.21524	-13.51266	-12.93761	-14.75991
RHO	=	0.26843	0.26799	0.25047	0.32183	0.25849	0.28061
LAP	=	-0.80116	-0.57260	-0.02300	-0.84745	-0.06381	-0.94350
ellip	=	0.06782	0.09555	0.05403	0.23432	0.08929	0.03757
K(r)	=	0.24725	0.22307	0.33533	0.33065	0.35132	0.27543
G(r)	=	0.04696	0.07992	0.32958	0.11879	0.33536	0.03955
BCP #	=	37	38	39	40		
n1-n2	=	27-28	29-28	35-27	36-30		
A - B	=	C - C	C - C	H - C	H - C		
x	=	6.24294	4.58906	8.45559	7.92005		
y	=	0.01565	0.00157	0.04831	0.02156		
z	=	-10.09539	-8.19115	-9.96483	-14.18609		
RHO	=	0.32315	0.25898	0.27562	0.27230		
LAP	=	-0.84789	-0.56191	-0.89971	-0.86207		
ellip	=	0.23496	0.06554	0.00393	0.01109		
K(r)	=	0.32941	0.20344	0.26735	0.26122		
G(r)	=	0.11744	0.06296	0.04243	0.04570		

Structure 13: 1-butyl-3-methylimidazolium i-butanoate

----- Bond critical points -----							
BCP #	=	1	2	3	4	5	6
n1-n2	=	2- 1	5- 1	6- 1	3- 2	5- 4	9-26
A - B	=	C - N	C - N	C - N	C - C	C - N	H - O
x	=	-0.00064	1.54890	-1.45004	1.21793	2.89319	2.63129
y	=	-0.00008	0.00217	0.00073	0.00004	0.00283	-0.00162
z	=	1.69280	-0.50489	-1.10358	3.00336	-0.09595	-4.01793
RHO	=	0.27709	0.32222	0.22172	0.32399	0.32472	0.03109
LAP	=	-0.58499	-0.74287	-0.25398	-0.84764	-0.78754	0.10590
ellip	=	0.03556	0.01600	0.04554	0.27063	0.00075	0.00928
K(r)	=	0.38495	0.49779	0.27646	0.32741	0.50175	0.00122
G(r)	=	0.23870	0.31208	0.21297	0.11550	0.30487	0.02769
BCP #	=	7	8	9	10	11	12
n1-n2	=	3- 4	7- 2	8- 3	13- 4	12-13	9- 5
A - B	=	C - N	H - C	H - C	C - N	C - C	H - C
x	=	2.96203	-1.08783	2.96884	5.74010	7.24436	2.75570
y	=	0.00060	0.00330	0.00229	-0.00898	-1.34891	0.00471
z	=	2.57693	3.30583	4.52877	1.07086	1.37592	-2.19284
RHO	=	0.27822	0.27822	0.27859	0.21416	0.23180	0.28027
LAP	=	-0.61452	-0.92852	-0.93222	-0.19715	-0.43807	-1.16196
ellip	=	0.03437	0.03251	0.03084	0.10339	0.05961	0.01247
K(r)	=	0.38415	0.27238	0.27303	0.26299	0.16790	0.31351
G(r)	=	0.23051	0.04025	0.03998	0.21370	0.05838	0.02302
BCP #	=	13	14	15	16	17	18
n1-n2	=	9-37	14- 6	15- 6	16- 6	15-26	29-26
A - B	=	H - O	H - C	H - C	H - C	H - O	C - O
x	=	4.21549	-2.90016	-1.76202	-2.90003	0.13124	3.84240

y	=	0.00018	-1.04397	0.00134	1.04590	-0.00476	-0.01379
z	=	-3.57645	-1.45600	-2.91733	-1.45544	-4.52173	-6.60759
RHO	=	0.01812	0.26872	0.27348	0.26871	0.00824	0.34505
LAP	=	0.06853	-0.81261	-0.88986	-0.81252	0.03543	-0.67765
ellip	=	0.73097	0.06667	0.04673	0.06669	0.11282	0.13742
K(r)	=	-0.00002	0.24944	0.26078	0.24942	-0.00128	0.54838
G(r)	=	0.01711	0.04629	0.03831	0.04629	0.00758	0.37897
BCP #	=	19	20	21	22	23	24
n1-n2	=	10-11	11-12	19-10	20-10	21-10	22-11
A - B	=	C - C	C - C	H - C	H - C	H - C	H - C
x	=	11.25024	9.25854	13.08821	11.40147	11.55556	10.99894
y	=	-3.88393	-2.59094	-5.13138	-6.05567	-5.50583	-2.26760
z	=	1.79486	1.58335	2.00288	1.33159	3.28716	0.29062
RHO	=	0.22655	0.22720	0.26035	0.25997	0.25869	0.26330
LAP	=	-0.41562	-0.41617	-0.74031	-0.73652	-0.72517	-0.75767
ellip	=	0.01385	0.02472	0.01353	0.01313	0.01404	0.01097
K(r)	=	0.16086	0.16162	0.23703	0.23616	0.23424	0.23969
G(r)	=	0.05696	0.05758	0.05196	0.05203	0.05295	0.05027
BCP #	=	25	26	27	28	29	30
n1-n2	=	23-11	24-12	25-12	17-37	17-13	18-13
A - B	=	H - C	H - C	H - C	H - O	H - C	H - C
x	=	11.15556	7.45882	7.30708	6.67847	6.98490	7.10756
y	=	-1.72239	-2.91296	-3.45583	0.24692	0.30211	0.88846
z	=	2.24094	2.85952	0.90223	-2.49534	-0.23339	1.80700
RHO	=	0.25945	0.25909	0.26326	0.01443	0.27684	0.26801
LAP	=	-0.72388	-0.71951	-0.75722	0.05701	-0.91451	-0.79710
ellip	=	0.01617	0.01577	0.01045	0.05374	0.04335	0.07050
K(r)	=	0.23399	0.23346	0.23983	-0.00104	0.26603	0.24659
G(r)	=	0.05302	0.05358	0.05053	0.01321	0.03740	0.04731
BCP #	=	31	32	33	34	35	36
n1-n2	=	32-30	32-31	32-29	27-30	33-30	36-30
A - B	=	C - C	C - C	C - C	H - C	H - C	H - C
x	=	5.05185	5.07447	5.11758	3.31695	4.99583	4.99056
y	=	-1.21126	1.17477	-0.01928	-2.42675	-3.44273	-2.41966
z	=	-10.18240	-10.18100	-8.19140	-10.86322	-10.28827	-12.04396
RHO	=	0.22512	0.22495	0.24149	0.26240	0.25913	0.25801
LAP	=	-0.40800	-0.40733	-0.47129	-0.75701	-0.72937	-0.71970
ellip	=	0.01126	0.01123	0.00777	0.01026	0.01406	0.01455
K(r)	=	0.15918	0.15898	0.17855	0.24008	0.23501	0.23343
G(r)	=	0.05718	0.05715	0.06073	0.05083	0.05266	0.05351
BCP #	=	37	38	39	40	41	
n1-n2	=	28-31	34-31	35-31	29-37	38-32	
A - B	=	H - C	H - C	H - C	C - O	H - C	
x	=	3.36314	5.06011	5.03736	5.24838	6.79957	
y	=	2.42342	3.40741	2.38744	-0.01149	-0.03486	
z	=	-10.86157	-10.28263	-12.04048	-6.15820	-9.48432	
RHO	=	0.26232	0.25924	0.25804	0.34989	0.26690	
LAP	=	-0.75627	-0.73033	-0.71991	-0.66622	-0.77541	
ellip	=	0.01044	0.01407	0.01463	0.12695	0.00292	
K(r)	=	0.23994	0.23516	0.23347	0.56036	0.24503	
G(r)	=	0.05087	0.05258	0.05349	0.39380	0.05118	

Structure 14: 1-ethyl-3-methylimidazolium octanoate

----- Bond critical points -----							
BCP #	=	1	2	3	4	5	6
n1-n2	=	2- 1	5- 4	5- 1	6- 1	2- 3	9- 5
A - B	=	C - N	C - N	C - N	C - N	C - C	H - C
x	=	-0.00305	2.88610	1.54281	-1.47345	1.20995	2.83001
y	=	0.01234	0.00078	0.00416	0.01021	0.01041	-0.00855
z	=	1.68575	-0.09295	-0.50287	-1.09832	3.00635	-2.17228
RHO	=	0.27792	0.32250	0.32374	0.21799	0.32412	0.27878
LAP	=	-0.60486	-0.75535	-0.77327	-0.20494	-0.84836	-1.15583
ellip	=	0.03639	0.01483	0.00539	0.08410	0.27064	0.01233
K(r)	=	0.38463	0.49788	0.50012	0.27127	0.32770	0.31192
G(r)	=	0.23341	0.30904	0.30680	0.22004	0.11561	0.02297

BCP #	=	7	8	9	10	11	12
n1-n2	=	9-26	3- 4	7- 2	8- 3	10- 4	11-10
A - B	=	H - O	C - N	H - C	H - C	C - N	C - C
x	=	2.44489	2.95385	-1.09480	2.95547	5.72119	7.23997
y	=	-0.03526	0.00479	0.01339	0.00386	0.00031	1.29990
z	=	-4.19114	2.58976	3.29962	4.53979	1.06946	1.42946
RHO	=	0.01697	0.27755	0.27839	0.27839	0.21740	0.23174
LAP	=	0.06709	-0.60116	-0.93045	-0.92977	-0.24557	-0.43931
ellip	=	3.88416	0.03422	0.03163	0.03155	0.07353	0.04901
K(r)	=	-0.00012	0.38406	0.27269	0.27265	0.26666	0.16785
G(r)	=	0.01666	0.23378	0.04008	0.04021	0.20527	0.05802
BCP #	=	13	14	15	16	17	18
n1-n2	=	9-22	17- 6	18- 6	19- 6	17-26	25-22
A - B	=	H - O	H - C	H - C	H - C	H - O	C - O
x	=	3.89412	-1.79316	-2.91188	-2.92366	-0.34525	4.25978
y	=	-0.03934	-0.00269	1.05920	-1.02717	-0.03099	-0.09563
z	=	-3.62721	-2.92524	-1.43360	-1.41697	-4.63472	-6.46866
RHO	=	0.03341	0.27460	0.26811	0.26811	0.01586	0.34505
LAP	=	0.11341	-0.92168	-0.80670	-0.80679	0.06198	-0.71467
ellip	=	0.02316	0.04403	0.07190	0.07185	0.00641	0.13055
K(r)	=	0.00137	0.26617	0.24846	0.24847	-0.00090	0.54805
G(r)	=	0.02972	0.03575	0.04678	0.04677	0.01460	0.36938
BCP #	=	19	20	21	22	23	24
n1-n2	=	25-26	15-10	16-10	15-22	12-11	13-11
A - B	=	C - O	H - C	H - C	H - O	H - C	H - C
x	=	2.83987	6.95585	7.09764	6.21253	9.06493	7.52098
y	=	-0.08819	-0.26187	-0.95217	-0.24069	2.46458	2.80083
z	=	-6.87784	-0.24328	1.74397	-2.65131	1.70581	3.00054
RHO	=	0.35146	0.27558	0.26947	0.00765	0.26135	0.26000
LAP	=	-0.65643	-0.89008	-0.81004	0.03331	-0.75255	-0.73456
ellip	=	0.12738	0.04498	0.06494	0.15353	0.01874	0.02028
K(r)	=	0.56411	0.26170	0.24903	-0.00129	0.23860	0.23638
G(r)	=	0.40000	0.03918	0.04652	0.00703	0.05046	0.05274
BCP #	=	25	26	27	28	29	30
n1-n2	=	14-11	23-24	24-25	20-23	23-29	29-30
A - B	=	H - C	C - C	C - C	H - C	C - C	C - C
x	=	7.38439	3.43591	4.08331	1.72332	2.85312	4.07817
y	=	3.45186	-0.16728	-0.13709	0.90062	-0.30684	0.64101
z	=	1.05620	-10.78358	-8.48325	-11.64274	-13.09695	-14.98431
RHO	=	0.26320	0.22975	0.24077	0.26141	0.22620	0.22680
LAP	=	-0.76606	-0.42575	-0.46745	-0.74011	-0.41269	-0.41340
ellip	=	0.01700	0.02211	0.03396	0.01564	0.01021	0.01690
K(r)	=	0.24139	0.16449	0.17801	0.23722	0.15989	0.16066
G(r)	=	0.04987	0.05806	0.06115	0.05219	0.05671	0.05731
BCP #	=	31	32	33	34	35	36
n1-n2	=	21-24	28-24	27-23	30-31	34-29	35-29
A - B	=	H - C	H - C	H - C	C - C	H - C	H - C
x	=	5.28376	5.22471	1.58824	5.20430	2.30196	3.98379
y	=	0.81413	-1.20626	-1.10522	1.61535	-0.61721	-1.51809
z	=	-9.95736	-9.93041	-11.47729	-16.88745	-15.22309	-14.57896
RHO	=	0.26095	0.25887	0.26356	0.22702	0.25892	0.25809
LAP	=	-0.73954	-0.72551	-0.75698	-0.41411	-0.71933	-0.71325
ellip	=	0.01442	0.01566	0.01528	0.01770	0.00986	0.00966
K(r)	=	0.23730	0.23368	0.24067	0.16092	0.23322	0.23181
G(r)	=	0.05242	0.05230	0.05143	0.05739	0.05339	0.05350
BCP #	=	37	38	39	40	41	42
n1-n2	=	31-32	36-30	37-30	32-33	38-31	39-31
A - B	=	C - C	H - C	H - C	C - C	H - C	H - C
x	=	6.39867	5.91584	4.20082	6.64105	4.49882	6.13340
y	=	2.51472	1.87997	2.81633	4.85002	1.41253	0.35883
z	=	-18.80822	-14.82895	-15.32897	-19.39009	-18.97565	-18.44299
RHO	=	0.22640	0.26004	0.26000	0.22574	0.25850	0.25945
LAP	=	-0.41313	-0.72663	-0.72620	-0.41189	-0.71681	-0.72382
ellip	=	0.00999	0.00842	0.00896	0.00948	0.00959	0.00991
K(r)	=	0.16001	0.23524	0.23520	0.15982	0.23245	0.23399
G(r)	=	0.05673	0.05358	0.05365	0.05684	0.05325	0.05304
BCP #	=	43	44	45	46	47	
n1-n2	=	40-32	41-32	42-33	43-33	44-33	

A - B	=	H - C	H - C	H - C	H - C	H - C
x	=	7.61910	8.31002	5.74571	4.95869	6.78813
y	=	3.23436	3.61767	6.59294	6.12844	7.00248
z	=	-20.50485	-18.65060	-18.29614	-20.11212	-19.98734
RHO	=	0.26011	0.25959	0.26049	0.25836	0.25893
LAP	=	-0.72891	-0.72598	-0.73809	-0.72308	-0.72761
ellip	=	0.01240	0.01138	0.01049	0.01082	0.01134
K(r)	=	0.23516	0.23423	0.23737	0.23375	0.23486
G(r)	=	0.05294	0.05274	0.05285	0.05298	0.05296

Structure 15: Im_c2h5 L-lactate (3b)

Bond critical points						
BCP #	=	1	2	3	4	5
n1-n2	=	2- 1	5- 4	5- 1	2- 3	12- 1
A - B	=	C - N	C - N	C - N	C - C	H - N
x	=	0.00736	2.87959	1.50372	1.20939	-1.23677
y	=	-0.01552	-0.00794	-0.00699	-0.01867	-0.00479
z	=	1.66009	-0.13686	-0.52252	2.97006	-1.03091
RHO	=	0.28541	0.31709	0.33565	0.32254	0.26360
LAP	=	-0.65256	-0.72940	-0.92124	-0.83911	-1.22046
ellip	=	0.01721	0.01007	0.05202	0.26459	0.01989
K(r)	=	0.40146	0.48449	0.52019	0.32414	0.34625
G(r)	=	0.23832	0.30214	0.28988	0.11436	0.04113
BCP #	=	7	8	9	10	11
n1-n2	=	8-17	3- 4	6- 2	7- 3	9- 4
A - B	=	H - O	C - N	H - C	H - C	C - N
x	=	1.70639	2.95351	-1.08951	2.97909	5.70298
y	=	0.00284	-0.01638	-0.01541	-0.01844	-0.03498
z	=	-3.86948	2.55971	3.28059	4.49517	1.06173
RHO	=	0.02049	0.27294	0.28010	0.27797	0.22496
LAP	=	0.07853	-0.52318	-0.95070	-0.92382	-0.33554
ellip	=	0.03537	0.04097	0.02525	0.03679	0.01929
K(r)	=	-0.00084	0.38015	0.27629	0.27186	0.27590
G(r)	=	0.01879	0.24936	0.03861	0.04091	0.19201
BCP #	=	13	14	15	16	17
n1-n2	=	24- 9	13-18	10- 9	11- 9	15-14
A - B	=	C - C	C - O	H - C	H - C	C - C
x	=	7.21774	-2.49404	6.99509	7.09567	-4.54295
y	=	-1.39663	0.01606	0.33631	0.82439	-1.07833
z	=	1.32209	-4.98530	-0.15152	1.85887	-8.23274
RHO	=	0.23127	0.34515	0.27147	0.27073	0.23371
LAP	=	-0.43740	-0.65029	-0.83060	-0.82255	-0.44662
ellip	=	0.04469	0.14583	0.05115	0.05451	0.04027
K(r)	=	0.16761	0.54901	0.25263	0.25117	0.17031
G(r)	=	0.05826	0.38644	0.04498	0.04553	0.05865
BCP #	=	19	20	21	22	23
n1-n2	=	14-16	13-17	19-14	20-15	21-15
A - B	=	C - O	C - O	H - C	H - C	H - C
x	=	-3.02584	-1.24946	-4.31182	-6.22530	-4.75428
y	=	0.10796	0.01299	1.17221	-2.17304	-3.23881
z	=	-8.88883	-5.77863	-8.11558	-7.36372	-8.33056
RHO	=	0.22958	0.35426	0.27138	0.26300	0.26068
LAP	=	-0.32912	-0.63198	-0.82340	-0.76312	-0.74254
ellip	=	0.05795	0.13737	0.04639	0.01608	0.01615
K(r)	=	0.27006	0.57095	0.25116	0.24134	0.23752
G(r)	=	0.18778	0.41295	0.04531	0.05056	0.05188
BCP #	=	25	26	27	28	29
n1-n2	=	23-16	23-17	25-24	26-24	27-24
A - B	=	H - O	H - O	H - C	H - C	H - C
x	=	-0.64411	-0.27818	7.43914	7.33728	9.02061
y	=	0.17110	0.10012	-3.03309	-3.50247	-2.60517
z	=	-9.88366	-8.23650	2.75246	0.75455	1.52246
RHO	=	0.34598	0.02419	0.26170	0.26279	0.26133
LAP	=	-1.72464	0.09535	-0.75062	-0.76194	-0.75207

ellip	=	0.02314	0.47184	0.02043	0.01882	0.02074
K(r)	=	0.49807	0.00030	0.23903	0.24069	0.23846
G(r)	=	0.06691	0.02414	0.05138	0.05020	0.05044

Structure 16: Im_c3h7 L-lactate (3c)

----- Bond critical points -----						
BCP #	=	1	2	3	4	5
n1-n2	=	2- 1	5- 4	5- 1	2- 3	12- 1
A - B	=	C - N	C - N	C - N	C - C	H - N
x	=	0.29303	3.16232	1.78604	1.49704	-0.95476
y	=	-0.37480	-0.70843	-0.74321	-0.19121	-0.76962
z	=	1.16301	-0.60804	-0.99115	2.45803	-1.49650
RHO	=	0.28535	0.31721	0.33560	0.32255	0.26396
LAP	=	-0.65137	-0.73126	-0.91985	-0.83915	-1.22313
ellip	=	0.01767	0.01060	0.05191	0.26458	0.01989
K(r)	=	0.40142	0.48468	0.52021	0.32414	0.34687
G(r)	=	0.23858	0.30186	0.29025	0.11435	0.04108
BCP #	=	7	8	9	10	11
n1-n2	=	8-17	3- 4	6- 2	7- 3	9- 4
A - B	=	H - O	C - N	H - C	H - C	C - N
x	=	1.98181	3.24036	-0.80083	3.26929	5.98732
y	=	-1.27160	-0.28718	-0.09542	0.01941	-0.60013
z	=	-4.29675	2.05500	2.76088	3.96560	0.58353
RHO	=	0.02041	0.27302	0.28007	0.27799	0.22521
LAP	=	0.07827	-0.52376	-0.95023	-0.92399	-0.33150
ellip	=	0.03537	0.04019	0.02537	0.03674	0.00952
K(r)	=	-0.00085	0.38035	0.27622	0.27189	0.27732
G(r)	=	0.01872	0.24941	0.03866	0.04089	0.19445
BCP #	=	13	14	15	16	17
n1-n2	=	24- 9	13-18	10- 9	11- 9	27-24
A - B	=	C - C	C - O	H - C	H - C	C - C
x	=	7.48383	-2.22075	7.28723	7.39837	9.45568
y	=	-1.95736	-1.35593	-0.41939	0.32178	-3.19687
z	=	1.02336	-5.40673	-0.66390	1.26693	1.38710
RHO	=	0.23117	0.34522	0.27057	0.26982	0.22616
LAP	=	-0.43536	-0.65055	-0.82268	-0.81478	-0.41385
ellip	=	0.05635	0.14558	0.05187	0.05506	0.01394
K(r)	=	0.16750	0.54917	0.25096	0.24954	0.16060
G(r)	=	0.05866	0.38654	0.04529	0.04584	0.05714
BCP #	=	19	20	21	22	23
n1-n2	=	14-13	14-16	13-17	19-14	20-15
A - B	=	C - C	C - O	C - O	H - C	H - C
x	=	-2.60292	-2.75780	-0.97783	-4.02087	-5.99900
y	=	-1.63570	-1.87930	-1.50984	-0.67958	-3.82256
z	=	-7.36991	-9.27549	-6.18782	-8.68442	-7.40927
RHO	=	0.24508	0.22955	0.35427	0.27136	0.26300
LAP	=	-0.48587	-0.32890	-0.63218	-0.82327	-0.76312
ellip	=	0.06769	0.05779	0.13723	0.04642	0.01605
K(r)	=	0.18154	0.27003	0.57097	0.25114	0.24134
G(r)	=	0.06007	0.18781	0.41292	0.04532	0.05056
BCP #	=	25	26	27	28	29
n1-n2	=	22-15	23-16	23-17	25-24	26-24
A - B	=	H - C	H - O	H - O	H - C	H - C
x	=	-5.82608	-0.37715	-0.00942	7.61520	7.50956
y	=	-4.07028	-2.02277	-1.83623	-3.38045	-4.09372
z	=	-9.44994	-10.26429	-8.62677	2.63836	0.73443
RHO	=	0.26209	0.34598	0.02419	0.26237	0.26349
LAP	=	-0.75470	-1.72465	0.09535	-0.74774	-0.75866
ellip	=	0.01587	0.02314	0.47088	0.01708	0.01528
K(r)	=	0.24001	0.49807	0.00030	0.23860	0.24024
G(r)	=	0.05133	0.06691	0.02414	0.05166	0.05057
BCP #	=	31	32			
n1-n2	=	29-27	30-27			

A - B	=	H - C	H - C
x	=	11.28859	11.31623
y	=	-3.06257	-4.35558
z	=	0.14524	1.72489
RHO	=	0.26021	0.26183
LAP	=	-0.73858	-0.75433
ellip	=	0.01721	0.01602
K(r)	=	0.23642	0.23950
G(r)	=	0.05178	0.05092

Structure 17: Im_c4h9 L-lactate (3d)

----- Bond critical points -----							
BCP #	=	1	2	3	4	5	6
n1-n2	=	2- 1	5- 4	5- 1	2- 3	12- 1	12-18
A - B	=	C - N	C - N	C - N	C - C	H - N	H - O
x	=	0.31858	2.94287	1.53483	1.66681	-1.23828	-2.16960
y	=	-0.69700	-0.54293	-0.66181	-0.55656	-0.88693	-0.98292
z	=	1.31187	-0.82610	-1.03880	2.46211	-1.20278	-2.10173
RHO	=	0.28536	0.31731	0.33553	0.32252	0.26414	0.06564
LAP	=	-0.65106	-0.73131	-0.91922	-0.83902	-1.22447	0.20449
ellip	=	0.01786	0.01097	0.05188	0.26453	0.01990	0.03518
K(r)	=	0.40149	0.48492	0.52007	0.32408	0.34718	0.00802
G(r)	=	0.23872	0.30209	0.29026	0.11433	0.04106	0.05914
BCP #	=	7	8	9	10	11	12
n1-n2	=	8-17	3- 4	6- 2	7- 3	9- 4	8- 5
A - B	=	H - O	C - N	H - C	H - C	C - N	H - C
x	=	1.32700	3.34265	-0.57035	3.60263	5.88443	2.48900
y	=	-0.77180	-0.43803	-0.71581	-0.36163	-0.31020	-0.62929
z	=	-4.38366	1.83920	3.05442	3.75530	0.01346	-2.81741
RHO	=	0.02036	0.27310	0.28006	0.27798	0.22504	0.28291
LAP	=	0.07810	-0.52401	-0.95001	-0.92397	-0.33099	-1.08007
ellip	=	0.03556	0.04012	0.02538	0.03673	0.00912	0.01441
K(r)	=	-0.00085	0.38054	0.27618	0.27188	0.27690	0.29687
G(r)	=	0.01867	0.24954	0.03868	0.04089	0.19415	0.02685
BCP #	=	13	14	15	16	17	18
n1-n2	=	24- 9	13-18	10- 9	11- 9	27-24	15-14
A - B	=	C - C	C - O	H - C	H - C	C - C	C - C
x	=	7.52868	-2.96769	6.98659	7.29637	9.63402	-5.30207
y	=	-1.56323	-1.12092	0.14265	0.65300	-2.65790	-2.49737
z	=	0.08384	-4.97055	-1.34919	0.63381	0.03646	-7.90272
RHO	=	0.23115	0.34525	0.27059	0.26987	0.22714	0.23373
LAP	=	-0.43556	-0.65072	-0.82281	-0.81509	-0.41559	-0.44668
ellip	=	0.05380	0.14546	0.05198	0.05515	0.02453	0.04031
K(r)	=	0.16761	0.54926	0.25099	0.24961	0.16150	0.17032
G(r)	=	0.05872	0.38658	0.04529	0.04584	0.05760	0.05865
BCP #	=	19	20	21	22	23	24
n1-n2	=	14-13	14-16	13-17	19-14	20-15	21-15
A - B	=	C - C	C - O	C - O	H - C	H - C	H - C
x	=	-3.58565	-3.97424	-1.83212	-5.23710	-6.77491	-5.35233
y	=	-1.20044	-1.22952	-1.06311	-0.23315	-3.67789	-4.66987
z	=	-6.89142	-8.77902	-5.91183	-7.88655	-6.79752	-7.90503
RHO	=	0.24507	0.22954	0.35427	0.27136	0.26300	0.26067
LAP	=	-0.48584	-0.32883	-0.63228	-0.82323	-0.76309	-0.74246
ellip	=	0.06765	0.05767	0.13719	0.04644	0.01603	0.01612
K(r)	=	0.18153	0.27001	0.57097	0.25113	0.24133	0.23750
G(r)	=	0.06007	0.18780	0.41290	0.04533	0.05056	0.05189
BCP #	=	25	26	27	28	29	30
n1-n2	=	22-15	23-16	23-17	25-24	26-24	30-27
A - B	=	H - C	H - O	H - O	H - C	H - C	C - C
x	=	-6.85724	-1.74305	-1.17531	7.98846	7.68321	11.72158
y	=	-3.66415	-1.02913	-1.00462	-3.15034	-3.63658	-3.82673
z	=	-8.85871	-10.06237	-8.47277	1.46907	-0.48416	0.00931
RHO	=	0.26208	0.34596	0.02422	0.26146	0.26259	0.22647
LAP	=	-0.75464	-1.72453	0.09543	-0.74013	-0.75091	-0.41540

ellip	=	0.01586	0.02314	0.46875	0.01629	0.01451	0.01282
K(r)	=	0.24000	0.49804	0.00031	0.23706	0.23869	0.16085
G(r)	=	0.05134	0.06691	0.02417	0.05203	0.05097	0.05700
BCP #	=	31	32	33	34	35	
n1-n2	=	28-27	29-27	31-30	32-30	33-30	
A - B	=	H - C	H - C	H - C	H - C	H - C	
x	=	11.52410	11.22555	12.26760	13.64556	11.96503	
y	=	-1.68323	-2.17031	-5.46647	-4.94078	-5.95773	
z	=	0.55598	-1.38644	1.39866	-0.00829	-0.55765	
RHO	=	0.26032	0.26092	0.25968	0.26098	0.26017	
LAP	=	-0.73131	-0.73651	-0.73365	-0.74577	-0.73814	
ellip	=	0.01337	0.01251	0.01593	0.01559	0.01554	
K(r)	=	0.23522	0.23611	0.23571	0.23798	0.23645	
G(r)	=	0.05239	0.05199	0.05230	0.05154	0.05191	

Structure 18: Im_c5h11 L-lactate (3e)

----- Bond critical points -----							
BCP #	=	1	2	3	4	5	6
n1-n2	=	2- 1	5- 4	5- 1	2- 3	3- 4	12- 1
A - B	=	C - N	C - N	C - N	C - C	C - N	H - N
x	=	0.60553	2.89132	1.49220	2.06528	3.61911	-1.23118
y	=	-1.43259	-0.49154	-0.76925	-1.32334	-0.84605	-1.35650
z	=	1.35705	-0.96063	-1.04720	2.36590	1.61195	-0.96728
RHO	=	0.28536	0.31738	0.33548	0.32250	0.27316	0.26423
LAP	=	-0.65088	-0.73212	-0.91874	-0.83891	-0.52433	-1.22511
ellip	=	0.01803	0.01129	0.05186	0.26448	0.04001	0.01990
K(r)	=	0.40150	0.48504	0.51997	0.32404	0.38065	0.34733
G(r)	=	0.23878	0.30201	0.29029	0.11431	0.24957	0.04106
BCP #	=	7	8	9	10	11	12
n1-n2	=	12-18	8-17	6- 2	7- 3	9- 4	8- 5
A - B	=	H - O	H - O	H - C	H - C	C - N	H - C
x	=	-2.25369	0.86459	-0.04004	4.11539	5.86817	2.19582
y	=	-1.41101	-0.26199	-1.91521	-1.10388	-0.00426	-0.25694
z	=	-1.76543	-4.30174	3.13947	3.46445	-0.39950	-2.86842
RHO	=	0.06559	0.02032	0.28005	0.27797	0.22491	0.28291
LAP	=	0.20447	0.07798	-0.94986	-0.92385	-0.32960	-1.07987
ellip	=	0.03522	0.03567	0.02540	0.03672	0.00919	0.01440
K(r)	=	0.00799	-0.00086	0.27616	0.27185	0.27677	0.29683
G(r)	=	0.05911	0.01864	0.03869	0.04088	0.19437	0.02686
BCP #	=	13	14	15	16	17	18
n1-n2	=	24- 9	13-18	10- 9	11- 9	27-24	15-14
A - B	=	C - C	C - O	H - C	H - C	C - C	C - C
x	=	7.64009	-3.39684	6.71983	7.22981	9.83379	-5.91039
y	=	-1.00062	-1.10831	0.87539	0.99599	-1.74603	-2.21770
z	=	-0.78601	-4.50188	-1.73275	0.27067	-1.28856	-7.39889
RHO	=	0.23090	0.34527	0.27065	0.26984	0.22659	0.23373
LAP	=	-0.43426	-0.65078	-0.82308	-0.81508	-0.41314	-0.44669
ellip	=	0.05363	0.14541	0.05216	0.05512	0.02147	0.04032
K(r)	=	0.16736	0.54930	0.25107	0.24958	0.16088	0.17032
G(r)	=	0.05879	0.38660	0.04530	0.04581	0.05759	0.05865
BCP #	=	19	20	21	22	23	24
n1-n2	=	14-13	14-16	13-17	19-14	20-15	21-15
A - B	=	C - C	C - O	C - O	H - C	H - C	H - C
x	=	-4.24568	-4.87060	-2.40896	-6.11720	-7.07354	-5.69839
y	=	-0.90548	-0.62707	-0.70729	-0.01361	-3.78860	-4.33337
z	=	-6.32286	-8.12484	-5.52276	-6.91916	-6.41713	-7.84767
RHO	=	0.24507	0.22953	0.35428	0.27136	0.26300	0.26067
LAP	=	-0.48580	-0.32881	-0.63232	-0.82320	-0.76309	-0.74243
ellip	=	0.06762	0.05760	0.13713	0.04644	0.01602	0.01611
K(r)	=	0.18151	0.27000	0.57100	0.25113	0.24133	0.23750
G(r)	=	0.06006	0.18780	0.41292	0.04533	0.05056	0.05189
BCP #	=	25	26	27	28	29	30
n1-n2	=	22-15	23-16	23-17	25-24	26-24	30-27
A - B	=	H - C	H - O	H - O	H - C	H - C	C - C

x	=	-7.42490	-2.86616	-2.10325	8.43885	7.96086	12.03720
y	=	-3.39105	0.13611	-0.06353	-2.76518	-2.85776	-2.55274
z	=	-8.41061	-9.56180	-8.06940	0.14713	-1.82899	-1.87679
RHO	=	0.26208	0.34595	0.02423	0.26289	0.26223	0.22608
LAP	=	-0.75461	-1.72452	0.09545	-0.74954	-0.74787	-0.41237
ellip	=	0.01586	0.02314	0.46815	0.01548	0.01551	0.01097
K(r)	=	0.23999	0.49804	0.00031	0.23966	0.23812	0.15994
G(r)	=	0.05134	0.06691	0.02417	0.05228	0.05115	0.05685
BCP #	=	31	32	33	34	35	36
n1-n2	=	30-33	28-27	29-27	31-30	32-30	34-33
A - B	=	C - C	H - C	H - C	H - C	H - C	H - C
x	=	13.15085	11.66449	11.13942	13.99779	12.39815	13.89224
y	=	-4.47665	-0.68831	-0.67667	-3.23224	-4.37652	-4.60637
z	=	-0.96174	-0.71864	-2.67300	-2.57341	-3.04173	1.13477
RHO	=	0.22599	0.25930	0.26049	0.26198	0.26078	0.25871
LAP	=	-0.41267	-0.72320	-0.73228	-0.74466	-0.73577	-0.72592
ellip	=	0.01189	0.01360	0.01284	0.01490	0.01486	0.01311
K(r)	=	0.16004	0.23349	0.23537	0.23797	0.23595	0.23423
G(r)	=	0.05687	0.05269	0.05231	0.05181	0.05201	0.05275
BCP #	=	37	38				
n1-n2	=	35-33	36-33				
A - B	=	H - C	H - C				
x	=	14.24893	12.37325				
y	=	-6.20591	-5.85776				
z	=	-0.07224	0.61798				
RHO	=	0.26045	0.26001				
LAP	=	-0.74124	-0.73364				
ellip	=	0.01232	0.01360				
K(r)	=	0.23716	0.23661				
G(r)	=	0.05185	0.05320				

Structure 19: Im_c6h13 L-lactate (3f)

----- Bond critical points -----							
BCP #	=	1	2	3	4	5	6
n1-n2	=	2- 1	5- 4	5- 1	2- 3	3- 4	12- 1
A - B	=	C - N	C - N	C - N	C - C	C - N	H - N
x	=	0.90098	2.95311	1.55735	2.44243	3.91367	-1.13656
y	=	-1.88090	-0.62754	-0.93413	-1.84046	-1.23941	-1.60432
z	=	1.25607	-1.13140	-1.12710	2.14086	1.31317	-0.87774
RHO	=	0.28537	0.31740	0.33546	0.32250	0.27320	0.26425
LAP	=	-0.65095	-0.73225	-0.91862	-0.83888	-0.52467	-1.22523
ellip	=	0.01811	0.01139	0.05184	0.26452	0.04014	0.01990
K(r)	=	0.40153	0.48510	0.51992	0.32403	0.38073	0.34736
G(r)	=	0.23879	0.30204	0.29027	0.11431	0.24956	0.04106
BCP #	=	7	8	9	10	11	12
n1-n2	=	12-18	8-17	6- 2	7- 3	9- 4	8- 5
A - B	=	H - O	H - O	H - C	H - C	C - N	H - C
x	=	-2.22506	0.63246	0.42600	4.57765	5.95852	2.08625
y	=	-1.60064	-0.09317	-2.57327	-1.68333	-0.11917	-0.20628
z	=	-1.58540	-4.23839	3.02286	3.07566	-0.77899	-2.93395
RHO	=	0.06559	0.02031	0.28004	0.27795	0.22486	0.28291
LAP	=	0.20448	0.07792	-0.94978	-0.92371	-0.32895	-1.07978
ellip	=	0.03522	0.03574	0.02540	0.03675	0.00888	0.01440
K(r)	=	0.00799	-0.00086	0.27614	0.27182	0.27671	0.29681
G(r)	=	0.05911	0.01862	0.03870	0.04089	0.19447	0.02687
BCP #	=	13	14	15	16	17	18
n1-n2	=	24- 9	13-18	10- 9	11- 9	27-24	15-14
A - B	=	C - C	C - O	H - C	H - C	C - C	C - C
x	=	7.70584	-3.61339	6.67107	7.35672	9.86083	-6.35378
y	=	-1.01610	-1.03419	0.92872	0.83641	-1.63781	-1.89283
z	=	-1.43119	-4.16184	-2.07165	-0.11994	-2.20048	-6.93570
RHO	=	0.23091	0.34527	0.27066	0.26980	0.22656	0.23373
LAP	=	-0.43434	-0.65080	-0.82318	-0.81476	-0.41298	-0.44668
ellip	=	0.05331	0.14539	0.05222	0.05521	0.02145	0.04032

K(r)	=	0.16740	0.54929	0.25109	0.24951	0.16092	0.17032
G(r)	=	0.05881	0.38659	0.04529	0.04582	0.05767	0.05865
BCP #	=	19	20	21	22	23	24
n1-n2	=	14-13	14-16	13-17	19-14	20-15	21-15
A - B	=	C - C	C - O	C - O	H - C	H - C	H - C
x	=	-4.62492	-5.41326	-2.72827	-6.55878	-7.39471	-6.14253
y	=	-0.65853	-0.20338	-0.49617	0.23896	-3.59415	-3.94003
z	=	-5.86865	-7.56766	-5.21353	-6.19794	-6.03761	-7.63344
RHO	=	0.24507	0.22953	0.35430	0.27136	0.26300	0.26067
LAP	=	-0.48580	-0.32881	-0.63231	-0.82320	-0.76307	-0.74243
ellip	=	0.06761	0.05757	0.13710	0.04645	0.01602	0.01610
K(r)	=	0.18151	0.27000	0.57103	0.25113	0.24133	0.23750
G(r)	=	0.06006	0.18780	0.41296	0.04533	0.05056	0.05189
BCP #	=	25	26	27	28	29	30
n1-n2	=	22-15	23-16	23-17	25-24	26-24	30-27
A - B	=	H - C	H - O	H - O	H - C	H - C	C - C
x	=	-7.92995	-3.55976	-2.66315	8.61120	7.96587	12.00519
y	=	-2.99191	0.76896	0.42978	-2.85439	-2.73112	-2.30784
z	=	-7.93662	-9.07897	-7.68972	-0.78280	-2.70789	-3.09734
RHO	=	0.26207	0.34595	0.02423	0.26269	0.26221	0.22539
LAP	=	-0.75459	-1.72452	0.09546	-0.74788	-0.74769	-0.40931
ellip	=	0.01585	0.02314	0.46813	0.01571	0.01562	0.01341
K(r)	=	0.23999	0.49803	0.00031	0.23932	0.23808	0.15916
G(r)	=	0.05134	0.06690	0.02418	0.05235	0.05116	0.05683
BCP #	=	31	32	33	34	35	36
n1-n2	=	33-30	33-36	28-27	29-27	31-30	32-30
A - B	=	C - C	C - C	H - C	H - C	H - C	H - C
x	=	13.17095	14.22919	11.71906	11.02149	13.92200	12.28860
y	=	-4.38516	-4.95707	-0.61641	-0.36442	-2.84346	-3.88365
z	=	-2.61490	-0.52413	-1.66114	-3.53821	-4.00892	-4.58754
RHO	=	0.22580	0.22590	0.26070	0.26024	0.26079	0.26058
LAP	=	-0.41021	-0.41210	-0.73232	-0.72987	-0.73517	-0.73338
ellip	=	0.01366	0.00997	0.01422	0.01426	0.01470	0.01468
K(r)	=	0.15926	0.16000	0.23597	0.23501	0.23594	0.23557
G(r)	=	0.05670	0.05698	0.05289	0.05254	0.05214	0.05222
BCP #	=	37	38	39	40	41	
n1-n2	=	34-33	35-33	37-36	38-36	39-36	
A - B	=	H - C	H - C	H - C	H - C	H - C	
x	=	14.19246	12.45402	16.01386	15.30921	14.28506	
y	=	-6.29982	-6.01280	-3.88887	-5.46450	-3.71593	
z	=	-2.26672	-1.29694	0.28849	1.36838	1.33980	
RHO	=	0.26144	0.26066	0.25908	0.26008	0.25910	
LAP	=	-0.74023	-0.73199	-0.72932	-0.73775	-0.72607	
ellip	=	0.01305	0.01476	0.01160	0.01132	0.01260	
K(r)	=	0.23717	0.23622	0.23479	0.23658	0.23530	
G(r)	=	0.05212	0.05322	0.05246	0.05214	0.05378	

Structure 20: Im_c7h15 L-lactate (3g)

----- Bond critical points -----							
BCP #	=	1	2	3	4	5	6
n1-n2	=	2- 1	5- 4	5- 1	2- 3	3- 4	12- 1
A - B	=	C - N	C - N	C - N	C - C	C - N	H - N
x	=	0.21540	2.96603	1.57107	1.49518	3.20755	-1.19122
y	=	-0.08302	-0.13196	-0.03460	-0.22417	-0.29383	0.14646
z	=	1.69063	-0.28771	-0.58234	2.91657	2.39339	-0.90731
RHO	=	0.28538	0.31742	0.33545	0.32249	0.27321	0.26428
LAP	=	-0.65097	-0.73220	-0.91859	-0.83885	-0.52478	-1.22547
ellip	=	0.01812	0.01141	0.05184	0.26453	0.04016	0.01991
K(r)	=	0.40156	0.48514	0.51989	0.32402	0.38075	0.34742
G(r)	=	0.23882	0.30209	0.29025	0.11430	0.24955	0.04105
BCP #	=	7	8	9	10	11	12
n1-n2	=	12-18	8-17	6- 2	7- 3	9- 4	8- 5
A - B	=	H - O	H - O	H - C	H - C	C - N	H - C
x	=	-2.06961	1.55925	-0.77568	3.35429	5.85380	2.63119

y	=	0.25396	0.14862	-0.11329	-0.40545	-0.38311	0.00296
z	=	-1.85753	-3.93004	3.37681	4.31964	0.71914	-2.29951
RHO	=	0.06557	0.02029	0.28004	0.27796	0.22484	0.28292
LAP	=	0.20444	0.07786	-0.94975	-0.92375	-0.32862	-1.07977
ellip	=	0.03526	0.03587	0.02540	0.03674	0.00886	0.01441
K(r)	=	0.00798	-0.00086	0.27614	0.27183	0.27670	0.29681
G(r)	=	0.05909	0.01860	0.03870	0.04089	0.19454	0.02687
BCP #	=	13	14	15	16	17	18
n1-n2	=	24- 9	13-18	10- 9	11- 9	27-24	15-14
A - B	=	C - C	C - O	H - C	H - C	C - C	C - C
x	=	7.30141	-2.69916	7.09340	7.34098	9.23799	-5.01115
y	=	-1.86211	0.45566	0.03447	0.30318	-3.22921	-0.34419
z	=	0.74241	-4.76404	-0.53186	1.50634	0.70292	-7.91937
RHO	=	0.23093	0.34528	0.27065	0.26979	0.22657	0.23373
LAP	=	-0.43446	-0.65085	-0.82309	-0.81465	-0.41298	-0.44669
ellip	=	0.05334	0.14537	0.05223	0.05527	0.02131	0.04033
K(r)	=	0.16744	0.54932	0.25107	0.24948	0.16092	0.17032
G(r)	=	0.05883	0.38661	0.04530	0.04582	0.05768	0.05865
BCP #	=	19	20	21	22	23	24
n1-n2	=	14-13	14-16	13-17	19-14	20-15	21-15
A - B	=	C - C	C - O	C - O	H - C	H - C	H - C
x	=	-3.20066	-3.47061	-1.50966	-4.63927	-6.69726	-5.35689
y	=	0.61453	0.78819	0.42608	1.87987	-1.38818	-2.48099
z	=	-6.71358	-8.61416	-5.63769	-7.70504	-6.99651	-8.11160
RHO	=	0.24508	0.22953	0.35429	0.27136	0.26300	0.26067
LAP	=	-0.48582	-0.32880	-0.63236	-0.82321	-0.76309	-0.74245
ellip	=	0.06760	0.05753	0.13709	0.04645	0.01601	0.01610
K(r)	=	0.18152	0.26999	0.57103	0.25113	0.24133	0.23751
G(r)	=	0.06006	0.18779	0.41294	0.04533	0.05056	0.05189
BCP #	=	25	26	27	28	29	30
n1-n2	=	22-15	23-16	23-17	25-24	26-24	30-27
A - B	=	H - C	H - O	H - O	H - C	H - C	C - C
x	=	-6.64823	-1.15688	-0.69169	7.42325	7.21705	11.17364
y	=	-1.20158	0.77123	0.59114	-3.62283	-3.86667	-4.67443
z	=	-9.05031	-9.75931	-8.14708	1.96895	-0.04001	0.55351
RHO	=	0.26207	0.34595	0.02424	0.26277	0.26220	0.22534
LAP	=	-0.75458	-1.72456	0.09551	-0.74850	-0.74764	-0.40906
ellip	=	0.01585	0.02314	0.46731	0.01571	0.01566	0.01256
K(r)	=	0.23999	0.49804	0.00031	0.23945	0.23807	0.15915
G(r)	=	0.05135	0.06690	0.02419	0.05233	0.05116	0.05689
BCP #	=	31	32	33	34	35	36
n1-n2	=	33-30	36-33	28-27	29-27	36-39	31-30
A - B	=	C - C	C - C	H - C	H - C	C - C	H - C
x	=	11.48236	11.82687	11.19480	10.97346	13.80564	12.94003
y	=	-6.77011	-7.00167	-2.63596	-2.74022	-6.31635	-5.93837
z	=	1.74513	4.14773	1.47853	-0.52445	5.35867	0.29095
RHO	=	0.22506	0.22579	0.26049	0.26019	0.22590	0.26215
LAP	=	-0.40704	-0.40993	-0.73063	-0.72945	-0.41216	-0.74402
ellip	=	0.01488	0.01253	0.01406	0.01413	0.00953	0.01533
K(r)	=	0.15839	0.15926	0.23564	0.23492	0.16000	0.23837
G(r)	=	0.05663	0.05678	0.05299	0.05256	0.05696	0.05237
BCP #	=	37	38	39	40	41	42
n1-n2	=	32-30	34-33	35-33	37-36	38-36	40-39
A - B	=	H - C	H - C	H - C	H - C	H - C	H - C
x	=	11.19139	11.76547	10.03271	12.04765	11.84394	15.62501
y	=	-6.61814	-8.70521	-7.74522	-7.22005	-5.34963	-5.33253
z	=	-0.44530	2.75001	3.09352	6.32836	5.62405	4.50138
RHO	=	0.26038	0.26027	0.26045	0.26098	0.25960	0.25990
LAP	=	-0.73138	-0.73092	-0.72964	-0.73623	-0.72345	-0.73293
ellip	=	0.01578	0.01240	0.01439	0.01146	0.01319	0.01261
K(r)	=	0.23528	0.23517	0.23583	0.23646	0.23471	0.23645
G(r)	=	0.05243	0.05244	0.05341	0.05240	0.05385	0.05322
BCP #	=	43	44				
n1-n2	=	41-39	42-39				
A - B	=	H - C	H - C				
x	=	15.80394	15.66444				
y	=	-7.26908	-5.78464				
z	=	5.09357	6.47865				

RHO	=	0.25909	0.25983
LAP	=	-0.72935	-0.73537
ellip	=	0.01215	0.01228
K(r)	=	0.23481	0.23620
G(r)	=	0.05248	0.05236

Structure 21: Im_c8h17 L-lactate (3h)

Bond critical points						
BCP #	=	1	2	3	4	5
n1-n2	=	2- 1	5- 4	5- 1	2- 3	3- 4
A - B	=	C - N	C - N	C - N	C - C	C - N
x	=	0.35000	3.07558	1.67902	1.64185	3.34642
y	=	-0.16228	-0.22393	-0.09895	-0.34440	-0.43350
z	=	1.75007	-0.26233	-0.53828	2.95782	2.41267
RHO	=	0.28538	0.31742	0.33545	0.32249	0.27322
LAP	=	-0.65094	-0.73218	-0.91855	-0.83888	-0.52484
ellip	=	0.01814	0.01141	0.05183	0.26456	0.04016
K(r)	=	0.40155	0.48515	0.51989	0.32402	0.38076
G(r)	=	0.23882	0.30211	0.29025	0.11430	0.24955
BCP #	=	7	8	9	10	11
n1-n2	=	12-18	8-17	6- 2	7- 3	9- 4
A - B	=	H - O	H - O	H - C	H - C	C - N
x	=	-1.97135	1.63030	-0.62121	3.51431	5.97065
y	=	0.27037	0.14006	-0.20389	-0.57912	-0.53834
z	=	-1.76402	-3.88211	3.44754	4.33498	0.70500
RHO	=	0.06555	0.02029	0.28004	0.27795	0.22484
LAP	=	0.20443	0.07786	-0.94973	-0.92376	-0.32860
ellip	=	0.03526	0.03587	0.02540	0.03673	0.00890
K(r)	=	0.00797	-0.00086	0.27613	0.27182	0.27671
G(r)	=	0.05908	0.01860	0.03870	0.04088	0.19456
BCP #	=	13	14	15	16	17
n1-n2	=	24- 9	13-18	10- 9	11- 9	27-24
A - B	=	C - C	C - O	H - C	H - C	C - C
x	=	7.39448	-2.63208	7.20142	7.47814	9.30817
y	=	-2.04042	0.53080	-0.12320	0.11324	-3.43740
z	=	0.69020	-4.65903	-0.55539	1.48308	0.60823
RHO	=	0.23093	0.34528	0.27064	0.26978	0.22658
LAP	=	-0.43449	-0.65088	-0.82302	-0.81456	-0.41304
ellip	=	0.05331	0.14534	0.05223	0.05528	0.02129
K(r)	=	0.16745	0.54933	0.25105	0.24946	0.16094
G(r)	=	0.05883	0.38661	0.04529	0.04582	0.05768
BCP #	=	19	20	21	22	23
n1-n2	=	14-13	14-16	13-17	19-14	20-15
A - B	=	C - C	C - O	C - O	H - C	H - C
x	=	-3.15408	-3.44386	-1.45370	-4.58365	-6.68611
y	=	0.73053	0.94066	0.49661	2.03545	-1.21054
z	=	-6.59939	-8.49342	-5.54744	-7.55202	-6.87335
RHO	=	0.24506	0.22953	0.35429	0.27136	0.26299
LAP	=	-0.48577	-0.32879	-0.63235	-0.82320	-0.76305
ellip	=	0.06759	0.05753	0.13708	0.04645	0.01601
K(r)	=	0.18150	0.26999	0.57103	0.25113	0.24133
G(r)	=	0.06006	0.18780	0.41294	0.04533	0.05056
BCP #	=	25	26	27	28	29
n1-n2	=	22-15	23-16	23-17	25-24	26-24
A - B	=	H - C	H - O	H - O	H - C	H - C
x	=	-6.65821	-1.14458	-0.66317	7.50288	7.26839
y	=	-0.99023	0.90556	0.69075	-3.81963	-4.03225
z	=	-8.92421	-9.66681	-8.06351	1.89105	-0.11841
RHO	=	0.26207	0.34594	0.02424	0.26278	0.26219
LAP	=	-0.75456	-1.72449	0.09548	-0.74862	-0.74752
ellip	=	0.01585	0.02314	0.46753	0.01571	0.01566
K(r)	=	0.23998	0.49802	0.00031	0.23947	0.23805
G(r)	=	0.05134	0.06690	0.02418	0.05232	0.05117
BCP #	=	30				
n1-n2	=	30-27				
A - B	=	C - C				
x	=	11.21857				
y	=	-4.91095				
z	=	0.41746				
RHO	=	0.22537				
LAP	=	-0.40917				
ellip	=	0.01260				
K(r)	=	0.15919				
G(r)	=	0.05690				

BCP #	=	31	32	33	34	35	36
n1-n2	=	33-30	36-33	28-27	29-27	39-36	31-30
A - B	=	C - C	C - C	H - C	H - C	C - C	H - C
x	=	11.50579	11.86236	11.28341	11.03622	13.86436	12.96145
y	=	-7.02672	-7.29312	-2.88484	-2.96065	-6.65052	-6.19908
z	=	1.57915	3.97831	1.36686	-0.63439	5.20619	0.11944
RHO	=	0.22492	0.22571	0.26049	0.26017	0.22731	0.26220
LAP	=	-0.40659	-0.40986	-0.73064	-0.72930	-0.41520	-0.74436
ellip	=	0.01482	0.01144	0.01402	0.01411	0.02044	0.01525
K(r)	=	0.15821	0.15921	0.23565	0.23488	0.16123	0.23847
G(r)	=	0.05656	0.05675	0.05299	0.05256	0.05743	0.05238
BCP #	=	37	38	39	40	41	42
n1-n2	=	32-30	34-33	35-33	37-36	38-36	39-40
A - B	=	H - C	H - C	H - C	H - C	H - C	C - C
x	=	11.19437	11.77171	10.05403	12.08639	11.91334	15.82303
y	=	-6.84157	-8.97791	-8.00104	-7.53992	-5.65786	-6.10532
z	=	-0.60587	2.55773	2.92474	6.15582	5.47337	6.48303
RHO	=	0.26036	0.26030	0.26046	0.26005	0.25870	0.22630
LAP	=	-0.73114	-0.73118	-0.72957	-0.72850	-0.71606	-0.41424
ellip	=	0.01570	0.01253	0.01461	0.00945	0.01086	0.01046
K(r)	=	0.23522	0.23522	0.23581	0.23486	0.23320	0.16051
G(r)	=	0.05244	0.05242	0.05341	0.05274	0.05419	0.05695
BCP #	=	43	44	45	46	47	
n1-n2	=	41-39	42-39	43-40	44-40	45-40	
A - B	=	H - C	H - C	H - C	H - C	H - C	
x	=	15.66139	15.80861	15.88871	17.61008	16.05944	
y	=	-5.70922	-7.63861	-4.56169	-5.58058	-6.50572	
z	=	4.32520	4.89488	8.09089	7.72479	8.66441	
RHO	=	0.26091	0.26000	0.25866	0.26001	0.25934	
LAP	=	-0.73359	-0.72913	-0.72540	-0.73727	-0.73082	
ellip	=	0.01060	0.01100	0.01266	0.01250	0.01224	
K(r)	=	0.23670	0.23485	0.23421	0.23647	0.23522	
G(r)	=	0.05330	0.05256	0.05285	0.05215	0.05251	

Structure 22: Im_c9h19 L-lactate (3i)

----- Bond critical points -----							
BCP #	=	1	2	3	4	5	6
n1-n2	=	2- 1	5- 4	5- 1	2- 3	12- 1	12-18
A - B	=	C - N	C - N	C - N	C - C	H - N	H - O
x	=	0.71947	3.36733	1.97073	2.04048	-0.78393	-1.69523
y	=	-0.24396	-0.40448	-0.20050	-0.51982	0.18201	0.38635
z	=	1.87874	-0.22970	-0.45348	3.03614	-0.63884	-1.54112
RHO	=	0.28538	0.31743	0.33545	0.32249	0.26431	0.06555
LAP	=	-0.65098	-0.73216	-0.91856	-0.83888	-1.22570	0.20442
ellip	=	0.01815	0.01142	0.05184	0.26456	0.01991	0.03529
K(r)	=	0.40155	0.48517	0.51989	0.32402	0.34747	0.00798
G(r)	=	0.23880	0.30213	0.29025	0.11430	0.04105	0.05909
BCP #	=	7	8	9	10	11	12
n1-n2	=	8-17	3- 4	6- 2	7- 3	9- 4	8- 5
A - B	=	H - O	C - N	H - C	H - C	C - N	H - C
x	=	1.81954	3.71820	-0.19380	3.94393	6.27315	2.95199
y	=	0.11440	-0.68623	-0.27162	-0.88235	-0.89091	-0.16908
z	=	-3.78753	2.42931	3.60835	4.34119	0.62814	-2.21699
RHO	=	0.02028	0.27322	0.28004	0.27795	0.22483	0.28293
LAP	=	0.07784	-0.52487	-0.94972	-0.92375	-0.32846	-1.07975
ellip	=	0.03601	0.04017	0.02540	0.03673	0.00892	0.01441
K(r)	=	-0.00086	0.38076	0.27613	0.27182	0.27671	0.29681
G(r)	=	0.01859	0.24955	0.03870	0.04088	0.19460	0.02688
BCP #	=	13	14	15	16	17	18
n1-n2	=	24- 9	13-18	10- 9	11- 9	27-24	15-14
A - B	=	C - C	C - O	H - C	H - C	C - C	C - C
x	=	7.61448	-2.44081	7.47978	7.83882	9.44798	-4.94343
y	=	-2.46448	0.74530	-0.51529	-0.33431	-3.95715	0.23209
z	=	0.53561	-4.40438	-0.66740	1.36390	0.36047	-7.47279
RHO	=	0.23094	0.34528	0.27063	0.26978	0.22659	0.23373
LAP	=	-0.43451	-0.65098	-0.82300	-0.81453	-0.41306	-0.44667

ellip	=	0.05329	0.14533	0.05224	0.05529	0.02126	0.04033
K(r)	=	0.16746	0.54933	0.25104	0.24946	0.16095	0.17032
G(r)	=	0.05884	0.38659	0.04529	0.04582	0.05769	0.05865
BCP #	=	19	20	21	22	23	24
n1-n2	=	14-13	14-16	13-17	19-14	20-15	21-15
A - B	=	C - C	C - O	C - O	H - C	H - C	H - C
x	=	-3.01763	-3.36048	-1.29708	-4.40761	-6.65510	-5.44614
y	=	1.01598	1.28381	0.66943	2.41525	-0.73064	-1.86681
z	=	-6.32048	-8.19828	-5.33452	-7.19459	-6.50950	-7.72677
RHO	=	0.24507	0.22953	0.35430	0.27136	0.26300	0.26067
LAP	=	-0.48578	-0.32881	-0.63234	-0.82320	-0.76306	-0.74243
ellip	=	0.06759	0.05751	0.13708	0.04645	0.01601	0.01609
K(r)	=	0.18151	0.26999	0.57103	0.25113	0.24133	0.23750
G(r)	=	0.06006	0.18779	0.41295	0.04533	0.05056	0.05189
BCP #	=	25	26	27	28	29	30
n1-n2	=	22-15	23-16	23-17	25-24	26-24	30-27
A - B	=	H - C	H - O	H - O	H - C	H - C	C - C
x	=	-6.68582	-1.10785	-0.58386	7.67032	7.35574	11.27043
y	=	-0.46580	1.15442	0.87852	-4.27042	-4.43045	-5.52406
z	=	-8.55505	-9.45267	-7.87241	1.69939	-0.30396	0.07574
RHO	=	0.26207	0.34594	0.02424	0.26279	0.26218	0.22537
LAP	=	-0.75455	-1.72446	0.09550	-0.74863	-0.74748	-0.40918
ellip	=	0.01585	0.02314	0.46694	0.01571	0.01567	0.01257
K(r)	=	0.23998	0.49801	0.00031	0.23948	0.23804	0.15920
G(r)	=	0.05134	0.06690	0.02419	0.05232	0.05117	0.05690
BCP #	=	31	32	33	34	35	36
n1-n2	=	33-30	36-33	28-27	29-27	39-36	31-30
A - B	=	C - C	C - C	H - C	H - C	C - C	H - C
x	=	11.48529	11.90885	11.47445	11.15467	13.98243	12.93207
y	=	-7.67431	-8.00607	-3.52309	-3.54650	-7.49081	-6.89472
z	=	1.18836	3.56839	1.05824	-0.93400	4.73532	-0.30618
RHO	=	0.22495	0.22559	0.26048	0.26015	0.22727	0.26222
LAP	=	-0.40676	-0.40937	-0.73056	-0.72918	-0.41519	-0.74456
ellip	=	0.01483	0.01150	0.01399	0.01413	0.01829	0.01523
K(r)	=	0.15825	0.15907	0.23563	0.23486	0.16122	0.23850
G(r)	=	0.05656	0.05672	0.05299	0.05257	0.05742	0.05236
BCP #	=	37	38	39	40	41	42
n1-n2	=	32-30	34-33	35-33	37-36	38-36	42-39
A - B	=	H - C	H - C	H - C	H - C	H - C	C - C
x	=	11.10990	11.68163	10.03104	12.19378	12.09405	16.02761
y	=	-7.43001	-9.65555	-8.59826	-8.30829	-6.40639	-7.07899
z	=	-0.98070	2.12182	2.56617	5.73112	5.09032	5.95469
RHO	=	0.26033	0.26033	0.26045	0.26010	0.25877	0.22761
LAP	=	-0.73094	-0.73143	-0.72950	-0.72882	-0.71653	-0.41682
ellip	=	0.01576	0.01243	0.01461	0.00951	0.01093	0.02136
K(r)	=	0.23518	0.23527	0.23579	0.23494	0.23333	0.16162
G(r)	=	0.05245	0.05241	0.05341	0.05274	0.05419	0.05741
BCP #	=	43	44	45	46	47	48
n1-n2	=	40-39	41-39	42-43	44-42	45-42	46-43
A - B	=	H - C	H - C	C - C	H - C	H - C	H - C
x	=	15.79424	15.86174	18.06869	16.27718	16.18347	19.99354
y	=	-6.61785	-8.56728	-6.66423	-7.55133	-5.60088	-7.72313
z	=	3.81407	4.32955	7.15641	8.09238	7.58126	6.77611
RHO	=	0.26001	0.25909	0.22656	0.26025	0.25953	0.25923
LAP	=	-0.72617	-0.72162	-0.41548	-0.73066	-0.72512	-0.73010
ellip	=	0.00860	0.00895	0.01078	0.01031	0.01085	0.01220
K(r)	=	0.23518	0.23331	0.16081	0.23524	0.23418	0.23505
G(r)	=	0.05364	0.05291	0.05694	0.05258	0.05290	0.05252
BCP #	=	49	50				
n1-n2	=	47-43	48-43				
A - B	=	H - C	H - C				
x	=	19.99949	19.89918				
y	=	-6.29366	-5.75607				
z	=	8.22401	6.26485				
RHO	=	0.25983	0.25899				
LAP	=	-0.73574	-0.72800				
ellip	=	0.01258	0.01236				

K(r) = 0.23621 0.23471
G(r) = 0.05228 0.05271

Structure 23: Im_c10h21 L-lactate (3j)

----- Bond critical points -----						
BCP #	=	1	2	3	4	5
n1-n2	=	2- 1	5- 4	5- 1	2- 3	12- 1
A - B	=	C - N	C - N	C - N	C - C	H - N
x	=	0.94194	3.54630	2.15209	2.27527	-0.59377
y	=	-0.37182	-0.52658	-0.27702	-0.72524	0.18635
z	=	2.02145	-0.14090	-0.33084	3.14308	-0.45056
RHO	=	0.28539	0.31743	0.33545	0.32249	0.26427
LAP	=	-0.65101	-0.73211	-0.91862	-0.83887	-1.22534
ellip	=	0.01817	0.01141	0.05186	0.26457	0.01991
K(r)	=	0.40157	0.48518	0.51987	0.32402	0.34739
G(r)	=	0.23882	0.30215	0.29021	0.11430	0.04106
BCP #	=	7	8	9	10	11
n1-n2	=	8-17	3- 4	6- 2	7- 3	9- 4
A - B	=	H - O	C - N	H - C	H - C	C - N
x	=	1.95085	3.93665	0.05927	4.19097	6.45248
y	=	0.16377	-0.91453	-0.43797	-1.18633	-1.12191
z	=	-3.64848	2.49918	3.76583	4.39818	0.64403
RHO	=	0.02028	0.27322	0.28004	0.27795	0.22484
LAP	=	0.07783	-0.52490	-0.94969	-0.92376	-0.32843
ellip	=	0.03586	0.04017	0.02540	0.03673	0.00894
K(r)	=	-0.00086	0.38077	0.27613	0.27182	0.27672
G(r)	=	0.01859	0.24955	0.03871	0.04088	0.19461
BCP #	=	13	14	15	16	17
n1-n2	=	24- 9	13-18	10- 9	11- 9	27-24
A - B	=	C - C	C - O	H - C	H - C	C - C
x	=	7.74844	-2.29995	7.64531	8.04578	9.53705
y	=	-2.72644	0.93192	-0.73295	-0.63365	-4.26028
z	=	0.47123	-4.16224	-0.66024	1.36896	0.20939
RHO	=	0.23094	0.34527	0.27063	0.26978	0.22660
LAP	=	-0.43453	-0.65087	-0.82296	-0.81451	-0.41309
ellip	=	0.05328	0.14535	0.05224	0.05530	0.02126
K(r)	=	0.16747	0.54930	0.25104	0.24945	0.16096
G(r)	=	0.05884	0.38659	0.04529	0.04582	0.05769
BCP #	=	19	20	21	22	23
n1-n2	=	14-13	14-16	13-17	19-14	20-15
A - B	=	C - C	C - O	C - O	H - C	H - C
x	=	-2.90339	-3.27249	-1.17562	-4.26963	-6.59067
y	=	1.28771	1.63300	0.85920	2.75492	-0.35202
z	=	-6.05607	-7.91618	-5.11597	-6.85275	-6.23874
RHO	=	0.24506	0.22953	0.35431	0.27136	0.26299
LAP	=	-0.48577	-0.32878	-0.63231	-0.82320	-0.76306
ellip	=	0.06759	0.05752	0.13705	0.04645	0.01601
K(r)	=	0.18150	0.27000	0.57107	0.25113	0.24133
G(r)	=	0.06006	0.18781	0.41299	0.04533	0.05056
BCP #	=	25	26	27	28	29
n1-n2	=	22-15	23-16	23-17	25-24	26-24
A - B	=	H - C	H - O	H - O	H - C	H - C
x	=	-6.65073	-1.04727	-0.50286	7.77590	7.42103
y	=	-0.01209	1.48897	1.14154	-4.57327	-4.65383
z	=	-8.27250	-9.21713	-7.65778	1.57001	-0.43137
RHO	=	0.26207	0.34595	0.02423	0.26279	0.26218
LAP	=	-0.75455	-1.72450	0.09547	-0.74865	-0.74744
ellip	=	0.01585	0.02314	0.46784	0.01572	0.01567
K(r)	=	0.23998	0.49803	0.00031	0.23948	0.23803
G(r)	=	0.05135	0.06690	0.02418	0.05232	0.05117
BCP #	=	31	32	33	34	35
n1-n2	=	33-30	36-33	28-27	29-27	39-36
A - B	=	C - C	C - C	H - C	H - C	C - C
x	=	11.48684	11.94284	11.58678	11.23052	14.04921
						12.92738

y	=	-8.05654	-8.48077	-3.90453	-3.85053	-8.06016	-7.26451
z	=	0.87152	3.23091	0.88287	-1.10257	4.37656	-0.62267
RHO	=	0.22495	0.22563	0.26048	0.26015	0.22715	0.26222
LAP	=	-0.40674	-0.40952	-0.73056	-0.72913	-0.41473	-0.74454
ellip	=	0.01484	0.01153	0.01397	0.01413	0.01844	0.01523
K(r)	=	0.15824	0.15911	0.23564	0.23485	0.16108	0.23849
G(r)	=	0.05656	0.05673	0.05300	0.05257	0.05740	0.05236
BCP #	=	37	38	39	40	41	42
n1-n2	=	32-30	34-33	35-33	37-36	38-36	42-39
A - B	=	H - C	H - C	H - C	H - C	H - C	C - C
x	=	11.07960	11.64648	10.03276	12.25692	12.19679	16.12494
y	=	-7.72760	-10.07310	-8.98905	-8.86458	-6.93978	-7.74328
z	=	-1.28062	1.73344	2.24355	5.37644	4.80240	5.57183
RHO	=	0.26032	0.26032	0.26044	0.26014	0.25880	0.22758
LAP	=	-0.73083	-0.73130	-0.72938	-0.72911	-0.71672	-0.41687
ellip	=	0.01577	0.01240	0.01459	0.00960	0.01101	0.01931
K(r)	=	0.23516	0.23524	0.23577	0.23500	0.23336	0.16162
G(r)	=	0.05245	0.05242	0.05342	0.05272	0.05418	0.05741
BCP #	=	43	44	45	46	47	48
n1-n2	=	40-39	41-39	43-42	44-42	45-42	43-48
A - B	=	H - C	H - C	C - C	H - C	H - C	C - C
x	=	15.86653	15.89086	18.20583	16.39994	16.34902	20.26328
y	=	-7.20420	-9.17106	-7.41888	-8.29424	-6.32535	-7.09728
z	=	3.45135	3.90010	6.76375	7.68813	7.24417	7.96206
RHO	=	0.26006	0.25915	0.22790	0.25935	0.25863	0.22651
LAP	=	-0.72649	-0.72195	-0.41817	-0.72323	-0.71773	-0.41524
ellip	=	0.00862	0.00904	0.02177	0.00834	0.00886	0.01078
K(r)	=	0.23526	0.23340	0.16195	0.23372	0.23266	0.16075
G(r)	=	0.05364	0.05291	0.05741	0.05291	0.05322	0.05694
BCP #	=	49	50	51	52	53	
n1-n2	=	46-43	47-43	49-48	50-48	51-48	
A - B	=	H - C	H - C	H - C	H - C	H - C	
x	=	20.05654	20.00542	20.58208	20.52949	22.14682	
y	=	-8.51327	-6.54340	-7.65493	-5.67023	-6.78644	
z	=	6.28305	5.84290	10.09801	9.65501	9.13062	
RHO	=	0.26014	0.25990	0.25911	0.25893	0.25983	
LAP	=	-0.73001	-0.72792	-0.72909	-0.72753	-0.73571	
ellip	=	0.01054	0.01092	0.01202	0.01213	0.01233	
K(r)	=	0.23509	0.23474	0.23489	0.23462	0.23621	
G(r)	=	0.05259	0.05276	0.05261	0.05274	0.05228	

Structure 24: Im_c12h25 L-lactate (3I)

----- Bond critical points -----							
BCP #	=	1	2	3	4	5	6
n1-n2	=	2- 1	5- 4	5- 1	2- 3	12- 1	12-18
A - B	=	C - N	C - N	C - N	C - C	H - N	H - O
x	=	1.43333	3.94519	2.53042	2.83513	-0.24292	-1.21672
y	=	-1.16213	-0.97380	-0.80927	-1.50308	-0.53181	-0.27071
z	=	2.55485	0.28825	0.17187	3.59385	0.19409	-0.62413
RHO	=	0.28539	0.31743	0.33544	0.32249	0.26429	0.06558
LAP	=	-0.65102	-0.73216	-0.91857	-0.83886	-1.22549	0.20448
ellip	=	0.01819	0.01143	0.05185	0.26457	0.01991	0.03526
K(r)	=	0.40157	0.48518	0.51987	0.32401	0.34743	0.00799
G(r)	=	0.23882	0.30214	0.29023	0.11430	0.04105	0.05911
BCP #	=	7	8	9	10	11	12
n1-n2	=	8-17	3- 4	6- 2	7- 3	9- 4	8- 5
A - B	=	H - O	C - N	H - C	H - C	C - N	H - C
x	=	2.15503	4.47572	0.63421	4.83046	6.91631	3.39513
y	=	-0.13937	-1.52733	-1.41866	-1.92017	-1.42017	-0.54224
z	=	-3.09160	2.87378	4.32173	4.73511	0.91266	-1.63224
RHO	=	0.02027	0.27323	0.28004	0.27795	0.22483	0.28293
LAP	=	0.07783	-0.52496	-0.94968	-0.92374	-0.32830	-1.07973
ellip	=	0.03593	0.04018	0.02541	0.03673	0.00892	0.01441
K(r)	=	-0.00086	0.38079	0.27613	0.27181	0.27672	0.29681
G(r)	=	0.01859	0.24955	0.03871	0.04088	0.19464	0.02688

BCP #	=	13	14	15	16	17	18
n1-n2	=	24- 9	13-18	10- 9	11- 9	27-24	15-14
A - B	=	C - C	C - O	H - C	H - C	C - C	C - C
x	=	8.30792	-2.15629	8.02238	8.50345	10.18212	-4.82865
y	=	-2.91275	0.36558	-0.85270	-0.87682	-4.29376	0.07912
z	=	0.56687	-3.38030	-0.40257	1.61135	0.11917	-6.33296
RHO	=	0.23094	0.34528	0.27063	0.26978	0.22660	0.23373
LAP	=	-0.43455	-0.65092	-0.82295	-0.81451	-0.41311	-0.44665
ellip	=	0.05326	0.14534	0.05225	0.05531	0.02126	0.04034
K(r)	=	0.16748	0.54931	0.25103	0.24945	0.16097	0.17031
G(r)	=	0.05884	0.38658	0.04529	0.04582	0.05769	0.05865
BCP #	=	19	20	21	22	23	24
n1-n2	=	14-13	14-16	13-17	19-14	20-15	21-15
A - B	=	C - C	C - O	C - O	H - C	H - C	H - C
x	=	-2.86429	-3.33647	-1.07237	-4.35947	-6.43748	-5.26647
y	=	0.81781	1.27381	0.44259	2.24057	-1.05898	-1.99988
z	=	-5.21648	-7.02882	-4.37940	-5.84446	-5.38364	-6.78994
RHO	=	0.24507	0.22953	0.35431	0.27136	0.26299	0.26067
LAP	=	-0.48578	-0.32880	-0.63230	-0.82325	-0.76303	-0.74242
ellip	=	0.06759	0.05751	0.13705	0.04645	0.01601	0.01609
K(r)	=	0.18150	0.27000	0.57106	0.25114	0.24132	0.23750
G(r)	=	0.06006	0.18780	0.41299	0.04533	0.05056	0.05189
BCP #	=	25	26	27	28	29	30
n1-n2	=	22-15	23-16	23-17	25-24	26-24	30-27
A - B	=	H - C	H - O	H - O	H - C	H - C	C - C
x	=	-6.60888	-1.16545	-0.53145	8.50660	8.07128	12.04140
y	=	-0.57371	1.38283	0.95937	-4.82969	-4.78578	-5.73738
z	=	-7.38126	-8.42147	-6.91584	1.51793	-0.46864	-0.44329
RHO	=	0.26207	0.34594	0.02424	0.26279	0.26217	0.22539
LAP	=	-0.75454	-1.72445	0.09549	-0.74866	-0.74740	-0.40922
ellip	=	0.01584	0.02314	0.46730	0.01572	0.01567	0.01258
K(r)	=	0.23998	0.49801	0.00031	0.23949	0.23802	0.15921
G(r)	=	0.05135	0.06690	0.02418	0.05232	0.05117	0.05691
BCP #	=	31	32	33	34	35	36
n1-n2	=	33-30	36-33	28-27	29-27	39-36	31-30
A - B	=	C - C	C - C	H - C	H - C	C - C	H - C
x	=	12.40814	12.99104	12.23065	11.78565	15.11061	13.72694
y	=	-7.98276	-8.54746	-3.84617	-3.67010	-8.06415	-6.98286
z	=	0.41186	2.71338	0.73916	-1.22115	3.80963	-1.07017
RHO	=	0.22494	0.22561	0.26049	0.26014	0.22722	0.26223
LAP	=	-0.40673	-0.40945	-0.73059	-0.72908	-0.41503	-0.74465
ellip	=	0.01486	0.01154	0.01396	0.01415	0.01847	0.01521
K(r)	=	0.15824	0.15909	0.23564	0.23484	0.16116	0.23851
G(r)	=	0.05656	0.05673	0.05299	0.05257	0.05740	0.05235
BCP #	=	37	38	39	40	41	42
n1-n2	=	32-30	34-33	35-33	37-36	38-36	42-39
A - B	=	H - C	H - C	H - C	H - C	H - C	C - C
x	=	11.88778	12.74067	11.07996	13.42058	13.20511	17.20858
y	=	-7.52409	-10.04127	-9.11527	-9.06644	-7.11357	-7.68506
z	=	-1.69162	1.10951	1.76068	4.80959	4.38846	4.94848
RHO	=	0.26031	0.26030	0.26042	0.26009	0.25876	0.22723
LAP	=	-0.73075	-0.73120	-0.72923	-0.72874	-0.71645	-0.41525
ellip	=	0.01578	0.01235	0.01457	0.00955	0.01090	0.01900
K(r)	=	0.23514	0.23522	0.23573	0.23493	0.23330	0.16121
G(r)	=	0.05246	0.05242	0.05343	0.05275	0.05418	0.05740
BCP #	=	43	44	45	46	47	48
n1-n2	=	40-39	41-39	43-42	44-42	45-42	48-43
A - B	=	H - C	H - C	C - C	H - C	H - C	C - C
x	=	16.82398	17.00195	19.31379	17.59002	17.41392	21.42450
y	=	-7.01658	-9.00357	-7.30925	-8.35693	-6.37017	-6.82897
z	=	2.88409	3.18444	6.07716	7.00539	6.70413	7.17921
RHO	=	0.26015	0.25904	0.22725	0.26061	0.25829	0.22568
LAP	=	-0.72702	-0.72134	-0.41521	-0.73096	-0.71501	-0.40991
ellip	=	0.00877	0.00899	0.01904	0.00763	0.00973	0.01222
K(r)	=	0.23539	0.23322	0.16120	0.23605	0.23213	0.15916
G(r)	=	0.05364	0.05289	0.05740	0.05331	0.05338	0.05668
BCP #	=	49	50	51	52	53	54
n1-n2	=	51-48	46-43	47-43	51-54	49-48	50-48

A - B	=	C - C	H - C	H - C	C - C	H - C	H - C
x	=	22.01476	21.21062	20.99508	22.48253	21.67909	23.33870
y	=	-7.40717	-8.27006	-6.31473	-9.63094	-5.33862	-6.28036
z	=	9.47763	5.50256	5.07810	10.29658	8.77683	8.12600
RHO	=	0.22570	0.26042	0.25949	0.22588	0.25937	0.25970
LAP	=	-0.40992	-0.73014	-0.72350	-0.41211	-0.72349	-0.72612
ellip	=	0.01314	0.01062	0.01191	0.00966	0.01216	0.01191
K(r)	=	0.15913	0.23569	0.23406	0.15999	0.23383	0.23430
G(r)	=	0.05665	0.05315	0.05319	0.05697	0.05296	0.05277
BCP #	=	55	56	57	58	59	
n1-n2	=	52-51	53-51	55-54	56-54	57-54	
A - B	=	H - C	H - C	H - C	H - C	H - C	
x	=	20.71542	22.51055	22.42241	23.02515	24.25126	
y	=	-8.47401	-7.84658	-11.53498	-11.66768	-10.83322	
z	=	10.92334	11.57740	9.11490	11.04653	9.65524	
RHO	=	0.26088	0.26056	0.25987	0.25952	0.25869	
LAP	=	-0.73385	-0.73256	-0.73275	-0.73274	-0.72587	
ellip	=	0.01293	0.01306	0.01153	0.01134	0.01131	
K(r)	=	0.23660	0.23585	0.23641	0.23575	0.23421	
G(r)	=	0.05313	0.05271	0.05323	0.05256	0.05275	

Structure 25: Im_ch3 L-lactate (3a)

----- Bond critical points -----						
BCP #	=	1	2	3	4	5
n1-n2	=	2- 1	5- 4	5- 1	2- 3	12- 1
A - B	=	C - N	C - N	C - N	C - C	H - N
x	=	0.33841	3.51630	2.29351	1.17228	-0.20525
y	=	0.09954	-0.71769	-0.73232	0.43079	-0.67868
z	=	1.18613	0.34628	-0.38947	2.72175	-1.62458
RHO	=	0.28548	0.31651	0.33598	0.32263	0.26236
LAP	=	-0.65563	-0.71496	-0.92703	-0.83982	-1.21119
ellip	=	0.01567	0.00645	0.05328	0.26446	0.01986
K(r)	=	0.40128	0.48388	0.52064	0.32431	0.34412
G(r)	=	0.23737	0.30514	0.28888	0.11436	0.04132
BCP #	=	7	8	9	10	11
n1-n2	=	8-18	3- 4	6- 2	7- 3	9- 4
A - B	=	H - O	C - N	H - C	H - C	C - N
x	=	3.29386	2.93614	-1.10172	2.50054	5.91618
y	=	-1.83967	0.15804	0.71659	0.78602	-0.54922
z	=	-3.39006	2.83751	2.36039	4.61341	2.23934
RHO	=	0.02062	0.27251	0.28022	0.27800	0.22923
LAP	=	0.07900	-0.50895	-0.95236	-0.92519	-0.35179
ellip	=	0.03612	0.04039	0.02483	0.03712	0.01479
K(r)	=	-0.00084	0.38035	0.27655	0.27203	0.28530
G(r)	=	0.01891	0.25311	0.03846	0.04073	0.19735
BCP #	=	13	14	15	16	17
n1-n2	=	14-19	10- 9	11- 9	13- 9	16-15
A - B	=	C - O	H - C	H - C	H - C	C - C
x	=	-0.45333	7.48433	7.30867	6.96276	-1.81248
y	=	-1.85529	-1.06738	0.50377	-1.47133	-3.79053
z	=	-5.58766	1.45776	2.82702	3.44241	-8.80468
RHO	=	0.34493	0.27046	0.26982	0.26983	0.23368
LAP	=	-0.64955	-0.83325	-0.82411	-0.82412	-0.44650
ellip	=	0.14646	0.05301	0.05729	0.05729	0.04022
K(r)	=	0.54849	0.25288	0.25130	0.25130	0.17028
G(r)	=	0.38610	0.04457	0.04527	0.04527	0.05866
BCP #	=	19	20	21	22	23
n1-n2	=	15-17	14-18	20-15	21-16	22-16
A - B	=	C - O	C - O	H - C	H - C	H - C
x	=	-0.01090	0.92735	-1.25558	-3.80810	-2.34009
y	=	-3.00423	-2.21504	-1.64993	-4.40789	-5.84120
z	=	-9.33094	-5.96402	-9.29594	-8.15682	-8.31698
RHO	=	0.22963	0.35431	0.27141	0.26300	0.26070
LAP	=	-0.32953	-0.63142	-0.82370	-0.76313	-0.74269

ellip	=	0.05839	0.13750	0.04632	0.01616	0.01622	0.01594
K(r)	=	0.27014	0.57109	0.25122	0.24134	0.23754	0.24007
G(r)	=	0.18776	0.41324	0.04529	0.05056	0.05187	0.05130
BCP #	=	25	26				
n1-n2	=	24-17	24-18				
A - B	=	H - O	H - O				
x	=	2.51769	2.45994				
y	=	-3.45633	-3.01264				
z	=	-9.59491	-7.96527				
RHO	=	0.34599	0.02413				
LAP	=	-1.72470	0.09520				
ellip	=	0.02314	0.47690				
K(r)	=	0.49808	0.00029				
G(r)	=	0.06691	0.02409				

Structure 26: Im_oc4h9 L-lactate (4a)

----- Bond critical points -----							
BCP #	=	1	2	3	4	5	6
n1-n2	=	2- 1	5- 4	5- 1	6- 1	2- 3	6-32
A - B	=	C - N	C - N	C - N	H - N	C - C	H - O
x	=	1.04102	2.71499	1.41111	-1.08482	2.56781	-2.17307
y	=	1.27201	-1.49788	-1.00738	0.13906	1.49565	-0.10542
z	=	-1.42521	-2.41337	-2.72196	-3.16435	-0.54459	-3.82196
RHO	=	0.28255	0.31466	0.33885	0.26336	0.32413	0.06606
LAP	=	-0.63831	-0.72611	-0.93295	-1.21904	-0.84848	0.20486
ellip	=	0.01707	0.00695	0.05199	0.01969	0.26728	0.03445
K(r)	=	0.39492	0.47866	0.52847	0.34586	0.32746	0.00824
G(r)	=	0.23535	0.29713	0.29523	0.04110	0.11534	0.05945
BCP #	=	7	8	9	10	11	12
n1-n2	=	9-31	3- 4	7- 2	8- 3	10- 4	10-11
A - B	=	H - O	C - N	H - C	H - C	C - N	C - O
x	=	0.23377	3.85477	0.77269	4.67429	5.52654	7.05423
y	=	-3.39179	0.27201	2.95936	1.56121	-2.17021	-2.21913
z	=	-4.76486	-0.70630	-0.46912	0.48188	-1.54664	-1.97311
RHO	=	0.02100	0.27140	0.28019	0.27934	0.24703	0.24691
LAP	=	0.08029	-0.49516	-0.95129	-0.94210	-0.53895	-0.46241
ellip	=	0.03585	0.01793	0.02667	0.03406	0.15734	0.19647
K(r)	=	-0.00080	0.37907	0.27651	0.27500	0.31032	0.29800
G(r)	=	0.01927	0.25528	0.03869	0.03947	0.17558	0.18240
BCP #	=	13	14	15	16	17	18
n1-n2	=	9- 5	27-32	29-28	12-11	16-10	17-10
A - B	=	H - C	C - O	C - C	C - O	H - C	H - C
x	=	1.72363	-3.73321	-7.17031	9.82389	6.08772	6.66931
y	=	-2.74888	-1.87920	-3.51675	-2.13608	-3.81592	-2.97770
z	=	-3.69870	-5.64243	-6.84384	-2.92341	-2.17206	-0.31435
RHO	=	0.28276	0.34527	0.23376	0.21279	0.27635	0.27585
LAP	=	-1.08530	-0.64947	-0.44686	-0.15719	-0.87071	-0.86336
ellip	=	0.01305	0.14582	0.04023	0.00821	0.03251	0.03474
K(r)	=	0.29770	0.54932	0.17038	0.25051	0.25885	0.25765
G(r)	=	0.02637	0.38695	0.05867	0.21121	0.04117	0.04180
BCP #	=	19	20	21	22	23	24
n1-n2	=	13-12	14-13	18-12	19-12	20-13	21-13
A - B	=	C - C	C - C	H - C	H - C	H - C	H - C
x	=	11.58254	13.74774	10.51478	11.13010	12.49395	11.88415
y	=	-1.57164	-1.25396	-3.60160	-2.83894	0.35729	-0.39057
z	=	-3.74773	-4.61217	-3.71985	-1.89110	-3.70262	-5.50063
RHO	=	0.23748	0.22692	0.26807	0.26746	0.26287	0.26352
LAP	=	-0.46674	-0.41464	-0.79520	-0.78966	-0.75324	-0.75931
ellip	=	0.05354	0.02562	0.05800	0.05901	0.01542	0.01455
K(r)	=	0.17655	0.16097	0.24510	0.24406	0.23945	0.24045
G(r)	=	0.05987	0.05731	0.04630	0.04665	0.05114	0.05062
BCP #	=	25	26	27	28	29	30
n1-n2	=	15-14	22-14	23-14	24-15	25-15	26-15
A - B	=	C - C	H - C	H - C	H - C	H - C	H - C
x	=	15.93219	14.96708	15.56928	16.33938	17.94708	16.94734

y	=	-0.85538	-2.84966	-2.11052	0.37556	-0.44018	1.11974
z	=	-5.51480	-5.50930	-3.72638	-7.31850	-6.36823	-5.52120
RHO	=	0.22644	0.26037	0.26006	0.25991	0.26051	0.25966
LAP	=	-0.41531	-0.73146	-0.72876	-0.73585	-0.74143	-0.73354
ellip	=	0.01198	0.01081	0.01125	0.01449	0.01493	0.01469
K(r)	=	0.16078	0.23534	0.23488	0.23607	0.23725	0.23570
G(r)	=	0.05695	0.05248	0.05269	0.05211	0.05189	0.05231
BCP #	=	31	32	33	34	35	36
n1-n2	=	28-27	28-30	27-31	33-28	34-29	35-29
A - B	=	C - C	C - O	C - O	H - C	H - C	H - C
x	=	-4.84706	-5.73409	-3.01335	-6.10638	-8.62435	-8.17657
y	=	-3.01594	-4.21902	-3.09881	-2.47394	-2.53429	-4.51340
z	=	-6.88624	-8.10208	-6.05780	-8.55074	-5.53865	-5.19613
RHO	=	0.24512	0.22956	0.35405	0.27134	0.26303	0.26068
LAP	=	-0.48616	-0.32905	-0.63185	-0.82316	-0.76336	-0.74255
ellip	=	0.06787	0.05821	0.13786	0.04639	0.01608	0.01617
K(r)	=	0.18163	0.27005	0.57045	0.25109	0.24138	0.23752
G(r)	=	0.06009	0.18779	0.41249	0.04530	0.05054	0.05189
BCP #	=	37	38	39			
n1-n2	=	36-29	37-30	37-31			
A - B	=	H - C	H - O	H - O			
x	=	-9.28290	-4.11928	-3.16757			
y	=	-3.99560	-6.16222	-5.26744			
z	=	-6.83740	-8.63316	-7.56331			
RHO	=	0.26210	0.34601	0.02420			
LAP	=	-0.75479	-1.72479	0.09541			
ellip	=	0.01591	0.02313	0.47002			
K(r)	=	0.24002	0.49812	0.00030			
G(r)	=	0.05133	0.06692	0.02416			

Structure 27: Im_oc5h11 L-lactate (4b)

----- Bond critical points -----							
BCP #	=	1	2	3	4	5	6
n1-n2	=	2- 1	5- 4	5- 1	6- 1	2- 3	6-31
A - B	=	C - N	C - N	C - N	H - N	C - C	H - O
x	=	0.89295	2.53387	1.21696	-1.29853	2.45371	-2.41176
y	=	1.27746	-1.60789	-1.16196	-0.08202	1.61814	-0.41270
z	=	-1.67336	-2.33143	-2.65223	-3.14881	-0.89572	-3.72095
RHO	=	0.28256	0.31467	0.33883	0.26331	0.32412	0.06610
LAP	=	-0.63835	-0.72609	-0.93298	-1.21860	-0.84842	0.20491
ellip	=	0.01713	0.00685	0.05205	0.01969	0.26726	0.03446
K(r)	=	0.39493	0.47868	0.52842	0.34576	0.32744	0.00826
G(r)	=	0.23535	0.29716	0.29517	0.04111	0.11534	0.05949
BCP #	=	7	8	9	10	11	12
n1-n2	=	9-30	3- 4	7- 2	8- 3	10- 4	10-11
A - B	=	H - O	C - N	H - C	H - C	C - N	C - O
x	=	-0.03573	3.73677	0.65861	4.60005	5.38060	6.89032
y	=	-3.80534	0.38052	3.08271	1.82118	-2.15984	-2.27121
z	=	-4.29180	-0.93691	-0.95276	0.02469	-1.49402	-1.96967
RHO	=	0.02097	0.27142	0.28018	0.27935	0.24697	0.24697
LAP	=	0.08019	-0.49531	-0.95121	-0.94214	-0.53841	-0.46287
ellip	=	0.03593	0.01791	0.02667	0.03404	0.15744	0.19648
K(r)	=	-0.00081	0.37912	0.27650	0.27501	0.31026	0.29810
G(r)	=	0.01924	0.25530	0.03870	0.03947	0.17566	0.18238
BCP #	=	13	14	15	16	17	18
n1-n2	=	9- 5	26-31	28-27	12-11	16-10	17-10
A - B	=	H - C	C - O	C - C	C - O	H - C	H - C
x	=	1.49499	-4.03960	-7.51815	9.62103	5.92133	6.57343
y	=	-3.02381	-2.41877	-4.19793	-2.32712	-3.87777	-2.79149
z	=	-3.38746	-5.21059	-6.03088	-3.02883	-1.90680	-0.20782
RHO	=	0.28277	0.34526	0.23376	0.21266	0.27633	0.27584
LAP	=	-1.08520	-0.64952	-0.44685	-0.15622	-0.87062	-0.86323
ellip	=	0.01306	0.14583	0.04023	0.00875	0.03249	0.03473
K(r)	=	0.29768	0.54928	0.17038	0.25032	0.25883	0.25761
G(r)	=	0.02638	0.38690	0.05867	0.21126	0.04117	0.04181

BCP #	=	19	20	21	22	23	24
n1-n2	=	13-12	14-13	18-12	19-12	20-13	21-13
A - B	=	C - C	C - C	H - C	H - C	H - C	H - C
x	=	11.34551	13.47091	10.28558	10.96777	12.26325	11.56136
y	=	-1.88656	-1.70866	-3.89090	-2.88165	0.02220	-0.95204
z	=	-3.99141	-4.97956	-3.63919	-1.95956	-4.24283	-5.89198
RHO	=	0.23724	0.22636	0.26803	0.26751	0.26249	0.26490
LAP	=	-0.46543	-0.41214	-0.79508	-0.78993	-0.75006	-0.76837
ellip	=	0.05321	0.02269	0.05794	0.05910	0.01635	0.01363
K(r)	=	0.17631	0.16032	0.24501	0.24412	0.23885	0.24296
G(r)	=	0.05995	0.05728	0.04624	0.04664	0.05133	0.05087
BCP #	=	25	26	27	28	29	30
n1-n2	=	15-14	15-37	22-14	23-14	24-15	25-15
A - B	=	C - C	C - C	H - C	H - C	H - C	H - C
x	=	15.67637	16.19357	14.64748	15.28166	17.72866	16.70059
y	=	-1.44065	-0.42342	-3.39934	-2.51980	-1.15573	0.49462
z	=	-5.94663	-8.06796	-5.75325	-4.04775	-6.66500	-6.11908
RHO	=	0.22612	0.22601	0.25939	0.25964	0.26147	0.26024
LAP	=	-0.41250	-0.41281	-0.72361	-0.72479	-0.74026	-0.73119
ellip	=	0.01077	0.01162	0.01091	0.01147	0.01382	0.01366
K(r)	=	0.15989	0.16006	0.23366	0.23418	0.23720	0.23518
G(r)	=	0.05677	0.05686	0.05276	0.05298	0.05214	0.05238
BCP #	=	31	32	33	34	35	36
n1-n2	=	27-26	27-29	26-30	32-27	33-28	34-28
A - B	=	C - C	C - O	C - O	H - C	H - C	H - C
x	=	-5.19993	-6.13232	-3.33398	-6.52732	-8.92064	-8.45394
y	=	-3.71483	-5.07327	-3.68670	-3.40684	-3.03855	-4.95179
z	=	-6.23706	-7.23599	-5.48011	-7.90844	-4.81766	-4.22066
RHO	=	0.24512	0.22956	0.35407	0.27134	0.26303	0.26068
LAP	=	-0.48616	-0.32904	-0.63177	-0.82319	-0.76335	-0.74254
ellip	=	0.06787	0.05819	0.13782	0.04639	0.01607	0.01617
K(r)	=	0.18163	0.27005	0.57051	0.25110	0.24138	0.23752
G(r)	=	0.06009	0.18779	0.41257	0.04530	0.05055	0.05189
BCP #	=	37	38	39	40	41	42
n1-n2	=	35-28	36-29	36-30	38-37	39-37	40-37
A - B	=	H - C	H - O	H - O	H - C	H - C	H - C
x	=	-9.62745	-4.53523	-3.54337	14.73343	15.67152	16.69457
y	=	-4.66488	-7.07655	-6.04391	0.41574	-1.32085	0.43773
z	=	-5.87184	-7.55522	-6.66028	-9.54115	-10.03775	-10.06454
RHO	=	0.26209	0.34601	0.02420	0.26049	0.25888	0.26002
LAP	=	-0.75478	-1.72479	0.09541	-0.73789	-0.72742	-0.73727
ellip	=	0.01591	0.02313	0.47026	0.01321	0.01305	0.01294
K(r)	=	0.24002	0.49812	0.00030	0.23733	0.23451	0.23652
G(r)	=	0.05133	0.06692	0.02416	0.05286	0.05265	0.05220

Structure 28: Im_oc6h13 L-lactate (4c)

----- Bond critical points -----							
BCP #	=	1	2	3	4	5	6
n1-n2	=	2- 1	5- 4	5- 1	6- 1	2- 3	6-31
A - B	=	C - N	C - N	C - N	H - N	C - C	H - O
x	=	0.83706	2.30489	0.99239	-1.49756	2.45523	-2.65648
y	=	1.51159	-1.52276	-1.05998	0.06648	1.88051	-0.28554
z	=	-2.09166	-2.39012	-2.70531	-3.22734	-1.45744	-3.68344
RHO	=	0.28256	0.31467	0.33884	0.26322	0.32411	0.06617
LAP	=	-0.63845	-0.72624	-0.93301	-1.21792	-0.84841	0.20499
ellip	=	0.01716	0.00682	0.05206	0.01969	0.26726	0.03445
K(r)	=	0.39493	0.47868	0.52842	0.34561	0.32744	0.00829
G(r)	=	0.23532	0.29712	0.29517	0.04113	0.11534	0.05954
BCP #	=	7	8	9	10	11	12
n1-n2	=	9-30	3- 4	7- 2	8- 3	10- 4	10-11
A - B	=	H - O	C - N	H - C	H - C	C - N	C - O
x	=	-0.47338	3.67687	0.72735	4.65967	5.16922	6.64049
y	=	-3.84704	0.58394	3.41382	2.10353	-2.09487	-2.35672
z	=	-3.85799	-1.37788	-1.64144	-0.69205	-1.62989	-2.16333
RHO	=	0.02096	0.27143	0.28018	0.27934	0.24697	0.24698

LAP	=	0.08015	-0.49543	-0.95118	-0.94206	-0.53826	-0.46289
ellip	=	0.03596	0.01793	0.02667	0.03404	0.15742	0.19655
K(r)	=	-0.00081	0.37912	0.27649	0.27499	0.31029	0.29813
G(r)	=	0.01923	0.25526	0.03870	0.03948	0.17573	0.18241
BCP #	=	13	14	15	16	17	18
n1-n2	=	9- 5	26-31	28-27	12-11	16-10	17-10
A - B	=	H - C	C - O	C - C	C - O	H - C	H - C
x	=	1.14240	-4.45875	-8.05651	9.29640	5.60641	6.40894
y	=	-3.02254	-2.40070	-4.09359	-2.71651	-3.88162	-2.58932
z	=	-3.16364	-4.76492	-5.12371	-3.34601	-1.80391	-0.32829
RHO	=	0.28277	0.34524	0.23376	0.21263	0.27633	0.27584
LAP	=	-1.08512	-0.64949	-0.44683	-0.15573	-0.87058	-0.86321
ellip	=	0.01306	0.14586	0.04023	0.00836	0.03250	0.03473
K(r)	=	0.29767	0.54924	0.17037	0.25031	0.25881	0.25761
G(r)	=	0.02639	0.38687	0.05867	0.21138	0.04117	0.04181
BCP #	=	19	20	21	22	23	24
n1-n2	=	13-12	14-13	18-12	19-12	20-13	21-13
A - B	=	C - C	C - C	H - C	H - C	H - C	H - C
x	=	10.97701	13.04478	9.85193	10.67974	11.96099	11.11834
y	=	-2.51820	-2.60419	-4.38749	-3.17483	-0.72059	-1.89356
z	=	-4.45574	-5.57011	-3.74407	-2.27803	-5.04528	-6.48580
RHO	=	0.23726	0.22624	0.26800	0.26749	0.26249	0.26494
LAP	=	-0.46550	-0.41183	-0.79487	-0.78979	-0.75006	-0.76864
ellip	=	0.05327	0.02280	0.05795	0.05913	0.01636	0.01364
K(r)	=	0.17634	0.16017	0.24496	0.24409	0.23885	0.24303
G(r)	=	0.05996	0.05721	0.04624	0.04664	0.05133	0.05087
BCP #	=	25	26	27	28	29	30
n1-n2	=	15-14	37-15	22-14	23-14	24-15	25-15
A - B	=	C - C	C - C	H - C	H - C	H - C	H - C
x	=	15.20539	15.66868	14.09744	14.86441	17.22902	16.30300
y	=	-2.59606	-1.92267	-4.44925	-3.36957	-2.52463	-0.76149
z	=	-6.67019	-8.95262	-6.14434	-4.61862	-7.51327	-7.17515
RHO	=	0.22607	0.22733	0.25942	0.25963	0.26054	0.25935
LAP	=	-0.41247	-0.41558	-0.72393	-0.72457	-0.73252	-0.72380
ellip	=	0.01005	0.02251	0.01101	0.01169	0.01218	0.01168
K(r)	=	0.15988	0.16121	0.23372	0.23414	0.23559	0.23367
G(r)	=	0.05676	0.05731	0.05273	0.05300	0.05246	0.05272
BCP #	=	31	32	33	34	35	36
n1-n2	=	37-40	27-26	27-29	26-30	32-27	33-28
A - B	=	C - C	C - C	C - O	C - O	H - C	H - C
x	=	16.21704	-5.73544	-6.78596	-3.82822	-7.14522	-9.33045
y	=	-1.31445	-3.77081	-5.21055	-3.73042	-3.64352	-2.69401
z	=	-11.20736	-5.52165	-6.25383	-4.87628	-7.14851	-4.02766
RHO	=	0.22630	0.24512	0.22957	0.35409	0.27134	0.26303
LAP	=	-0.41429	-0.48617	-0.32904	-0.63175	-0.82320	-0.76335
ellip	=	0.01092	0.06787	0.05819	0.13779	0.04639	0.01607
K(r)	=	0.16053	0.18163	0.27006	0.57055	0.25110	0.24138
G(r)	=	0.05696	0.06009	0.18780	0.41261	0.04530	0.05055
BCP #	=	37	38	39	40	41	42
n1-n2	=	34-28	35-28	36-29	36-30	38-37	39-37
A - B	=	H - C	H - C	H - O	H - O	H - C	H - C
x	=	-8.91524	-10.17136	-5.30254	-4.21358	14.15945	14.99143
y	=	-4.51976	-4.41860	-7.32147	-6.22193	-1.25953	-3.07889
z	=	-3.17386	-4.78564	-6.34986	-5.67427	-10.42458	-10.69735
RHO	=	0.26068	0.26209	0.34600	0.02420	0.26149	0.25978
LAP	=	-0.74255	-0.75477	-1.72479	0.09540	-0.73833	-0.72702
ellip	=	0.01617	0.01591	0.02313	0.47062	0.01014	0.01149
K(r)	=	0.23752	0.24002	0.49811	0.00030	0.23756	0.23452
G(r)	=	0.05189	0.05133	0.06692	0.02415	0.05298	0.05276
BCP #	=	43	44	45			
n1-n2	=	41-40	42-40	43-40			
A - B	=	H - C	H - C	H - C			
x	=	17.44214	16.78212	18.27304			
y	=	0.46084	-0.72107	-1.37298			
z	=	-11.76905	-13.28829	-12.06562			
RHO	=	0.25908	0.26007	0.25921			
LAP	=	-0.72895	-0.73781	-0.72964			
ellip	=	0.01280	0.01284	0.01270			

K(r)	=	0.23482	0.23658	0.23502
G(r)	=	0.05258	0.05212	0.05261

Structure 29: Im_oc7h13 L-lactate (4d)

----- Bond critical points -----						
BCP #	=	1	2	3	4	5
n1-n2	=	2- 1	5- 4	5- 1	6- 1	2- 3
A - B	=	C - N	C - N	C - N	H - N	C - C
x	=	0.70065	2.13326	0.81613	-1.67802	2.33978
y	=	1.69963	-1.36606	-0.92814	0.15874	2.12145
z	=	-2.49924	-2.47797	-2.80870	-3.39017	-1.95876
RHO	=	0.28256	0.31469	0.33881	0.26341	0.32411
LAP	=	-0.63829	-0.72615	-0.93281	-1.21938	-0.84838
ellip	=	0.01713	0.00681	0.05201	0.01969	0.26726
K(r)	=	0.39497	0.47873	0.52836	0.34594	0.32743
G(r)	=	0.23539	0.29720	0.29516	0.04110	0.11534
BCP #	=	7	8	9	10	11
n1-n2	=	9-30	3- 4	7- 2	8- 3	10- 4
A - B	=	H - O	C - N	H - C	H - C	C - N
x	=	-0.70628	3.55210	0.62028	4.56753	5.01355
y	=	-3.81387	0.82890	3.64279	2.40694	-1.87857
z	=	-3.58217	-1.76080	-2.27426	-1.28737	-1.73524
RHO	=	0.02096	0.27143	0.28018	0.27935	0.24692
LAP	=	0.08018	-0.49539	-0.95117	-0.94215	-0.53804
ellip	=	0.03599	0.01791	0.02667	0.03404	0.15750
K(r)	=	-0.00081	0.37913	0.27649	0.27501	0.31019
G(r)	=	0.01924	0.25528	0.03870	0.03947	0.17568
BCP #	=	13	14	15	16	17
n1-n2	=	9- 5	26-31	28-27	12-11	16-10
A - B	=	H - C	C - O	C - C	C - O	H - C
x	=	0.93594	-4.70461	-8.32531	9.08802	5.43068
y	=	-2.93273	-2.43769	-4.11882	-2.74137	-3.67837
z	=	-3.03582	-4.54186	-4.59659	-3.47306	-1.71115
RHO	=	0.28277	0.34527	0.23376	0.21259	0.27633
LAP	=	-1.08520	-0.64958	-0.44687	-0.15533	-0.87060
ellip	=	0.01306	0.14578	0.04023	0.00822	0.03248
K(r)	=	0.29768	0.54932	0.17039	0.25024	0.25882
G(r)	=	0.02638	0.38692	0.05867	0.21141	0.04117
BCP #	=	19	20	21	22	23
n1-n2	=	13-12	14-13	18-12	19-12	20-13
A - B	=	C - C	C - C	H - C	H - C	H - C
x	=	10.73972	12.77703	9.62052	10.49599	11.71899
y	=	-2.69224	-2.92871	-4.45323	-3.08507	-0.98639
z	=	-4.64146	-5.78935	-3.68557	-2.39451	-5.46442
RHO	=	0.23726	0.22627	0.26800	0.26748	0.26248
LAP	=	-0.46555	-0.41198	-0.79490	-0.78976	-0.74987
ellip	=	0.05326	0.02284	0.05797	0.05916	0.01640
K(r)	=	0.17636	0.16021	0.24496	0.24408	0.23881
G(r)	=	0.05997	0.05721	0.04623	0.04664	0.05134
BCP #	=	25	26	27	28	29
n1-n2	=	15-14	37-15	22-14	23-14	24-15
A - B	=	C - C	C - C	H - C	H - C	H - C
x	=	14.90844	15.31566	13.80307	14.61571	16.90960
y	=	-3.07020	-2.67416	-4.83821	-3.59305	-3.11823
z	=	-6.93622	-9.29277	-6.16770	-4.79979	-7.83133
RHO	=	0.22596	0.22730	0.25946	0.25962	0.26059
LAP	=	-0.41201	-0.41565	-0.72416	-0.72447	-0.73282
ellip	=	0.01008	0.02035	0.01092	0.01168	0.01220
K(r)	=	0.15975	0.16123	0.23376	0.23412	0.23567
G(r)	=	0.05675	0.05731	0.05272	0.05301	0.05247
BCP #	=	31	32	33	34	35
n1-n2	=	40-37	27-26	27-29	26-30	32-27
A - B	=	C - C	C - C	C - O	C - O	H - C
x	=	15.80750	-6.01409	-7.09751	-4.08853	-7.46950
y	=	-2.34790	-3.87276	-5.37681	-3.77852	-3.92286
						-2.58427

z	=	-11.63394	-5.09463	-5.62076	-4.51259	-6.68511	-3.63967
RHO	=	0.22758	0.24512	0.22956	0.35407	0.27133	0.26303
LAP	=	-0.41679	-0.48614	-0.32903	-0.63181	-0.82312	-0.76335
ellip	=	0.02182	0.06786	0.05817	0.13782	0.04639	0.01607
K(r)	=	0.16161	0.18162	0.27004	0.57049	0.25108	0.24138
G(r)	=	0.05741	0.06009	0.18778	0.41253	0.04531	0.05055
BCP #	=	37	38	39	40	41	42
n1-n2	=	34-28	35-28	36-29	36-30	38-37	39-37
A - B	=	H - C	H - C	H - O	H - O	H - C	H - C
x	=	-9.13056	-10.43207	-5.63488	-4.51754	13.77624	14.57933
y	=	-4.30061	-4.37660	-7.50130	-6.34239	-2.16812	-4.01957
z	=	-2.58676	-4.16352	-5.50741	-4.99810	-10.79614	-10.87052
RHO	=	0.26068	0.26209	0.34600	0.02420	0.26060	0.25886
LAP	=	-0.74255	-0.75475	-1.72478	0.09542	-0.73090	-0.71950
ellip	=	0.01616	0.01591	0.02313	0.47016	0.00835	0.00954
K(r)	=	0.23752	0.24002	0.49811	0.00030	0.23604	0.23297
G(r)	=	0.05189	0.05133	0.06692	0.02416	0.05331	0.05310
BCP #	=	43	44	45	46	47	48
n1-n2	=	40-43	41-40	42-40	44-43	45-43	46-43
A - B	=	C - C	H - C	H - C	H - C	H - C	H - C
x	=	16.28039	17.03912	17.83031	14.75669	15.55175	16.66681
y	=	-2.02208	-0.68345	-2.53877	-1.48242	-3.35299	-1.74351
z	=	-13.96707	-12.38465	-12.48271	-15.50248	-15.60015	-16.15234
RHO	=	0.22657	0.25997	0.26011	0.25918	0.25914	0.25982
LAP	=	-0.41549	-0.72870	-0.72948	-0.72966	-0.72931	-0.73559
ellip	=	0.01108	0.01067	0.01083	0.01231	0.01233	0.01267
K(r)	=	0.16082	0.23481	0.23504	0.23499	0.23492	0.23620
G(r)	=	0.05694	0.05264	0.05267	0.05258	0.05260	0.05230

Structure 30: Im_oc8h17 L-lactate (4e)

----- Bond critical points -----							
BCP #	=	1	2	3	4	5	6
n1-n2	=	2- 1	5- 4	5- 1	6- 1	2- 3	6-31
A - B	=	C - N	C - N	C - N	H - N	C - C	H - O
x	=	0.44935	1.93763	0.59750	-1.94274	2.10577	-3.12823
y	=	1.79503	-1.22582	-0.84915	0.12523	2.30160	-0.32323
z	=	-2.55843	-2.22578	-2.53921	-3.12100	-2.16282	-3.38532
RHO	=	0.28256	0.31470	0.33881	0.26335	0.32411	0.06608
LAP	=	-0.63837	-0.72621	-0.93287	-1.21891	-0.84840	0.20489
ellip	=	0.01715	0.00679	0.05202	0.01969	0.26726	0.03448
K(r)	=	0.39495	0.47873	0.52837	0.34584	0.32744	0.00825
G(r)	=	0.23536	0.29718	0.29515	0.04111	0.11534	0.05947
BCP #	=	7	8	9	10	11	12
n1-n2	=	9-30	3- 4	7- 2	8- 3	10- 4	10-11
A - B	=	H - O	C - N	H - C	H - C	C - N	C - O
x	=	-0.90877	3.35030	0.34464	4.35910	4.86103	6.29106
y	=	-3.82753	1.05917	3.74995	2.69655	-1.60551	-1.99356
z	=	-2.86116	-1.86747	-2.57669	-1.65134	-1.57767	-2.14505
RHO	=	0.02095	0.27143	0.28018	0.27934	0.24693	0.24702
LAP	=	0.08015	-0.49549	-0.95116	-0.94211	-0.53801	-0.46312
ellip	=	0.03602	0.01793	0.02667	0.03404	0.15746	0.19660
K(r)	=	-0.00081	0.37913	0.27649	0.27500	0.31023	0.29823
G(r)	=	0.01923	0.25526	0.03870	0.03947	0.17573	0.18245
BCP #	=	13	14	15	16	17	18
n1-n2	=	9- 5	26-31	28-27	12-11	16-10	17-10
A - B	=	H - C	C - O	C - C	C - O	H - C	H - C
x	=	0.74272	-4.97523	-8.56236	8.85549	5.31189	6.20447
y	=	-2.86476	-2.63163	-4.34922	-2.63567	-3.38241	-1.77319
z	=	-2.51743	-3.77533	-3.42731	-3.40745	-1.34731	-0.29601
RHO	=	0.28277	0.34526	0.23376	0.21259	0.27632	0.27582
LAP	=	-1.08517	-0.64957	-0.44684	-0.15514	-0.87055	-0.86309
ellip	=	0.01306	0.14580	0.04024	0.00817	0.03248	0.03473
K(r)	=	0.29768	0.54930	0.17037	0.25025	0.25880	0.25758
G(r)	=	0.02638	0.38691	0.05867	0.21147	0.04117	0.04181
BCP #	=	19	20	21	22	23	24

n1-n2	=	13-12	14-13	18-12	19-12	20-13	21-13
A - B	=	C - C	C - C	H - C	H - C	H - C	H - C
x	=	10.44352	12.42303	9.40798	10.32331	11.34716	10.42060
y	=	-2.71708	-3.07460	-4.35418	-2.82161	-1.11930	-2.60865
z	=	-4.65937	-5.87509	-3.42844	-2.37086	-5.74399	-6.78521
RHO	=	0.23727	0.22628	0.26799	0.26748	0.26247	0.26494
LAP	=	-0.46558	-0.41201	-0.79487	-0.78973	-0.74982	-0.76868
ellip	=	0.05323	0.02277	0.05798	0.05917	0.01641	0.01364
K(r)	=	0.17637	0.16022	0.24495	0.24407	0.23880	0.24303
G(r)	=	0.05998	0.05722	0.04623	0.04664	0.05135	0.05086
BCP #	=	25	26	27	28	29	30
n1-n2	=	15-14	37-15	22-14	23-14	24-15	25-15
A - B	=	C - C	C - C	H - C	H - C	H - C	H - C
x	=	14.49515	14.77385	13.46348	14.32189	16.44843	15.51900
y	=	-3.33589	-3.23911	-5.00443	-3.58539	-3.47377	-1.68052
z	=	-7.10662	-9.51252	-6.06229	-4.90852	-8.09318	-8.12319
RHO	=	0.22599	0.22718	0.25944	0.25960	0.26062	0.25945
LAP	=	-0.41209	-0.41518	-0.72404	-0.72433	-0.73313	-0.72443
ellip	=	0.01008	0.02049	0.01093	0.01168	0.01226	0.01182
K(r)	=	0.15978	0.16108	0.23374	0.23410	0.23573	0.23382
G(r)	=	0.05675	0.05729	0.05273	0.05301	0.05245	0.05272
BCP #	=	31	32	33	34	35	36
n1-n2	=	40-37	27-26	27-29	26-30	32-27	33-28
A - B	=	C - C	C - C	C - O	C - O	H - C	H - C
x	=	15.13944	-6.28443	-7.36518	-4.33398	-7.81759	-9.77012
y	=	-3.20776	-4.14054	-5.71180	-3.95056	-4.40854	-2.72080
z	=	-11.89855	-4.07345	-4.34877	-3.60966	-5.56611	-2.60711
RHO	=	0.22755	0.24512	0.22956	0.35408	0.27134	0.26303
LAP	=	-0.41681	-0.48615	-0.32903	-0.63179	-0.82319	-0.76334
ellip	=	0.01976	0.06786	0.05816	0.13780	0.04639	0.01607
K(r)	=	0.16161	0.18163	0.27005	0.57051	0.25110	0.24138
G(r)	=	0.05741	0.06009	0.18780	0.41256	0.04530	0.05055
BCP #	=	37	38	39	40	41	42
n1-n2	=	34-28	35-28	36-29	36-30	38-37	39-37
A - B	=	H - C	H - C	H - O	H - O	H - C	H - C
x	=	-9.26093	-10.63928	-5.85990	-4.73977	13.14981	13.98318
y	=	-4.28513	-4.57527	-7.78736	-6.56015	-2.94812	-4.78387
z	=	-1.37087	-2.85473	-4.04576	-3.74552	-10.98276	-10.86454
RHO	=	0.26068	0.26209	0.34600	0.02420	0.26065	0.25892
LAP	=	-0.74254	-0.75476	-1.72478	0.09542	-0.73123	-0.71985
ellip	=	0.01616	0.01591	0.02313	0.47014	0.00836	0.00960
K(r)	=	0.23752	0.24002	0.49811	0.00030	0.23612	0.23307
G(r)	=	0.05189	0.05133	0.06692	0.02416	0.05332	0.05310
BCP #	=	43	44	45	46	47	48
n1-n2	=	43-40	41-40	42-40	43-46	44-43	45-43
A - B	=	C - C	H - C	H - C	C - C	H - C	H - C
x	=	15.49556	16.29997	17.11931	15.86657	13.87673	14.69260
y	=	-3.17127	-1.63740	-3.48120	-3.13068	-2.85788	-4.70257
z	=	-14.29005	-12.91853	-12.82396	-16.66279	-15.75095	-15.65491
RHO	=	0.22790	0.25907	0.25922	0.22651	0.26011	0.26006
LAP	=	-0.41819	-0.72132	-0.72209	-0.41526	-0.72965	-0.72924
ellip	=	0.02209	0.00877	0.00889	0.01087	0.01081	0.01082
K(r)	=	0.16195	0.23329	0.23352	0.16076	0.23505	0.23497
G(r)	=	0.05740	0.05296	0.05300	0.05694	0.05264	0.05266
BCP #	=	49	50	51			
n1-n2	=	47-46	48-46	49-46			
A - B	=	H - C	H - C	H - C			
x	=	17.03159	16.26882	17.85278			
y	=	-1.55803	-3.06668	-3.41667			
z	=	-17.73247	-18.86371	-17.63646			
RHO	=	0.25901	0.25980	0.25902			
LAP	=	-0.72824	-0.73548	-0.72828			
ellip	=	0.01200	0.01227	0.01201			
K(r)	=	0.23474	0.23617	0.23475			
G(r)	=	0.05268	0.05230	0.05268			

Structure 31: Im_oc9h19 L-lactate (4f)

----- Bond critical points -----						
BCP #	=	1	2	3	4	5
n1-n2	=	2- 1	5- 4	5- 1	6- 1	2- 3
A - B	=	C - N	C - N	C - N	H - N	C - C
x	=	0.23607	1.78012	0.42311	-2.15243	1.89964
y	=	1.93488	-1.05050	-0.70419	0.21293	2.47840
z	=	-2.48123	-2.08810	-2.36128	-2.87716	-2.17466
RHO	=	0.28256	0.31470	0.33881	0.26335	0.32411
LAP	=	-0.63836	-0.72617	-0.93287	-1.21895	-0.84839
ellip	=	0.01716	0.00679	0.05202	0.01969	0.26725
K(r)	=	0.39495	0.47874	0.52836	0.34584	0.32743
G(r)	=	0.23536	0.29719	0.29514	0.04111	0.11534
BCP #	=	7	8	9	10	11
n1-n2	=	9-30	3- 4	7- 2	8- 3	10- 4
A - B	=	H - O	C - N	H - C	H - C	C - N
x	=	-1.05174	3.17292	0.10244	4.16586	4.73254
y	=	-3.71238	1.26516	3.88590	2.92281	-1.36581
z	=	-2.50014	-1.88064	-2.57421	-1.77237	-1.54544
RHO	=	0.02095	0.27144	0.28018	0.27935	0.24693
LAP	=	0.08015	-0.49549	-0.95115	-0.94212	-0.53798
ellip	=	0.03602	0.01792	0.02667	0.03403	0.15748
K(r)	=	-0.00081	0.37914	0.27649	0.27500	0.31022
G(r)	=	0.01923	0.25527	0.03870	0.03947	0.17573
BCP #	=	13	14	15	16	17
n1-n2	=	9- 5	26-31	28-27	12-11	16-10
A - B	=	H - C	C - O	C - C	C - O	H - C
x	=	0.59821	-5.16875	-8.71387	8.66558	5.21809
y	=	-2.71519	-2.60721	-4.35423	-2.41680	-3.12595
z	=	-2.26402	-3.29410	-2.72970	-3.49264	-1.26287
RHO	=	0.28277	0.34526	0.23376	0.21258	0.27632
LAP	=	-1.08516	-0.64956	-0.44686	-0.15503	-0.87054
ellip	=	0.01306	0.14580	0.04023	0.00815	0.03248
K(r)	=	0.29767	0.54929	0.17038	0.25024	0.25880
G(r)	=	0.02638	0.38690	0.05867	0.21149	0.04117
BCP #	=	19	20	21	22	23
n1-n2	=	13-12	14-13	18-12	19-12	20-13
A - B	=	C - C	C - C	H - C	H - C	H - C
x	=	10.20331	12.13806	9.24232	10.17627	11.03842
y	=	-2.52848	-2.90884	-4.12722	-2.54048	-0.96469
z	=	-4.80370	-6.08280	-3.46639	-2.50982	-5.98808
RHO	=	0.23727	0.22628	0.26799	0.26748	0.26246
LAP	=	-0.46560	-0.41203	-0.79487	-0.78973	-0.74978
ellip	=	0.05320	0.02274	0.05797	0.05918	0.01642
K(r)	=	0.17638	0.16023	0.24495	0.24407	0.23879
G(r)	=	0.05998	0.05722	0.04623	0.04663	0.05135
BCP #	=	25	26	27	28	29
n1-n2	=	15-14	37-15	22-14	23-14	24-15
A - B	=	C - C	C - C	H - C	H - C	H - C
x	=	14.16345	14.34536	13.19971	14.08127	16.07818
y	=	-3.19200	-3.19096	-4.83029	-3.35348	-3.34279
z	=	-7.38520	-9.80239	-6.23355	-5.17356	-8.44276
RHO	=	0.22599	0.22722	0.25944	0.25959	0.26061
LAP	=	-0.41208	-0.41532	-0.72402	-0.72421	-0.73300
ellip	=	0.01005	0.02055	0.01092	0.01169	0.01223
K(r)	=	0.15978	0.16112	0.23373	0.23407	0.23570
G(r)	=	0.05676	0.05729	0.05273	0.05302	0.05245
BCP #	=	31	32	33	34	35
n1-n2	=	40-37	27-26	27-29	26-30	32-27
A - B	=	C - C	C - C	C - O	C - O	H - C
x	=	14.61566	-6.46705	-7.53536	-4.50234	-8.05516
y	=	-3.25241	-4.14371	-5.73865	-3.90990	-4.49295
z	=	-12.20033	-3.47648	-3.64264	-3.10141	-4.89292
RHO	=	0.22744	0.24512	0.22956	0.35407	0.27134
LAP	=	-0.41634	-0.48615	-0.32903	-0.63182	-0.82313
ellip	=	0.01991	0.06786	0.05816	0.13780	0.04639
K(r)	=	0.16147	0.18163	0.27005	0.57051	0.25109
G(r)	=					

G(r)	=	0.05738	0.06009	0.18779	0.41255	0.04531	0.05055
BCP #	=	37	38	39	40	41	42
n1-n2	=	34-28	35-28	36-29	36-30	38-37	39-37
A - B	=	H - C	H - C	H - O	H - O	H - C	H - C
x	=	-9.32979	-10.76254	-5.98930	-4.87571	12.65985	13.52741
y	=	-4.21360	-4.58264	-7.78060	-6.52783	-2.98478	-4.80160
z	=	-0.65080	-2.06392	-3.31736	-3.11385	-11.21646	-11.05755
RHO	=	0.26068	0.26209	0.34600	0.02420	0.26068	0.25894
LAP	=	-0.74255	-0.75475	-1.72476	0.09542	-0.73145	-0.72006
ellip	=	0.01616	0.01591	0.02313	0.47025	0.00842	0.00967
K(r)	=	0.23752	0.24002	0.49811	0.00030	0.23616	0.23310
G(r)	=	0.05189	0.05133	0.06692	0.02416	0.05330	0.05309
BCP #	=	43	44	45	46	47	48
n1-n2	=	43-40	41-40	42-40	46-43	44-43	45-43
A - B	=	C - C	H - C	H - C	C - C	H - C	H - C
x	=	14.87601	15.70834	16.56191	15.14618	13.19544	14.04668
y	=	-3.31012	-1.70810	-3.53367	-3.36584	-3.08283	-4.90932
z	=	-14.60340	-13.32815	-13.19120	-17.00492	-16.01030	-15.87212
RHO	=	0.22786	0.25912	0.25927	0.22787	0.25921	0.25915
LAP	=	-0.41820	-0.72166	-0.72243	-0.41804	-0.72219	-0.72182
ellip	=	0.02001	0.00879	0.00893	0.02179	0.00880	0.00881
K(r)	=	0.16195	0.23338	0.23361	0.16191	0.23352	0.23344
G(r)	=	0.05740	0.05297	0.05300	0.05740	0.05297	0.05298
BCP #	=	49	50	51	52	53	54
n1-n2	=	46-49	47-46	48-46	50-49	51-49	52-49
A - B	=	C - C	H - C	H - C	H - C	H - C	H - C
x	=	15.40124	16.24272	17.09351	13.72679	14.58432	15.58024
y	=	-3.42767	-1.82408	-3.64966	-3.19329	-5.03278	-3.51278
z	=	-19.39401	-18.13553	-17.99754	-20.84911	-20.71001	-21.62348
RHO	=	0.22651	0.25993	0.25994	0.25909	0.25907	0.25966
LAP	=	-0.41523	-0.72823	-0.72827	-0.72889	-0.72870	-0.73421
ellip	=	0.01075	0.01053	0.01052	0.01188	0.01190	0.01235
K(r)	=	0.16075	0.23478	0.23479	0.23485	0.23482	0.23595
G(r)	=	0.05694	0.05273	0.05273	0.05263	0.05265	0.05240

Structure 32: Im_oc10h21 L-lactate (4g)

Bond critical points							
BCP #	=	1	2	3	4	5	6
n1-n2	=	2- 1	5- 4	5- 1	6- 1	2- 3	6-31
A - B	=	C - N	C - N	C - N	H - N	C - C	H - O
x	=	0.15383	1.72233	0.35435	-2.24272	1.82648	-3.43684
y	=	2.11869	-0.81824	-0.49813	0.36846	2.68759	-0.12126
z	=	-2.60253	-1.99803	-2.24747	-2.74234	-2.41414	-2.84692
RHO	=	0.28256	0.31470	0.33881	0.26338	0.32411	0.06606
LAP	=	-0.63835	-0.72621	-0.93284	-1.21914	-0.84840	0.20487
ellip	=	0.01716	0.00678	0.05202	0.01969	0.26726	0.03449
K(r)	=	0.39495	0.47875	0.52835	0.34589	0.32744	0.00824
G(r)	=	0.23536	0.29720	0.29514	0.04110	0.11534	0.05945
BCP #	=	7	8	9	10	11	12
n1-n2	=	9-30	3- 4	7- 2	8- 3	10- 4	10-11
A - B	=	H - O	C - N	H - C	H - C	C - N	C - O
x	=	-1.11496	3.11453	0.01008	4.10544	4.69507	6.08268
y	=	-3.50556	1.50619	4.05287	3.16642	-1.08323	-1.53027
z	=	-2.04937	-2.06074	-2.86944	-2.14552	-1.54718	-2.17339
RHO	=	0.02095	0.27144	0.28018	0.27935	0.24692	0.24703
LAP	=	0.08014	-0.49550	-0.95115	-0.94213	-0.53793	-0.46320
ellip	=	0.03605	0.01792	0.02667	0.03403	0.15749	0.19661
K(r)	=	-0.00081	0.37914	0.27649	0.27500	0.31022	0.29826
G(r)	=	0.01923	0.25526	0.03870	0.03947	0.17573	0.18246
BCP #	=	13	14	15	16	17	18
n1-n2	=	9- 5	26-31	28-27	12-11	16-10	17-10
A - B	=	H - C	C - O	C - C	C - O	H - C	H - C
x	=	0.53993	-5.26431	-8.77816	8.55123	5.19733	6.13929
y	=	-2.49163	-2.47658	-4.16273	-2.30996	-2.80998	-1.06806
z	=	-1.97236	-2.77577	-1.91061	-3.54475	-1.12332	-0.36838

RHO	=	0.28278	0.34527	0.23377	0.21257	0.27632	0.27582
LAP	=	-1.08517	-0.64957	-0.44688	-0.15494	-0.87054	-0.86305
ellip	=	0.01306	0.14579	0.04023	0.00810	0.03248	0.03474
K(r)	=	0.29768	0.54931	0.17039	0.25025	0.25880	0.25757
G(r)	=	0.02638	0.38692	0.05867	0.21151	0.04117	0.04181
BCP #	=	19	20	21	22	23	24
n1-n2	=	13-12	14-13	18-12	19-12	20-13	21-13
A - B	=	C - C	C - C	H - C	H - C	H - C	H - C
x	=	10.03571	11.91914	9.13500	10.10044	10.81689	9.84140
y	=	-2.54274	-3.04015	-4.01050	-2.34178	-1.09562	-2.71988
z	=	-4.90053	-6.21551	-3.38318	-2.61615	-6.25737	-7.01294
RHO	=	0.23727	0.22629	0.26799	0.26748	0.26246	0.26494
LAP	=	-0.46561	-0.41206	-0.79484	-0.78974	-0.74976	-0.76866
ellip	=	0.05319	0.02273	0.05798	0.05918	0.01642	0.01363
K(r)	=	0.17638	0.16023	0.24494	0.24407	0.23879	0.24303
G(r)	=	0.05998	0.05722	0.04624	0.04663	0.05135	0.05086
BCP #	=	25	26	27	28	29	30
n1-n2	=	15-14	37-15	22-14	23-14	24-15	25-15
A - B	=	C - C	C - C	H - C	H - C	H - C	H - C
x	=	13.89190	13.97694	12.98106	13.89874	15.76328	14.79687
y	=	-3.44274	-3.66546	-4.96727	-3.39856	-3.69106	-1.92760
z	=	-7.56634	-9.97863	-6.23014	-5.34771	-8.68140	-8.87271
RHO	=	0.22599	0.22722	0.25944	0.25958	0.26061	0.25943
LAP	=	-0.41210	-0.41532	-0.72400	-0.72415	-0.73300	-0.72429
ellip	=	0.01005	0.02047	0.01092	0.01169	0.01222	0.01179
K(r)	=	0.15978	0.16112	0.23373	0.23406	0.23570	0.23379
G(r)	=	0.05676	0.05729	0.05273	0.05302	0.05245	0.05272
BCP #	=	31	32	33	34	35	36
n1-n2	=	40-37	27-26	27-29	26-30	32-27	33-28
A - B	=	C - C	C - C	C - O	C - O	H - C	H - C
x	=	14.15185	-6.56374	-7.63252	-4.58636	-8.20615	-9.94757
y	=	-3.94927	-4.02286	-5.62593	-3.75621	-4.50080	-2.44972
z	=	-12.36948	-2.76335	-2.73854	-2.49091	-4.07653	-1.21702
RHO	=	0.22747	0.24512	0.22956	0.35407	0.27133	0.26303
LAP	=	-0.41647	-0.48614	-0.32904	-0.63182	-0.82309	-0.76335
ellip	=	0.01995	0.06785	0.05815	0.13780	0.04639	0.01607
K(r)	=	0.16151	0.18162	0.27005	0.57050	0.25108	0.24138
G(r)	=	0.05739	0.06009	0.18779	0.41255	0.04531	0.05055
BCP #	=	37	38	39	40	41	42
n1-n2	=	34-28	35-28	36-29	36-30	38-37	39-37
A - B	=	H - C	H - C	H - O	H - O	H - C	H - C
x	=	-9.31080	-10.79774	-6.06775	-4.95108	12.23587	13.11456
y	=	-3.83057	-4.32797	-7.62967	-6.36400	-3.59018	-5.38502
z	=	0.16950	-1.14483	-2.28902	-2.24692	-11.33722	-11.04530
RHO	=	0.26068	0.26209	0.34600	0.02421	0.26065	0.25892
LAP	=	-0.74256	-0.75475	-1.72477	0.09543	-0.73129	-0.71993
ellip	=	0.01616	0.01591	0.02313	0.46990	0.00839	0.00962
K(r)	=	0.23753	0.24002	0.49811	0.00030	0.23612	0.23307
G(r)	=	0.05189	0.05133	0.06692	0.02416	0.05330	0.05309
BCP #	=	43	44	45	46	47	48
n1-n2	=	43-40	41-40	42-40	46-43	44-43	45-43
A - B	=	C - C	H - C	H - C	C - C	H - C	H - C
x	=	14.31623	15.19464	16.05764	14.49130	12.58031	13.44015
y	=	-4.22900	-2.51702	-4.32319	-4.50681	-4.13008	-5.93737
z	=	-14.76528	-13.67767	-13.40689	-17.15984	-16.11803	-15.84547
RHO	=	0.22775	0.25915	0.25930	0.22783	0.25926	0.25921
LAP	=	-0.41774	-0.72189	-0.72266	-0.41805	-0.72255	-0.72216
ellip	=	0.02017	0.00885	0.00899	0.01975	0.00885	0.00886
K(r)	=	0.16180	0.23342	0.23365	0.16190	0.23361	0.23353
G(r)	=	0.05737	0.05295	0.05298	0.05739	0.05297	0.05299
BCP #	=	49	50	51	52	53	54
n1-n2	=	49-46	47-46	48-46	49-52	50-49	51-49
A - B	=	C - C	H - C	H - C	C - C	H - C	H - C
x	=	14.66005	15.53937	16.39828	14.83913	12.92359	13.78312
y	=	-4.78708	-3.07786	-4.88515	-5.05927	-4.68833	-6.49495
z	=	-19.55643	-18.47134	-18.19957	-21.93705	-20.91087	-20.63966
RHO	=	0.22788	0.25903	0.25904	0.22649	0.26003	0.26001
LAP	=	-0.41805	-0.72083	-0.72090	-0.41519	-0.72905	-0.72885

ellip	=	0.02172	0.00850	0.00848	0.01071	0.01069	0.01071
K(r)	=	0.16192	0.23326	0.23327	0.16074	0.23494	0.23490
G(r)	=	0.05740	0.05305	0.05305	0.05695	0.05268	0.05269
BCP #	=	55	56	57			
n1-n2	=	53-52	54-52	55-52			
A - B	=	H - C	H - C	H - C			
x	=	15.88222	15.06553	16.74835			
y	=	-3.63060	-5.28453	-5.45043			
z	=	-23.29709	-24.15352	-23.02367			
RHO	=	0.25898	0.25967	0.25897			
LAP	=	-0.72792	-0.73430	-0.72786			
ellip	=	0.01169	0.01205	0.01169			
K(r)	=	0.23469	0.23596	0.23468			
G(r)	=	0.05271	0.05239	0.05271			

Structure 33: Im_oc11h23 L-lactate (4h)

----- Bond critical points -----							
BCP #	=	1	2	3	4	5	6
n1-n2	=	2- 1	5- 4	5- 1	6- 1	2- 3	6-31
A - B	=	C - N	C - N	C - N	H - N	C - C	H - O
x	=	-0.12627	1.59067	0.19832	-2.45650	1.53128	-3.63465
y	=	2.14814	-0.67484	-0.42286	0.31166	2.78714	-0.22515
z	=	-2.65601	-1.92524	-2.10955	-2.50110	-2.62235	-2.48912
RHO	=	0.28256	0.31469	0.33881	0.26335	0.32411	0.06608
LAP	=	-0.63836	-0.72617	-0.93288	-1.21891	-0.84838	0.20489
ellip	=	0.01717	0.00677	0.05205	0.01969	0.26725	0.03450
K(r)	=	0.39495	0.47873	0.52836	0.34584	0.32743	0.00825
G(r)	=	0.23536	0.29719	0.29514	0.04111	0.11534	0.05947
BCP #	=	7	8	9	10	11	12
n1-n2	=	9-30	3- 4	7- 2	8- 3	10- 4	10-11
A - B	=	H - O	C - N	H - C	H - C	C - N	C - O
x	=	-1.13701	2.88411	-0.36203	3.80201	4.59384	5.95644
y	=	-3.45248	1.68294	4.04822	3.36361	-0.80077	-1.24924
z	=	-1.58017	-2.26150	-3.06468	-2.54124	-1.64938	-2.32733
RHO	=	0.02094	0.27144	0.28018	0.27935	0.24692	0.24704
LAP	=	0.08012	-0.49550	-0.95114	-0.94214	-0.53793	-0.46323
ellip	=	0.03609	0.01791	0.02668	0.03403	0.15749	0.19661
K(r)	=	-0.00081	0.37915	0.27649	0.27501	0.31021	0.29828
G(r)	=	0.01922	0.25527	0.03870	0.03947	0.17572	0.18247
BCP #	=	13	14	15	16	17	18
n1-n2	=	9- 5	26-31	28-27	12-11	16-10	17-10
A - B	=	H - C	C - O	C - C	C - O	H - C	H - C
x	=	0.47869	-5.36061	-8.74554	8.36393	5.18891	6.10667
y	=	-2.37994	-2.62763	-4.35702	-2.05236	-2.46940	-0.64093
z	=	-1.69084	-2.11462	-0.89386	-3.79061	-1.12473	-0.57168
RHO	=	0.28278	0.34527	0.23377	0.21257	0.27631	0.27581
LAP	=	-1.08515	-0.64959	-0.44687	-0.15489	-0.87050	-0.86303
ellip	=	0.01307	0.14579	0.04023	0.00811	0.03248	0.03474
K(r)	=	0.29767	0.54930	0.17039	0.25024	0.25879	0.25757
G(r)	=	0.02639	0.38690	0.05867	0.21152	0.04117	0.04181
BCP #	=	19	20	21	22	23	24
n1-n2	=	13-12	14-13	18-12	19-12	20-13	21-13
A - B	=	C - C	C - C	H - C	H - C	H - C	H - C
x	=	9.76992	11.58669	9.02279	9.96752	10.40866	9.45277
y	=	-2.34245	-2.87932	-3.71345	-1.95643	-0.98320	-2.69526
z	=	-5.21719	-6.60822	-3.53488	-2.96443	-6.73039	-7.29239
RHO	=	0.23727	0.22629	0.26799	0.26748	0.26246	0.26494
LAP	=	-0.46562	-0.41206	-0.79485	-0.78972	-0.74974	-0.76868
ellip	=	0.05319	0.02272	0.05798	0.05919	0.01643	0.01363
K(r)	=	0.17639	0.16023	0.24495	0.24406	0.23879	0.24303
G(r)	=	0.05998	0.05722	0.04623	0.04663	0.05135	0.05086
BCP #	=	25	26	27	28	29	30
n1-n2	=	15-14	37-15	22-14	23-14	24-15	25-15
A - B	=	C - C	C - C	H - C	H - C	H - C	H - C
x	=	13.48695	13.43222	12.72021	13.62833	15.29455	14.24992
y	=	-3.32097	-3.73274	-4.76408	-3.09948	-3.59350	-1.88507

z	=	-8.04789	-10.43613	-6.54158	-5.84440	-9.25837	-9.52337
RHO	=	0.22599	0.22722	0.25943	0.25957	0.26060	0.25942
LAP	=	-0.41210	-0.41533	-0.72400	-0.72409	-0.73295	-0.72425
ellip	=	0.01005	0.02047	0.01091	0.01169	0.01221	0.01179
K(r)	=	0.15978	0.16113	0.23373	0.23404	0.23569	0.23379
G(r)	=	0.05676	0.05730	0.05273	0.05302	0.05245	0.05272
BCP #	=	31	32	33	34	35	36
n1-n2	=	40-37	27-26	27-29	26-30	32-27	33-28
A - B	=	C - C	C - C	C - O	C - O	H - C	H - C
x	=	13.47092	-6.59526	-7.59686	-4.61679	-8.29574	-9.93602
y	=	-4.20044	-4.21123	-5.84253	-3.85614	-4.84963	-2.63435
z	=	-12.80411	-1.89654	-1.67661	-1.77450	-3.05897	-0.26285
RHO	=	0.22746	0.24512	0.22957	0.35408	0.27133	0.26303
LAP	=	-0.41643	-0.48613	-0.32906	-0.63179	-0.82310	-0.76335
ellip	=	0.01988	0.06785	0.05815	0.13780	0.04639	0.01607
K(r)	=	0.16150	0.18162	0.27005	0.57052	0.25108	0.24138
G(r)	=	0.05739	0.06009	0.18779	0.41257	0.04531	0.05055
BCP #	=	37	38	39	40	41	42
n1-n2	=	34-28	35-28	36-29	36-30	38-37	39-37
A - B	=	H - C	H - C	H - O	H - O	H - C	H - C
x	=	-9.16116	-10.70590	-5.92999	-4.86325	11.60939	12.57393
y	=	-3.87590	-4.52847	-7.74866	-6.44652	-3.82571	-5.56044
z	=	1.18381	0.01172	-1.17312	-1.30306	-11.68153	-11.30841
RHO	=	0.26068	0.26209	0.34600	0.02421	0.26064	0.25892
LAP	=	-0.74255	-0.75474	-1.72474	0.09544	-0.73124	-0.71990
ellip	=	0.01616	0.01591	0.02313	0.46955	0.00838	0.00961
K(r)	=	0.23753	0.24001	0.49810	0.00030	0.23610	0.23307
G(r)	=	0.05189	0.05133	0.06691	0.02416	0.05330	0.05309
BCP #	=	43	44	45	46	47	48
n1-n2	=	43-40	41-40	42-40	46-43	44-43	45-43
A - B	=	C - C	H - C	H - C	C - C	H - C	H - C
x	=	13.49811	14.37462	15.32227	13.53752	11.68053	12.62255
y	=	-4.66463	-2.84255	-4.59098	-5.12833	-4.73124	-6.48183
z	=	-15.17686	-14.28351	-13.92991	-17.54919	-16.41932	-16.06175
RHO	=	0.22780	0.25913	0.25926	0.22748	0.25923	0.25927
LAP	=	-0.41797	-0.72167	-0.72242	-0.41646	-0.72243	-0.72249
ellip	=	0.02024	0.00881	0.00893	0.01966	0.00881	0.00902
K(r)	=	0.16187	0.23339	0.23359	0.16149	0.23354	0.23362
G(r)	=	0.05737	0.05297	0.05299	0.05738	0.05293	0.05299
BCP #	=	49	50	51	52	53	54
n1-n2	=	49-46	47-46	48-46	52-49	52-55	50-49
A - B	=	C - C	H - C	H - C	C - C	C - C	H - C
x	=	13.56138	14.45803	15.38559	13.60149	14.51332	11.75709
y	=	-5.59189	-3.77613	-5.53664	-6.13415	-4.77671	-5.61510
z	=	-19.92058	-19.01791	-18.67816	-22.28810	-24.06646	-21.18931
RHO	=	0.22724	0.26053	0.25870	0.22637	0.22580	0.25891
LAP	=	-0.41525	-0.73043	-0.71823	-0.41301	-0.41206	-0.72020
ellip	=	0.01895	0.00771	0.00937	0.01021	0.00992	0.01003
K(r)	=	0.16116	0.23597	0.23276	0.15997	0.15986	0.23304
G(r)	=	0.05735	0.05336	0.05321	0.05672	0.05685	0.05299
BCP #	=	55	56	57	58	59	60
n1-n2	=	51-49	53-52	54-52	56-55	57-55	58-55
A - B	=	H - C	H - C	H - C	H - C	H - C	H - C
x	=	12.61758	13.69819	15.44254	13.60657	15.26881	15.42870
y	=	-7.38939	-6.79017	-6.65790	-2.85582	-3.49039	-2.74090
z	=	-20.76013	-24.39166	-23.38820	-24.75088	-25.73403	-23.85632
RHO	=	0.25979	0.26074	0.25965	0.25858	0.25942	0.26019
LAP	=	-0.72642	-0.73418	-0.72643	-0.72488	-0.73196	-0.73536
ellip	=	0.01053	0.01261	0.01232	0.01132	0.01155	0.01148
K(r)	=	0.23451	0.23610	0.23432	0.23405	0.23559	0.23694
G(r)	=	0.05290	0.05256	0.05271	0.05283	0.05260	0.05310

Structure 34: Im_oc12h25 L-lactate (4i)

----- Bond critical points -----							
BCP #	=	1	2	3	4	5	6
n1-n2	=	2- 1	5- 4	5- 1	6- 1	2- 3	6-31
A - B	=	C - N	C - N	C - N	H - N	C - C	H - O
x	=	-0.06293	1.55975	0.17864	-2.44679	1.61126	-3.63977
y	=	2.44214	-0.44367	-0.14791	0.67073	3.03228	0.16771
z	=	-2.44626	-1.74609	-1.94889	-2.37028	-2.37064	-2.38969
RHO	=	0.28256	0.31470	0.33881	0.26337	0.32411	0.06606
LAP	=	-0.63832	-0.72612	-0.93285	-1.21908	-0.84838	0.20488
ellip	=	0.01716	0.00677	0.05205	0.01969	0.26725	0.03449
K(r)	=	0.39495	0.47874	0.52835	0.34588	0.32743	0.00824
G(r)	=	0.23537	0.29722	0.29513	0.04111	0.11534	0.05946
BCP #	=	7	8	9	10	11	12
n1-n2	=	9-30	3- 4	7- 2	8- 3	10- 4	10-11
A - B	=	H - O	C - N	H - C	H - C	C - N	C - O
x	=	-1.25132	2.92550	-0.23726	3.89569	4.55273	5.91435
y	=	-3.14834	1.88233	4.35626	3.54127	-0.66169	-1.13440
z	=	-1.50657	-2.01009	-2.81861	-2.23840	-1.42119	-2.08451
RHO	=	0.02095	0.27144	0.28018	0.27935	0.24691	0.24704
LAP	=	0.08013	-0.49545	-0.95114	-0.94217	-0.53792	-0.46326
ellip	=	0.03604	0.01789	0.02668	0.03403	0.15753	0.19660
K(r)	=	-0.00081	0.37915	0.27649	0.27501	0.31020	0.29828
G(r)	=	0.01922	0.25528	0.03870	0.03947	0.17572	0.18246
BCP #	=	13	14	15	16	17	18
n1-n2	=	9- 5	26-31	28-27	12-11	16-10	17-10
A - B	=	H - C	C - O	C - C	C - O	H - C	H - C
x	=	0.39573	-5.43955	-8.89290	8.32450	5.09061	6.04944
y	=	-2.12053	-2.19162	-3.84774	-1.97498	-2.35754	-0.56842
z	=	-1.56696	-2.09532	-0.96831	-3.52214	-0.92279	-0.31354
RHO	=	0.28277	0.34527	0.23376	0.21256	0.27632	0.27581
LAP	=	-1.08515	-0.64959	-0.44685	-0.15482	-0.87052	-0.86302
ellip	=	0.01307	0.14578	0.04024	0.00811	0.03247	0.03473
K(r)	=	0.29767	0.54931	0.17038	0.25023	0.25879	0.25756
G(r)	=	0.02639	0.38691	0.05867	0.21153	0.04117	0.04181
BCP #	=	19	20	21	22	23	24
n1-n2	=	13-12	14-13	18-12	19-12	20-13	21-13
A - B	=	C - C	C - C	H - C	H - C	H - C	H - C
x	=	9.74752	11.57331	8.93099	9.91479	10.45238	9.45839
y	=	-2.27501	-2.83442	-3.65945	-1.94299	-0.90278	-2.57400
z	=	-4.92967	-6.29978	-3.29115	-2.66587	-6.40123	-7.01736
RHO	=	0.23727	0.22629	0.26799	0.26748	0.26246	0.26494
LAP	=	-0.46563	-0.41208	-0.79485	-0.78973	-0.74972	-0.76865
ellip	=	0.05317	0.02271	0.05798	0.05919	0.01643	0.01362
K(r)	=	0.17639	0.16024	0.24495	0.24406	0.23878	0.24302
G(r)	=	0.05998	0.05722	0.04623	0.04663	0.05135	0.05086
BCP #	=	25	26	27	28	29	30
n1-n2	=	15-14	37-15	22-14	23-14	24-15	25-15
A - B	=	C - C	C - C	H - C	H - C	H - C	H - C
x	=	13.48641	13.46409	12.65098	13.59335	15.30752	14.31729
y	=	-3.29969	-3.65782	-4.75227	-3.13026	-3.59823	-1.85484
z	=	-7.71481	-10.11219	-6.25486	-5.50478	-8.89856	-9.14415
RHO	=	0.22600	0.22722	0.25943	0.25957	0.26060	0.25942
LAP	=	-0.41211	-0.41534	-0.72398	-0.72405	-0.73297	-0.72425
ellip	=	0.01004	0.02046	0.01092	0.01168	0.01222	0.01178
K(r)	=	0.15979	0.16113	0.23373	0.23403	0.23569	0.23379
G(r)	=	0.05676	0.05730	0.05273	0.05302	0.05245	0.05272
BCP #	=	31	32	33	34	35	36
n1-n2	=	40-37	27-26	27-29	26-30	32-27	33-28
A - B	=	C - C	C - C	C - O	C - O	H - C	H - C
x	=	13.53321	-6.72234	-7.77365	-4.73700	-8.41993	-10.04459
y	=	-4.07503	-3.74315	-5.34914	-3.44777	-4.30790	-2.10496
z	=	-12.48889	-1.93157	-1.76329	-1.76863	-3.13561	-0.32065
RHO	=	0.22748	0.24512	0.22956	0.35408	0.27134	0.26303
LAP	=	-0.41649	-0.48614	-0.32902	-0.63180	-0.82315	-0.76334
ellip	=	0.01989	0.06785	0.05815	0.13779	0.04639	0.01607
K(r)	=	0.16151	0.18162	0.27005	0.57051	0.25109	0.24138

G(r)	=	0.05739	0.06009	0.18779	0.41256	0.04531	0.05055
BCP #	=	37	38	39	40	41	42
n1-n2	=	34-28	35-28	36-29	36-30	38-37	39-37
A - B	=	H - C	H - C	H - O	H - O	H - C	H - C
x	=	-9.33053	-10.87273	-6.17084	-5.06540	11.66266	12.57029
y	=	-3.39821	-3.98141	-7.31265	-6.03917	-3.67103	-5.44056
z	=	1.11194	-0.09941	-1.27218	-1.35642	-11.39170	-11.04002
RHO	=	0.26068	0.26209	0.34600	0.02420	0.26064	0.25891
LAP	=	-0.74254	-0.75474	-1.72477	0.09542	-0.73122	-0.71985
ellip	=	0.01616	0.01591	0.02313	0.47014	0.00838	0.00960
K(r)	=	0.23752	0.24002	0.49811	0.00030	0.23610	0.23306
G(r)	=	0.05189	0.05133	0.06692	0.02416	0.05330	0.05310
BCP #	=	43	44	45	46	47	48
n1-n2	=	43-40	41-40	42-40	46-43	44-43	45-43
A - B	=	C - C	H - C	H - C	C - C	H - C	H - C
x	=	13.59135	14.50208	15.39341	13.66032	11.79512	12.68377
y	=	-4.48879	-2.71201	-4.49403	-4.89968	-4.47839	-6.26136
z	=	-14.87034	-13.92166	-13.58955	-17.25118	-16.14501	-15.81155
RHO	=	0.22777	0.25913	0.25927	0.22777	0.25927	0.25921
LAP	=	-0.41785	-0.72171	-0.72252	-0.41783	-0.72257	-0.72217
ellip	=	0.02017	0.00881	0.00894	0.01999	0.00888	0.00889
K(r)	=	0.16184	0.23338	0.23361	0.16182	0.23362	0.23352
G(r)	=	0.05737	0.05295	0.05298	0.05737	0.05298	0.05298
BCP #	=	49	50	51	52	53	54
n1-n2	=	49-46	47-46	48-46	52-49	50-49	51-49
A - B	=	C - C	H - C	H - C	C - C	H - C	H - C
x	=	13.72256	14.63272	15.52224	13.79214	11.92210	12.82581
y	=	-5.31500	-3.53896	-5.32093	-5.71851	-5.31344	-7.09118
z	=	-19.63349	-18.68635	-18.35274	-22.01437	-20.89561	-20.58156
RHO	=	0.22749	0.25905	0.25916	0.22724	0.26062	0.25877
LAP	=	-0.41648	-0.72108	-0.72159	-0.41523	-0.73118	-0.71872
ellip	=	0.01958	0.00853	0.00869	0.01886	0.00784	0.00952
K(r)	=	0.16150	0.23328	0.23345	0.16115	0.23611	0.23286
G(r)	=	0.05738	0.05301	0.05306	0.05734	0.05332	0.05318
BCP #	=	55	56	57	58	59	60
n1-n2	=	55-52	55-58	53-52	54-52	56-55	57-55
A - B	=	C - C	C - C	H - C	H - C	H - C	H - C
x	=	13.91669	12.07999	15.68348	14.71873	13.11935	14.13023
y	=	-6.18178	-6.18374	-6.07176	-4.34412	-8.01980	-6.74704
z	=	-24.39681	-25.96665	-23.07614	-23.47076	-25.32409	-26.51778
RHO	=	0.22636	0.22581	0.25969	0.25879	0.25969	0.26064
LAP	=	-0.41298	-0.41209	-0.72555	-0.71925	-0.72680	-0.73332
ellip	=	0.01018	0.00993	0.01031	0.00980	0.01214	0.01265
K(r)	=	0.15996	0.15987	0.23436	0.23287	0.23438	0.23596
G(r)	=	0.05671	0.05685	0.05297	0.05306	0.05268	0.05263
BCP #	=	61	62	63			
n1-n2	=	59-58	60-58	61-58			
A - B	=	H - C	H - C	H - C			
x	=	9.93935	10.40561	10.99556			
y	=	-5.69259	-6.09885	-4.34314			
z	=	-25.51608	-27.44786	-26.61038			
RHO	=	0.26030	0.25943	0.25852			
LAP	=	-0.73634	-0.73203	-0.72438			
ellip	=	0.01152	0.01166	0.01146			
K(r)	=	0.23710	0.23560	0.23397			
G(r)	=	0.05301	0.05259	0.05288			

Appendix 3: The data processing script written in Matlab 7.10.

```
for scr=1:1000

disp
('~~~~~')
disp(' ')
disp('Program script for MATLAB 7.10 is running (Alex, 2010-2014)')
disp(' ')
disp
('~~~~~')
disp(' ')

% loading multiple .csv files from current working directory
files = dir('*.csv');
files={files.name};
files=files';

% experimental ec50 values
% manual input in the script in the corresponding to .csv
files sequence
ec50a=[...];
ec50_d={...};
ec50=log(1./ec50a);

%%%%%%%%%
% bootstrapping started
corr=[files, ec50_d'] %visual check for consistency between
concentrations and names of the chemical structures

for k=length(files);
ind_files_cell1=cvpartition(k, 'kfold', 2);

for i = 1:ind_files_cell1.NumTestSets;
trIdx_files1 = ind_files_cell1.training(i);
teIdx_files1 = ind_files_cell1.test(i);
end
end

train_set1=files(trIdx_files1);
test_set1=files(teIdx_files1);

train_set_ec50_1=ec50(trIdx_files1);
test_set_ec50_1=ec50(teIdx_files1);

train_set_ec50_d=ec50_d(trIdx_files1);
test_set_ec50_d=ec50_d(teIdx_files1);

train_set_data=[train_set1, train_set_ec50_d']
test_set_data=[test_set1, test_set_ec50_d']

%%%%%%%%%
```

```

%*****train set*****

for k=1:length(train_set1);
    input_data{k}=importdata(train_set1{k,1});
    length_array{k}=length(input_data{k});
    length_matrix=cell2mat(length_array);
end
% The longest array in the set of .csv files is found
longest_array_a=max(length_matrix);

for d=1:length(test_set1);
    input_data_1{d}=importdata(test_set1{d,1});
    length_array_1{d}=length(input_data_1{d});
    length_matrix_1=cell2mat(length_array_1);
end

longest_array_b=max(length_matrix_1);
longest=[longest_array_a, longest_array_b];
longest_array=max(longest);

% Zero padding to the longest array started
for k=1:length(train_set1);
    input_levelled=input_data{k};
    input_levelled(9,longest_array)=0;
    n{k}=input_levelled;
end
qsar_mult_arr=cat(3,n{1:length(train_set1)});

qsar_mult_arr(isnan(qsar_mult_arr))==0;

% normalizing data from each file

data_norm=zscore(qsar_mult_arr);

qsar_mult_array=data_norm
%%

% Replacing zero's with NaN's to use nanmean to centre the
data by mean
% subtraction from each column
qsar_mult_array_nan=qsar_mult_array;
qsar_mult_array_nan(find(qsar_mult_array_nan==0)) = NaN;

%Mean centering of the data
for k=1:length(train_set1);
    qsar_detrend_array{k}=detrend(qsar_mult_array_nan(:, :, k),
'constant');
end
qsar_meancentr_array=cat(3, qsar_detrend_array{:});

%replacing NaN's with 0 for PCA analysis, as it does not
handle NaN's
qsar_array_zero=qsar_meancentr_array;

```

```

qsar_array_zero(isnan(qsar_array_zero))=0;
qsar_array_zero1=permute(qsar_array_zero,[2,1,3]);

%%%%%%%%%%%%%%%%%%%%%%%%%%%%%%%%%%%%%%%%%%%%%%%%%%%%%%%%%%%%%%%%%%%%%%%% REGRESSION %%%%%%%%%%%%%%%%%%%%%%%%%%%%%%%%%%%%%%%%%%%%%%%%%%%%%%%%%%%%%%%%%%%%%%%%%
a=longest_array*9;
train_array_2d=reshape(qsar_array_zero1,[a,length(train_set1)]
);
train_array_2d=train_array_2d';

[breg, bint, rreg]=regress(train_set_ec50_1',train_array_2d);

pred_ec50_train_regress = train_array_2d*breg +rreg;
%%

%%%%%%%%%%%%%%%%%%%%%%%%%%%%%%%%%%%%%%%%%%%%%%%%%%%%%%%%%%%%%%%%%%%%%%%% PCA %%%%%%%%%%%%%%%%%%%%%%%%%%%%%%%%%%%%%%%%%%%%%%%%%%%%%%%%%%%%%%%%%%%%%%%%%

% PCA on the data in each file started
for k=1:length(train_set1);
[COEFF,SCORE,latent]=princomp(qsar_array_zero1(:, :, k));
C{k}=COEFF;
S{k}=SCORE;
l{k}=latent;
end
pca_coeff=cat(3,C{:});
pca_score=cat(3,S{:});
pca_latent=cat(3,l{:});

for k=1:length(train_set1);
percent_explained =
100*pca_latent(:, :, k)/sum(pca_latent(:, :, k));
perc_expl{k}=percent_explained;

end
pca_percent=cat(3,perc_expl{:});
post_pca_array_train=pca_score(:,1:2,:);
%%

%%%%%%%%%%%%%%%%%%%%%%%%%%%%%%%%%%%%%%%%%%%%%%%%%%%%%%%%%%%%%%%%%%%%%%%% PCR %%%%%%%%%%%%%%%%%%%%%%%%%%%%%%%%%%%%%%%%%%%%%%%%%%%%%%%%%%%%%%%%%%%%%%%%%

pca_p1_train=squeeze(post_pca_array_train(:,1,:));
pca_pcl_train=pca_p1_train';

[b, binta, r]=regress(train_set_ec50_1',pca_pcl_train);
pred_ec50_train_pcr = pca_pcl_train*b +r;
ec50_pred_pcr=pred_ec50_train_pcr';

train_set_ec50_1;

%check
sse=sqrt(sum((train_set_ec50_1-ec50_pred_pcr).^2));
tse=sum((train_set_ec50_1-mean(train_set_ec50_1)).^2);
r_sq=1-(sse/tse);

%%

%%%%%%%%%%%%%%%%%%%%%%%%%%%%%%%%%%%%%%%%%%%%%%%%%%%%%%%%%%%%%%%%%%%%%%%% PCA/PLS %%%%%%%%%%%%%%%%%%%%%%%%%%%%%%%%%%%%%%%%%%%%%%%%%%%%%%%%%%%%%%%%%%%%%%%%%

```

```

[xl_p,yl_p,xs_p,ys_p,BETA_p,PCTVAR_p, MSE_p,
stats_p]=plsregress...
    (pca_pcl_train,train_set_ec50_1',6);

yfit_train= [ones(size(pca_pcl_train,1),1)
pca_pcl_train]*BETA_p;

%plot(1:6,cumsum(100*PCTVAR_p(2,:)),'-bo');
%title('LVs for PLS on training dataset')

%%%%%%%%%%%%%%%%%%%%%%%%%%%%%%%%%%%%%%%%%%%%%%%%%%%%%%%%%%%%%%%%%%%%%%%%PLS%%%%%%%%%%%%%%%%%%%%%%%%%%%%%%%%%%%%%%%%%%%%%%%%%%%%%%%%%%%%%%%%%%%%%%%%

[xl,yl,xs,ys,BETA,PCTVAR, MSE,
stats]=plsregress(train_array_2d,...
    train_set_ec50_1',6);

pred_ec50_train_pls= [ones(size(train_array_2d,1),1)
train_array_2d]*BETA;

plot(1:6,cumsum(100*PCTVAR(2,:)),'-bo');
%title('LVs for PLS on training dataset')

%%%%%%%%%%%%%%%%%%%%%%%%%%%%%%%%%%%%%%%%%%%%%%%%%%%%%%%%%%%%%%%%%%%%%%%%

%%

%*****test set*****8

% Zero padding to the longest array started
for k=1:length(train_set1);
    input_levelled_1=input_data_1{k};
    input_levelled_1(9,longest_array)=0;
    n_1{k}=input_levelled_1;
end
qsar_mult_arr_1=cat(3,n_1{1:length(train_set1)});

qsar_mult_arr_1(isnan(qsar_mult_arr_1))=0;

% normalizing data from each file

data_norm_1=zscore(qsar_mult_arr_1);

qsar_mult_array_1=data_norm_1

% Replacing zero's with NaN's to use nanmean to centre the
data by mean
% subtraction from each column
qsar_mult_array_nan_1=qsar_mult_array_1;
qsar_mult_array_nan_1(find(qsar_mult_array_nan_1==0)) = NaN;

%Mean centering of the data

```

```

for k=1:length(test_set1);
qsar_detrend_array_1{k}=detrend(qsar_mult_array_nan_1(:,:,k),
'constant');
end
qsar_meancentr_array_1=cat(3, qsar_detrend_array_1{:});

%replacing NaN's with 0 for PCA analysis, as it does not
handle NaN's
qsar_array_zero_1=qsar_meancentr_array_1;
qsar_array_zero_1(isnan(qsar_array_zero_1))=0;
qsar_array_zero1_1 = permute(qsar_mult_array_1, [2,1,3]);

%%

%%%%%%%%%%%%%%%%%%%%%%%%%%%%%%%%%%%%%%%%%%%%%%%%%%%%%%%%%%%%%%%%%%%%%%%% REGRESSION %%%%%%%%%%%%%%%%%%%%%%%%%%%%%%%%%%%%%%%%%%%%%%%%%%%%%%%%%%%%%%%%%%%%%%%%%

test_array_2d=reshape(qsar_array_zero1_1,[a,length(test_set1)]
);
test_array_2d_cent=bsxfun(@minus, test_array_2d,
mean(train_array_2d'));
% train equation fit
yfit_test1_reg=test_array_2d_cent'*breg +rreg;
ec50_pred_test_regress=yfit_test1_reg';

%%%%%%%%%%%%%%%%%%%%%%%%%%%%%%%%%%%%%%%%%%%%%%%%%%%%%%%%%%%%%%%%%%%%%%%%PCR %%%%%%%%%%%%%%%%%%%%%%%%%%%%%%%%%%%%%%%%%%%%%%%%%%%%%%%%%%%%%%%%%%%%%%%%%
qsar_array_zero1_1cent=bsxfun(@minus, qsar_array_zero1_1,
mean(qsar_array_zero1));

for p=1:length(test_set1);
S_test{p}=qsar_array_zero1_1cent(:,:,p)*pca_coeff(:,:,p);
end

pca_score_test=cat(3,S_test{:});
post_pca_array_test=pca_score_test(:,1:2,:);
pca_p1_test=squeeze(post_pca_array_test(:,1,:));
pca_pcl_test=pca_p1_test';

pca_pcl_test_cent=bsxfun(@minus, pca_pcl_test',
mean(pca_pcl_train'));
% train equation fit

yfit_test1_pcr = pca_pcl_test_cent'*b +r;
ec50_pred_test_pcr=yfit_test1_pcr';

%%%%%%%%%%%%%%%%%%%%%%%%%%%%%%%%%%%%%%%%%%%%%%%%%%%%%%%%%%%%%%%%%%%%%%%% PCA/PLS %%%%%%%%%%%%%%%%%%%%%%%%%%%%%%%%%%%%%%%%%%%%%%%%%%%%%%%%%%%%%%%%%%%%%%%%%

% train equation fit
yfit_test1_pca_pls= [ones(size(pca_pcl_test_cent',1),1) ...
pca_pcl_test_cent']*BETA_p+stats_p.Yresiduals;

ec50_pred_test_pca_pls=yfit_test1_pca_pls';

%%

%%%%%%%%%%%%%%%%%%%%%%%%%%%%%%%%%%%%%%%%%%%%%%%%%%%%%%%%%%%%%%%%%%%%%%%% PLS %%%%%%%%%%%%%%%%%%%%%%%%%%%%%%%%%%%%%%%%%%%%%%%%%%%%%%%%%%%%%%%%%%%%%%%%%

```

```

test_array_2d=reshape(qsar_array_zero1_1,[a,length(test_set1)]
);
test_array_2d_central=bsxfun(@minus, test_array_2d,
mean(train_array_2d'));

% train equation fit
yfit_test1_pls= [ones(size(test_array_2d_central',1),1) ...
test_array_2d_central']*BETA+stats.Yresiduals;

ec50_pred_test_pls=yfit_test1_pls'

%%

%%%%%%%%%%%%%%%%%%%%%%%%%%%%%%%%%%%%%%%%%%%%%%%%%%%%%%%%%%%%%%%%%%%%%%%% STATISTICS %%%%%%%%%%

% R.^2 predicted for the test set:
PRESS_regress=sum((ec50_pred_test_regress-
test_set_ec50_1).^2);
PRESS_pcr=sum((ec50_pred_test_pcr-test_set_ec50_1).^2);
PRESS_pca_pls=sum((ec50_pred_test_pca_pls-
test_set_ec50_1).^2);
PRESS_pls=sum((ec50_pred_test_pls-test_set_ec50_1).^2);

SS_test_test=sum((test_set_ec50_1-mean(train_set_ec50_1)).^2);

r_sq_pred_test_regress=1-(PRESS_regress/SS_test_test);
r_sq_pred_test_pcr=1-(PRESS_pcr/SS_test_test);
r_sq_pred_test_pca_pls=1-(PRESS_pca_pls/SS_test_test);
r_sq_pred_test_pls=1-(PRESS_pls/SS_test_test);

% R.^2 for the test set:

stat_regress=regstats(test_set_ec50_1,
ec50_pred_test_regress);
stat_pcr=regstats(test_set_ec50_1, ec50_pred_test_pcr);
stat_pca_pls=regstats(test_set_ec50_1,
ec50_pred_test_pca_pls);
stat_pls=regstats(test_set_ec50_1, ec50_pred_test_pls);

r_squared_test_regress=stat_regress.rsquare;
r_squared_test_pcr=stat_pcr.rsquare;
r_squared_test_pca_pls=stat_pca_pls.rsquare;
r_squared_test_pls=stat_pls.rsquare;

% RMSE for the test set:

rmse_test_regress=sqrt(stat_regress.mse);
rmse_test_pcr=sqrt(stat_pcr.mse);
rmse_test_pca_pls=sqrt(stat_pca_pls.mse);
rmse_test_pls=sqrt(stat_pls.mse);

%concordance correlation coefficient
p1_regress=2*(sum((test_set_ec50_1-
mean(test_set_ec50_1)*(ec50_pred_test_regress-
mean(ec50_pred_test_regress))))))
p2_regress=sum((test_set_ec50_1-mean(test_set_ec50_1)).^2) +
sum((ec50_pred_test_regress-mean(ec50_pred_test_regress)).^2)
+17*((mean(test_set_ec50_1)-mean(ec50_pred_test_regress)).^2)

```

```

pc_regress=p1_regress/p2_regress

p1_pcr=2*(sum((test_set_ec50_1-
mean(test_set_ec50_1)*(ec50_pred_test_pcr-
mean(ec50_pred_test_pcr))))))
p2_pcr=sum((test_set_ec50_1-mean(test_set_ec50_1)).^2) +
sum((ec50_pred_test_pcr-mean(ec50_pred_test_pcr)).^2)
+17*((mean(test_set_ec50_1)-mean(ec50_pred_test_pcr)).^2)
pc_pcr=p1_pcr/p2_pcr

p1_pca_pls=2*(sum((test_set_ec50_1-
mean(test_set_ec50_1)*(ec50_pred_test_pca_pls-
mean(ec50_pred_test_pca_pls))))))
p2_pca_pls=sum((test_set_ec50_1-mean(test_set_ec50_1)).^2) +
sum((ec50_pred_test_pca_pls-mean(ec50_pred_test_pca_pls)).^2)
+17*((mean(test_set_ec50_1)-mean(ec50_pred_test_pca_pls)).^2)
pc_pca_pls=p1_pca_pls/p2_pca_pls

p1=2*(sum((test_set_ec50_1-
mean(test_set_ec50_1)*(ec50_pred_test_pls-
mean(ec50_pred_test_pls))))))
p2=sum((test_set_ec50_1-mean(test_set_ec50_1)).^2) +
sum((ec50_pred_test_pls-mean(ec50_pred_test_pls)).^2)
+17*((mean(test_set_ec50_1)-mean(ec50_pred_test_pls)).^2)
pc_pls=p1/p2

%%%%%%%%%%%%%%%%%%%%%%%%%%%%%%%%%%%%%%%%%%%%%%%%%%%%%%%%%%%%%%%%%%%%%%%%
results_regress=[r_sq_pred_test_regress,
r_squared_test_regress,...
    rmse_test_regress, pc_regress];
results_pcr=[r_sq_pred_test_pcr, r_squared_test_pcr,
rmse_test_pcr, pc_pcr];
results_pca_pls=[r_sq_pred_test_pca_pls,
r_squared_test_pca_pls, ...
    rmse_test_pca_pls, pc_pca_pls];
results_pls=[r_sq_pred_test_pls, r_squared_test_pls,
rmse_test_pls, pc_pls];

for scr=scr
mat_regress{scr}=results_regress;
mat_pcr{scr}=results_pcr;
mat_pca_pls{scr}=results_pca_pls;
mat_pls{scr}=results_pls;
end

%clearvars -except mat_regress mat_pcr mat_pca_pls mat_pls

mat1=cat(3,mat_regress{:});
mat2=permute(mat1,[2,1,3]);
test_results_regress=squeeze(mat2(:,:,:));

mat1a=cat(3,mat_pcr{:});
mat2a=permute(mat1a,[2,1,3]);
test_results_pcr=squeeze(mat2a(:,:,:));

```

```

mat1b=cat(3,mat_pca_pls{:});
mat2b=permute(mat1b,[2,1,3]);
test_results_pca_pls=squeeze(mat2b(:,:,:));

mat1c=cat(3,mat_pls{:});
mat2c=permute(mat1c,[2,1,3]);
test_results_pls=squeeze(mat2c(:,:,:));

end

%%

% Dr Mike Croucher is acknowledged for generating a template
% for a simultaneous display of multiple subplots on the
screen
% A plot of R.^2 predicted calculated over 'scr' runs.
scrsz = get(0,'ScreenSize');
fig1=figure()
set(fig1,'OuterPosition',[1 scrsz(4)/2 scrsz(3)/2
scrsz(4)/2]);

[n,xout] = hist(test_results_regress(1,:))
subplot(2,2,1),bar(xout,n)
title(' R^2 predicted values for Regression of imidazolium
carboxylates')
xlabel('R^2 predicted value')
ylabel('Number of runs')

[n1,xout1] = hist(test_results_pcr(1,:))
subplot(2,2,2),bar(xout1,n1)
title(' R^2 predicted values for PCR of imidazolium
carboxylates')
xlabel('R^2 predicted value')
ylabel('Number of runs')

[n2,xout2] = hist(test_results_pca_pls(1,:))
subplot(2,2,3),bar(xout2,n2)
title(' R^2 predicted values for PCA/PLS of imidazolium
carboxylates')
xlabel('R^2 predicted value')
ylabel('Number of runs')

[n3,xout3] = hist(test_results_pls(1,:))
subplot(2,2,4),bar(xout3,n3)
title(' R^2 predicted values for PLS of imidazolium
carboxylates')
xlabel('R^2 predicted value')
ylabel('Number of runs')

% A plot of RMSE calculated over 'scr' runs.

fig2=figure()
set(fig2,'OuterPosition',[scrsz(3)/2 scrsz(4)/2 scrsz(3)/2
scrsz(4)/2]);

[n4,xout4] = hist(test_results_regress(3,:))

```



```

subplot(2,2,1),bar(xout4,n4)
title(' RMSE values for Regression of imidazolium
caboxylates')
xlabel('RMSE predicted value')
ylabel('Number of runs')

[n5,xout5] = hist(test_results_pcr(3,:))
subplot(2,2,2),bar(xout5,n5)
title(' RMSE values for PCR of imidazolium caboxylates')
xlabel('RMSE predicted value')
ylabel('Number of runs')

[n6,xout6] = hist(test_results_pca_pls(3,:))
subplot(2,2,3),bar(xout6,n6)
title(' RMSE values for PCA/PLS of imidazolium caboxylates')
xlabel('RMSE predicted value')
ylabel('Number of runs')

[n7,xout7] = hist(test_results_pls(3,:))
subplot(2,2,4),bar(xout7,n7)
title(' RMSE values for PLS of imidazolium caboxylates')
xlabel('RMSE predicted value')
ylabel('Number of runs')

% A plot of R.^2 for test set calculated over 'scr' runs.

fig3=figure()
set(fig3,'OuterPosition',[1 1 scrsz(3)/2 scrsz(4)/2]);

[n8,xout8] = hist(test_results_regress(2,:))
subplot(2,2,1),bar(xout8,n8)
title(' R^2 values for Regression of imidazolium caboxylates')
xlabel('R^2 calculated value')
ylabel('Number of runs')

[n9,xout9] = hist(test_results_pcr(2,:))
subplot(2,2,2),bar(xout9,n9)
title(' R^2 values for PCR of imidazolium caboxylates')
xlabel('R^2 calculated value')
ylabel('Number of runs')

[n10,xout10] = hist(test_results_pca_pls(2,:))
subplot(2,2,3),bar(xout10,n10)
title(' R^2 values for PCA/PLS of imidazolium caboxylates')
xlabel('R^2 calculated value')
ylabel('Number of runs')

[n11,xout11] = hist(test_results_pls(2,:))
subplot(2,2,4),bar(xout11,n11)
title(' R^2 values for PLS of imidazolium caboxylates')
xlabel('R^2 calculated value')
ylabel('Number of runs')

save('stat_reg', 'test_results_regress')
save('stat_pcr', 'test_results_pcr')
save('stat_pca_pls', 'test_results_pca_pls')
save('stat_pls', 'test_results_pls')

```

```

fig4=figure()
set(fig4,'OuterPosition',[scrsz(3)/2 1 scrsz(3)/2
scrsz(4)/2]);

[n12,xout12] = hist(test_results_regress(4,:))
subplot(2,2,1),bar(xout8,n8)
title(' CCC values for Regression of imidazolium caboxylates')
xlabel('CCC calculated value')
ylabel('Number of runs')

[n13,xout13] = hist(test_results_pcr(4,:))
subplot(2,2,2),bar(xout9,n9)
title(' CCC values for PCR of imidazolium caboxylates')
xlabel('CCC calculated value')
ylabel('Number of runs')

[n14,xout14] = hist(test_results_pca_pls(4,:))
subplot(2,2,3),bar(xout10,n10)
title(' CCC values for PCA/PLS of imidazolium caboxylates')
xlabel('CCC calculated value')
ylabel('Number of runs')

[n15,xout15] = hist(test_results_pls(4,:))
subplot(2,2,4),bar(xout11,n11)
title(' CCC values for PLS of imidazolium caboxylates')
xlabel('CCC calculated value')
ylabel('Number of runs')

%clear

disp(' ')
disp
('~~~~~')
disp(' ')
disp('Program script for Matlab 7.10 is finished (Alex, 2010-
2014)')
disp(' ')
disp
('~~~~~')
disp(' ')

end

```